Pulmonary delivery of antibiotic-loaded lipid nanoparticles for the treatment of *Pseudomonas aeruginosa* infections associated with cystic fibrosis

María Moreno Sastre
Vitoria-Gasteiz 2016

Pulmonary delivery of antibiotic-loaded lipid nanoparticles for the treatment of *Pseudomonas aeruginosa* infections associated with cystic fibrosis

María Moreno Sastre

University of the Basque Country (UPV/EHU)

Laboratory of Pharmaceutics

Faculty of Pharmacy

Vitoria-Gasteiz, 2016

AGRADECIMIENTOS

ACKNOWLEDGEMENTS

ESKER ONAK

Parece que fue ayer pero ya han pasado tres años desde que comencé mi aventura en este departamento. Para mí el doctorado ha sido como una montaña rusa, tan rápido estás arriba como de repente te encuentras abajo para empezar de nuevo de cero o puede que después de tantas vueltas no sepas donde te encuentras. Esta etapa ha estado llena de emociones, retos y aprendizaje y ha estado marcada por momentos muy duros pero también por otros muy bonitos. Por eso quiero aprovechar este espacio para agradecer a todas esas personas que me han acompañado a lo largo de este camino y que de alguna manera han aportado su granito de arena.

En primer lugar quiero dar las gracias a mis directores de tesis; José Luis por haberme dado la oportunidad de trabajar en el grupo de investigación NanoBioCel y por haberme guiado en la realización de la tesis. Amaia, gracias por toda la ayuda que me has ofrecido durante estos años, tu compresión y dedicación a este trabajo. Además, he tenido la suerte de haber contado con una tercera directora, Marta, muchas gracias por compartir tus conocimientos conmigo e introducirme en el mundo de las "nanos", por tu ayuda incondicional, por tu paciencia y por estar siempre ahí, en los buenos y en los malos momentos. Ha sido un autentico placer haber trabajado a tu lado y haber aprendido tanto contigo, no tengo palabras para agradecerte todo tu esfuerzo, sin ti esta tesis no hubiera sido posible, mila esker!!

Asimismo quiero dar las gracias a Gustavo y a Jon por acogerme con los brazos abiertos cuando empecé el proyecto de fin de máster, por contagiarme vuestro entusiasmo por la ciencia y por haberme dado la confianza suficiente para continuar en el camino de la investigación.

Me gustaría también agradecerle al resto de los integrantes del departamento de Farmacia y Tecnología Farmacéutica: Rosa, Manoli, Gorka, Marian, Ana, Begoña, Arantxa… a todos los compañeros de Tecnalia, Fer, Sergio, Amanda, Sonia, Arantza, Ana, Noe, Estis, Aitziber, Leires, Zuriñe… por vuestro tiempo y colaboración cuando la he necesitado. También a Ángela, Andrés y Blanca por vuestra amabilidad y por estar siempre disponibles. Muchas gracias a todos!

I would like to thank Dr. Ben Forbes for giving me the opportunity of working during four months in his group "Drug Delivery" at King´s College of London. Thank you so much to all the people I met there, especially Kate, for your kindness and support during my placement. Mais, although we met at the end, we had really a good time together. Miro, I will always remember our trip to Edinburg, I enjoyed it very much! Masirah, thanks for sharing your knowledge about microbiology with me, and for encouraging me that "there is always hope". I am sure you will be a great doctor soon! Thank you so much also to my roommates. Tanya, Peter and Joel thanks for helping me my first days in London, the parties and the seasons watching the Lord of the Rings. Sarah, it was a pleasure living with you and thanks for your advices. Issy, thanks for your attention and your positive attitude to adversity, for teaching me to cook typical English dishes, for our shoppings days and making everyday much funnier. Dominga, thanks for being my friend and listening to me when I needed. Hope to see you all again!

Y por supuesto, también me gustaría dedicar esta tesis a todos los miembros de mi familia por todo el apoyo que me han brindado siempre para poder conseguir todo lo que me he propuesto. A mi madre, que siempre ha estado cuando más la he necesitado, por darme fuerza para seguir adelante y por sus sabios consejos, eres todo un ejemplo a seguir! A mi padre, que desde pequeñita me ha enseñado que con esfuerzo, trabajo y constancia todo se consigue y son la clave para poder alcanzar todas mi metas, gracias por tu sacrificio para poder darnos unos estudios. Espero que los dos os sintáis orgullosos de mí. A mi hermano, por tu generosidad, tu simpatía, tu continuo interés en todo lo que hago y por preocuparte por mis "celulitas" o mis "particulitas". Gracias por confiar en mí, os quiero!

Al resto de mi familia, tíos, primos y a mi abuela Luisa y también a mi otra familia, Juanjo, Mariasun, Leire, Diego y Amagoia por vuestro cariño y a mis sobris, Iraia y Ziortza por haberme dado tantos momentos de alegría en este último añito, gracias a todos!

Y por último y no por ello menos importante, quiero dar las gracias a mis dos grandes amores. A Iraitz por formar parte de mi vida, por estar siempre a mi lado y por animarme a perseguir este sueño. Miles de gracias por aguantar mi mal humor, por tu paciencia infinita y por sacarme siempre una sonrisa en los momentos más difíciles. Sin ti, sin tu apoyo no podría haber llegado tan lejos. Te quiero! Y como no podría faltar, a mi gato, Argi, que es capaz de darme un cariño igualable al de un humano y su terapia antiestrés me ha servido de mucho durante este tiempo. Te adoro!

MUCHAS GRACIAS A TODOS!

THANK YOU VERY MUCH!

ESKERRIK ASKO GUZTIOI!

ACKNOWLEDGEMENT FOR FINANCIAL SUPPORT

ACKNOWLEDGMENT TO THE EDITORIALS

Authors would like to thank the editorials for granting permission to reuse their previously published articles in this thesis.

The links to the final published versions are the following:

Moreno-Sastre *et al*. J Antimicrob Chemother*.* 2015*;* 70 (11): 2945-2955
http://jac.oxfordjournals.org/content/early/2015/07/21/jac.dkv192.

Pastor *et al.* Int J Pharm. 2014; 477 (1–2):485-494.
http://www.sciencedirect.com/science/article/pii/S0378517314007716

Moreno-Sastre *et al*. Int J Pharm. 2016; 498 (1): 263-273
http://www.sciencedirect.com/science/article/pii/S0378517315304270

A mis padres, Gilberto y Chelo,

mi hermano, David, y a Iraitz

Lo importante es no dejar de cuestionar.

La curiosidad tiene su propia razón de existir.

(Albert Einstein)

GLOSSARY

ABU: arbitrary brightness units

ACI: Andersen cascade impactor

AFM: atomic force microscope

AM/EthD-1: acetoxy-methyl and ethidium homodimer-1

AM: artificial mucus

AMR: antimicrobial resistance

ANOVA: analysis of variance

API: active pharmaceutical ingredient

ATCC: American type culture collection

AUC: area under the curve

BIEDT: bismuth-ethanedithiol

BP: beclomethasone dipropionate

cAMP: cyclic adenosine monophosphate

CB: comassie blue

CCK-8: cell counting kit 8

CF: cystic fibrosis

CFTR: cystic fibrosis transmembrane conductance regulator

CFU: colony forming units

CH: cholesterol

CMC: carboxymethylcysteine

COPD: chronic obstructive pulmonary disease

DCP: dicethylphosphate

DDS: drug delivery system

DLS: dynamic light scattering

DMEM: Dulbecco´s modified eagle growth medium

DMPC: 1,2-dimyristoyl-sn-glycero-3 phosphocholine

DMPG: 1,2-dimyristoyl-sn-glycero-3-phosphorylglycerol

DMSO: dimethyl sulfoxide

DNA: deoxyribonucleic acid

DPBS: Dulbecco´s phosphate-buffered saline

DPI: dry powder inhaler

DPPC: 1,2-dipalmitoyl-sn-glycero-3-phosphocholine

DPTA: diethylenetriaminepentaacetic acid

DSPC: 1,2- distearoyl-sn- glycerol-3-phosphorylcholine

ED: emitted dose

EE: encapsulation efficiency

ELF: epithelial lung fluid

EMA: European Medicine Agency

ESE: emulsification-solvent-evaporation

FBS: fetal bovine serum

FDA: Food and Drug Administation

FPD: fine particle deposition

FPF: fine particle fraction

HEC: hydroxyethylcellulose

HPLC: high performance liquid chromatography

HPO: 3-hydroxypyridin-4-one

IC50: median inhibition concentration

ICH: International Conference of Harmonization

IR: infrared

MAC: *Mycobacterium avium complex*

MBC: minimum bactericidal concentration

MBIC: minimum biofilm inhibitory concentration

MEM-NEAA: minimum essential medium-non essential amino acids

MHA: Mueller-Hinton agar

MHBCA: Mueller-Hinton broth cation-adjusted

MIC: minimum inhibitory concentration

MMAD: mass median aerodynamic diameter

MRSA: methicillin resistant *Staphyloccocus aureus*

MRT: mean residence time

MsLI: multi-stage liquid impinger

MTT: 3-4.5-dimethylthiazole-2-yl-diphenyltetrazolium bromide

MVL: multilayer vesicle

MWCO: molecular weight cut-off

NCFBC: non-cystic fibrosis bronchiectasis

NGI: next generation impactor

NIR: near infra-red

NLC: nanostructured lipid carrier

NNI: Nanotechnology Initiative

NP: nanoparticle

NPC: nanoprecipitation

PA: *Pseudomonas aeruginosa*

PANAM: polyamidoamine

PBS: phosphate buffered saline

PCL: poly-ε-caprolactone

PDI: polidispersity index

PEG: poly (ethylene glycol)

PGA: poly (glycolic acid)

PLA: poly (L-lactide)

PLGA: poly (lactic-co-glycolic acid)

pMDI: pressurized metered dose inhaler

PVA: poly (vinyl alcohol)

PVP: poly (vinylpyrrolidone)

RES: reticuloendothelial system

RGB: red green blue

RH: relative humidity

SD: standard desviation

SEM: scanning electron microscopy

SLN: solid lipid nanoparticle

SLV: single layer vesicle

TB: tuberculosis

TEM: transmission electron microscopy

TIP: tobramycin inhalation powder

TIS: tobramycin inhalation solution

TSA: tryptic soy agar

TSI: twin stage impinger

USP: United States Pharmacopeia

UV: ultraviolet

WHO: Word Health Organization

ZP: zeta potential

INDEX

INTRODUCTION

The use of nanoparticles for antimicrobial delivery

New weapons to control bacterial growth

Springer (2016)

Editors: Tomás G. Villa and Miguel Viñas

The use of nanoparticles for antimicrobial delivery

María Moreno-Sastre[1,2,*] Marta Pastor[1,2,*], Amaia Esquisabel[1,2], José Luis Pedraz[1,2]

[1]NanoBioCel Group, Laboratory of Pharmaceutics, University of the Basque Country (UPV/EHU), School of Pharmacy, Paseo de la Universidad 7, Vitoria-Gasteiz 01006, Spain

[2]Biomedical Research Networking Center in Bioengineering, Biomaterials and Nanomedicine (CIBER-BBN), Vitoria-Gasteiz, Spain

*These authors equally contrIbuted to the chapter

Abstract

Many currently used antibiotics suffer from some drawbacks such as local and systemic side effects, inadequate therapeutic index and high antimicrobial resistance to bacteria. Since the emergence of multidrug resistant bacteria, new antibiotic approaches are required. In recent years, nanotechnology has appeared as a successful tool for the encapsulation of antibiotics into nanoparticles (NPs) aiming to treat bacterial infections and overcoming, at the same time, some of the limitations of traditional antimicrobial therapeutics. Drug delivery systems (DDS) provide several advantages over the free drug such as protection from environmental inactivation and specific target site that can lead to an improvement in the treatment of such diseases. Moreover NPs can overcome tissue and cellular barriers, thereby can treat infections caused by intracellular microorganisms. NPs are capable of reducing drug dose and toxicity as well as dosing frequency which improve patient compliance. Many nanostructures including liposomes, nanoparticles or dendrimers have demonstrated their ability to increase the therapeutic efficacy of antibiotics and fight against infectious diseases. In this chapter we provide an overview of the current progress of the latest nanosystems developed to delivery antibiotics to combat microbial infection.

---

1. Introduction

Since the discovery of penicillin in 1928, antibiotics have made significant improvement in public health reducing the morbidity and mortality associated with infection diseases. However, the growth of bacterial resistance over the last decades forces an enormous economic and social problem on the healthcare system worldwide (Huttner *et al*. 2013). The main causes of this phenomenon are the overuse and misuse of anti-infection drugs that contribute to the development of new defense mechanism of bacteria by means of innate resistance, genetic mutations or acquisition of resistance genes. In addition, bacteria can modify the antibiotic by inactivation or enzymatic modification, alteration of the antibiotic target or changes in cell permeability and efflux (Brooks and Brooks 2014). Figure 1 summarizes the main mechanisms bacteria have for antibiotic resistance.
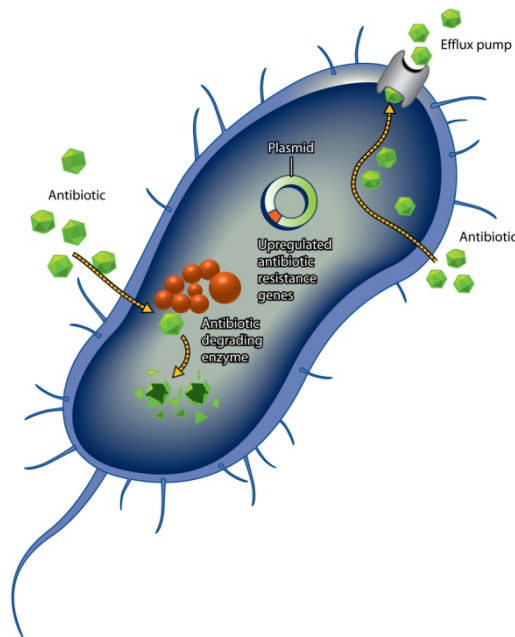
Figure 1. Main antibiotic resistance strategies used by bacteria. Reproduced with permission (Brooks and Brooks 2014).

The emergence of drug resistant microorganisms, such as methicillin-resistant *Staphylococcus aureus* (MRSA), vancomycin-resistant *Enterococcus*, fluoroquinolone-resistant *Escherichia coli* and multidrug-resistant mycobacteria intensifies the needs for new antimicrobial agents with novel drug targets (Yang 2014). Besides that, another important challenge in antimicrobial therapy is the treatment of chronic infections, which are often caused by intracellular microbes or by extracellular microorganisms able to form biofilms. Intracellular infections are more difficult to treat than the extracellular ones due to the low availability of drug inside the cells, the intracelullar location of the microorganism which protects them from the host defense mechanisms and also because the drugs are unable to penetrate the cell efficiently (Ray *et al.* 2009).

Currently, a great number of pathologies are caused by intracellular microorganisms such as leishmaniasis, tuberculosis, legionellosis (pneumonia) or salmonellosis. The antibiotics mainly used today to treat these infections (aminoglycosides and beta-lactams) have a limited capacity to penetrate the cells, hindering their treatment, with only a few (quinolones, macrolides) being efficient in the treatment of phagocytic cells (Briones *et al.* 2008).

Taking all the above into account, the failure of current therapies of bacterial infectious diseases could be related with:

- Low bioavailability of antibiotics
- Side effects of antibiotics
- Rapid clearance of antibiotics from organs
- The environmental deactivation of the drug
- Tissue and cellular barriers (mucosal barriers of the ocular, gastrointestinal and respiratory tissues)

- Biofilm formation (renders the bacterial less susceptible, i.e. 10 to 1000-fold to antimicrobial agents compared to their planktonic cell counterparts) (Mah and O'Toole 2001).
- Intracellular bacterial infection
- Emergence of resistant bacteria
- No specific accumulation

This chapter is aimed to raise the awareness of an urgent need for new therapies to fight against multidrug-resistant pathogens in the treatments of infectious diseases. In this regard, nanotechnology has emerged as an approach to encapsulate antibiotics in drug delivery systems (DDS) in order to improve the therapeutic indexes of antimicrobial drugs (Zhang *et al.* 2010). DDS including dendrimers, micelles, polymeric nanoparticles (NP), liposomes, solid lipid nanoparticles (SLNs) or nanostructured lipid carriers (NLCs) are structures in the nanometric range (Figure 2) that have been explored for the delivery of different antimicrobial agents showing high bactericidal activity *in vitro* with an improvement on conventional therapies (Kalhapure *et al.* 2015).
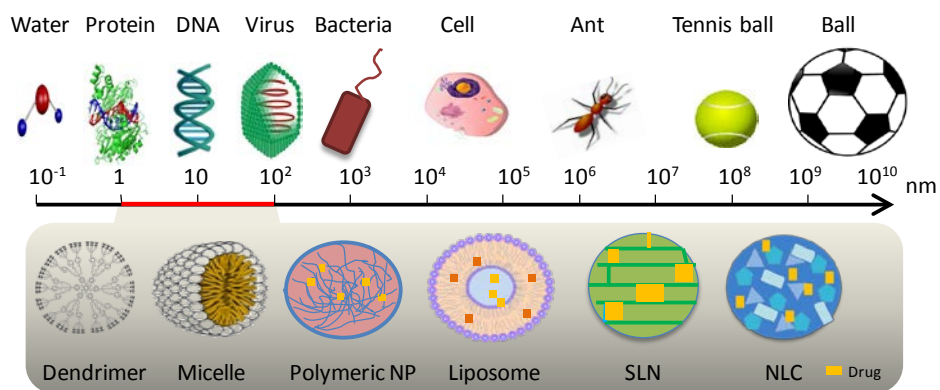
Figure 2. Main nanoparticles employed for antibiotic delivery.

Antimicrobial nano-DDS can provide several advantages over other conventional drugs that are enumerated in Figure 3. Besides them, other advantages also worth it to mention are: high drug payload, ability to encapsulate a wide range of molecules and to increase drug solubility of hydrophobic drugs, target the drugs to specific cells, tissues or organs, reduction side effects or toxicity of the drug as well as their ability to facilitate transport across critical and specific barriers. Moreover, NPs are also able to combat intracellular bacteria as they are small enough to be phagocytozed by host immune cells and release high concentrations of antimicrobial drugs inside the infected cell (Huh and Kwon 2011, Xiong *et al*. 2014).
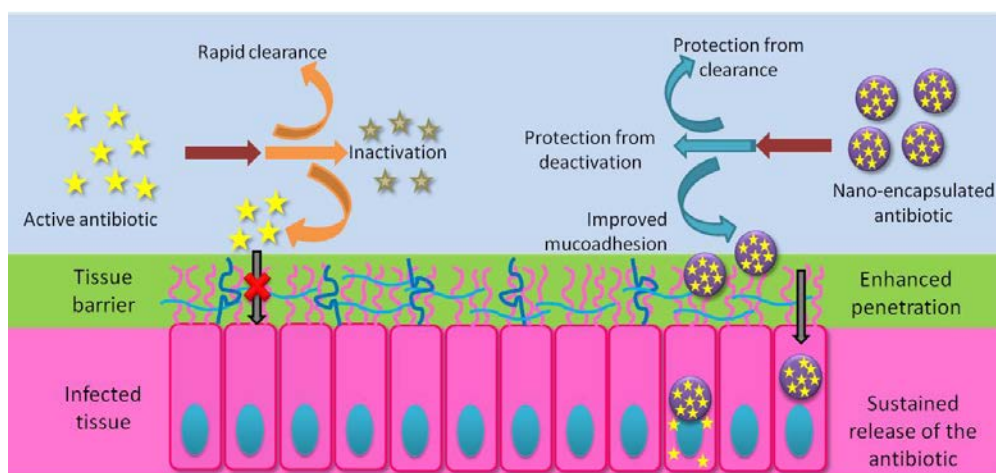
Figure 3. Main advantages of nano-encapsulated antibiotics over free antibiotics. Adapted from Xiong *et al*. 2014.

In general, NPs are well-tolerated systems for oral, parenteral, inhalational, ocular and dermal applications. The administration route plays an important role in their therapeutic efficiency. When NPs are administrated intravenously, they rapidly accumulate in the cells of mononuclear phagocyte system (MPS), therefore are useful in the treatment of infections involving these cells, particularly in the liver and spleen. On

the other hand, oral administration is effective in treating intestinal tract infections and the pulmonary route is commonly use to the treatment of respiratory infections such as tuberculosis, cystic fibrosis and chronic obstructive pulmonary disease (Pinto-Alphandary *et al.* 2000). The main applications of nanoparticles to the treatment of infectious diseases will be revised in part 4 of this chapter.

Although these new drug delivery systems promises a number of benefits for the treatment of infectious diseases, there is a lack of evidence of the potential toxicity of nanoantibiotics to human health at the moment mainly related to their small size (El-Ansary and Al-Daihan 2009).

2. State-of-the-art

Since 2009 only two new antibiotics (telavancin and cetaroline fosamil) have been introduced into the market (Infectious Diseases Society of America (IDSA), 2011).

Nanomedicine has altered the landscape of the pharmaceutical and biotechnology industries but the marketing process of nano-DDS by the FDA is long and difficult as evidenced by the few FDA approved products in the market at the moment (Duncan and Gaspar 2011). Up to date, more than 10 nanoparticle-based products have been marketed for bacterial diagnosis, antibiotic delivery and medical devices (Etheridge *et al.* 2013).

Before reaching the market, many pre-clinical and clinical studies should be carried out in order to confirm that the DDS are safe and viable and can provide therapeutic benefits to humans. Nanotechnology has become a promising strategy to improve the limitations of conventional formulations and to treat resistance to antibiotic drugs. This chapter aims to provide an overview of the latest DDS approaches. Firstly, the different types of nanoparticulate systems loaded with antibiotics are described, secondly different

approaches of antibiotic nanoencapsulation classified according to their administration route are reviewed and finally the limitations and new challenges are discussed.

3. Drug Delivery Systems (DDS) for nanoencapsulation

Nanocarriers used in drug delivery systems are structures of sizes in the nanoscale ranging from 1 to 100 nm in at least one dimension as it is defined by National Nanotechnology Initiative (NNI). However, the literature describes nanoparticles of up to 1000 nm size.

The way of incorporating the active compound such as antibiotic drugs into the nanocarrier and the strategy for its targeting is highly important for a targeted therapy. The nanoparticulate systems (NPs) can load drugs through physical encapsulation, adsorption, or chemical conjugation and are able to deliver their payloads into host cells through different pathways, e.g., contact release, absorption and endocytosis. These antimicrobial delivery systems may allow sufficiently high concentrations and extended release mechanism to effectively eradicate resistant microorganisms. The behavior (intracellular delivery, biodistribution, release profile or antibacterial effect, for instance) of the NPs can be controlled by their composition or properties, e.g., targeted NPs delivery to the infection site could also be achieved by surface modification with targeting ligands or by microenvironment responsiveness. Once the nanoparticles reach the target site, the therapeutic agents are released in a controlled manner which depends on the nature of the delivery system, pH, osmotic gradient, and the surrounding environment (Wilczewska *et al.* 2012).

Nanoparticles used for medical applications must be biocompatible, biodegradable and non-toxic**.** Undesirable effects of nanoparticles strongly depend on their hydrodynamic size, shape, amount, surface chemistry, the route of administration, reaction of the immune systems and residence time in the bloodstream (Ai *et al.* 2011).

For that reason, it is important to consider several parameters such as physicochemical properties of the compounds used, the drug to be loaded, particle size and polydispersity index (PDI), surface charge, stability in storage, reproducibility and feasibility for scale-up before their utilization as DDS. Liposomes, lipid nanoparticles, polymeric nanoparticles, dendrimers or metallic nanoparticles are examples of nanocarriers that have been tested as drug delivery systems for antibacterial treatment and that are evaluated in the following section. Table 1 summarizes the main approaches described in the recent literature for the delivery of antibiotic drugs by means of these systems.

3.1 Lipid Nanoparticles

3.1.1 Liposomes

Liposomes are widely investigated for drug delivery since Doxil® (doxorubicin-encapsulating PEGylated liposomes (liposomes with polyethylene glycol chains in their surface)) became the first liposomal drug approved by the FDA in 1995 (Lian, Ho 2001). Liposomes are spherical vesicles comprising one or more phospholipid bilayers with an aqueous core. Those with a single bilayer are known as single-layer vesicles (SLV) and the others as multilayer vesicles (MLV). They are usually made of natural or synthetic phospholipids and cholesterol. Liposomes can encapsulate hydrophilic or hydrophobic drugs; soluble drugs such as aminoglycosides are enclosed in the aqueous phase, whereas hydrophobic molecules as penicillins are incorporated into the lipid bilayer (Samad *et al*. 2007).

The most commonly applied methods for liposome elaboration include sonication, reverse-phase evaporation technique, thin film hydration or ethanol injection (Vemuri and Rhodes 1995). Sonication is one of the most extensively used methods for liposome preparation by using a bath sonicator or a probe sonicator under a passive atmosphere. However, the main disadvantages of this method include a low encapsulation efficacy (EE)

or possible degradation of the phospholipids or compounds to be encapsulated. When preparing liposomes by ethanol injection, a lipid solution of the ethanol is quickly injected into a huge excess of buffer. This technique, however, presentes some disadvantages because the liposomes are not homogenous, they are much diluted and removal all the ethanol is difficult to achieve. Reverse-phase evaporation is based on the formation of inverted micelles that are shaped by sonication with an aqueous phase containing water-soluble molecules (to be encapsulated inside) and an organic phase in which the amphiphilic molecules are solubilized. The slow elimination of the organic solvent leads to the formation of a complete bilayer around the residual micelles forming the liposomes (Akbarzadeh *et al*. 2013).The physicochemical properties of liposomes can be modified and optimized depending on their therapeutic application. For example, cationic or anionic liposomes can be prepared by using cationic or anionic ingredients in the formulation (Immordino *et al*. 2006).

Interactions of liposomes with cells can be realized by: adsorption, fusion, endocytosis, and lipid transfer. Among the mechanism of action, they can release the drug incorporated in two different ways: a) antibiotics are released inside the bacterial cells after the liposomes fuse with the microbial cell walls, b) antibiotics are released outside the bacterial cells by the liposomes adsorbed on the cell walls, followed by the diffusion into the bacteria. Both mechanisms resulted in a high concentration of antimicrobial drug into the plasma membrane or cytoplasm (Zhang *et al*. 2010).

An important benefit of using liposomes for infectious diseases is that they can treat extracellular or intracellular infections. As the most popular route for liposomal administration is the parenteral one, they are rapidly uptake by the reticuloendothelial system (RES), especially liver and spleen, which may be advantageous for the treatment of intracellular infections involving this type of cells (Allen *et al*. 1989). However, in some cases, it is necessary to incorporate or conjugate them with other materials such as

polyethyleneglycol (PEG) or glycolipids in order to improve their stability and prolong their circulation time.

During the last decade there have been a surmountable number of approaches for the delivery of antibiotics by means of liposomes (Table 1). The encapsulation of the drug into liposomes has proven to be an effective method for reducing minimum inhibitory concentration (MIC), compared to the free drug, as it is the case of gentamicin. Liposomal gentamicin showed significantly lower MIC values than those of free drug (32 mg/L versus 512 mg/L) tested in a gentamicin-resistant non-mucoid strains of *Pseudomonas aeruginosa* isolated from cystic fibrosis (CF) patients (Rukholm *et al*. 2006).

Another advantage of the use of liposomes is the reduction of the drug side effects. Liposomes containing polymixin B have shown to reduce its nephotoxicity, ototoxicity and neuromuscular blockade after a systemic administration while improving its antimicrobial activity against *P. aeruginosa.* Together with this, polymixin-loaded liposomes fuse with the bacteria´s membrane causing its deformation and delivering a high dosage of antimicrobial agents inside the bacteria that prevent drug resistance of microbes by saturation of the efflux pumps (Alipour *et al*. 2008).

In another study, Ong *et al* developed ciprofloxacin-loaded liposomes for the treatment of bacterial infections in cystic fibrosis (CF) and non-CF bronchiectasis patients, achieving the same antimicrobial activity *in vitro* against *Pseudomonas aeruginosa* and *Staphylococcus aureus* as the free drug. In addition, liposomal ciprofloxacin presented lower minimum bactericidal concentration (MBC) against *P. aeruginosa* than the free drug. However, it did not provide bactericidal activity against *S. aureus* (Ong *et al*. 2012).

Moreover, by modifying the surface properties by PEGylation, liposomes have shown to increase the activity of ciprofloxacin and vancomycin in respiratory infections, reducing at the same time the adverse effects of the drugs incorporated (Chono *et al*. 2011, Muppidi *et al*. 2011).

Besides the previous strategies, liposomes have been widely used for the treatment of respiratory diseases, and in particular, tuberculosis. Pulmonary tuberculosis is treated by a standard short term tuberculosis chemotherapy, which consists of a daily oral administration of isoniazid, rifampicin, ethambutol, or pyrizinamide. The co- encapsulation of isoniazid and rifampicin in liposomes for tuberculosis treatment showed a significant reduction of mycobacterias in lungs, liver and spleen of infected mice compared with untreated animals (Labana *et al*. 2002). Changsan *et al* investigated the properties of liposomes containing rifampicin and different amount of cholesterol and soybean L-α-phosphatidycholine prepared by the chloroform-film method. The liposomes particles were a mixture of unilamellar and multilamellar vesicles in a size range of 200-300 nm**.** The MICs of liposome containing rifampicin and free rifampicin were 0.2 and 0.8 µM, respectively, determined against *Mycobacterium bovis* for all formulations (Changsan *et al*. 2009).

In another approach, Zaru *et al.* (2009) carried out *in vitro* and *in vivo* studies to investigate the targeting of rifampicin-loaded liposomes to alveolar macrophages. In order to improve the stability problems associated with low transition temperature, lecithin and Phospholipon 90 with or without cholesterol were used to prepare the liposomes via the film hydration method followed freeze-drying. These authors tested different drug containing liposomal formulations, observing that the formulation with the lowest drug concentration (0.05 µg/mL) showed a complete inhibition of the growth of *Mycobacterium avium* complex (MAC) in infected alveolar macrophages (J774 cells) whereas the free drug exhibited a 80% reduction in bacterial growth. In the *in vivo* experiments, rifampicin-loaded liposomes were administered into rats by nebulization, showing that they were able to reach the lowest airways in comparison with the free drug.

Similarly, other antibiotics with successful results have been incorporated to liposomes demonstrating effective antimicrobial activity against different organisms, as they are illustrated in Table 1.

To sum up, antibiotic-loaded liposomes are effective against a wide range of microorganisms, have a potential for treating numerous diseases, reducing toxicity, and achieving a sustained drug release. However, the use of liposomes for antibiotic delivery over the last few years has decreased, probably due to the introduction of newer DDS, discussed later in this chapter, that overcome some of their drawbacks e.g, low stability in the bloodstream and during storage, low encapsulation efficiency or the presence of residues of toxic solvents in the final preparation (Barratt 2003).

3.1.2 Niosomes

Niosomes are very similar to liposomes but they are prepared with non-ionic surfactants, which give them more stability, compared to liposomes. Moreover, the surfactants used are biodegradable, biocompatible and non-immunogenic. As is the case of liposomes, niosomes have a bilayer structure which can enclose aqueous or lipophilic drugs. There are numerous methods of preparation such as thin film hydration, ether injection, reverse phase evaporation or active trapping techniques, as those revised in the previous section (Sankhyan, Pawar 2012).

Different drugs have been reported to be delivered using niosomes. A niosomal formulation of isoniazid showed a high cellular uptake (≈61%) by macrophages cells, as consequence, dose and frequency could be reduced with an enhancement of patient compliance (Singh *et al*. 2011). Similar findings were found with pyrazinamide-loaded niosomes that were effective in killing tubercle bacilli and decrease toxicity (El-Ridy *et al*. 2011). Akbari *et al* prepared niosomes containing ciprofloxacin by remote loading method followed by sonication. The MIC values of ciprofloxacin-loaded niosomes were from 2 to 8 times lower than MICs of free drug against intracellular *S. aureus* infection of murine macrophage-like (J774 cells) and provide a high intracellular antimicrobial activity (Akbari *et al*. 2013).

Others examples of antibiotics encapsulated into niosomes are cefuroxime (Sambhakar *et al*. 2011) and gallidermin (Manosroi *et al*. 2010), although these studies did not test antimicrobial efficacy.

3.1.3 Solid lipid nanoparticles (SLN and NLC)

Solid lipid nanoparticles (SLNs) appeared as an alternative drug delivery system in the early 90's, thanks to their advantages such as the use of biocompatible materials, high EE of lipophilic drugs, controlled release, protection of drug against degradation, tissue tolerance and large-scale production (Müller *et al*. 2000). SLNs are made of solid lipids (e.g., stearic acid, palmitic acid, glycerol behenate or glyceryl monostearate) stabilized by surfactants (e.g., poloxamer 188, 182, 407, 908, Tween 20 or 80 and solutol HS15) (Kovacevic *et al*. 2011).

The main methods for the production of SLNs are high-pressure homogenization, emulsion-solvent-evaporation and microemulsion technique (Mehnert and Mäder 2001). The most recurrent technique of elaboration is by emulsion-solvent-evaporation where the aqueous phase containing a surfactant as stabilizer agent is added to lipid phase (drug and organic solvent). After the emulsification step the volatile solvent is removed through evaporation while magnetic stirring leading to the formation of drug-loaded nanoparticles with a lipid matrix solid at room and body temperature (Pardeike *et al*. 2009). Figure 4 shows a schematic representation of the method.

Many studies are reported with SLN-based antibiotic delivery systems. Jain and Banerjee encapsulated ciprofloxacin into SLNs that provided a prolong release of the drug in a controlled manner (Jain and Banerjee 2008). Similarly, tilmicosin-SLNs demonstrated an improvement antibacterial activity *in vitro* and *in vivo* against *S. aureus* (Wang *et al*. 2012a). In a further research, norfloxacin-loaded SLNs were found to be stable 9 months at 4°C and with a sustained release until 48 hours. Also demonstrate *in vitro* antibacterial activity and in mice against *E. coli* (Wang *et al*. 2012b).

Kalhapure *et al.* developed a compritol-based SLN formulation of vancomycin and linoleic acid using an ion paring mechanism. SLNs were active against *S. aureus* and MRSA strains (MICs of 31.25 and 15.62 µg/mL, respectively) suggesting that the co-encapsulation of a fatty acid with an antibiotic may enhance its antibacterial activity (Kalhapure *et al*. 2014). Ghaffari and colleages encapsulated amikacin into SLNs leading to an increasing antimicrobial activity against *P. aeruginosa* than the free drug (Ghaffari *et al*. 2011).

For the treatment of tuberculosis, a multidrug solid lipid particle loaded with rifampicin, isoniazid and pyrazinamide was developed by Pandey *et al.* The formulations were produced by the emulsion solvent diffusion technique and achieved drug incorporation efficiencies between 41-51% for the three drugs. After their pulmonary administration in *Mycobacterium tuberculosis*-infected guinea pigs, no colony forming units (CFU) could be detected in the lungs and spleen after seven times one dose weekly of treatment whereas 46 daily oral doses of free drugs were required to obtain the same therapeutic effect. Moreover, those nanoparticles did not cause hepatotoxicity. Thus, nebulization of SLN-based antitubercular drugs could be a higher potential anti-tuberculosis therapy improving drug bioavailability and patient compliance (Pandey and Khuller 2005).

Although SLNs have shown great therapeutic potential for delivering drugs they presented some disadvantages such as a low soluble-drug loading capacity, the possibility of drug expulsion after crystallization, and a relative high water content of the dispersions (Müller *et al*. 2002). Nanostructured lipid carriers (NLCs) have been developed to overcome these limitations of conventional SLNs and represented the second generation of lipid nanoparticles. The main difference between them is that NLCs are produced by mixing solid lipids with liquid lipids, which leads to imperfections in the lipid matrix with an increased payload and prevented drug expulsion (Das *et al*. 2012). Hot melt homogenization or emulsification is one of the main methods used to elaborate NLCs that consists on heating the oil phase (drug and lipids) and the aqueous solution (surfactants)

at the same temperature, high enough to able to melt the lipid compounds, mixing then afterwards by sonication in order to obtain an emulsion containing the nanoparticles (Figure 4). By using this method, recently, Pastor *et al*. reported a novel formulation of NLCs for the encapsulation of sodium colistimethate to reduce its side effects, more precisely, nephrotoxicity, neuromuscular blockage and ototoxicity while improving its antimicrobial activity. The nanoparticles were more effective against clinically isolated *P. aeruginosa* strains than free drug and the authors suggested that Colist-NLCs administered by the pulmonary route could be an alternative for the treatment of the infections associated to cystic fibrosis patients (Pastor *et al*. 2014).
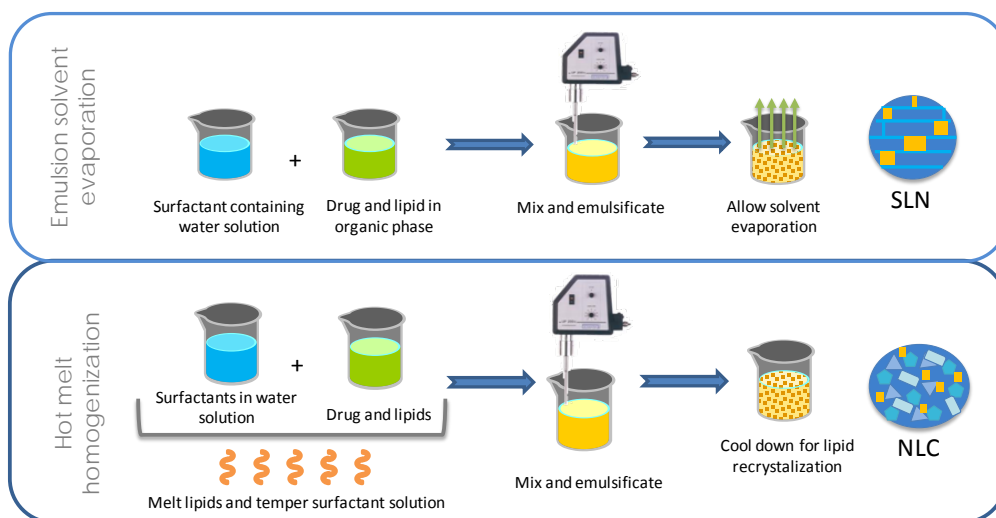
Figure 4. Schematic representation of emulsion solvent-evaporation and hot-melt homogenization techniques.

3.2 Polymeric Nanoparticles

Polymeric nanoparticles are solid colloidal particles composed by polymers. Polymers can be divided into natural, e.g., albumin, chitosan, gelatin or alginate or synthetic such as poly-ε-caprolactone (PCL), poly(L-lactide) (PLA), poly-glycolide (PGA), polyvinyl alcohol (PVA), poly (lactic-co-glycolic acid) (PLGA) and polyethylene glycol (PEG) (Pinto-Alphandary *et al*. 2000). PLGA is widely use for NPs preparation as it is approved by FDA for therapeutic use in humans and has biodegradable and biocompatible properties (Makadia and Siegel 2011).

There are a considerable number of methods for polymeric particles elaboration reported in the literature, being the most common ones; emulsion polymerization, nanoprecipitation, emulsification-solvent diffusion or solvent evaporation method. Drugs can be entrapped, adsorbed, or covalently attached in the polymeric matrix and may be released by desorption, diffusion, or nanoparticle erosion in the target tissue (Kumari *et al*. 2010).

Emulsion diffusion is a method which begins by dissolving the pre-formed polymer in an organic solvent that is partially miscible with water (e.g. ethyl acetate, dichloromethane, or acetone/methanol). Then, an aqueous solution containing a stabilizer is added to emulsify the solution. The mixture is then stirred while a large quantity of water is added promoting the formation of oil-in-water emulsions. Under continuous stirring, the organic solvent evaporates from the emulsions which results in the formation of NPs. Emulsion-evaporation is another method used for the elaboration of polymeric NPs. It involves the emulsification of an organic solvent with the polymer and the compound to be encapsulated into an aqueous phase containing a stabilizer. A high shear stress is then applied to break the emulsion droplets into even smaller ones. The size of the droplet is directly related to the size of the NPs that will be formed. Finally the organic solvent is removed through evaporation causing the precipitation of the polymer and the

formation of NP. Nanoprecipitation is also known as solvent diffusion or solvent displacement technique. Firstly, the polymer must be dissolved in a water miscible solvent. Secondly, this mixture is added to an aqueous solution containing a stabilizer. This causes NPs to precipitate instantly due to solvent diffusion into the aqueous matrix. The NPs can be purified by removing the remaining organic solvent (Lai *et al*. 2014). High pressure homogenization is a scalable method and has been commercially used for several FDA approved drugs. The drug and the stabilizer are pressurized with an intensifier pump to 100–2000 bars. The high pressure stream then passes through a relief valve where cavitation, high shear force, and collision between the particles are induced by a sudden release of pressure which gives rise to a progressively reduction of particle size and results in a homogeneous and uniform product (Keck and Müller 2006).

Due to their polymeric composition, polymeric-NPs may have greater stability than liposomes in biological fluids and under storage. Their main characteristics for antibiotic delivery include: structural stability, ability to control their physicochemical properties (size, zeta potential and release profile) by the selection of appropriate components during preparation (polymers, surfactants and organic solvents) and possibility to introduce functional groups onto the surface of NP by using drug moieties or targeting ligands (Zhang *et al*. 2010).

Since the 21st century, scientists have focused on the use of biodegradable and biocompatible materials, such as PLGA. Initially, Dillen *et al.* (2004), studied the antibacterial activity of ciprofloxacin PLGA NPs, modified or not with a cationic polymers (Eudragit RS100 or RL100) against *P. aeruginosa* and *S. aureus*. In the case of PLGA nanoparticles no differences in activity were found. However, when Eudragit was added into PLGA NPs, the drug was less active in killing *S. aureus* compared with *P. aeruginosa* (Dillen *et al*. 2006). Using the same antibiotic, Jeong *et al*. (2008) developed PLGA NPs, obtaining particle size between 100-300 nm and demonstrating higher antibacterial activity *in vivo* than the free drug although *in vitro* was superior. This fact was explained by

the sustained release of the drug that lasted for 14 days whereas the *in vitro* study was only performed for 24 hours. Other NPs formulated using PLGA have been shown to improve the delivery of azithromycin and rifampicin aimed to treat intracellular *Chlamydia* infections (Toti *et al.* 2011).

In another approach, Moghaddam and co-workers encapsulated clarithromycin into PLGA nanoparticles by the emulsification-solvent-evaporation technique using PVA as emulsifying agent. Drug release studies showed a biphasic profile lasting for 2 days. They developed a respirable formulation adding leucine to the NP formulation for the treatment of pulmonary infections (Moghaddam *et al.* 2013).

Cheow *et al.* elaborated levofloxacin and ciprofloxacin-loaded PLGA or poly-ε-caprolactone NPs by nanoprecipitation or emulsification-solvent-evaporation methods. Their biphasic release over 6 days period permitted a high initial drug concentration at the beginning and the extended release profile above the MIC value able to inhibit the biofilm growth, both in biofilm cells and in biofilm-derived planktonic cells (Figure 5) (Cheow *et al.* 2010a, Cheow *et al.* 2010b).
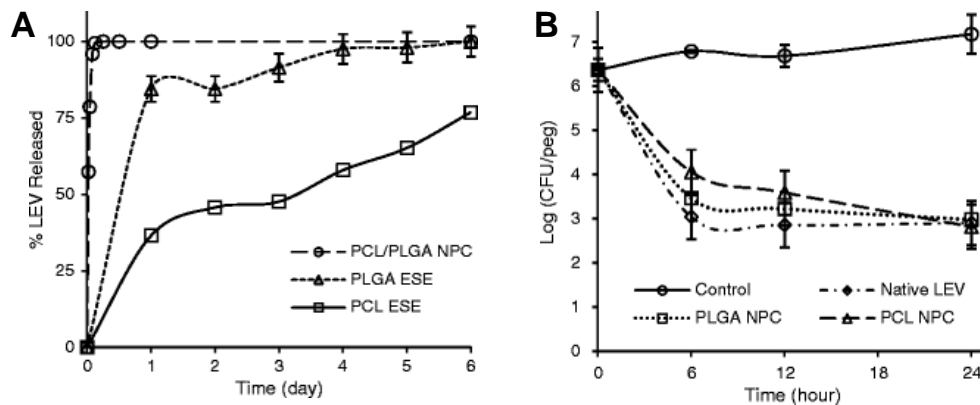
Figure 5. A) *In vitro* release profiles of the LEV-loaded nanoparticle formulations. B) Effect of encapsulation on the LEV antibacterial activity. Reproduced with permission (Cheow *et al.* 2010b).

Tobramycin encapsulation was described by Ungaro *et al.* An emulsion-solvent diffusion technique was slightly modified for the preparation of PLGA nanoparticles including different types of hydrophilic polymers, such as cationic chitosan (CS) and non-ionic polyvinylalcohol (PVA). When chitosan or PVA were added in an appropriate concentration, i.e. PVA/PLGA 3:5 w/w and CS/PLGA 1:20 w/w, the nanoparticles obtained displayed a 250-300 nm diameter and a positive or neutral charge, respectively. Moreover, by adding alginate in the internal phase of the emulsion, the EE increased up to 80% and the relase profile was characterized with a bust released followed by a sustained drug release for a month. The MIC values of the PLGA formulations against *P. aeruginosa* in planktonic cells were higher than that of the free antibiotic. This fact could be due to the biphasic extended antibiotic release profiles of the nanoparticles that liberated small amounts of the drug into the media, very likely below the MIC. Moreover, the nanoparticles were able to inhibit the growth of planktonic cells even at low antibiotic loadings (i.e. <2%, w/w) (Ungaro *et al*. 2012).

Apart from PLGA, chitosan alone is another interesting polymer for NPs preparation because of its antimicrobial and antifungal inherent activities. It is considered that the positive charge of chitosan bind with the negative charge of the bacteria cell walls destabilizing the cell and altering the permeability, subsequently it might get attached to DNA and inhibit the replication (Kong *et al*. 2010). Successful examples using this polymer are tetracycline encapsulated O-carboxymethyl chitosan NPs for the eradication on intracellular *S. aureus* infections (Maya *et al*. 2012) and amoxicillin-entrapped chitosan/heparin NPs to eradicate *Helicobacter pylori* (Lin *et al*. 2013).

3.3 Other DDS

3.3.1 Dendrimers

Dendrimers are polymers with a well-defined monodispersed structure: a core, dendrons, and surface active groups (which determinate the biocompatibility and physicochemical or biological properties). Both hydrophobic and hydrophilic drugs may be entrapped in the internal structure of dendrimers or it can be chemically attached or physically adsorbed on their surface (Menjoge *et al*. 2010). Functionalization of the surface with specific antibodies may enhance potential targeting. The main mechanism of antimicrobial action is directly by destroying the cell membrane of bacterials or by disrupting multivalent binding interactions between the microorganism and host cell (Chen and Cooper 2002).

Dendrimers are normally synthesized from a central polyfunctional core by repetitive addition of monomers. The core is characterized by a number of functional groups. Addition of monomers to each functional group results into next dendrimer generation as well as expression of end groups for further reaction. The size of dendrimers increases as the generation number increases. Divergent and convergent methods are the most frequently used for dendrimer synthesis (Kesharwani *et al*. 2014).

The first family of dendrimers and the most frequently used in biomedical application is poly (amido amine) known as PANAM. They have gained much attention for drug delivery because of their nanosize, globular shape, multivalency, tunable inner cavities, and physicochemical properties (Kalhapure *et al*. 2013). PANAM dendrimers grow through generations from G1 to G10 and their sizes increases from 1.1 to 12.4 nm (Tomalia 2005).

Many researchers have used dendrimers to enhance the properties of antibiotics. These drug-loaded dendrimeric nanostructrures have been explored for improving drug solubility, antibacterial activity and achieving a sustained release *in vitro*. In an attempt to increase the poor aqueous solubility of quinolones, Cheng *et al.* (2007) investigated the

encapsulation of nadifloxaxin and prulifloxacin into PANAM dendrimers, resulting in an improvement in their aqueous solubility and similar bacterial activity as the free drugs. In a further study they prepared sulfamethoxazole dendrimers, finding a higher activity against *E. coli* than the free drug (Ma *et al*. 2007). Mishra *et al.* carried out a study with a macrolide antibiotic, azitromycin, with a G4-PAMAM dendrimer for the treatment of *Chlamydia trachomatis* infections using them as intracellular drug delivery vehicles and showing that the conjugate was significantly superior to the free drugs in the prevention of productive infections (Mishra *et al*. 2011).

Recently, Zhou *et al.* reported a synergistic effect of norfloxacin in combination with 3-hydroxypyridin-4-one (HPO) hexadentate-based dendrimeric chelator against Gram positive (*B. subtilis* and *S. aureus*) and Gram-negative (*E. coli and P. aeruginosa*) bacteria. It was postulated that the large molecular weight of the complex penetrate slowly through the membranes and with lower toxicity than the smaller ones (Zhou *et al*. 2014).

Little published data are available on the toxicity of this class of particles but it is known that the size and charge of higher-generation (G4-G8) PANAM dendrimers affects their citotoxicity (Shah *et al*. 2011) probably due to their high cationic charge density as proved when tested in Caco-2 cells (Kitchens *et al*. 2006).

3.3.2 Metallic nanoparticles

Apart from microbiological agents, many organic and inorganic nanomaterials (silver, tellurium, bismuth, copper, zinc, titanium, etc) have also demonstrated to possess potent antimicrobial properties making them attractive candidates to treat infectious diseases (Huh and Kwon 2011). The most used are silver (Ag) nanoparticles that are able to kill Gram positive and Gram negative bacteria and are effective against many drug-resistant-microbes as the metals nanoparticles have multiple mechanisms of action. Moreover, Ag NPs have shown to inhibit biofilm growth (Knetsch and Koole 2011).

Table 1. Summary of the main approaches used for the development of drug delivery systems containing antibiotic drugs. MIC, minimum inhibitory concentration; MBC, minimum bactericidal concentration; MRSA, methicillin-resistant *Staphylococcus aureus*; CFU, colony forming units; CF, cystic fibrosis; NP, nanoparticle.

Drug Delivery System (DDS)	Antibiotic	Bacteria tested	Main findings	References
Liposomes	Gentamicin	*Pseudomonas aeruginosa*	MICs of liposomal gentamicin for all clinical isolates of *P. aeruginosa* were lower than the MICs of free gentamicin. Liposomal gentamicin altered the susceptibilities of these clinical isolates from gentamicin resistant to either intermediate or susceptible	Mugabe et al. 2005
		Pseudomonas aeruginosa	MIC values significantly lower than free drug against gentamicin- sensitive and resistant strains. Improved killing time and prolonged antimicrobial activity	Rukholm et al. 2006
	Polymixin B	*Pseudomonas aeruginosa*	Improve antimicrobial activity. Prevent drug resistant of microbes by saturation of the efflux pumps.	Alipour et al. 2008
	Ciprofloxacin	*Pseudomonas aeruginosa, Haemophillus influenza, Streptococcus pneumoniae*	High antimicrobial activity	Chono et al. 2011
		Pseudomonas aeruginosa, Staphylococcus aureus	Same antimicrobial activity as the free drug. Lower MBC against *P. aeruginosa*	Ong et al. 2012
	Vancomycin	None	Increased lung tissue concentration of vancomycin for effective treatment of pneumonia caused by MRSA with a reduction of nephrotoxicity	Muppidi et al. 2011
	Rifampicin	*Mycobacterium bovis*	MIC values lower than the free drug. Less negatively charged liposome displayed the greatest activity against intracellular growth of *M. bovis*.	Changsan et al. 2009
		MAC (*Mycobacterium avium* complex)	Able to inhibit the growth of MAC in infected macrophages (J774 cells) and to reach the lower airways in rats.	Zaru et al. 2009
	Tobramycin	*Pseudomonas aeruginosa*	The MIC of bismuth–ethanedithiol-loaded tobramycin was 16-folf lower than free drug. Less CFU in the lungs of treated rats with the liposomal formulation compared to free drug and untreated animals	Alhariri et al 2013
Lipidic NPs	Meropenem	*Pseudomonas aeruginosa*	Enhancement of antibiotic activity None of the studied liposomal forms of meropenem	Drulis-

		Drug	Bacteria	Findings	Reference
Lipidic NPs				exhibited bactericidal activity against drug-resistant isolates strains.	Kawa et al. 2006
		Benzyl penicillin	Staphylococcus aureus	Lower drug concentrations and shorter time of exposure. Enhanced the inhibition of bacterial biofilms growth	Kim et al. 2004
		Clarithromycin	Pseudomonas aeruginosa	The highly resistant strains of *P. aeruginosa* isolated from CF patients became susceptible to liposome-encapsulated clarithromycin. Liposomal clarithromycin reduced the bacterial growth within the biofilm, significantly attenuated virulence factor production, and reduced bacterial twitching, swarming, and swimming motilities and were less cytotoxic than the free drug	Alhajlan et al. 2013
	Niosomes	Isoniazid	None	High cellular uptake by macrophages cells (J744) capable of achieving effective treatment of tuberculosis	Singh et al. 2011
		Pyrazinamide	*Mycobacterium tuberculosis*	Target maximum concentration of drug to the affected site (lungs) and able to exclude undesirable side effects and decrease toxicity	El-Ridy et al. 2011
		Ciprofloxacin	Staphylococcus aureus	Niosomes were 2-8 times lower than MICs of free drug. High intracellular antimicrobial activity	Akbari et al. 2013
		Ciprofloxacin	None	Sustained and prolong drug release	Jain et al 2008
	SLN	Tilmicosin	Staphylococcus aureus	Sustained drug release. Improved antibacterial activity *in vitro* and *in vivo*	Wang et al. 2012a
		Norfloxacin	Escherichia coli	Sustained drug release. Improved antibacterial activity *in vitro* and *in vivo*	Wang et al. 2012b
		Vancomycin	Staphylococcus aureus and MRSA strains	Lower MICs. Con-encapsulation an antibiotic and a fatty acid (linoleic acid) enhance encapsulation efficiency and antibacterial activity	Kalhapure et al. 2014
		Amikacin	Pseudomonas aeruginosa	Higer antimicrobial activity than the free drug taking into account the profile release over 6 days	Ghaffari et al. 2011
		Rifampicin, isoniazid and pyrazinamide	*Mycobacterium tuberculosis*	After pulmonary administration to tuberculosis-infected guinea pig no CFU in lung and spleen. No hepatotoxicity	Pandey et al 2005

	Material	Drug	Bacteria	Description	Reference
Polymeric NPs	NLC	Sodium colistimethate	*Pseudomonas aeruginosa*	More effective than free drug against clinically isolated strains from CF patients	*Pastor et al. 2014*
	PLGA-NP	Ciprofloxacin	*Pseudomonas aeruginosa, Staphylococcus aureus*	Prolonged drug release. The same activity as free drug	*Dillen et al. 2004, Dillen et al. 2006*
		Ciprofloxacin	*Escherichia coli*	Superior effectiveness to inhibit the growth of bacteria *in vivo* than the free drug due to the sustained release of the NPs	*Jeong et al. 2008*
		Azithromycin, rifampicin	*Chlamydia trachomatis*	Enhanced effectiveness of the antibiotic in microbial burden by intracellular targeting	*Toti et al. 2011*
		Levofloxacin and ciprofloxacin	*Escherichia coli*	Biofilm inhibition activity	*Cheow et al 2010a; Cheow et al 2010b*
	PLGA, PVA, chitosan and alginate	Tobramycin	*Pseudomonas aeruginosa*	Good *in vitro* antibacterial activity of NP formulations according to the biphasic release profile	*Ungaro et al. 2012*
	O-carboxymethyl chitosan	Tetracycline	*Staphylococcus aureus*	Sustained release, improved bioavailability and intracellar targeting	*Maya et al. 2012*
	Chitosan and herparin	Amoxicillin	*Helicobacter pylori*	A multifunctional NP system for targeting *H. pylori*, clearance effect and decrease gastric inflamation	*Lin et al. 2013*
Dendrimers		Nadifloxacin and prulifloxacin	*Escherichia coli*	Improved solubility without affecting antibacterial activity	*Cheng et al. 2007*
	PANAM	Sulfamethoxazole	*Escherichia coli*	Increased antibacterial activity via enhanced penetration of antibiotics through the bacteria membrane	*Ma et al. 2007*
		Azithromycin	*Chlamydia trachomatis*	The conjugations with the drug was efficient to treat intracellular infections	*Mishra et al. 2011*
	HPO hexadentate-based dendrimeric quelator	Norfloxacin	*Bacillus subtilis, Staphylococcus aureus, Escherichia coli, Pseudomonas aeruginosa*	Synergistic bactericidal effect	*Zhou et al. 2014*

Recent efforts have attempted to couple gold (Au) nanoparticles with a variety of antibiotics (e.g., ciprofloxacin, vancomycin, gentamicin etc.) against all types of microorganism (Burygin *et al.* 2009). For example, chitosan-capped Au coupled with ampicillin displayed 2-fold increase in antimicrobial activity compared to free drug. The antimicrobial activity of Au NPs seems to be mediated by strong electrostatic attractions to the negatively charge bilayer of the cell membrane (Chamundeeswari *et al*. 2010).

An important advantage of using these types of metal nanoparticles as antimicrobial agents is that they have anti-biofilm activity as the same time it is difficult for microbes to develop resistant to them, however, their limited applications is partially due to safety concerns (Zhu *et al*. 2014).

4. Approaches of antibiotic nanoencapsulation classified according to their administration route

In this part of the chapter, different nanoparticle approaches will be reviewed classified by the administration route intended for its use. More precisely, the ocular, topical, pulmonary, oral and systemic routes will be addressed.

Once administered, antibiotics should overcome the barriers that some tissues represent. These barriers might be the ocular barrier, the gastrointestinal, or the respiratory tissue, for instance. This issue could be addressed by antibiotic encapsulation that in one hand could enhance barriers trespassing and on the other hand protects the antibiotic from different inactivation processes. In addition, nanoparticles might also improve the mucoadhesion and enhance the penetration across the extra cellular matrix that in turns might allow the penetration of the particle into the infected tissue and permit a sustained drug release in the target site (Alonso 2004; Xiong *et al*. 2014).

4.1. Ocular administration

The first administration route that will be addressed herein is the ocular administration. Drug delivery to the eye is still nowadays a great challenge. The main advantage of this administration route is the feasibility of achieving a local effect avoiding systemic exposure to the drug. However, drugs display low bioavailability after ocular administration due to rapid drain out by blinking, tear turn-over, liquid drainage, tear evaporation and systemic absorption that in turns results in less than 5% of the drug penetrating the ocular parenchyma (Hon-Leung and Robinson 1979; Xiong *et al*. 2014).

In order to overcome such limitations tailored nanoparticles represent an alternative drug delivery system. In this regard, the utility of tobramycin loaded SLNs for ocular application was firstly reported by Cavalli and colleagues. The nanoparticles elaborated displayed a 100 nm size and 2.5% drug load of tobramycin as an ion-pair complex with hexadecyl phosphate. Firstly, the eye disposition was studied using fluorescently labelled nanoparticles without drug and compared to fluorescent dye solution. From this study it could be confirmed that the SLNs presented a prolonged residence time on the corneal surface and in the conjunctival sac. In a further experiment, tobramycin-loaded SLN were administered to rabbits and the drug level in aqueous humour was quantified for 6h. It was verified that SLNs were able to improve the bioavailability of tobramycin (Cavalli *et al*. 2002).

Another example of SLNs for ocular administration was reported by Abul Kalam *et al.* In this research article the authors developed gatifloxacin-loaded SLNs following an o/w emulsion method and using two different lipid mixtures, stearic acid and Compritol® (SLN-C) or stearic acid and Gelucire® (SLN-D), both at a 4:1 proportion. Besides, the addition of stearylamine led to positively charged nanoparticles. The optimized lipid nanoparticles presented a 250-305 nm size and a positively charged zeta potential, i.e. ≈29-36 mV. SLN-C displayed higher EE values than SLN-D, 79% vs. 47%. The authors postulate that

Compritol® together with stearic acid might form less perfect crystals, compared to Gelucire®, allowing the drug to incorporate within the spaces of the crystals leading to higher encapsulation efficiency. Moreover, the drug released from both SLN-C and SLN-D showed a slower drug release profile compared to the commercially available one, i.e., SLNs released 60-80% of the drug in 12h, whereas the commercial eye drop liberated the 80% within the first two hours (Abul Kalam *et al*. 2013a,b). In a following article the authors compared eye drops based on the gatifloxacin-loaded SLN-C and SLN-D and the commercial eye drop Gate® formulation. The aim of the study was to test whether the SLNs were able to improve the residence time in the eye, enhance bioavailability and decrease ocular irritation. To cope with this, the authors performed a Draize test to measure potential irritation in eyes and precorneal retention of ^{99m}Tc-radiolabeled SLNs. In addition, an *ex vivo* goat permeability model was also carried out using gatifloxacin-loaded SLNs. This first *ex vivo* experiment showed that SLNs, as well as eye drops, were capable of maintaining corneal hydration at almost 80%, meaning that the formulations did not exert eye damage. Furthermore, the corneal permeation profiles showed that the SLNs were able to provide a more sustained release of the drug. Moreover, the SLN-C displayed a slower release profile than SLN-D. In the following *in vivo* rabbit experiments, no sign of discomfort was detected, both at long-term and acute studies. Likewise, for cornea, conjunctiva and eyelids no irritation was detected, grade 0. After a repeated administration, the SLN group showed a slight mucoid discharge (grade 1), very likely related to the aggregation of the nanoparticles. Overall, this study suggests that SLNs represent a relatively safe drug delivery system for ocular administration. In the subsequent gamma scintigraphy studies, it was observed that 20 minutes after administration the SLNs presented an increased activity in the preocular area compared to the marketed eye drops. Nanoparticles might display an extended preocular residence time due to their positive charges that could interact with the negatively charged mucin layer of the corneal surface. Ocular pharmacokinetic studies were performed by analysing

the drug content by high-performance liquid chromatography (HPLC) at the aqueous humour, confirming that the SLNs were able to increase the relative bioavailability of drug 3.37-fold. In addition, the increase in drug half-life when encapsulated was 2.34-fold (Figure 6). Altogether, these assays suggest that gatifloxacin incorporated in solid lipid nanoparticles leads to a significant improvement of the ocular bioavailability and residence time into the eye (Abul Kalam *et al*. 2013a,b).
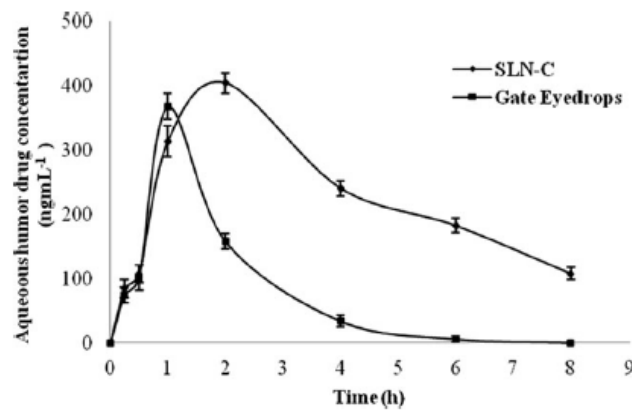
Figure 6. Aqueous humour concentration–time profile of gatifloxacin after topical instillation of SLN-C and Gate® Eyedrops to rabbit eyes (n = 3, ±SD) up to 8-h study period. The ocular bioavailability and relative bioavailability of GAT were significantly increased with the SLN-C as compared to Gate® Eyedrops formulation. Reuse with permission Abul Kalam *et al*. 2013.

A ciprofloxacin encapsulation approach was described by Garhwal and colleagues. In this occasion the authors chose pullulan and poli-ε-caprolactone as core polymer for the nanoparticles, embedding them after their preparation in hydrogel-based contact lens. Nanoparticles showed 142 ± 12 nm particle sizes and displayed a sustained release profile. Next, two different contact lens were elaborated, both using (hydroxyethylmethacrylate) HEMA polymer, one presenting a thin thickness (30 ± 4 mg) and the other displaying a thicker (≈60 mg) composition. These lenses incorporated the nanoencapsulated ciprofloxacin in the matrix as nanoparticles were added during the preparation process. The resulting lenses were clear and presented a prolonged drug release over 15 day. The

microbiological assays revealed that both types of lenses were able to prevent *Pseudomonas aeruginosa* and *Staphylococcus aureus* growth, whereas the control group presented a log-phase growth within the first 2h of incubation. In addition, when the culture media was replaced with fresh bacterial broth, the lenses inhibited their growth for other 24h. When testing the thin lens against higher *S. aureus* inoculums, 10^9 CFU/mL, these lenses were able to prevent bacterial growth during 48h, but failed to avoid proliferation for the third day. Yet, thicker lenses, which contained higher amount of nanoencapsulated ciprofloxacin, were able to inhibit microbe growth for three days. Therefore, the authors postulated that the thin lenses could be appropriate for the treatment of milder infection, counting 10^6 bacterial, whereas the thicker lenses could be useful for more severe infections such as corneal bacterial ulcers (Garhwal *et al*. 2012).

Levofloxacin nanoencapsulation has also gained much attention. For example, Gupta *et al*. described levofloxacin-loaded poly-L-lactic-co-glycolic acid (PLGA) nanoparticles as a successful approach for ocular administration. They described 190-195 nm size nanoparticles showing -25 mV zeta potential and 85% of encapsulation efficiency. Nanoparticles were able to release the drug content during 24h after an initial burst phase. Antimicrobial test showed that levofloxacin-PLGA nanoparticles displayed a similar inhibition area compared to the commercially available eye drops. The subsequent animal experiments revealed that nanoparticles displayed an appropriate spread and retention in the precorneal area. In addition, authors performed the HET-CAM test (Hen's Egg Test Chorioallantoic Membrane) in order to assess the potential irritancy of the formulation for the mucous-membrane. Test score was 0.33 meaning that no irritancy was detected (Gupta *et al*. 2011). In a following study by the same group, the previously described levofloxacin-PLGA nanoparticles were embedded in an *in situ* forming chitosan gel in order to enhance the disposition of the formulation in the eye. This new formulation was also studied by γ-scintigraphy in rabbits and revealed that chitosan gels containing levofloxacion-PLGA nanoparticles presented good spread and retention properties in the

precorneal area. Besides, the formulation clearance was slowed down by gel embedding and showed longer permanency compared to the commercial eye drops, labelled nanoparticles alone and labelled chitosan gel (Gupta *et al*. 2013).

4.2. Topical administration

Nanoencapsulation has also been reported as a successful approach for the antimicrobial activity in the skin. In this regard, in the following part of this chapter, the latest nanoparticles as antibacterial and antifungal carriers for topical administration will be highlighted.

Sanchez *et al*. (2014) reported a very interesting work on amphotericin B encapsulation to fight against *Candida spp* in burn wounds. Pursuing this goal, polyethylene glycol and chitosan were selected for the preparation of the hydrogel/glassy composite ranging 91.3–101.9 nm in size. The drug was released in a sustained manner and the released amount of the drug was tested by means of MIC determination and confirmed 99% of antifungal activity. Besides, the anti-proliferative effect of nanoparticulated amphotericin B was tested by XTT (2,3-bis-(2-methoxy-4-nitro-5-sulfophenyl)-2H-tetrazolium-5-carboxanilide) cell viability assay against *C. albicans* SC5314. It was observed that after 4h incubation 95.9% of growth was inhibited and 82% post-24h. There were no differences between the amphotericin B solution and the nanoencapsulated drug, suggesting that the released drug was active. In a further experiment, clinical strains of non-albicans *Candida* were assessed and it was shown that the growth inhibition of the nanoparticles was 72.4-98.3% after 4 hour incubation. On the contrary, amphotericin B solution was not able to reach those inhibition levels, *P*>0.01. Nanoparticles were also tested against biofilm bearing fungi and it was observed that amphotericin B-loaded nanoparticles were capable of reducing the metabolic activity of the fungi at 80-95% level. Moreover, when tested in mature biofilms, nanoencapsulated

amphoterin B showed enhanced inhibitory results compared to amphoterin B in solution (*P*<0.05). It is worth it to mentioning that when *C parapsilosis* strain #75 was tested these differences were only remarkable at lower concentrations (Figure 7).
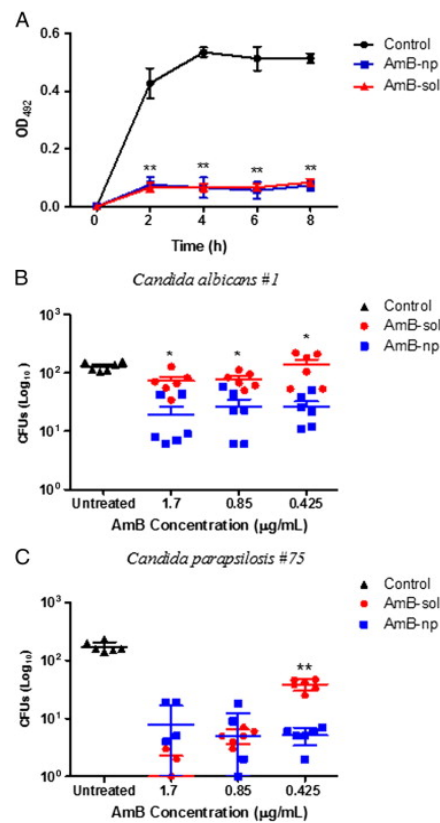
Figure 7. Amphotericin B-nanoparticle inhibits biofilm formation and reduces mature biofilm viability. A) *C. albicans* biofilm development after being subjected to Amphotericin B-nanoparticle, Amphotericin B-solution, and no treatment. Outlined statistical differences comparing amphotericin B solution and nanoparticles to control. B and C) Clinical strains of *C. albicans* (Ca#1) and *C.parapsilosis* (Cp#75) produced mature biofilms after 48h. Subsequent to Amphotericin B-nanoparticles, drug solution, or PBS application, samples were plated for CFU tabulations.* denotes *P*-value significance (*P< 0.05, **P< 0.001) calculated by two-way ANOVA statistical analysis. Both experiments were performed twice and similar results were obtained. OD, optical density. Reused with permission, Sanchez *et al*. 2014.

In a following step nanoparticles were tested in a murine infected burn wound model, where nanoparticulated amphotericin B showed improved anti-fungal effectiveness compared to amphotericin B solution at day 3, meaning that the nanoparticles were able to speed up the drug effect resulting in a lower CFU account. On the following days, amphotericin B solution and nanoparticles presented no statistically significant differences. However, as the histological studies revealed, the group treated with nanoparticles displayed a more advanced re-epithelialisation, organized dermal proliferation and appropriate dermal remodelling. Hence, it might be postulated that a faster *Candida* reduction plays a role in a proper healing process, although it did not accelerate the wound closure. This work underlined three important points of the usefulness of nanoparticles, i) that encapsulation did not affect the drug activity, ii) that nanoparticles were active against plantonik and biofilm *Candida*, and iii) that nanoparticles exerted *in vivo* activity. Altogether, amphotericin B nanoparticles seem a feasible alternative to the oral administration of amphotericin B in burn wounds avoiding systemic exposure and side effects of the orally administered drug (Sanchez *et al*. 2014).

Another approach against burn wound infection was reported by Krausz *et al*. (2015), but in this work methicillin-resistant *Staphylococcus aureus,* MRSA, and *Pseudomonas aeruginosa* were the pathogenic targets. For that purpose, curcumin was selected as nanoencapsulation candidate due to its antimicrobial, anti-inflammatory and antioxidant effect. Besides, nanoencapsulation could improve some of the drawbacks that curcumin presents, such as low oral bioavailability, poor aqueous solubility and rapid degradation. Chitosan, polyethylene glycol 4000 and tetramethyl orthosilicate were chosen as core polymers resulting in 222 ± 14 nm nanoparticles showing a sustained release profile of 81.5% of the drug in 24h. The cytotoxicity of nanoparticles was tested in cell cultures of PAM212 keratinocytes and by the embryonic zebrafish assay. Both studies confirmed the safety of the formulation as no toxic effect was detected compared to the controls. The *in vitro* bioactivity assay against MRSA and *P. aeruginosa* showed that nanoparticles were

able to inhibit their growth from the 8th hour onwards. When tested against 10[7] CFU/mL inoculums, the nanoparticles were able to inhibit bacterial growth in 97% and 59.2% for MRSA and *P. aeruginosa*, respectively. In order to get insight into the cell-nanoparticle relationship, 5 mg/mL of nanoparticles with and without curcumin were added to the bacterial strain and observed over time under transmission electron microscopy, TEM (Figure 8). Unloaded nanoparticles (with no curcumin) interacted with bacteria, but there were no observable changes in the cell (Figure 8B). Whereas, when adding curcumin-loaded nanoparticles (Figure 8C and D), after 6h-incubation the cell displayed a modified shape and oedema and lysis was undertaken by the 24th hour.
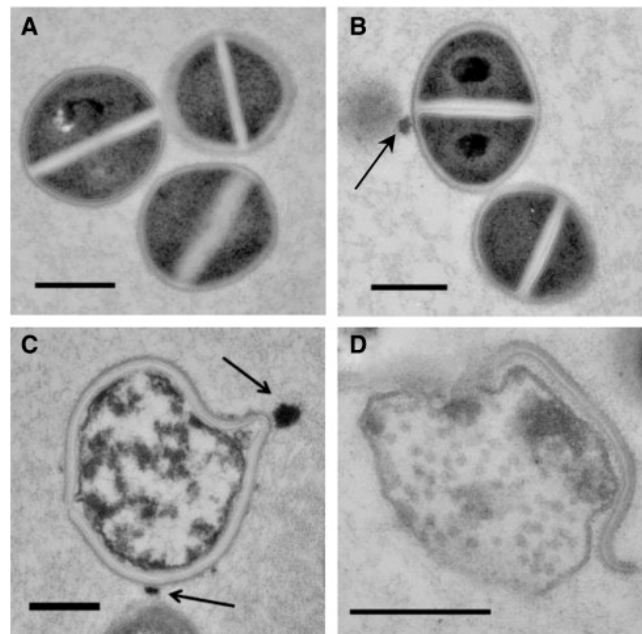
Figure 8. Curcumin-nanoparticles induce cellular damage of MRSA. High-power TEM demonstrated interaction of nanoparticles (arrows) with MRSA cells. A) Untreated MRSA showed uniform cytoplasmic density and central cross wall surrounding a highly contrasting splitting system. B) After 24 hours, cells incubated with control nanoparticles at 5 mg/mL did not exhibit changes in cellular morphology compared to untreated control. C) After 6 hours, cells incubated with Curcumin-nanoparticles at 5 mg/mL exhibited distortion of cellular architecture and oedema, followed by lysis and extrusion of cytoplasmic contents after 24 hours (D). All scale bars = 500 nm. With permission from Krausz *et al*. 2015.

Next, the efficacy of the nanoparticles was assessed in an *in vivo* murine MRSA infected burn wound model. It was observed that on days 3 and 7, curcumin-loaded nanoparticle treated groups presented a lower CFU account. In addition, it was observed that curcumin-loaded nanoparticles were able to accelerate the healing process and to enhance re-epithelisation and granulation processes leading to a more mature epidermis/dermis compared to the control groups (Krausz *et al*. 2015).

4.3. Pulmonary administration of antimicrobial-loaded nano-carriers

Approaching the lung from an inhalatory point of view is very interesting as an anti-infective strategy due to the possibility of targeting lung infections in a direct manner, avoiding plasmatic high drug concentrations. In this regard, one successful example, approved by the FDA, has been already reported, which is tobramycin encapsulation by Pulmosphere™ technology that gives rise to a dry powder of porous microparticles (Geller *et al*. 2011). The success of these microparticles has encouraged many other groups to keep on working on other drug delivery systems, such as liposomes, for the administration of different antibiotics, i.e., amikacin and ciprofloxacin.

Liposomal amikacin consisting of DPPC and cholesterol is also known as Arikace™. These liposomes display ≈300 nm in size and after nebulization they are able to penetrate sputum in cystic fibrosis, as fluorescently labelled liposomes has revealed. Besides, these liposomes have shown to release amikacin in a sustained manner even in a *P. aeruginosa* environment. Furthermore, *in vivo* studies in rats revealed that the liposomes increased drug concentrations in the lungs compared to the free drug. In addition, when rats were infected using a mucoid strain of *Pseudomonas* (PA3064) embedded in agarose beads, and treated with 6 mg/kg three times a week with free amikacin, no CFU decrease was observed, whereas liposomal amikacin reduced bacterial account in two orders of magnitude. In a next study, a single administration of liposomal amikacin was tested

against tobramycin twice daily. It was confirmed that liposomal amikacin was as effective as free tobramycin administered twice a day. Remarkably, it was also observed that amikacin liposomes administered every other day displayed similar results to tobramycin twice daily (Meers *et al*. 2008).

In a further study, Weers *et al*. administered radiolabelled Arikace™ to healthy volunteers, determining that the lung deposition was around 32% of the emitted dose and that 24 h after administration the retention percentage was 60.4%, decreasing to 38.3% after 48 h. Furthermore, no adverse effects such as cough or bronchospasm were observed (Weers *et al*. 2009).

A phase II clinical trial was carried out in order to evaluate short term, 28-day, once daily Arikace™ safety, tolerability, and effectiveness against chronically *P. aeruginosa* colonised cystic fibrosis patients. The design of this clinical trial was set as a randomized, double-blind, placebo-controlled, multiple-dose, multicentre trial including 105 patients. Four doses were tested, i.e., 70 mg, 140 mg, 280 mg, and 560 mg against placebo. The adverse effects were similar for the placebo and treated groups, e.g. 20% for 560 mg Arikace™ and 22% for the placebo group. Lung function, studied by spirometry, presented an improvement only with the two high doses. In fact, the 560 mg Arikace™ group showed an enhanced lung function that was maintained until day 56, i.e., 28 days after the last dose. The microbiological results showed that especially the highest dose rapidly reduced the bacterial density in the sputum of patients (Clancy *et al*. 2013). In order to gain insight into a longer treatment period with cycles of 28 days on treatment followed by 28 days off treatment, a Phase III trial is currently being conducted with CF patients colonized by *P. aeruginosa* in Europe, Australia, and Canada (2011-000441-20). The goal of this trial is to study whether Arikace™ treated groups show an improvement in lung function and a reduction in *P. aeruginosa* counts compared to TOBI®. After the analysis of some preliminary results, the authors deduced that liposomal amikacin was effective and safe and its effectiveness was not reduced after three cycles of 28 days on and 28 days off

treatment. A single daily dose of liposomal amikacin showed better results that TOBI® twice daily, especially in terms of the respiratory symptoms (Bilton *et al*. 2013; Ehsan *et al*. 2014).

Altogether, Arikace™ seems to be close to be released on the market in the EU and US. Hence, the efforts that Insmed Inc. (Monmouth Junction, NJ) has made are about to be a successful approach of a lab-scale to clinical framework of a drug delivery system that could be defined as a milestone for the application of nanotechnology for infectious treatments.

Another successful example, which also reached clinical trial, is illustrated by Lipoquin® and Pulmoquin® from Aradigm Corporation (Hayward, CA). Lipoquin® is based on ciprofloxacin hydrochloride liposomes, which presents a 90 nm size and has already shown to be safe, capable of reducing *P. aeruginosa* CFU account and improving lung function in a Phase II clinical trial.

On the other hand, Pulmoquin® is composed of free ciprofloxacin and liposomal ciprofloxacin at a 1:1 volume ratio. Pulmoquin® is prepared using hydrogenated soybean phosphatidylcholine and cholesterol. Pulmoquin® underwent phase II B clinical trial, termed ORBIT-1, aiming at non-cystic fibrosis bronchiectasis patients. The study was designed as randomized, double-blind, placebo-controlled (empty liposomes) and focused on safety, tolerability and efficacy of either 150 or 300 mg of Lipoquin®. Liposomes were administered once daily either 300 or 150 mg dose with a 28-day treatment phase and a 28-day off stage with a follow-up period. It was observed that ciprofloxacin was safe and well-tolerated for both doses. Lung function presented no changes and adverse effects were mild to moderate and detected in two patients in the placebo group and two patients in the treatment group (Bilton *et al*. 2011). Similarly, Pulmaquin® was studied in another Phase II-B clinical trial, ORBIT 2, designed as a randomized, double blind, placebo controlled trial aiming at the non-cystic fibrosis bronchiectasis population suffering from

P. aeruginosa infection. For this trial, the 210 mg dose was selected and three cycles were fixed, consisting of 28 days of treatment and 28 days off. Besides, Lipoquin® patients presented a low incidence of adverse effects and the formulation was overall well-tolerated (Serisier *et al*. 2013). Pulmaquin® is currently ongoing another evaluation in a Phase III clinical trial (ARD-3150-1201, ORBIT-3).

4.4. Oral route

Nanotechnology has been also applied for drug administration by the oral route, as it protects the drug from the acidic environment in the stomach and from enzymatic degradation throughout the gut. In addition, the nano-carriers themselves may also improve drug absorption (He *et al*. 2012).

A pioneering work was first reported by Cavalli and colleagues when tobramycin was encapsulated into SLNs in order to study its pharmacokinetic profile. SLNs showed an 85 ± 5 nm size, a negative zeta potential of around -20 mV and 2.5% of drug loading. These nanoparticles were administered intra-duodenally or intra-venously to rats and compared to a tobramycin solution i.v. administered. Firstly, it was observed that i.v.-administered SLNs were able to increase the AUC (area under the curve) of the drug 4.85-fold compared to the free drug. More interestingly, when tobramycin-loaded SLNs were administered intra-duodenally the AUC was increased 25-fold in comparison to the i.v.-administered tobramycin-SLN and this increase was 120-fold in contrast to the free tobramycin solution. Turning to the maximum drug concentration in plasma, i.v. SLNs showed the highest value, followed by the intra-duodenally administered SLNs. The authors postulated that these differences among intra-duodenal and i.v. routes were related to the transmucosal transport of the SLNs mainly to the lymphatic system instead of to the bloodstream (Cavalli *et al*. 2000). In a following study, Bargoni *et al* analysed the tissue distribution of tobramycin after i.v. administration and tobramycin-loaded SLN after i.v. and intra-

duodenal administration. They observed that the clearance of nanoparticulated tobramycin was 10-fold slower than the clearance of the tobramycin solution. In addition, it was also determined that the intra-duodenal administration led to a lower kidney concentration of the drug compared to the i.v. administration of both, tobramycin solution and tobramycin-SLNs. It is also worth mentioning that 24h after the administration, intra-duodenally administered SLNs displayed the highest lung concentration. This finding could be very useful for the therapy of cystic fibrosis. Finally, it was also remarkable that SLNs were able to cross the blood-brain-barrier, especially when administered intravenously. The authors hypothesized that the SLNs may aid masking the drug and improving its passive transport by protecting the drug from the e-flux pump or other type of mechanisms that may avoid drug absorption or passage. Altogether, they demonstrated that intra-duodenally administered SLNs were efficiently absorbed and the pharmacokinetic profile was improved, presenting extended AUC and half-life ($t_{½}$) (Bargoni *et al*. 2001).

The oral route is also the most appropriate approach for *Helicobacter pylori* eradication. Lin and co-workers explored the use of a chitosan/heparin nanoemulsion as an amoxicillin carrier candidate. The nanoemulsion prepared showed ≈300 nm particle size, positive zeta potential around 30 mV, and a 54.3% encapsulation efficiency that gave rise to 19.2% drug loading and a sustained drug release. Moreover, the particles were found to be stable at pH 1.2-6. Besides, confocal microscopy confirmed that the particles were able to interact with the bacteria. In order to assess nanoemulsion efficiency, mice were infected with 10^9 CFU/mL of *H. pylori* once daily for 7 consecutive days and treated for another 7 days with deionized water, amoxicillin solution or amoxicillin bearing nanoemulsion. It was determined that non-treated animals presented the highest *H. pylori* CFU account per stomach, 137.3, followed by animals treated with amoxicillin solution, 45.2, whereas nanoemulsionated amoxicillin showed lower CFU account, 11.3. Altogether this work represents a new strategy to fight against *H. pylori* infection (Lin *et al*. 2012).

4.5. Systemic route

Sande and co-workers reported liposomal vancomycin encapsulation to fight against methicillin-resistant *Staphylococcus aureus* (MRSA). Two different liposomal formulations were designed, DCP liposomes composed of DSPC, DCP and cholesterol and DMPG liposomes composed of DPC, DMPG and cholesterol. Both displayed ≈530 nm in size and showing 9% and 20% of encapsulation efficiency for DCP and DMPG liposomes, respectively. Both formulations were able to decrease MIC values 2- to 4-fold compared to free vancomycin against different hospital associated-MRSA. DCP liposome showed the most promising results, so these were further characterized by time-kill assays. Three different concentrations were assessed, 0.3, 0.6 and 1.25 mg/L against NRS-35, a hospital-associated MRSA (HA-MRSA) strain from NARSA; and LAC a CA-MRSA strain of the pulsotype USA300. The results revealed that after 3 h incubation all the three concentrations were active against LAC. Likewise, liposomes at 1.25 mg/L concentration were more effective than the free drug in killing NRS-35 at the 3rd and 6th hours. The animal studies using LAC infected mice showed that liposomal vancomycin was able to reduce 2-3 log the bacterial CFU in spleen and kidneys compared to the PBS control. Yet, when comparing with the free drug, the liposomes presented a 1-log reduction in the bacterial account for the kidney but spleen CFU fail to present statistically significant differences (Sande *et al.* 2012).

Van de Ven and colleagues designed PLGA nanoparticles and nanosuspensions to encapsulate amphotericin B by nanoprecipitation. The particles presented an 86-153 nm size and where freeze dried using 5% mannitol cryo-preservative. All the formulations displayed a negative zeta potential, with EE ranging from 54 to 63%. Nanoparticles showed an increased activity against intracellular *L. infantum* amastigotes compared to the free drug, IC$_{50}$ 0.03 vs. 0.16 µg/mL, respectively. When testing the formulations against *C albicans*, it was also observed that the nanoparticles (IC50, 0.04 ± 0.01 µg/mL) were 10 times more active against the fungal strain than the commercially available

formulations, Fungizone® or AmBisome®, (IC50, 0.34 ± 0.12 μg/mL and 0.40 ± 0.09 μg/mL). The nanoformulations also revealed to be less cytotoxic. The nanoparticles were next assessed against an *Aspergillus fumigatus* infection model and compared to Fungizone® or AmBisome® at the same dosing schedule. Amphotericin B loaded nanoparticles and nanosuspension were more active than Fungizone® (Figure 9).
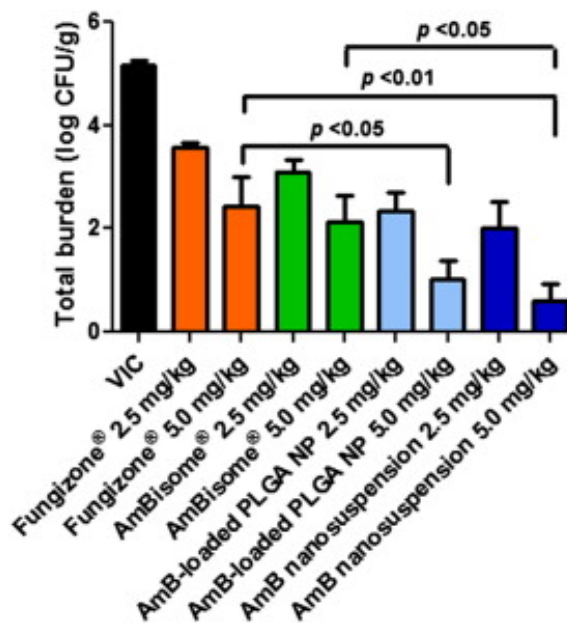
Figure 9. Total burden (liver, kidneys and spleen) of mice infected with *A. fumigatus* and treated with either 5.0% (w/v) mannitol (Vehicle-treated infected-control group, VIC, sacrificed at day 4 post-infection) or the various amphotericin B nanoformulations at 2.5 or 5.0 mg/kg (sacrificed at day 10 post-infection) (data represented as mean ± sem; n = 4 for VIC and n = 5 minimum for the different treatment groups). Significant differences between groups are indicated; in addition, all treatment groups were significantly (p ≤ 0.001) different from VIC (except p < 0.01 for Fungizone® 2.5 mg/kg vs. VIC), Fungizone® 2.5 mg/kg significantly (p < 0.05) different from amphotericin B-loaded PLGA nanoparticle 2.5 mg/kg, Fungizone® 2.5 mg/kg significantly (p < 0.01) different from amphotericin B nanosuspension 2.5 mg/kg. The percentage of reduction of fungal burden (compared to mannitol) amounted to 99.4% for treatment with Fungizone® 5.0 mg/kg and 99.8% for treatment with AmBisome® 5.0 mg/kg. With permission, Van de Ven *et al*. 2011.

Indeed, the nanosuspension was more effective against fungi than PLGA nanoparticles. These experiments underlined that the nanosuspension was the most efficacious of all formulations and that it could allow a dose reduction from 5 mg/kg to 2.5 mg/kg maintaining the same therapeutic efficacy than the free drug (Van de Ven *et al*. 2011).

5. Conclusions and future perspectives

Over the last years, the pharmaceutical industry has decreased its efforts to develop new antibiotics, mainly due to the low potential returns of this therapeutic group and to the different interests in the development of other drugs. As a consequence, it seems that breakthrough innovations are needed to effectively manage microbial infections. In this regard, the application of nanotechnologies to medicine seems as an interesting tool, with over 100 nanomedicine products being approved for clinical use, and 10 nanoparticulate formulations being already marketed.

The application of nanomedicines in antimicrobial therapy aims at combating resistance to antibiotics and reducing the appearance of adverse effects. In addition, they show promise especially in the treatment of chronic infections as they may inhibit biofilm formation and may also target intracellular microorganisms. Moreover, the delivery of antimicrobial agents could improve considerably the current therapy of infectious diseases, as they could decrease the systemic toxic effects of antibiotics, increase uptake and decrease the efflux of drugs, act on biofilm formation and be more effective in intracellular bacterial infections.

Besides that, DDS are quite versatile as allow the targeting to the infection site by the use of ligands, may improve the solubility of hydrophobic drugs, prolong drug systemic circulation and allow a sustained release of the drug, which leads to a reduction in the frequency of administration.

This review covers a range of diverse drug delivery systems in the submicron range such as liposomes, polymeric nanoparticles, solid lipid nanoparticles or dendrimers that have been investigated *in vitro* for antibiotic delivery with successful results together with some *in vivo* studies confirming the enhanced activity against sensitive and resistant bacteria.

Taking into account the studies revised in this chapter, antimicrobial nanomedicine has a potential impact, although their clinical development still faces important challenges. The first one is the availability of biomaterials and the regulatory requirements that they have to meet before entering the market, especially in terms of biocompatibility and long-term safety. Another major concern is the scalability of the processes used in the preparation of DDS. They should allow a feasible translation into industry-scale manufacturing providing appropriate reproducibility.

References

Abul Kalam M, Sultana Y, Ali A *et al* (2013a) Part I: Development and optimization of solid-lipid nanoparticles using Box-Behnken statistical design for ocular delivery of gatifloxacin. J Biomed Mater Res A 101 (6): 1813-27.

Abul Kalam M, Sultana Y, Ali A *et al* (2013b) Part II: Enhancement of transcorneal delivery of gatifloxacin by solid lipid nanoparticles in comparison to commercial aqueous eye drops. J Biomed Mater Res A. 101 (6): 1828-36.

Ai J, Biazar E, Jafarpour M *et al* (2011) Nanotoxicology and nanoparticle safety in biomedical designs. Int J Nanomedicine 6: 1117-1127.

Akbari V, Abedi D, Pardakhty A *et al* (2013) Ciprofloxacin nano-niosomes for targeting intracellular infections: an *in vitro* evaluation. J. Nanoparticle Res 15 (4): 1-14.

Akbarzadeh A, Rezaei-Sadabady R, Davaran S *et al* (2013) Liposome: classification, preparation, and applications. Nanoscale Res Lett 8 (1): 102.

Alhajlan M, Alhariri M, Omri A. (2013) Efficacy and safety of liposomal clarithromycin and its effect on *Pseudomonas aeruginosa* virulence factors. Antimicrob Agents Chemother 57 (6): 2694-2704.

Alhariri M, Azghani A, Omri A (2013) Liposomal antibiotics for the treatment of infectious diseases. Expert Opin Drug Deliv 10 (11):1515-1532.

Alipour M, Halwani M, Omri A *et al* (2008) Antimicrobial effectiveness of liposomal polymyxin B against resistant Gram-negative bacterial strains. Int J Pharm 355 (1–2): 293-298.

Allen TM, Hansen C, Rutledge J (1989) Liposomes with prolonged circulation times: factors affecting uptake by reticuloendothelial and other tissues. BBA-Biomembranes 981 (1): 27-35.

Alonso MJ (2004) Nanomedicines for overcoming biological barriers. Biomed Pharmacother 58(3): 168-172.

Bargoni A, Cavalli R, Zara GP *et al* (2001) Transmucosal transport of tobramycin incorporated in SLN after duodenal administration to rats. Part II- Tissue distribution. Pharmacol Res 43 (5): 497-502.

Barratt G (2003) Colloidal drug carriers: achievements and perspectives. Cell Mol Life Sci 60 (1): 21-37.

Bilton D, Pressler T, Falac I *et al* (2013) Phase 3 efficacy and safety data from randomized, multicenter study of liposomal amikacin for inhalation (Arikace®) compared with TOBI® in cystic fibrosis patients with chronic infection due to *Pseudomonas aeruginosa*. In: Abstracts of North America Cystic Fibrosis Conference, Sant Lake, UT. 2013; Poster 235. Cystic Fibrosis Foundation, Bethesda, MD, USA.

Bilton D, Serisier DJ, De Soyza AT *et al* (2011) Multicenter, randomized, double-blind, placebo-controlled study (ORBIT 1) to evaluate the efficacy, safety, and tolerability of once daily ciprofloxacin for inhalation in the management of *Pseudomonas aeruginosa* infections in patients with non-cystic fibrosis bronchiectasis. Eur Respiratory J 38 (Suppl 55): 1925.

Briones E, Colino CI, Lanao JM (2008) Delivery systems to increase the selectivity of antibiotics in phagocytic cells. J Control Release 125 (3): 210-227.

Brooks BD, Brooks AE (2014) Therapeutic strategies to combat antibiotic resistance. Adv Drug Deliv Rev 78: 14-27.

Burygin G, Khlebtsov B, Shantrokha A *et al* (2009) On the enhanced antibacterial activity of antibiotics mixed with gold nanoparticles. Nanoscale Res Lett 4 (8): 794-801.

Cavalli R, Gasco RM, Chetoni P *et al* (2002) Solid lipid nanoparticles (SLN) as ocular delivery system for tobramycin. Int J Pharm 238 (1-2): 241-245.

Cavalli R, Zara GP, Caputo O *et al* (2000) Transmucosal transport of tobramycin incorporated in SLN after duodenal administration to rats. Part I—A pharmacokinetic study. Pharmacol Res 42 (6): 541-545.

Chamundeeswari M, Sobhana S, Jacob JP *et al* (2010) Preparation, characterization and evaluation of a biopolymeric gold nanocomposite with antimicrobial activity. Biotech Appl Biochem 55 (1): 29-35.

Changsan N, Nilkaeo A, Pungrassami P *et al* (2009) Monitoring safety of liposomes containing rifampicin on respiratory cell lines and *in vitro* efficacy against *Mycobacterium bovis* in alveolar macrophages. J Drug Target 17 (10): 751-762.

Chen CZ, Cooper S.L (2002) Interactions between dendrimer biocides and bacterial membranes. Biomaterials 23 (16): 3359-3368.

Cheng Y, Qu H, Ma M *et al* (2007) Polyamidoamine (PAMAM) dendrimers as biocompatible carriers of quinolone antimicrobials: an *in vitro* study. Eur J Med Chem 42 (7): 1032-1038.

Cheow WS, Chang MW, Hadinoto K (2010a) Antibacterial efficacy of inhalable antibiotic-encapsulated biodegradable polymeric nanoparticles against *E. coli* biofilm cells. J Biomed Nanotech 6 (4): 391-403.

Cheow WS, Chang MW, Hadinoto K (2010b) Antibacterial efficacy of inhalable levofloxacin-loaded polymeric nanoparticles against *E. coli* biofilm cells: the effect of antibiotic release profile. Pharm Res 27 (8) 1597-1609.

Chono S, Suzuki H, Togami K *et al* (2011) Efficient drug delivery to lung epithelial lining fluid by aerosolization of ciprofloxacin incorporated into PEGylated liposomes for treatment of respiratory infections. Drug Dev Ind Pharm 37 (4): 367-372.

Clancy JP, Dupont L, Konstan MW *et al* (2013) Phase II studies of nebulised arikace in CF patients with *Pseudomonas aeruginosa* infection. Thorax 68: 818-25.

Das S, Ng WK, Tan RBH (2012) Are nanostructured lipid carriers (NLCs) better than solid lipid nanoparticles (SLNs): Development, characterizations and comparative evaluations of clotrimazole-loaded SLNs and NLCs? Eur J Pharm Sci 47 (1): 139-151.

Dillen K, Vandervoort J, Van den Mooter G *et al* (2006) Evaluation of ciprofloxacin-loaded Eudragit® RS100 or RL100/PLGA nanoparticles. Int J Pharm. 314 (1): 72-82.

Dillen K, Vandervoort J, Van den Mooter G *et al* (2004) Factorial design, physicochemical characterisation and activity of ciprofloxacin-PLGA nanoparticles. Int J Pharm 275 (1): 171-187.

Drulis-Kawa Z, Gubernator J, Dorotkiewicz-Jach A *et al* (2006) *In vitro* antimicrobial activity of liposomal meropenem against *Pseudomonas aeruginosa* strains. Int J Pharm 315 (1): 59-66.

Duncan R, Gaspar R (2011) Nanomedicine(s) under the microscope. Mol Pharm 8 (6): 2101-2141.

Ehsan Z, Wetzel JD, Clancy JP (2014) Nebulized liposomal amikacin for the treatment of *Pseudomonas aeruginosa* infection in cystic fibrosis patients. Expert Opin Investig Drugs 23: 743-9.

El-Ansary A, Al-Daihan S (2009) On the toxicity of therapeutically used nanoparticles: an overview. J Toxicol, ID:754810, 1-9.

El-Ridy MS, Abdelbary A, Nasr EA *et al* (2011) Niosomal encapsulation of the antitubercular drug, pyrazinamide. Drug Dev Ind Pharm 37 (9): 1110-1118.

Etheridge ML, Campbell SA, Erdman AG *et al* (2013) The big picture on nanomedicine: the state of investigational and approved nanomedicine products. Nanomed Nanotech Biol Med 9 (1): 1-14.

Garhwal R, Shady SF, Ellis EJ *et al* (2012) Sustained ocular delivery of ciprofloxacin using nanospheres and conventional contact lens materials. Iovs 53 (3): 1341-52.

Geller DE, Weers J, Heuerding S (2011) Development of an inhaled dry-powder formulation of tobramycin using PulmoSphere™ technology. J Aerosol Med Pulm Drug Deliv. 24: 175-82.

Ghaffari S, Varshosaz J, Saadat A *et al* (2011) Stability and antimicrobial effect of amikacin loaded SLN. Int J Nanomedicine 6: 35-43.

Gupta H, Aqil M, Khar RK *et al* (2011) Biodegradable levofloxacin nanoparticles for sustained ocular drug delivery. J Drug Target 19 (6): 409-17.

Gupta H, Aqil M, Khar RK *et al* (2013) Nanoparticles laden *in situ* gel of levofloxacin for enhanced ocular retention. Drug Deliv 20 (7): 306-9.

He C, Yin L, Tang C *et al* (2012) Size-dependent absorption mechanism of polymeric nanoparticles for oral delivery of protein drugs. Biomaterials 33(33): 8569-8578.

Hon-Leung Lee V, Robinson JR (1979) Mechanistic and quantitative evaluation of precorneal pilocarpine disposition in albino rabbits. J Pharm Sci 68, (6): 673–68.

Huh AJ, Kwon YJ (2011) Nanoantibiotics: A new paradigm for treating infectious diseases using nanomaterials in the antibiotics resistant era. J Control Release 156 (2): 128-145.

Huttner A, Harbarth S, Carlet J *et al* (2013) Antimicrobial resistance: a global view from the 2013 World Healthcare-Associated Infections. Antimicrob Resist Infect 18 (2): 31.

Immordino ML, Dosio F, Cattel L (2006) Stealth liposomes: review of the basic science, rationale, and clinical applications, existing and potential. Int J Nanomed 1 (3): 297-315.

Infectious Diseases Society of America (IDSA), Spellberg B, Blaser M *et al* (2011) Combating antimicrobial resistance: policy recommendations to save lives. Clin Infect Dis 52 (5): 397-428.

Jain D, Banerjee R (2008) Comparison of ciprofloxacin hydrochloride-loaded protein, lipid, and chitosan nanoparticles for drug delivery. J Biomed Mater Res Part B: Appl Biomaterials 86 (1): 105-112.

Jeong Y, Na H, Seo D *et al* (2008) Ciprofloxacin-encapsulated poly (DL-lactide-co-glycolide) nanoparticles and its antibacterial activity. Int J Pharm 352 (1): 317-323.

Kalhapure RS, Kathiravan MK, Akamanchi KG *et al* (2013) Dendrimers-from organic synthesis to pharmaceutical applications: an update. Pharm Dev Tech 20 (1): 22-40.

Kalhapure RS, Mocktar C, Sikwal DR *et al* (2014) Ion pairing with linoleic acid simultaneously enhances encapsulation efficiency and antibacterial activity of vancomycin in solid lipid nanoparticles. Colloids Surf B 117: 303-311.

Kalhapure RS, Suleman N, Mocktar C *et al* (2015) Nanoengineered drug delivery systems for enhancing antibiotic therapy. J Pharm Sci, 104 (3): 872-905.

Keck CM, Müller RH (2006) Drug nanocrystals of poorly soluble drugs produced by high pressure homogenisation. Eur J Pharm Biopharm 62 (1): 3-16.

Kesharwani P, Jain K, Jain NK (2014) Dendrimer as nanocarrier for drug delivery. Prog Pol Sci 39 (2): 268-307.

Kim H, Jones MN (2004) The delivery of benzyl penicillin to *Staphylococcus aureus* biofilms by use of liposomes. J Liposome Res 14 (3-4):123-139.

Kitchens KM, Kolhatkar RB, Swaan, P.W *et al* (2006) Transport of poly (amidoamine) dendrimers across Caco-2 cell monolayers: influence of size, charge and fluorescent labeling. Pharm Res 23 (12): 2818-2826.

Knetsch ML, Koole LH (2011) New strategies in the development of antimicrobial coatings: the example of increasing usage of silver and silver nanoparticles. Polymers 3 (1): 340-366.

Kong M, Chen XG, Xing K *et al* (2010) Antimicrobial properties of chitosan and mode of action: A state of the art review. Int J Food Microbiol, 144 (1): 51-63.

Kovacevic A, Savic S, Vuleta G *et al* (2011) Polyhydroxy surfactants for the formulation of lipid nanoparticles (SLN and NLC): effects on size, physical stability and particle matrix structure. Int J Pharm 406 (1): 163-172.

Krausz AE, Adler BL, Cabral V *et al* (2015) Curcumin-encapsulated nanoparticles as innovative antimicrobial and wound healing agent. Nanomedicine 11 (1): 195-206.

Kumari A, Yadav S.K., Yadav S.C (2010) Biodegradable polymeric nanoparticles based drug delivery systems. Colloids Surf B 75 (1): 1-18

Labana S, Pandey R, Sharma S *et al* (2002) Chemotherapeutic activity against murine tuberculosis of once weekly administered drugs (isoniazid and rifampicin) encapsulated in liposomes. Int J Antimicrob Ag 20 (4): 301-304.

Lai P, Daear W, Löbenberg R *et al* (2014) Overview of the preparation of organic polymeric nanoparticles for drug delivery based on gelatine, chitosan, poly(D,L-lactide-co-glycolic acid) and polyalkylcyanoacrylate. Colloids Surf B 118: 154-163.

Lian T, Ho R.J (2001) Trends and developments in liposome drug delivery systems. J Pharm Sci 90 (6): 667-680.

Lin Y, Tsai S, Lai C *et al* (2013) Genipin-cross-linked fucose–chitosan/heparin nanoparticles for the eradication of Helicobacter pylori. Biomaterials 34 (18): 4466-4479.

Lin YH, Chious SF, Lai CH (2012) Formulation and evaluation of water-in-oil amoxicillin-loaded nanoemulsions using for Helicobacter pylori eradication. Process Biochem 47(10):1469-1478.

Ma M, Cheng Y, Xu Z *et al* (2007) Evaluation of polyamidoamine (PAMAM) dendrimers as drug carriers of anti-bacterial drugs using sulfamethoxazole (SMZ) as a model drug. Eur J Med Chem 42 (1): 93-98.

Mah TC, O'Toole GA (2001) Mechanisms of biofilm resistance to antimicrobial agents. Trends Microbiol 9 (1): 34-39.

Makadia HK, Siegel SJ (2011) Poly Lactic-co-Glycolic acid (PLGA) as biodegradable controlled drug delivery carrier. Polymers 3 (3):1377-1397.

Manosroi A, Khanrin P, Lohcharoenkal W *et al* (2010) Transdermal absorption enhancement through rat skin of gallidermin loaded in niosomes. Int J Pharm 392 (1–2): 304-310.

Maya S, Indulekha S, Sukhithasri V *et al* (2012) Efficacy of tetracycline encapsulated O-carboxymethyl chitosan nanoparticles against intracellular infections of *Staphylococcus aureus*. Int J Biol Macromol 51 (4): 392-399.

Meers P, Neville M, Malinin V *et al* (2008) Biofilm penetration, triggered release and *in vivo* activity of inhaled liposomal amikacin in chronic *Pseudomonas aeruginosa* lung infections. J Antimicrob Chemother 61: 859-68.

Mehnert W, Mäder K (2001) Solid lipid nanoparticles: production, characterization and applications. Adv Drug Deliv Rev 47 (2):165-196.

Menjoge AR, Kannan RM, Tomalia DA (2010) Dendrimer-based drug and imaging conjugates: design considerations for nanomedical applications. Drug Discov Today 15 (5):171-185.

Mishra MK, Kotta K, Hali M *et al* (2011) PAMAM dendrimer-azithromycin conjugate nanodevices for the treatment of *Chlamydia trachomatis* infections. Nanomed Nanotech Biol Med 7 (6): 935-944.

Moghaddam PH, Ramezani V, Esfandi E *et al* (2013) Development of a nano–micro carrier system for sustained pulmonary delivery of clarithromycin. Powder Technol 239 (0): 478-483.

Mugabe C, Azghani, AO, Omri A (2005) Liposome-mediated gentamicin delivery: development and activity against resistant strains of *Pseudomonas aeruginosa* isolated from cystic fibrosis patients. J Antimicrob Chemother 55 (2): 269-271.

Müller R, Radtke M, Wissing S (2002) Nanostructured lipid matrices for improved microencapsulation of drugs", Int J Pharm 242 (1):121-128.

Müller RH, Mäder K, Gohla S (2000) Solid lipid nanoparticles (SLN) for controlled drug delivery – a review of the state of the art. Eur J Pharm Biopharm 50 (1): 161-177.

Muppidi K, Wang J, Betageri G *et al* (2011) PEGylated liposome encapsulation increases the lung tissue concentration of vancomycin. Antimicrob Ag Chemother 55 (10): 4537-4542.

Ong HX, Traini D, Cipolla D *et al* (2012) Liposomal nanoparticles control the uptake of ciprofloxacin across respiratory epithelia. Pharm Res 29 (12): 3335-3346.

Pandey R, Khuller GK (2005) Solid lipid particle-based inhalable sustained drug delivery system against experimental tuberculosis. Tuberculosis (Edinburgh, Scotland) 85 (4): 227-234.

Pardeike J, Hommoss A, Muller RH (2009) Lipid nanoparticles (SLN, NLC) in cosmetic and pharmaceutical dermal products. Int J Pharm 366 (1-2): 170-184.

Pastor M, Moreno-Sastre M, Esquisabel A *et al* (2014) Sodium colistimethate loaded lipid nanocarriers for the treatment of *Pseudomonas aeruginosa* infections associated with cystic fibrosis. Int J Pharm 477 (1–2): 485-494.

Pinto-Alphandary H, Andremont A, Couvreur P (2000a) Targeted delivery of antibiotics using liposomes and nanoparticles: research and applications. Int J Antimicrob Ag 13 (3): 155-168.

Ray K, Marteyn B, Sansonetti PJ *et al* (2009) Life on the inside: the intracellular lifestyle of cytosolic bacteria, Nat Rev Microbiol 7 (5): 333-340.

Rukholm G, Mugabe C, Azghani AO *et al* (2006) Antibacterial activity of liposomal gentamicin against *Pseudomonas aeruginosa*: a time–kill study. Int J Antimicrob Ag 27 (3): 247-252.

Samad A, Sultana Y, Aqil M (2007) Liposomal drug delivery systems: an update review. Curr Drug Deliv 4 (4): 297-305.

Sambhakar S, Singh B, Paliwal S *et al* (2011) Niosomes as a potential carrier for controlled release of cefuroxime axetil. Asian J. Biochem Pharm Res (1):126-136.

Sanchez DA, Schairer D, Tuckmann-Vernon C *et al* (2014) Amphotericin B releasing nanoparticle topical treatment of *Candida* spp. in the setting of a burn wound. Nanomedicine 10 (1): 269-77.

Sande L, Sanchez M, Montes J *et al* (2012) Liposomal encapsulation of vancomycin improves killing of methicillin-resistant *Staphylococcus aureus* in a murine infection mode. J Antimicrob Chemother 67(9):2191-94.

Sankhyan A, Pawar P (2012) Recent trends in niosome as vesicular drug delivery system. J Appl Pharm Sci 2 (6):20-32

Serisier DJ, Bilton D, De Soyza A *et al* (2013) Inhaled, dual release liposomal ciprofloxacin in non-cystic fibrosis bronchiectasis (ORBIT-2): A randomised, double-blind, placebo-controlled trial. Thorax. 68 (9): 812-7.

Shah N, Steptoe RJ, Parekh HS (2011) Low-generation asymmetric dendrimers exhibit minimal toxicity and effectively complex DNA. J Pept Sci, 17 (6): 470-478.

Singh G, Dwivedi H, Saraf SK *et al* (2011) Niosomal delivery of isoniazid-development and characterization. Trop J Pharm Res 10 (2): 203-210.

Tomalia DA (2005) Birth of a new macromolecular architecture: dendrimers as quantized building blocks for nanoscale synthetic polymer chemistry. Prog Pol Sci 30 (3): 294-324.

Toti US, Guru BR, Hali M *et al* (2011) Targeted delivery of antibiotics to intracellular chlamydial infections using PLGA nanoparticles. Biomaterials 32 (27): 6606-6613.

Ungaro F, d'Angelo I, Coletta *et al* (2012) Dry powders based on PLGA nanoparticles for pulmonary delivery of antibiotics: modulation of encapsulation efficiency, release rate and lung deposition pattern by hydrophilic polymers. J Control Release 157 (1): 149-159.

Van de Ven H, Paulussen C, Feijens PB *et al* (2011) PLGA nanoparticles and nanosuspensions with amphotericin B: Potent *in vitro* and *in vivo* alternatives to Fungizone and AmBisome. J Control Release 161 (3): 795-803.

Vemuri S, Rhodes C (1995) Preparation and characterization of liposomes as therapeutic delivery systems: a review. Pharm Act Helv 70 (2): 95-111.

Wang X, Zhang S, Zhu L *et al* (2012a) Enhancement of antibacterial activity of tilmicosin against *Staphylococcus aureus* by solid lipid nanoparticles *in vitro* and *in vivo*. Vet J 191 (1): 115-120.

Wang Y, Zhu L, Dong Z *et al* (2012b) Preparation and stability study of norfloxacin-loaded solid lipid nanoparticle suspensions. Colloids Surf B 98: 105-111.

Weers J, Metzheiser B, Taylor G *et al* (2009) A gamma scintigraphy study to investigate lung deposition and clearance of inhaled amikacin-loaded liposomes in healthy male volunteers. J Aerosol Med Pulm Drug Deliv 22: 131-8.

Wilczewska, AZ, Niemirowicz, K, Markiewicz *et al* (2012) Nanoparticles as drug delivery systems. Pharmacol Rep 64 (5): 1020-1037.

Xiong MH, Bao Y, Yang XZ *et al* (2014) Delivery of antibiotics with polymeric particles. Adv Drug Deliv Rev 79: 63-76.

Yang YY (2014) Emergence of multidrug-resistant bacteria: important role of macromolecules and drug delivery systems. Adv Drug Deliv Rev 78: 1-2.

Zaru M, Sinico C, De Logu A *et al* (2009) Rifampicin-loaded liposomes for the passive targeting to alveolar macrophages: *in vitro* and *in vivo* evaluation. J Liposome Res 19 (1): 68-76.

Zhang L, Pornpattananangkul D, Hu C *et al* (2010) Development of nanoparticles for antimicrobial drug delivery. Curr Med Chem 17 (6):585-594.

Zhou YJ, Zhang MX, Hider RC *et al* (2014) *In vitro* antimicrobial activity of hydroxypyridinone hexadentate-based dendrimeric chelators alone and in combination with norfloxacin. FEMS microbiology letters 355 (2): 124-130.

Zhu X, Radovic-Moreno AF, Wu J *et al* (2014) Nanomedicine in the management of microbial infection–Overview and perspectives. Nano today 9 (4): 478-498.

Pulmonary drug delivery: a review on nanocarriers for antibacterial chemotherapy

Pulmonary drug delivery: a review on nanocarriers for antibacterial chemotherapy

M. Moreno-Sastre[1,2]†, M. Pastor[1,2]†, C.J. Salomon[3,4], A. Esquisabel[1,2] and J.L. Pedraz[1,2]

[1]NanoBioCel Group, Laboratory of Pharmaceutics, School of Pharmacy, University of the Basque Country (UPV/EHU), Paseo de la Universidad 7, 01006 Vitoria-Gasteiz, Spain
[2]Biomedical Research Networking Center in Bioengineering, Biomaterials and Nanomedicine (CIBER-BBN), Vitoria-Gasteiz, Spain.
[3]Laboratory of Pharmaceutical Technology, Biochemical and Pharmaceutical Sciences Faculty, National University of Rosario, Suipacha 531, 2000 Rosario, Argentina
[4]Rosario Chemistry Institute, IQUIR-CONICET, Suipacha 531, 2000 Rosario, Argentina.

† Both authors contributed equally

Abstract

As the WHO stated, lower respiratory infections are the third leading cause of death. In addition, it is remarkable that antimicrobial resistance represents a huge threat. Thus, new therapeutic weapons are required. Among the possible alternatives, antibiotic encapsulation in nanoparticles has gained much attention in terms of improved tolerability, activity and ability to combat the resistance mechanisms of bacteria. In this regard, this reviewarticle focuses on the latest nanocarrier approaches for inhalatory therapy of antibiotics. First, the technology related to lung disposition will be reviewed. Then, nanocarrier systems will be introduced and the challenges required to perform adequate pulmonary deposition analysed. In the following part, drug delivery systems (DDSs) on the market or in clinical trials are described and, finally, new approaches of nanoparticles that have reached preclinical stage are enumerated. Altogether, this review aims at gathering together the novel nanosystems for anti-infectious therapy, underlining the potential of DDSs to improve and optimize currently available antibiotic therapies in the context of lung infections.

Introduction

According to the WHO, lower respiratory infection is the third leading cause of death, giving rise to 3.2 million deaths per year. Major contributors are the 1 million deaths per year caused by TB and the augmented risk of life-threatening pulmonary infections in chronic obstructive pulmonary disease (COPD) and cystic fibrosis (CF) patients.[1,2] Antimicrobial resistance (AMR) is a key issue to take into account regarding the therapy of infectious diseases. For example, hospital infections due to multiresistant bacteria, such as MRSA[3,4] or Gram-negative multiresistant bacteria, are currently serious threats.[5,6] Although bacterial evolution and resistance are natural phenomena, the misuse of antimicrobial drugs has accelerated the development of resistance.[7] In this context, there is an urgent need to optimize currently available antiinfectious therapies to overcome drug resistance.[8]

Nanotechnology has emerged as a promising approach to encapsulate antibiotics in order to avoid drug toxicity and reduce AMR. Drug delivery systems (DDSs) administered by the pulmonary route have gained increasing attention for the treatment of several pathologies, including asthma and COPD, since the inhalation process gives more direct access to the drug target than traditional routes.

Bearing this in mind, the aim of this review is to analyse the latest nanosystems to treat lung infections by the pulmonary route. First, factors affecting the lung disposition of various DDSs will be assessed and then nanotechnology advances and challenges for infectious pulmonary diseases will be discussed. However, pulmonary TB will be set aside from the scope of this review as the literature on anti-TB therapy is prolific and could be reviewed separately.[9–12]

Drug delivery to the lung

Pulmonary deposition

The lungs are constituted of two functional parts: the tracheobronchial region, from the larynx to the terminal
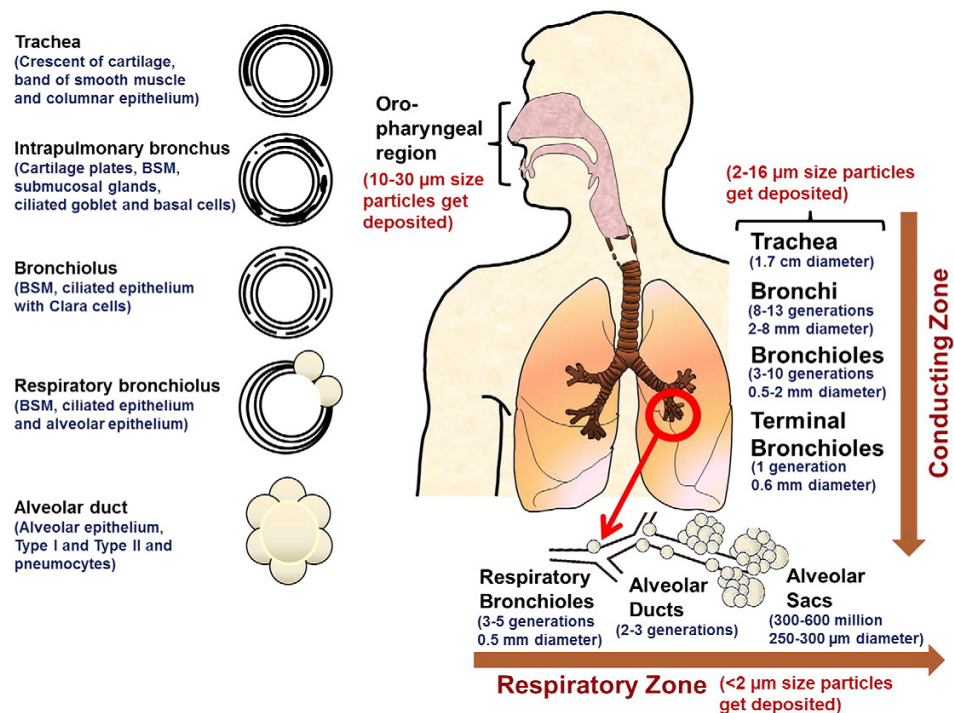
Figure 1. Representation of the particle deposition in the lungs according to different mechanisms related to particle size. BSM, bronchial smooth-muscle. Reproduced with permission from Nahar *et al*.[22]

bronchioles; and the alveolar region, comprising the respiratory bronchioles and alveoli. The respiratory tract is highly bifurcated and >95% of the total surface area of the lungs is composed of the alveolar area ($\approx$ 90-100 m^2) and a thin (0.1-0.2 µm) alveolar–vascular epithelium with a large capillary network. One of the factors influencing the efficacy of pulmonary drug delivery is the dose able to reach targets in the lung. The most important mechanisms of particle deposition in the respiratory tract are inertial impaction, gravitational sedimentation and diffusion (Brownian motion) (Figure 1).[13] Larger particles

(>10 μm) are retained in the oropharyngeal region and the larynx by inertial impaction. Particles having a size between 2 and 10 μm are usually deposited in the tracheobronchial region.[14] The deposition of particles, mainly of small size (0.5 2 μm), in the small conducting airways and alveoli is the result of gravitational sedimentation.[15] Particles having a size <0.5 μm, as a consequence of Brownian diffusion, are generally not deposited and are expelled upon exhalation.[16] Up to 80% of small aerosol particles (<1 μm) can be exhaled during breathing; however, nanoparticles (NPs) ≈100 nm are able to deposit in the alveolar region in acceptable amounts.[17,18] Drug NPs usually deposit by sedimentation after being released from the aerosol device due to an agglomeration process in the lung. These agglomerated NPs are able to sediment for longer periods in the tracheobronchial section, thereby improving the biological activity of the delivered therapeutic agent.

Models for studying deposition patterns of inhaled therapeutics

The deposition of inhaled particles in the respiratory airways depends on a number of parameters related to the particles, including size, charge, density, shape, solubility and lipophilicity, together with many physiological and anatomical factors of the respiratory system.[19,20]

One of the key issues for studying deposition and evaluating aerosol characteristics is the determination of the aerodynamic behaviour of the particles. Several methods are used for this purpose with the following equipment: (i) twin-stage impinger (TSI); (ii) multistage liquid impinger (MSLI); (iii) Andersen cascade impactor (ACI); and (iv) next-generation impactor (NGI). The TSI is relatively easy to use as it operates on the principle of liquid impingement to divide the dose emitted from the inhaler into non-respirable (stage 1) and respirable (stage 2) fractions. More recently developed equipment such as the MSLI, ACI and NGI consist of an administration device coupled to a spacer simulating the throat followed by stages

1–8 where the particles are deposited according to their size. Each stage of the impactor comprises a series of nozzles (progressively reducing jet diameters through which the sample-laden air is drawn) and a collection plate. At the end of the test, particles are removed from each plate using a suitable solvent and then analysed, to quantify the amount of drug actually present at each stage. Mathematical programs can be applied to calculate the emitted dose (ED, the total mass of drug emitted from the inhaler), fine particle dose (FPD, the mass of drug deposited in the cascade), fine particle fraction (FPF, the mass fraction of particles smaller than 5 µm) and, subsequently, mass median aerodynamic diameter (MMAD, the median of the distribution of airborne particle mass with respect to the aerodynamic diameter). The interpretation of these parameters predicts the deposition patterns of particulate drug carriers in the respiratory tract. In order to reach the alveolar region of the lung, particles must present a high FPF and an adequate MMAD, ranging from ≈1 to 5 µm.[21]

After the *in vitro* characterization, in vivo studies should be carried out. In this regard, different approaches have been proposed in order to reach animal lungs, i.e. aerosol inhalation by means of a nebulization chamber or intratracheal instillation by different syringes such as the Penn-Century® device.[22]

Table 1. Features of the devices currently used for pulmonary delivery.

Device	Mechanism	Characteristics	Inconveniences
Nebulizer	Air-jet or ultrasonic nebulization	Vibrating mesh technology Generates aerosol droplets from liquids	Long inhalation times cleaning times Frequent administration
pMDI	Generates aerosol droplets from a drug suspension in volatile liquids (propellant)	Unit dosing Inexpensive Correct size to deposit in the lung	Propellant requirement Lung deposition <60% Coordination difficulties
DPI	Dry powder	Store drug in dry state: stability and sterility Small portable devices Short administration	Requires high inspiratory effort

Delivery devices

Aerosols are an effective method to deliver therapeutic agents to the lung. There are different kinds of devices available on the market useful for pulmonary administration. Depending on the type of formulation, the most commonly used are nebulizers, pressurized metered-dose inhalers (pMDIs) and dry powder inhalers (DPIs), whose main characteristics are summarized in Table 1. Drug delivery by means of DPIs is considered the most convenient, as it is free of propellant and is chemically stable and patient friendly. Usually, however, drug or nanocarriers have to undergo additional formulation steps in order to be suitable for DPI administration.[23]

Nanosystems

Definition and types

NPs are solid colloidal particles ranging in size between 1 and 100 nm, but depending on the context, most of the NPs described in the literature are 50–500 nm in diameter. They can be made of biodegradable and biocompatible materials where active compounds such as antibiotics can be adsorbed, attached to their surface or entrapped into the matrix. Several methods for the elaboration of nanoparticulate systems have been reported, e.g. the emulsion–solvent evaporation technique, the high-pressure homogenization technique or nanoprecipitation.[24,25]

Among nanoparticulate DDSs, liposomes have deserved special attention. Liposomes are sphere-shaped vesicles consisting of one or more phospholipid bilayers, which can trap both hydrophobic and lipophilic drugs; water-soluble drugs are entrapped in the aqueous core whereas oil-soluble drugs are located in the lipid bilayer.[26]

On the other hand, polymeric NPs are more stable than liposomes as they present a higher structural integrity afforded by the rigidity of the polymer matrix. However, they might poorly encapsulate water-soluble drugs due to the fast leakage of the drug from NPs

during the high-energy emulsification step commonly employed during their preparation. In addition, polymeric NPs usually require the use of organic solvents to dissolve the polymers. Poly(lactic-co-glycolic acid) (PLGA) is an FDA-approved polymer for therapeutic use in humans and an attractive candidate for NP preparation owing to its minimal toxicity, biodegradability and biocompatibility properties.[27] Other biodegradable polymers that are currently being extensively explored are chitosan, dextran, alginates, polyvinyl alcohol (PVA), polyethylene glycol (PEG), etc.[28,29]

Solid lipid nanoparticles (SLNs) have emerged during the last decades as an alternative approach for drug encapsulation. SLNs possess a solid lipid matrix that, due to changes in the lipid polymorphism, can leak out the drug. To overcome this limitation they have been modified, leading to the introduction of nanostructured lipid carriers (NLCs), which represent the second generation of lipid NPs. The main difference between them is the configuration of the lipid matrix: in

NLCs it is a less ordered matrix consisting of a mixture of solid and liquid lipids, increasing drug loading and preventing leakage.[30,31] Apart from these NPs, there are many other DDSs, including niosomes, dendrimers, nanocapsules, etc.[32,33]

Advantages and disadvantages of nanosystems

Nano-DDSs have some advantages for the treatment of lung infection compared with the free drug (Figure 2):

(i) Protection of the antibiotics from enzymatic (e.g. degradation by β-lactamases) or chemical degradation.

(ii) The possibility of achieving mucoadhesive properties to the formulation. Nanocarriers can be decorated with different molecules in order achieve target delivery to specific airway tissue/cells, e.g. penetrate the mucus barrier or remain attached to he bacterial biofilm.[34,35]

(iii) Sustained drug release. Drug is released in a controlled manner, avoiding too high drug

concentrations and prolonging the resdence time in lung tissue over several weeks.[36,37]

(iv) The ability to escape from alveolar macrophages.
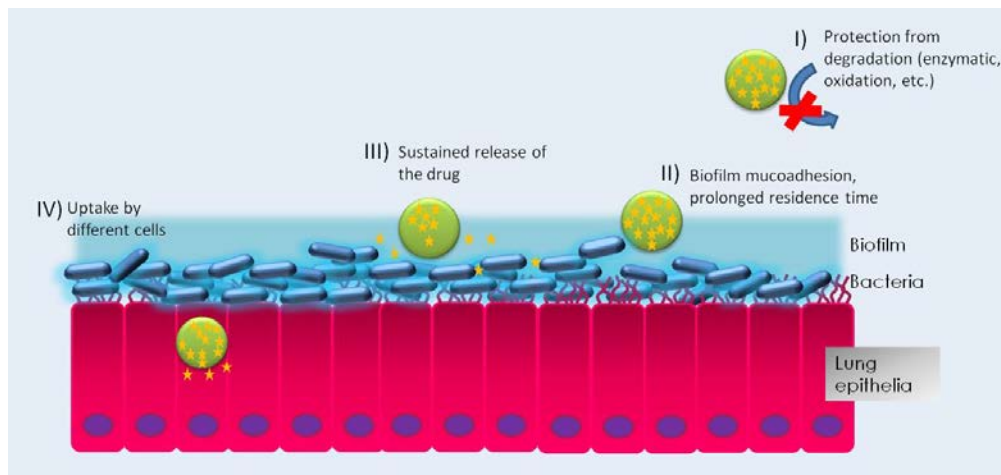
Figure 2. Advantages of nanosystems for the treatment of lung infections. (I) DDS protect drugs from degradation, e.g. enzymatic degradation or oxidation. (II) DDS can be tailored to present mucoadhesive properties. (III) Sustained drud release. (IV) DDS uptake by different cells such as alveolar macrophages enabling intracellular infection treatment.

Overall, these characteristics enhance the antimicrobial activity by decreasing the MIC, hence giving rise to an improved treatment. The advantages that different DDSs might present over free-drug administration depend on the nature of the DDS itself (Figure 3).[38–41]

The major disadvantage of nano-DDSs is their potential toxicity. Nanotoxicology has gained much attention in recent decades, especially in the health–pollution field, due to the prevalence of NPs in air. However, most of the NPs for drug delivery are usually made with well-tolerated materials, generally recognized as safe (GRAS), avoiding the possibility of toxicity effects.[42,43] Therefore, when designing NPs, *in vitro* and *in vivo* toxicity

studies should be carefully performed to ensure their safety for human health. Another issue that should be overcome before inhalable NPs reach the complexity of the NP production could be a disadvantage (Figure 3).
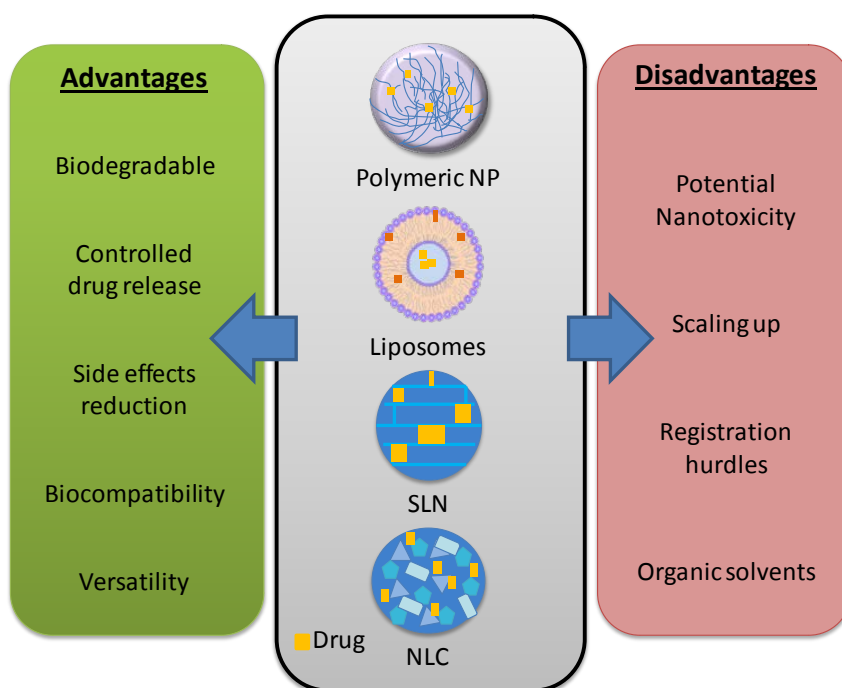
Figure 3. Main advantages and disadvantages of NP.

Challenges faced by NPs before reaching the deep lung

The pulmonary route can be approached to provide a systemic or a local effect. The enthusiasm regarding this route for local targeting is based on the following:

(i) The DDS or the drug comes into direct contact with the pulmonary epithelium, allowing a fast onset of the therapeutic effect.

(ii) High systemic drug concentrations are avoided and thus adverse effects are minimized or prevented.

(iii) Drug degradation is slowed down due to low intra- and extracellular enzymatic activity in the lung environment.[44–46]

The fate of inhaled drug after lung deposition strongly depends on its interaction with the different components of the biological environment. Among them, lung lining fluids, lung cell populations and bacterial biofilm are the most critical factors. In certain pathological conditions, the natural airway mucus can be thicker, enabling bacterial growth and hampering drug action. Another important point is the different cell populations present in the lung. For example, alveolar macrophages may phagocytose the particles, which could be interesting for TB treatment, but disadvantageous when treating other types of bacteria. Finally, overcoming bacterial biofilms also plays a major role in antibiotic therapy. Biofilms are intricate bacterial communities enclosed by an extracellular matrix composed of polymeric substances, DNA and proteins. Bacterial biofilms exhibit high resistance to antimicrobial agents that together with the complex and well coordinated biofilm mode of growth are the main causes of chronic infections development, e.g. in CF patients, clusters of *Pseudomonas aeruginosa* are embedded in a thick, stationary mucus layer overlying airway epithelial cells.[47]

The development of inhalable pharmaceutical forms using nanocarriers represents a huge challenge. Due to their particle size, they lack suitable aerodynamic flow properties and are exhaled during breathing. In order to overcome this limitation, two main strategies have been followed: nebulization of nanocarriers as a colloidal suspension or associating the system with microsized carriers.
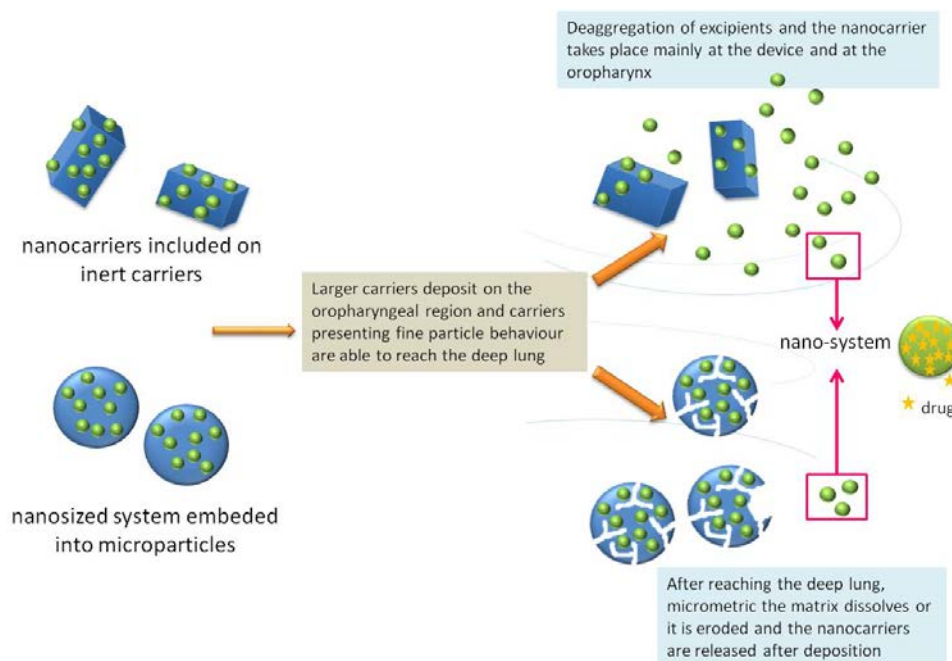
Figure 4. Improvement of the aerodynamic properties of the nanocarriers can be achieved following, e.g., two different approaches that are represented in the scheme.

The latter approach could be accomplished by either mixing nanocarriers along with inert carriers such as inhalable lactose or mannitol or by embedding the nanosized system into microparticles (Figure 4).[48] Furthermore, another hurdle for the formulation development step is caused by the limited number of excipients approved for inhalation therapy.[49] Carbohydrates, especially lactose and mannitol, are generally used as carriers or excipients for DPIs since they are approved by the FDA, non-toxic and degradable. The amino acid leucine is another candidate to be taken into consideration, since it prevents aggregation due to surfactant behaviour and antiadherent properties at low concentration. Dipalmitoyl-phosphatidylcholine (DPPC) is a phospholipid normally used to prepare nanosystems for pulmonary delivery

because it is the major lipid component of lung surfactant and is relatively non-toxic.[50]

In order to prepare inhalable powders, the spray-drying technique is widely used. This method of producing dry powder is based on evaporating the solvent from a liquid or suspension, achieving solid-state particles presenting appropriate MMAD that ensures drug deposition in the tracheobronchial and deep alveolar regions. Lyophilization, or freeze-drying, has also been explored as an approach to produce stable dry powder that could be administered by DPIs or after rehydration in the appropriate buffer. Both methods produce a powder form that will enhance NP stability, avoiding polymer hydrolysis and drug loss.

As with other inhalable drugs, NPs should meet quality measures of isotonicity, sterility, neutral pH value between 3 and 8.5 (in European Pharmacopeia), biocompatibility, good aerosolization properties and production on an industrial scale.[51]

Current state of clinical therapy

Recently, the FDA approved an inhalation powder containing tobramycin (tobramycin inhalation powder, TOBI Podhaler™)[52,53] to treat *P. aeruginosa* lung infection in CF patients. This product is based on a tobramycin DDS prepared by means of PulmoSphere™ technology, which is an emulsion-based spraydrying process that enables the production of light porous particles. The success of this product has encouraged new developments in this field. In this regard, two more antibiotics, ciprofloxacin (Lipoquin® and Pulmaquin®)[54,55] and amikacin (Arikace™)[56] both as nebulized liposomal formulations, have reached Phase II and Phase III in clinical trials for CF and non-CF bronchiectasis.

More precisely, Phase II trial of ciprofloxacin formulations confirmed that a single administration of Lipoquin® was safe and capable of reducing the *P. aeruginosa* cfu account and improving lung function.[57] Another Phase IIb clinical trial, ORBIT-1 and ORBIT-2, focused on non-CF bronchiectasis patients suffering

from *P. aeruginosa* infection. Both liposomal formulations were administered once daily with a 28 day treatment phase and a 28 day off stage with a follow-up period. In this case, patients presented a low incidence of adverse effects and the formulations were overall well tolerated.[55] Pulmaquin® is currently under evaluation in a Phase III clinical trial for the non-CF bronchiectasis population (ARD-3150-1201, ORBIT-3 and ORBIT-4).

Arikace™ is a formulation based on liposomes containing amikacin.[58] After nebulization, it is able to penetrate the characteristic sputum of CF patients. A Phase III trial is currently being conducted with CF patients colonized by *P. aeruginosa* in Europe, Australia and Canada (2011-000441-20, Insmed Incorporated). After analysis of some preliminary results, the authors postulated that liposomal amikacin was safe and effective. A single daily dose of liposomal amikacin showed better results than TOBI® twice daily, especially in terms of respiratory symptoms.[59,60]

New approaches for antibiotic DDSs

The efforts of the scientific community in the development of respirable DDSs have given rise to an extensive literature on antibiotic-loaded NPs that will be overviewed in the following section according to therapeutic group.

Macrolides

Moghaddam *et al.*[61] described an approach for the encapsulation of clarithromycin into PLGA NPs that were freeze- and spray-dried with different excipients, i.e. lactose, mannitol and leucine. Drug release studies showed a biphasic profile releasing 100% of the drug after 2 days (Figure 5). Finally, the aerodynamic study of the NPs was performed by means of a TSI using a Cyclohaler® device. It was observed that the addition of leucine to the formulations led to the best FPF (53.77%) and ED (75.85%). These results could be explained by the non-polar side chain of leucine, which improves flowability due to its antiadherent properties.
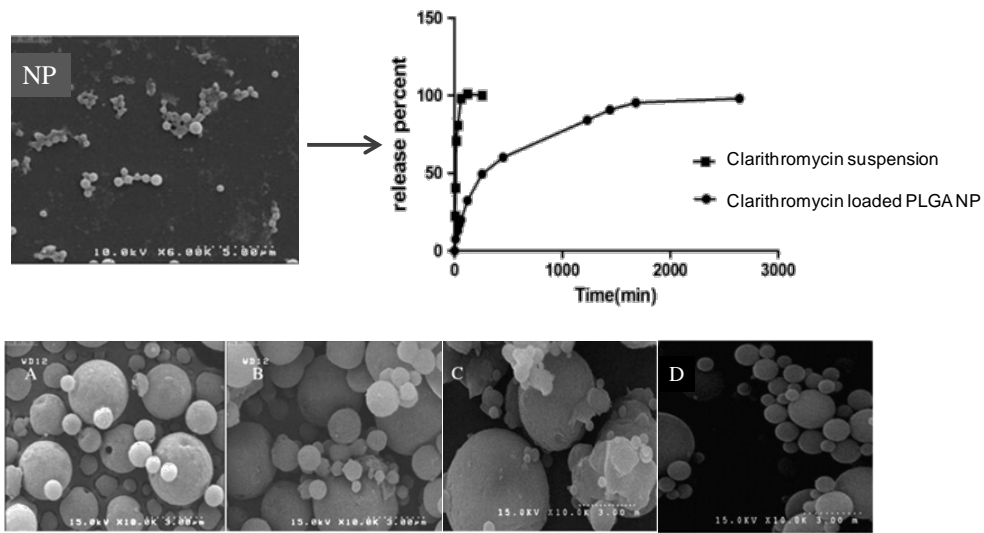
Figure 5. Top row, left: scanning electron microscopy image of clarithromycin-loaded nanoparticles (NP). Top row, right: release profile of clarithromycin-loaded polymeric NPs. Botton row: four SEM micrographs of clarithromycin-loaded PLGA NP after spray-drying with different excipients, A) mannitol and L-leucine NPs; B) lactose and L-leucine NPs; C) mannitol and D) lactose. Reproduced with permission from Moghaddam *et al.*[61]

Quinolones

Cheow *et al.*[62] developed levofloxacin- and ciprofloxacin-loaded PLGA or poly-ε-caprolactone NPs that presented high activity against *Escherichia coli* in biofilm cells and biofilm-derived planktonic cells. In a subsequent study,[63] these nanoformulations were evaluated against *E. coli* in biofilms. NPs displayed biphasic release profiles over a 6 day period. This biphasic release permitted a high initial antibiotic concentration followed by an extended release profile presenting a drug concentration above the minimum biofilm inhibitory concentration value (i.e. 1.10 mg/L) that is able to inhibit biofilm growth of the surviving persisting *E. coli* cells for 4 days. This biphasic profile seems to be required for the successful eradication of the biofilm and to minimize the exacerbation due to the higher

antibiotic susceptibility of the surviving cells.

Another work investigating quinolone encapsulation was reported by Duan *et al.*[64] The spray-drying technique was selected for moxifloxacin and ofloxacin encapsulation. *In vitro* aerosol dispersion of the spray-dried powders was performed using an NGI. When moxifloxacin was spray-dried along with DPPC, high values of ED (>90%) and FPF (>67%) were achieved, together with an appropriate MMAD (<5.24 μm) suitable for reaching the smaller airways without rendered crystallinity. However, ofloxacin powders retained partial crystallinity in certain compositions depending on the DPPC ratio. Hence, on this occasion, the use of DPPC improved the aerosol dispersion of moxifloxacin NPs after spray-drying, leading to powder-form carriers useful for the treatment of pulmonary infections.

Chono *et al.*[65] evaluated the aerosolization of ciprofloxacin incorporated into PEGylated liposomes. In the *in vivo* study, drug distribution in epithelial lining fluid (ELF) was analysed after the aerosolization of PEGylated liposomes and uncoated liposomes and it was observed that the elimination rate of ciprofloxacin from ELF was significantly slower for PEGylated liposomes compared with uncoated liposomes and also the AUC and mean residence time were higher. Moreover, the evaluation of their antibacterial effects against pathogenic microorganisms in ELF showed strong activity against bacteria such as *P. aeruginosa*, *Haemophilus influenzae* and *Streptococcs pneumoniae*. Finally, they also observed that the liposomes led to no lung tissue damage and that PEGylated liposomes did not show cytotoxic effects at the dose assessed. Altogether, the authors concluded that PEGylated liposomes may be a suitable pulmonary DDS allowing ciprofloxacin dose reduction against lung infections.
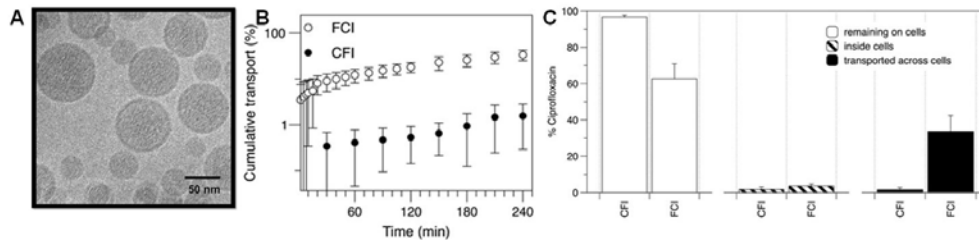
Figure 6. A) Cryotransmission electron microscopy image of liposomal ciprofloxacin. B) Apical-basal cumulative transport of nebulised free ciprofloxacin (FCI) and liposomal ciprofloxacin (CFI) on a Calu-3 air-interface cell line (n ≤ 5, ± SD). C) Intracellular distribution of ciprofloxacin, remaining on the Calu-3 epithelial cells and transported across the epithelial cells after 4 h, free ciprofloxacin (FCI) and liposomal ciprofloxacin (CFI). Reproduced with permission from Ong *et al*.[66]

Ong *et al*.[66] worked on the development of ciprofloxacinloaded liposomal NPs for the treatment of bacterial infections in cystic fibrosis and non-CF bronchiectasis. The characterization of nebulized aerosols by NGI studies revealed liposome diameters of 4.43 μm, similar to the free drug. The respirable fraction of the formulation was quantified at 70.5 ± 2.03%, i.e the formulation was able to reach deep-lung regions. Moreover, when the nebulizer-adapted TSI was coupled to a Calu-3 cell culture, it was demonstrated that the formulation allowed slow and controlled release of the drug. In addition, >95% of the liposomal ciprofloxacin remained in the apical chamber of the inserts, meaning that the drug can be released where the bacterial infection takes place (Figure 6). Liposomal ciprofloxacin was found to be as active as the free drug against *P. aeruginosa* and *Staphylococcus aureus*. In addition, MBC testing showed that the liposomal formulation against *P. aeruginosa* presented a significantly lower value than the free drug. On the other hand, the ciprofloxacin-loaded liposomes did not provide an improvement in the bactericidal activity against *S. aureus*, very likely due to the presence of the dense peptidoglycan cell wall in Gram-positive bacteria (Table 2).

Table 2. *In vitro* activity against *S. aureus* and *P. aeruginosa* of nebulized liposomal ciprofloxacin and free ciprofloxacin. Reproduced with permission from Ong *et al.*[66]

Formulation	S. aureus		P. aeruginosa	
	MIC (mg/L)	MBC (mg/L)	MIC (mg/L)	MBC (mg/L)
Free ciprofloxacin	0.125	0.5-1	0.25-0.5	4
Liposomal ciprofloxacin	0.125	1	0.5-1	2*
Empty liposomes	>32	>32	>32	>32

*p<0.05 compared with free ciprofloxacin.

Nonetheless, in order to provide an in-depth analysis of ciprofloxacin liposomes, the same group[67] used different *in vitro* and *ex vivo* methodologies to examine the release mechanisms from the inhalation delivery systems and their effect on drug disposition, comparing them with an *in vivo* assay performed by Yim *et al.*[68] As the results were qualitatively similar, they underlined the usefulness of *in vitro/ex vivo* models for the prediction of *in vivo* results.

Sweeney *et al.*[69] also developed a ciprofloxacin-loaded liposomal powder formulation using a spray and freeze-drying process that showed adequate aerodynamic properties measured by ACI.

By means of a numerical deposition model developed by Finlay *et al.*,[70] the drug concentration in the airway surface liquid was calculated to be 5 mg/L. This drug concentration would be above the MIC and thus could inhibit the growth of many pathogens, such as *P. aeruginosa*, *Streptococcus pyogenes*, *Neisseria gonorrhoeae*, *Bacillus anthracis* and many other aerobes. Nonetheless, more experimental outcomes should be provided in order to ensure the robustness of these estimations.

As another strategy, Liu *et al.*[71] encapsulated ciprofloxacin into liposomes presenting sustained *in vitro* release in simulated lung fluid over 36 h. Liposomes were administered to rats by intratracheal instillation. The drug concentration in the lung was higher for the liposomal antibiotic than for the free drug, e.g. liposomal ciprofloxacin presented 18.7 h $t_{1/2}$ in the lung and 151.2 mg/g C_{max}, representing 7.21- and 4.99-fold increases, respectively, over those of the free drug. Bioavailability results also confirmed that liposomal ciprofloxacin was able to reach

the lung and provide high drug concentrations at the target site. In addition, an *in vivo* pulmonary irritation test showed ciprofloxacin liposomes were able to minimize modification and irritation of the lungs after intratracheal instillation in rats. From these results, it can be inferred that successful pulmonary delivery of a liposomal formulation was achieved with a high concentration of ciprofloxacin at the target site.

Aminoglycosides

Alhariri *et al.*[72] developed tobramycin-loaded liposomes incorporating bismuth-ethanedithiol (BiEDT) (LipoBiEDT-TOB). Previous work described that BiEDT in the presence of tobramycin has a synergistic effect against *P. aeruginosa* and *Burkholderia cepacia in vitro*.[73,74] The MIC of LipoBiEDT-TOB was 16-fold lower than that of free tobramycin and 4-fold lower than that of free tobramycin together with BiEDT. In a further *in vivo* assay, intratracheal administration of the liposomes was studied in rats chronically infected with *P. aeruginosa*. It could be observed that, after 24 h, LipoBiEDT-TOB decreased the bacterial counts in the lungs up to 10^3 cfu/lung, whereas untreated animals and the free antibiotic group displayed $10^{7.4}$ and $10^{4.7}$ cfu/lung, respectively. After the last dose of LipoBiEDT-TOB, no tobramycin was detected in the kidneys, whereas the free drug was found in the kidneys and lungs. Taken together, the authors concluded that pulmonary administration of LipoBiEDT-TOB could improve the treatment of chronic *P. aeruginosa* infection in CF patients.

Another tobramycin-loaded formulation was evaluated by Pilcer *et al.*[75] In this case, a mixture of microparticle and NP formulation was developed. The aerodynamic behaviour of the spraydried tobramycin formulations was evaluated by an MSLI using an Aerolizer® as the inhalation device. It was confirmed that the NP-coated tobramycin increased the FPD during inhalation, which was explained by the fact that coating the drug with NPs could reduce powder agglomeration and cohesion with other particles. Similarly, it was found that an

increase in the amount of sodium glycocholate in the spray-dried suspension led to an enhancement in FPF from 36% to 61%. In conclusion, mixing tobramycin-loaded NPs and microparticle dry powders with low levels of sodium glycocholate resulted in a suitable DDS for treating lung diseases as it offered effective pulmonary delivery.

Tobramycin encapsulation was also described by Ungaro *et al*.,[76] although this group selected PLGA as the core polymer. Spray-drying was performed in order to obtain micrometre-sized dry powder particles using lactose as an inert carrier. The drug release was optimal, providing a burst release followed by a maintained liberation of the drug for a month. Chitosan-coated PLGA NPs were able to penetrate through an artificial mucus layer. The MIC values of the PLGA formulations for *P. aeruginosa* planktonic cells were much higher than that of the free antibiotic. This could be due to the biphasic extended antibiotic release profiles of the NPs that in turn liberated small amounts of drug into the media that

were very likely below the MIC. The aerosolization properties of the formulations were investigated *in vitro* using an MSLI coupled to a Turbospin®. The results confirmed that both powders presented suitable properties of MMAD and FPF with an ED of 100%. *In vivo* biodistribution studies in rats, after intratracheal delivery using the Penn-Century® device, showed that PVA-modified alginate PLGA NPs reached the deep lung, whereas chitosan-modified NPs were located to a greater extent in the upper airways. Hence, PVA preparations led to the development of respirable lactose–PLGA carriers suitable for lung delivery.

Rukholm *et al*.[77] proposed the encapsulation of gentamicin into liposomes. MIC and time-kill studies were performed with free and liposomal gentamicin against *P. aeruginosa*. The most remarkable difference among the two gentamicin preparations was observed for the MIC values, where liposomal gentamicin showed significantly lower values (32 mg/L) than those of the

free form (512 mg/L) for a non-mucoid clinical strain of P. *aeruginosa* isolated from the lungs of a CF patient that was resistant to gentamicin. The authors explained these results by the possible fusion of the liposomes with the outer bacterial membrane, which may have led to increased penetration of the antibiotic. Finally, in *in vitro* time-kill studies, only the 4-fold MIC liposomal formulation demonstrated improved antimicrobial activity against the antibiotic-resistant strain by achieving complete bacterial eradication in 6 h, whereas the free drug needed 24 h to eradicate the bacteria. The authors concluded that the liposomal gentamicin formulation was effective, presenting an improved killing time and prolonged antimicrobial activity against *P. aeruginosa.*

In an attempt to decrease drug toxicity and improve dosing by drug targeting, Ghaffari *et al.*[78] encapsulated amikacin into SLNs for pulmonary delivery and a lyophilization step was carried out for the stabilization of the formulation. It could be determined that SLNs, whether as a freeze-dried powder or as a dispersion, were able to release >95% of the drug during 6 days of incubation. Both SLNs presented activity against *P. aeruginosa*. Nonetheless, testing of amikacin-loaded SLNs showed that SLNs increased the MIC and MBC values compared with the free drug. However, as the incubation period of this test was set at 48 h, it should be kept in mind that only the 25% of the drug was released from the SLNs; hence, the authors postulated that SLNs *in vivo* might present half the MIC and MBC compared with the free drug. The authors hypothesized that besides the sustained drug release profile, SLNs have the advantage of improving the antibacterial activity of amikacin due to diffusion enhancement across the bacterial membrane.

In a further study related to amikacin, Varshosaz *et al.*[79] analysed the biodistribution in the lungs and kidneys of ^{99m}Tc-labelled amikacin SLNs after pulmonary delivery to assess whether amikacin encapsulation could increase the drug concentration in the lungs and thus

reduce side effects of CF treatment. The drug release profile displayed a continuous and sustained pattern for 144 h. In the subsequent *in vivo* experiment, [99mTc]-labelled amikacin SLNs or free [99mTc]-amikacin were administered by the inhalation route, detecting a similar signal in the lung for both formulations. It is worth mentioning that pulmonary-administered SLNs presented higher drug concentrations in the stomach than intravenous administration, which might be related to swallowing exhaled particles after administration. Finally, the authors concluded that SLNs seem to be a promising inhaled carrier for improving the efficacy of amikacin in CF as well as reducing the dose frequency due to sustained drug release and could, therefore, decrease drug toxicity, especially nephrotoxicity.

Polypeptides

Pastor *et al.*[80] recently reported the utility of lipid NPs for the encapsulation of sodium colistimethate. More precisely, SLNs and NLCs were elaborated. Both lipid NPs presented antimicrobial activity

against clinically isolated P. *aeruginosa* strains at a concentration of 1–2 mg/L. Cell experiments using the A549 cell line showed that lipid NPs were able to significantly reduce antibiotic toxicity. Next, an *in vivo* biodistribution assay was conducted after nebulizing infrared (IR)-labelled NLCs into mice. It was observed that NLCs spread homogenously throughout the lungs, whereas no signal could be detected in other organs. The IR intensity was detectable 48 h after administration, suggesting that the dosing interval could be prolonged by the use of these NPs.

Conclusions

Pulmonary infections are often persistent and recurrent. A potential therapeutic approach is to target the delivery of antibiotics directly to the site of infection as a mechanism to increase and maintain the local drug concentration. In recent years, the encapsulation of antimicrobial drugs into nanocarriers has appeared as a powerful tool for enhancing therapeutic effectiveness against infectious diseases

and minimizing side effects of the drugs. The inhalation route has gained much attention as a promising alternative administration route for the treatment of pulmonary infections. Tight control over the geometric size and morphology of particles resulted in aerosols with narrow aerodynamic size distributions that would be able to reach the deep-lung region and appropriately deliver the antibiotic to the site of infection.

Here, the current progress and challenges in synthesizing NP systems for delivering various antimicrobial drugs are reviewed. The published data stated that DDSs for inhalation therapy are able to decrease the antibiotic dose administered, thereby reducing toxicity as well as enhancing patient compliance and adherence to the treatment. Much has been studied in order to overcome the resistance of common antibiotics, yet additional efforts are needed. We need to gain insight into the complex context that surrounds the infection by better understanding the interaction of different fields, such as microbiology, physiopathology, immunology, pharmacokinetics/ pharmacodynamics, pharmacology, microtechnology and nanotechnology.

Overall, the scientific community should pay attention to the formulation of DDSs to improve lung deposition and anti-infective therapy. Therefore, further tailoring of currently available DDSs is required in order to translate this technological advance into clinical benefits.

Acknowledgements

Funding

References

1 WHO. The Top 10 Causes of Death. Fact Sheet 310.http://www.who.int/mediacentre/factsheets/fs310/en/index.html.

2 Heijerman H, Westerman E, Conway S *et al*. Inhaled medication and inhalation devices for lung disease in patients with cystic fibrosis: a European consensus. J Cyst Fibros 2009; 8: 295–315.

3 Sader HS, Jones RN. Antimicrobial susceptibility of gram-positive bacteria isolated from US medical centers: results of the daptomycin surveillance program (2007–2008). Diagn Microbiol Infect Dis 2009; 65: 158–62.

4 Porto JP, Santos RO, Gontijo PPF *et al*. Active surveillance to determine the impact of methicillin resistance on mortality in patients with bacteremia and influences of the use of antibiotics on the development of MRSA infection. Rev Soc Bras Med Trop 2013; 46: 713–8.

5 Haase R, Worlitzsch F, Schmidt F *et al*. Colonization and infection due to multi-resistant bacteria in neonates: a single center analysis. Klin Padiatr 2014; 226: 8–12.

6 Viswanathan R, Singh AK, Basu S *et al*. Multi-drug resistant Gramnegative bacilli causing early neonatal sepsis in India. Arch Dis Child Fetal Neonatal Ed 2012; 97: F182–7.

7 WHO. The Evolving Threat of Antimicrobial Resistance: Options for Actions. Geneva: WHO, 2012.

8 Gould I, Bal A. New antibiotic agents in the pipeline and how they can help overcome microbial resistance. Virulence 2013; 4: 185–91.

9 Costa H, Grenha A. Natural carriers for application in tuberculosis treatment. J Microencapsul 2013; 30: 295–306.

10 Mehanna MM, Mohyeldin SM, Elgindy NA. Respirable nanocarriers as a promising strategy for antitubercular drug delivery. J Control Release 2014; 187: 183–97.

11 Sosnik A, Carcaboso AM, Glisoni RJ *et al*. New old challenges in tuberculosis: potentially effective nanotechnologies in drug delivery. Adv Drug Deliv Rev 2010; 62: 547–59.

12 Pandey R, Ahmad Z. Nanomedicine and experimental tuberculosis: facts, flaws, and future. Nanomedicine 2011; 7: 259–72.

13 Hinds WC. Aerosol Technology: Properties, Behavior, and Measurement of Airborne Particles. 2nd edn. New Jersey: John Wiley & Sons, 1999.

14 Schulz H, Muhle H. Chapter 16—respiration. In: Krinke GJ, ed. The Laboratory Rat. London: Academic Press, 2000; 323–44.

15 Newman SP, Pavia D, Garland N *et al*. Effects of various inhalation modes on the deposition of radioactive pressurized aerosols. Eur J Respir Dis Suppl 1982; 119: 57–65.

16 Heyder J, Svartengren MU. Basic principles of particle behavior in the human respiratory tract. In: Bisgaard H, O'Callaghan C, Smaldone GC, eds. Drug Delivery to the Lung. 1st edn. New York: Marcel Dekker, 2002; 21–45.

17 Patton JS. Unlocking the opportunity of tight glycaemic control. Diabetes Obes Metab 2005; 7: S5–8.

18 Courrier HM, Butz N, Vandamme TF. Pulmonary drug delivery systems: recent developments and prospects. Crit Rev Ther Drug Carrier Syst 2002; 19: 425–98.

19 Rabanel JM, Aoun V, Elkin I *et al*. Drug-loaded nanocarriers: passive targeting and crossing of biological barriers. Curr Med Chem 2012; 19: 3070–102.

20 Geiser M, Kreyling WG. Deposition and biokinetics of inhaled nanoparticles. Part Fibre Toxicol 2010; 7: 2.

21 Wong W, Crapper J, Chan HK *et al*. Pharmacopeial methodologies for determining aerodynamic mass distributions of ultra-high dose inhaler medicines. J Pharm Biomed Anal 2010; 51: 853–7.

22 Nahar K, Gupta N, Gauvin R *et al*. *In vitro, in vivo* and ex vivo models for studying particle deposition and drug absorption of inhaled pharmaceuticals. Eur J Pharm Sci 2013; 49: 805–18.

23 Timsina MP, Martin GP, Marriott C *et al*. Drug delivery to the respiratory tract using dry powder inhalers. Int J Pharm 1994; 101: 1–13.

24 Corrias F, Lai F. New methods for lipid nanoparticles preparation. Recent Pat Drug Deliv Formul 2011; 5: 201–13.

25 Bilati U, Alle´mann E, Doelker E. Development of a nanoprecipitation method intended for the entrapment of hydrophilic drugs into nanoparticles. Eur J Pharm Sci 2005; 24: 67–75.

26 Ulrich AS. Biophysical aspects of using liposomes as delivery vehicles. Biosci Rep 2002; 22: 129–50.

27 Makadia HK, Siegel SJ. Poly lactic-co-glycolic acid (PLGA) as biodegradable controlled drug delivery carrier. Polymers (Basel) 2011; 3: 1377–97.

28 Peniche H, Peniche C. Chitosan nanoparticles: a contribution to nanomedicine. Polym Int 2011; 60: 883–9.

29 Chan JM, Zhang L, Yuet KP *et al*. PLGA–lecithin–PEG core–shell nanoparticles for controlled drug delivery. Biomaterials 2009; 30: 1627–34.

30 Das S, Ng WK, Tan RBH. Are nanostructured lipid carriers (NLCs) better than solid lipid nanoparticles (SLNs): development, characterizations and comparative evaluations of clotrimazole-loaded SLNs and NLCs? Eur J Pharm Sci 2012; 47: 139–51.

31 Das S, Chaudhury A. Recent advances in lipid nanoparticle formulations with solid matrix for oral drug delivery. AAPS PharmSciTech 2011; 12: 62–76.

32 Akbari V, Abedi D, Pardakhty A *et al*. Ciprofloxacin nano-niosomes for targeting

intracellular infections: an *in vitro* evaluation. J Nanopart Res 2013; 15: 1556.

33 Kavruk M, Celikbicak O, Ozalp V *et al*. Antibiotic loaded nanocapsules functionalized with aptamer gates for targeted destruction of pathogens. Chem Commun (Camb) 2015; 51: 8492–5.

34 d'Angelo I, Conte C, La Rotonda MI *et al*. Improving the efficacy of inhaled drugs in cystic fibrosis: challenges and emerging drug delivery strategies. Adv Drug Deliv Rev 2014; 75: 92–111.

35 Andrade F, Rafael D, Videira M *et al*. Nanotechnology and pulmonary delivery to overcome resistance in infectious diseases. Adv Drug Deliv Rev 2013; 65: 1816–27.

36 Abed N, Couvreur P. Nanocarriers for antibiotics: a promising solution to treat intracellular bacterial infections. Int J Antimicrob Agents 2014; 43: 485–96.

37 Todoroff J, Vanbever R. Fate of nanomedicines in the lungs. Curr Opin Colloid Interface Sci 2011; 16: 246–54.

38 Pouton CW. Lipid formulations for oral administration of drugs: non-emulsifying, self-emulsifying and 'self-microemulsifying' drug delivery systems. Eur J Pharm Sci 2000; 11 Suppl 2: S93–8.

39 Gainza G, Aguirre JJ, Pedraz JL *et al*. rhEGF-loaded PLGA-alginate microspheres enhance the healing of full-thickness excisional wounds in diabetised Wistar rats. Eur J Pharm Sci 2013; 50: 243–52.

40 Ungaro F, d'Angelo I, Coletta C *et al*. Dry powders based on PLGA nanoparticles for pulmonary delivery of antibiotics: modulation of encapsulation efficiency, release rate and lung deposition pattern by hydrophilic polymers. J Control Release 2012; 157: 149–59.

41 Beloqui A, Solinıs MA, Gascon AR *et al*. Mechanism of transport of saquinavir-loaded nanostructured lipid carriers across the intestinal barrier. J Control Release 2013; 166: 115–23.

42 Donaldson K, Stone V, Tran CL *et al*. Nanotoxicology. Occup Environ Med 2004; 61: 727–8.

43 Borm PJ, Kreyling W. Toxicological hazards of inhaled nanoparticlespotential implications for drug delivery. J Nanosci Nanotechnol 2004; 4: 521–31.

44 Jesús Valle MJD, González López F, Sánchez Navarro A. Pulmonary versus systemic delivery of levofloxacin: the isolated lung of the rat as experimental approach for assessing pulmonary inhalation. Pulm Pharmacol Ther 2008; 21: 298–303.

45 Bur M, Henning A, Hein S *et al*. Inhalative nanomedicine: opportunities and challenges. Inhal Tox 2009; 21 Suppl 1: 137–43.

46 Weber S, Zimmer A, Pardeike J. Solid lipid nanoparticles (SLN) and nanostructured lipid carriers (NLC) for pulmonary application: a review of the state of the art. Eur J Pharm Biopharm 2014; 86: 7–22.

47 Bjarnsholt T, Jensen PO, Fiandaca MJ *et al*. *Pseudomonas aeruginosa* biofilms in the respiratory tract of cystic fibrosis patients. Pediatr Pulmonol 2009; 44: 547–58.

48 Loira-Pastoriza C, Todoroff J, Vanbever R. Delivery strategies for sustained drug release in the lungs. Adv Drug Deliv Rev 2014; 75: 81–91.

49 Healy AM, Amaro MI, Paluch KJ *et al*. Dry powders for oral inhalation free of lactose carrier particles. Adv Drug Deliv Rev 2014; 75: 32–52.

50 Pilcer G, Amighi K. Formulation strategy and use of excipients in pulmonary drug delivery. Int J Pharm 2010; 392: 1–19.

51 European Council, 2014. European Pharmacopeia 8.0. Council of Europe: European Directorate for the Quality of Medicines and Healthcare, Strasbourg; 363–5.

52 Konstan MW, Flume PA, Kappler M *et al*. Safety, efficacy and convenience of tobramycin inhalation powder in cystic fibrosis patients: the EAGER trial. J Cyst Fibros 2011; 10: 54–61.

53 Konstan MW, Geller DE, Minic P *et al*. Tobramycin inhalation powder for P. *aeruginosa* infection in cystic fibrosis: the EVOLVE trial. Pediatr Pulmonol 2011; 46: 230–8.

54 Bilton D, Serisier DJ, De Soyza A *et al*. Multicenter, randomized, double-blind, placebo-controlled study (ORBIT 1) to evaluate the efficacy, safety, and tolerability of once daily ciprofloxacin for inhalation in the management of *Pseudomonas aeruginosa* infections in patients with non-cystic fibrosis bronchiectasis. Eur Respiratory J 2011; 38 Suppl 55; 1925.

55 Serisier DJ, Bilton D, De Soyza A *et al*. Inhaled, dual release liposomal ciprofloxacin in non-cystic fibrosis bronchiectasis (ORBIT-2): a randomised, double-blind, placebo-controlled trial. Thorax 2013; 68: 812–7.

56 Waters V, Ratjen F. Inhaled liposomal amikacin. Expert Rev Respir Med 2014; 8: 401–9.

57 Cipolla D, Shekunov B, Blanchard J *et al*. Lipid-based carriers for pulmonary products: preclinical development and case studies in humans. Adv Drug Deliv Rev 2014; 75: 53–80.

58 Meers P, Neville M, Malinin V *et al*. Biofilm penetration, triggered release and *in vivo* activity of inhaled liposomal amikacin in chronic *Pseudomonas aeruginosa* lung infections. J Antimicrob Chemother 2008; 61: 859–68.

59 Bilton D, Pressler T, Falac I *et al*. Phase 3 efficacy and safety data from randomized, multicenter study of liposomal amikacin for inhalation (Arikace™) compared with TOBI® in cystic fibrosis patients with chronic infection due to *Pseudomonas aeruginosa*. In: Posters of the North American Cystic Fibrosis Conference, Salt Lake City, UT, 2013. Poster 235. Cystic Fibrosis Foundation, Bethesda, MD, USA.

60 Ehsan Z, Wetzel JD, Clancy JP. Nebulized liposomal amikacin for the treatment of *Pseudomonas aeruginosa* infection in cystic fibrosis patients. Expert Opin Investig Drugs 2014; 23: 743–9.

61 Moghaddam PH, Ramezani V, Esfandi E *et al*. Development of a nano– micro carrier system for sustained pulmonary delivery of clarithromycin. Powder Technol 2013; 239: 478–83.

62 Cheow WS, Chang MW, Hadinoto K. Antibacterial efficacy of inhalable levofloxacin-loaded polymeric nanoparticles against *E. coli* biofilm cells: the effect of antibiotic release profile. Pharm Res 2010; 27: 1597–609.

63 Cheow WS, Chang MW, Hadinoto K. Antibacterial efficacy of inhalable antibiotic-encapsulated biodegradable polymeric nanoparticles against *E. coli* biofilm cells. J Biomed Nanotechnol 2010; 6: 391–403.

64 Duan J, Vogt FG, Li X *et al*. Design, characterization, and aerosolization of organic solution advanced spray-dried moxifloxacin and ofloxacin dipalmitoylphosphatidylcholine (DPPC) microparticulate/ nanoparticulate powders for pulmonary inhalation aerosol delivery. Int J Nanomedicine 2013; 8: 3489–505.

65 Chono S, Suzuki H, Togami K *et al*. Efficient drug delivery to lung epithelial lining fluid by aerosolization of ciprofloxacin incorporated into PEGylated liposomes for treatment of

respiratory infections. Drug Dev Ind Pharm 2011; 37: 367–72.

66 Ong H, Traini D, Cipolla D *et al*. Liposomal nanoparticles control the uptake of ciprofloxacin across respiratory epithelia. Pharm Res 2012; 29: 3335–46.

67 Ong HX, Benaouda F, Traini D *et al*. *In vitro* and ex vivo methods predict the enhanced lung residence time of liposomal ciprofloxacin formulations for nebulisation. Eur J Pharm Biopharm 2014; 86: 83–9.

68 Yim D, Blanchard JD, Mudumba S *et al*. The development of inhaled liposome-encapsulated ciprofloxacin to treat cystic fibrosis. In: Dalby RN, Byron PR, Peart J *et al*., eds. Respiratory Drug Delivery. River Grove, IL: Davis Healthcare International, 2006; 425–8.

69 Sweeney LG, Wang Z, Loebenberg R *et al*. Spray-freeze-dried liposomal ciprofloxacin powder for inhaled aerosol drug delivery. Int J Pharm 2005; 305: 180–5.

70 Finlay W, Lange C, Li W*et al*. Validating deposition models in disease: what is needed? J Aerosol Med 2000; 13: 381–5.

71 Liu C, Shi J, Dai Q *et al*. In-vitro and in-vivo evaluation of ciprofloxacin liposomes for pulmonary administration. Drug Dev Ind Pharm 2015; 41: 272–8.

72 Alhariri M, Omri A. Efficacy of liposomal bismuth-ethanedithiol-loaded tobramycin after intratracheal administration in rats with pulmonary *Pseudomonas aeruginosa* infection. Antimicrob Agents Chemother 2013; 57: 569–78.

73 Halder KK, Mandal B, Debnath MC *et al*. Chloramphenicol-incorporated poly lactide-co-glycolide (PLGA) nanoparticles: formulation, characterization, Technetium-99m labeling and biodistribution studies. J Drug Target 2008; 16: 311–20.

74 Veloira WG, Domenico P, LiPuma JJ *et al*. *In vitro* activity and synergy of bismuth thiols and tobramycin against Burkholderia cepacia complex. J Antimicrob Chemother 2003; 52: 915–9.

75 Pilcer G, Vanderbist F, Amighi K. Preparation and characterization of spray-dried tobramycin powders containing nanoparticles for pulmonary delivery. Int J Pharm 2009; 365: 162–9.

76 Ungaro F, d'Angelo I, Coletta C *et al*. Dry powders based on PLGA nanoparticles for pulmonary delivery of antibiotics: modulation of encapsulation efficiency, release rate and lung deposition pattern by hydrophilic polymers. J Control Release 2012; 157: 149–59.

77 Rukholm G, Mugabe C, Azghani AO *et al*. Antibacterial activity of liposomal gentamicin against *Pseudomonas aeruginosa*: a time–kill study. Int J Antimicrob Agents 2006; 27: 247–52.

78 Ghaffari S, Varshosaz J, Saadat A *et al*. Stability and antimicrobial effect of amikacin loaded SLN. Int J Nanomedicine 2011; 6: 35–43.

79 Varshosaz J, Ghaffari S, Mirshojaei SF *et al*. Biodistribution of amikacin solid lipid nanoparticles after pulmonary delivery. Biomed Res Int 2013; 2013: 136859.

80 Pastor M, Moreno-Sastre M, Esquisabel A *et al*. Sodium colistimethate loaded lipid nanocarriers for the treatment of *Pseudomonas aeruginosa* infections associated with cystic fibrosis. Int J Pharm 2014; 477:485-94

OBJECTIVES

Cystic fibrosis (CF) is a genetic disorder that affects an estimate of 80,000 individuals worldwide, being chronic pulmonary infections with *Pseudomonas aeruginosa* the main cause of morbidity and mortality in these patients. Lung infections are treated with antibiotics but since the rise of bacterial resistances and the lack of new antibiotics coming into the market, nanoengineered drug delivery systems (DDS) have emerged as a promising strategy to combat infectious diseases. The use of these DDS may overcome some of the limitations associated with conventional antimicrobial agents such as inadequate drug concentrations at target infections sites or severe side effects. Nowadays, both tobramycin and sodium colistimethate are the first-choice options for inhaled therapy to treat respiratory infections in CF patients. Moreover, the pulmonary route allows to deliver high doses of drug directly to the site of infection, while minimizing systemic exposure and risk of toxicity.

Taking all the above into account, the main objective of the present work was to develop and evaluate lipid nanoparticles as vehicles for antibiotic delivery by pulmonary administration for the treatment of lung infections associated with cystic fibrosis. To accomplish this purpose, three specific goals were considered:

1. To develop, optimize and *in vitro* characterize solid lipid nanoparticles (Colist-SLNs) and nanostructured lipid carriers (Colist-NLCs) for the delivery of sodium colistimethate. To analyze their antimicrobial activity against *P. aeruginosa* clinical isolates from CF patients. The last scope of this work was to gain insight into the biodistribution of the nanoformulations after their pulmonary administration to mice.

2. To evaluate the stability of sodium colistimethate-loaded lipid nanoparticles (Colist-SLNs and Colist-NLCs) after 12 months of storage according to the International Conference of Harmonization (ICH Q1 A, R2) specifications: i) 5$^{\text{o}}$C, ii) 25$^{\text{o}}$C and 60% relative humidity (RH), iii) 30$^{\text{o}}$C and 65% RH and iv) 40$^{\text{o}}$C and 75% RH by means of their physico-

chemical characteristics, biopharmaceutical properties and antimicrobial activity in order to establish the most suitable conditions for their storage.

3. To elaborate and fully characterize *in vitro* tobramycin-loaded nanostructured lipid carriers (Tb-NLCs) able to exert an effective antibacterial activity against *P. aeruginosa* infections. To evaluate the capacity of the nanoparticles to overcome an artificial mucus barrier and, finally, to examine their biodistribution after pulmonary administration to mice.

EXPERIMENTAL DESIGN

Chapter 1

Sodium colistimethate loaded lipid nanocarriers for the treatment of *Pseudomonas aeruginosa* infections in cystic fibrosis

Sodium colistimethate-loaded lipid nanocarriers for the treatment of *Pseudomonas aeruginosa* infections in cystic fibrosis

Marta Pastor[a,b], María Moreno-Sastre[a,b], Amaia Esquisabel[a,b], Eulàlia Sans[c], Miguel Viñas[c] Daniel Bachiller[d,e], Víctor José Asensio[d], Ángel Del Pozo[f], Eusebio Gainza[f], José Luis Pedraz[a,b]

[a]NanoBioCel Group, Laboratory of Pharmaceutics, University of the Basque Country (UPV/EHU), School of Pharmacy, Paseo de la Universidad 7, 01006 Vitoria-Gasteiz, Spain.
[b]Biomedical Research Networking Center in Bioengineering, Biomaterials and Nanomedicine (CIBER-BBN). Vitoria-Gasteiz, Spain.
[c]Department of Pathology and Experimental Therapeutics. Medical School. University of Barcelona-IDIBELL, Barcelona, Spain.
[d]Fundación Investigaciones Sanitarias Islas Baleares (FISIB), Development and Regeneration Program, Ctra. Sóller km 12, Bunyola (Balearic Islands) 7110, Spain.
[e]Consejo Superior de Investigaciones Científicas (CSIC), Ctra. Sóller km 12, Bunyola (Balearic Islands) 7110, Spain.
[f]B.R.A.I.E., Hermanos Lumiere 5, Miñano 01510, Spain.

Abstract

Lung impairment is the most life-threatening factor for cystic fibrosis patients. Indeed, *Pseudomonas aeruginosa* is the main pathogen in the pulmonary infection of these patients. In this work, we developed sodium colistimethate loaded lipid nanoparticles, namely, solid lipid nanoparticles (SLN) and nanostructured lipid carriers (NLC), as a strategy to enhance the antimicrobial therapy against *P. aeruginosa* in cystic fibrosis patients. The nanoparticles obtained displayed a 200-400 nm size, high drug entrapment (79-94%) and a sustained drug release profile. Moreover, both SLN and NLC presented antimicrobial activity against clinically isolated *P. aeruginosa*. The integrity of the nanoparticles was not affected by nebulization through a mesh vibrating nebulizer. Moreover, lipid nanoparticles appeared to be less toxic than free sodium colistimethate in cell culture. Finally, an *in vivo* distribution experiment showed that nanoparticles spread homogenously through the lung and there was no migration of lipid nanoparticles to other organs, such as liver, spleen or kidneys.

1. Background

Cystic fibrosis (CF) is an autosomal recessive disorder caused by mutations in the gene encoding for the CF transmembrane conductance regulator (CFTR) protein (Gibson *et al*., 2003). The absence of functional CFTR protein in the membrane of epithelial cells leads to chronic pulmonary disease, recidivant respiratory infections, pancreatic dysfunction, high electrolytes level in sweat and male infertility (WHO, 2002). It is estimated that 1 out of 2500 Caucasian newborns might be affected by CF, being the most common autosomal recessive disease (Sims *et al*., 2005). CFTR mutations cause malfunctioning of the membrane-bound cAMP regulated chloride channel, which in turn, produces plugs of mucus, obstruction and bronchial infections in the lung, constituting the main limiting factor of the disease in terms of morbidity and mortality (Heijerman *et al*., 2009; Ratjen *et al*., 2009). Among the pathogens that affect the CF patients, *Pseudomonas aeruginosa* (PA) is the most prevalent, but

the treatment of its infections is often difficult due to the wide range of antimicrobial resistance of this species. This resistance to antimicrobials is a well documented phenomenon due to several molecular mechanisms such as the restricted outer membrane permeability, the presence of integron, insertion sequences, and the biosynthesis of degrading-enzymes (Fuste *et al*., 2013; Ruiz-Martinez *et al*., 2011a; Ruiz-Martinez *et al*., 2011b). *P. aeruginosa* infections usually start as an acute infection that finally becomes chronic. One of the main pathogenicity factors that favors P. *aeruginosa* colonization and resistance is its ability to develop a biofilm-like mucus layer in the viscous hypoxic media of CF patients' respiratory tract (Koch, 2002; Worlitzsch *et al*., 2002).

Currently, the preferred treatment is a high dose of inhaled antibiotic along with oral ciprofloxacin (Proesmans *et al*., 2013). The spread of multi-resistant bacteria strains together with the lack of new antibacterial agents drove the

recovery of old antibiotics to treat CF patients and to apply new technologies, such as nanotechnology, to fight infections. Nowadays, both tobramycin and sodium colistimethate are the first-choice option for inhaled therapy to treat respiratory infections in CF patients (Heijerman *et al*., 2009). Although both the antibiotics proved to be effective against *P. aeruginosa,* they produced local side effects. Moreover, their administration is time consuming, is conditioned by unpredictable systemic drug absorption and needs education and training. All these facts together induces poor adherence to the treatment (Heijerman *et al*., 2009).

Over the last decades, lipid nanoparticles have emerged as a promising drug delivery system that could overcome some limitations of the already existing drugs. Since only a few new antimicrobial entities have been discovered over the last years (Gould and Bal, 2013), nano-encapsulation of antibiotics is a good alternative for improving current treatments. Pulmonary delivery of lipid nanoparticles presents many advantages, such as, mucoadhesion, biodegradability, avoidance of first pass effect and hence the possibility to reduce the dose, good tolerability, deep lung deposition of drug and a sustained release of the API that leads to a longer dosing interval (Andrade *et al*., 2013; Weber *et al*., 2014). Many research groups have focused their efforts in developing inhalable nanoparticles to fight against bacterial resistances by encapsulating different drugs, such as amikacin (Ghaffari *et al*., 2011), tobramycin (Ungaro *et al*., 2012), ciprofloxacin (Chono *et al*., 2008; Wong *et al*., 2003), itraconazole (Alvarez *et al*., 2007) or amphotericin B (Gilani *et al*., 2011).

Taking the above into consideration, the aim of this work is to elaborate and fully characterize sodium colistimethate loaded lipid nanoparticles to be used in the treatment of infections in CF patients. Furthermore, the antimicrobial activity of the nanoparticles was assessed against a collection of P. *aeruginosa* strains isolated from CF patients. Finally, the *in vivo* pulmonary distribution was assessed.

2. Methods

2.1. Preparation of lipid nanoparticles

Two sodium colistimethate loaded formulations were elaborated, namely solid lipid nanoparticles (Colist-SLN) and nanostructured lipid carriers (Colist-NLC). An emulsion solvent evaporation technique was chosen for the preparation of Colist-SLN by modifying the procedure reported elsewhere (Soares *et al.*, 2013). Briefly, 10 mg of antibiotic (Sigma-Aldrich, St. Louis, MO, USA) were mixed with a 5% (w/v) Precirol® ATO 5 (Gattefossé, Madrid, Spain) dichloromethane solution. Then, the organic phase and an aqueous surfactant containing solution (Poloxamer 188 at 1% w/v and Polysorbate 80 at 1% w/v) were mixed and emulsified by sonication at 20 W for 30 s (Branson Sonifier 250, Danbury, CT, US). The solvent was allowed to evaporate by magnetic stirring for 2 h at room temperature. Subsequently, the resulting SLNs were washed by centrifugation in Amicon® centrifugal filtration units (100,000 MWCO, Merck Millipore) at 2500 rpm for 15 min three times. For the Colist-NLC

elaboration, a hot melt homogenization technique was selected (Beloqui *et al.*, 2013; Obeidat *et al.*, 2010). In brief, Precirol1 ATO 5 and Miglyol® 812 (Sasol, Johannesburg, South Africa) were selected as the lipid core. Those lipids were mixed with the API and heated above the melting temperature of the solid lipid. The surfactant solution consisted of 1.3% (w/v) of Polysorbate 80 and 0.6% (w/v) of Poloxamer 188. The lipid and aqueous solutions were heated to the same temperature and then emulsified by sonication for 15 s at 20 W. Nanoparticles were stored at 4⁰C overnight to allow lipid re-crystallization and particle formation. Then, a washing step was undergone by centrifugation at 2500 rpm in Amicon® centrifugal filtration units (100,000 MWCO) three times. All the nanoparticles prepared were freeze-dried with two different cryoprotectants, either D-mannitol or trehalose (15%).

For the preparation of infrared (IR) labeled NLC, the IR-783 dye was selected (Sigma-Aldrich). The use of IR-labeled NLC enables particle observation in the near infra-red

(NIR) region that it is known to avoid tissue auto-fluorescence problems. NIR dye has been previously encapsulated in heparin–folic conjugates and demonstrated its ability to remain inside the nanoparticles (Yue *et al.*, 2013). The NLCs were prepared just as mentioned previously, but by adding 50 mg of IR-783 instead of the antibiotic. The washing step was performed three times by centrifugal filtration and trehalose 15% (w/w) was added prior to the freeze drying.

2.2. Characterization of lipid nanoparticles

2.2.1. Size and zeta potential

The particle size and zeta potential (ζ) were measured in a Zetasizer Nano ZS (Malvern Instruments, Worcestershire, UK) based on dynamic light scattering (DLS).

2.2.2. Microscopy analysis

Lipid nanoparticles were analyzed under transmission electron microscopy (TEM). Firstly, a negative staining was performed and after that the samples were observed. In addition, lipid nanoparticles were imaged in air by using an Atomic Force Microscope (AFM) XE-70 (Park Systems, Suwon, Korea). All images were collected in a non-contact mode. Four types of images were simultaneously acquired with several scan sizes (100 μm^2, 25 μm^2 and 6.25 μm^2) at a scan rate of 0.3 - 0.5 Hz.

2.2.3. Encapsulation efficiency

Non-entrapped sodium colistimethate was determined from the supernatants recollected after centrifugation. The amount of non-encapsulated drug was detected by HPLC (see Section 2.2.4). For the IR-labeled nanoparticles, dye loading was calculated spectrophotometrically at 800 nm. The supernatant samples were diluted to 10 ml and compared to a calibration curve (5-80 $\mu g/ml$). In both cases, the encapsulation efficiency (EE) was calculated following this equation:

$$EE\,(\%) = 100 \times \frac{\text{Drug or dye}_{initial} - \text{Drug or dye}_{non\text{-}encapsulated}}{\text{Drug or dye}_{initial}}$$

2.2.4. Determination of sodium colistimethate by HPLC

The quantification of sodium colistimethate was conducted by a high performance liquid chromatographic (HPLC) technique adapted from Cancho Grande *et al.* (2000) and using a Waters 1525HPLC Binary Pump, UV-detector Waters 2487 and Waters 717 plus autosampler (Waters Corp., Milford, USA). The system was controlled by the Empower software. The column selected was a Novapak C18 x 150 mm with a 4 mm pore size. The mobile phase consisted of 77% of an aqueous solution and 23% of acetonitrile. The aqueous phase was prepared by dissolving (7.1 g) sodium sulphate, (0.6 g) acetic acid and (2.2 g) phosphoric acid and adjusted to pH 2.5 with tryethylamine up to 1 l. Sodium colistimethate was detected at 206 nm wavelength. The flow rate was fixed at 1.5 ml/min for isocratic elution, and 50 µl were set as an injected sample volume. This analytic technique was validated following EMA guidance for bioanalytical methods (Committee for Medicinal Products for Human Use, CHMP, 2011).

The assay was found to be linear for 100–800 µg/ml. Absence of interference was confirmed as the mobile phase and surfactant presented no peak under these conditions at this wavelength.

2.2.5. *In vitro* release profile

An amount ranging from 25 to 35 mg of each formulation was accurately weighed and incubated in 4 ml of PBS. At pre-established time points samples were centrifuged in Amicon® centrifugal filtration units (100,000 MWCO) for 15 min. The supernatants were then analyzed for drug quantification by HPLC. The PBS withdrawn was replaced with fresh medium. Results were expressed as percentage of drug released compared to the total encapsulated drug. The assay was run in triplicate for each formulation, Colist-SLN, Colist-NLC and IR-NLC.

2.2.6. Nebulization study

In order to study whether the nebulization through a mesh vibrating equipment (eFlow® rapid, PARI GmbH, Starnberg, Germany) could affect lipid nanoparticles properties, different analysis were

performed after nebulization, i.e., size and zeta potential determination and TEM observation, as previously mentioned at Sections 2.2.1 and 2.2.2.

2.2.7. Microbiological experiment

2.2.7.1. Isolation of *P. aeruginosa* strains.

Samples were recovered from the sputum of CF patients. Further steps were performed in order to select and identify the different P. *aeruginosa* strains (Ruiz *et al.*, 2004). In brief, the samples obtained were harvested and microbiological assays were performed, i.e., morphology observation of short Gram-negative bacilli. Moreover, colony observation was performed in McConkey agar, Blood agar, TSA and MHA at 37 ^{o}C for 24–48 h. Furthermore, several biochemical assays were conducted such as, oxidase test, oxidative/ fermentative test (O/F), and Kliger medium assay. These isolated strains were compared to control strains *P. aeruginosa* ATCC 27853, *E. coli* ATCC 25922, *Staphylococcus aureus* ATCC 29213 and *Enterococcus faecalis* ATCC 29212.

2.2.7.2. MIC determination

Nanoparticles and free sodium colistimethate were tested in 31 *P. aeruginosa* isolates from patients (see Section 2.2.7.1) selected for these experiments, among whose 13 were mucoid and 18 non-mucoid. Freeze-dried nanoparticles were resuspended in MHBCA and placed in the first row of 96-well plates. Next, starting from 32 µg/ml of antimicrobial agent, decreasing concentrations of nanoparticles were obtained by serial two-fold dilutions. Then, 5 ml of 10^4 CFU/ml of bacteria was used as inoculums, and added to each well. Finally, plates were incubated for 24 h at 37°C. Negative controls were defined as well without both bacteria and antimicrobial whereas positive bacterial growth controls were antibiotic-lacking wells. In addition, free antibiotic was also assessed. The minimum inhibitory concentration (MIC) was defined as the lowest antibiotic concentration that can prevent visible bacterial growth. The assay was run by triplicates.

2.2.8. Cell experiments

2.2.8.1. Inhibition concentration 50, IC50.

Cells were grown in Dulbecco's Modified Eagle Growth Medium (DMEM) supplemented with 10% foetal bovine serum (FBS), 1% L-glutamine, 1% penicillin/streptomycin solution and 1% of minimum essential medium-non essential amino acids 100x (MEM-NEAA) at 37°C and 5% CO_2. The median inhibition concentration (IC50) was determined for Colist-SLN and Colist- NLC on A549 and H441 cells (ATCC). For this purpose, decreasing concentrations of nanoparticles starting from 10 mg/ml to 0.07812 mg/ml were added to the cells and incubated at 37 ± 2°C and 5% CO_2 for 24 h. First, cells were seeded at a density of 12,000 cells per well in a 96-well plate and after overnight incubation, lipid nanoparticles were added to the wells and diluted in DMEM supplemented with 0.5% serum. Cell viability was assessed by means of the Cell Counting Kit 8 (CCK-8, Sigma- Aldrich) after a washing step. With this aim, 10% of CCK-8 reagent was added to each well and incubated in a wet chamber for 4 h at 37 ± 2°C and 5% CO_2. Subsequently, the absorbance was read at 450 nm and at 650 nm as the reference wavelength. The absorbance was directly proportional to the number of living cells in culture. The results are given as 50% of living cells (IC50), meaning that this dose inhibits the growth of the 50% of the population. The test was run in triplicates for each sample.

2.2.8.2. *In vitro* cytotoxicity.

The cytotoxicity of Colist-SLN and Colist-NLC was determined against A549 and H441 cells by incubating them with different concentrations of nanoparticles for 24, 48 and 72 h at 37 ± 2°C and 5% CO_2. Cells were seeded at a density of 12,000 cells per well and after overnight incubation, lipid nanoparticles, diluted in DMEM supplemented with 0.5% serum, were added to the wells from 78.1 up to 2500 µg/ml. After performing a washing step, cell viability was analyzed by means of the CCK-8. Subsequently, 10% of CCK-8 reagent was added to each well and incubated in a wet chamber for 4 h at

$37 \pm 2°C$ and 5% CO_2. The test was run in triplicates for each sample.

2.3. *In vivo* biodistribution study

Mice were treated in accordance with the Directive 2010/63/EU of the European Parliament and of the Council of 22 September 2010 on the protection of animals used for scientific purposes. This animal study was approved by the Bioethics Committee of the Balearic Islands University (CEEA 06/11/13). Certified animal technicians observed mice regularly in all the studies and took steps to maintain animal welfare and prevented undue suffering. The animals were maintained under controlled environmental conditions (20-24 $\pm$ 1°C, 40-65% $\pm$ 5% humidity, and 12-hour light/dark cycle), with free access to standard food (A04 diet, Panlab) and tap water in makrolon III cages (Tecniplast). Eight B6SJLF1 males (Charles River) were used to study the biodistribution of IR-labeled lipid nanoparticles.

Each mouse was administered 1.66 mg of IR-labeled NLCs by means of an inhalation tower (Buxco, Wilmington, NC, USA). At 0, 2.5, 4, 24 and 48 h after inhalation, groups of two mice were sacrificed by ketamin/xylazin anaesthesia overdose. Skin and peritoneal tissue were removed and lungs dissected for imaging. IR recordings were performed with a LI-COR Pearl® impulse small animal imaging system (LI-COR Corporate). The image J (NIH, USA) Java-based image analysis program was chosen for RGB brightness measurement of the images of the 800 nm channel. In brief, the whole lung area was selected and the mean brightness value of the green channel in ABU (arbitrary brightness units) was calculated.

2.4. Statistical analysis

All data are expressed as mean $\pm$ standard deviation (SD). All statistical calculations were carried out using the SPSS® 19.0 (SPSS® Inc., Chicago, IL, US). Kruskal-Wallis and one-way ANOVA program and post-hoc test were used for multiple group comparisons.

Table 1. Characteristics of sodium colistimethate loaded lipid nanoparticles.

Formulation	Cryoprotectant	Size (nm)[a]	Polydispersity index (PDI)[a]	Zeta potential (mV)[a]
Colist-NLC	Trehalose	412.5 ± 13.9	0.442	-21.97 ± 1.72
	D-Mannitol	254.5 ± 20.3	0.339	-26.10 ± 7.05
Colist-SLN	Trehalose	303.4 ± 39.5	0.276	-20.80 ± 1.63
	D-Mannitol	302.6 ± 20.5	0.361	-20.50 ± 6.09
IR-NLC	Trehalose	439.3 ± 20.1	0.439	-23.03 ± 1.80

[a] The results are expressed as the mean ± S.D (n=3).

3. Results

### 3.1. Nanoparticle characterization

Nanoparticles displayed a mean diameter size of 412.5 ± 13.9 nm and 303.4 ± 39.5 nm, for Colist-NLC and Colist-SLN, respectively, when trehalose was used as cryoprotectant. The addition of D-mannitol led to particle sizes of 254.5 ± 20.3 nm for Colist-NLC and 302.6 ± 20.5 nm for Colist-SLN. In addition, the polydispersity index was below 0.5, i.e., 0.442 and 0.276 for trehalose containing Colist-NLC and Colist-SLN and 0.361 and 0.339 for D-Mannitol Colist-NLC and Colist-SLN, respectively. All the nanoparticles elaborated presented a negative zeta potential, around -21 mV. Likewise, IR-labelled NLC displayed a 439.3 ± 20.1 nm size and -23.03 ± 1.8 mV of charge, very similar to the antibiotic loaded NLCs. Table 1 summarizes the characterization data of the nanoparticles prepared. As Figure 1 shows, TEM images revealed that the nanoparticles presented an almost spherical shape. Similarly, in the topography images obtained by AFM it becomes possible to observe the shape, structure and differences of the sample surface, confirming that particles were spherical and presented a smooth surface. Amplitude images accentuating the edges give roughness and height information, showing that particles were mainly smooth and flat. Finally, the phase images showed variations in elasticity and viscoelasticity of the sample.

The impact of nebulization on the properties of lipid nanoparticles was studied in terms of size, zeta potential and TEM. A mesh vibrating nebulizer was selected for this purpose. Size distribution and polydispersity index varied from thepre-nebulization to the post-nebulization sample, i.e. from 488 nm to 573 nm. Similarly, zeta potential changed from -20.8 to -25.3 mV, although it remained to be negative. These slight variations were not statistically significant.

As TEM images showed (Figure 1), nebulization did not affect nanoparticle morphology. Once the nanoparticles were prepared, the supernatants were quantified by HPLC in order to calculate the EE indirectly (Figure 2). High encapsulation efficiencies were achieved for Colist-SLN, Colist-NLC and IR-NLC, i.e., $79.70 \pm 6.06\%$, $94.79 \pm 4.20\%$ and $98.94 \pm 0.01\%$, respectively.
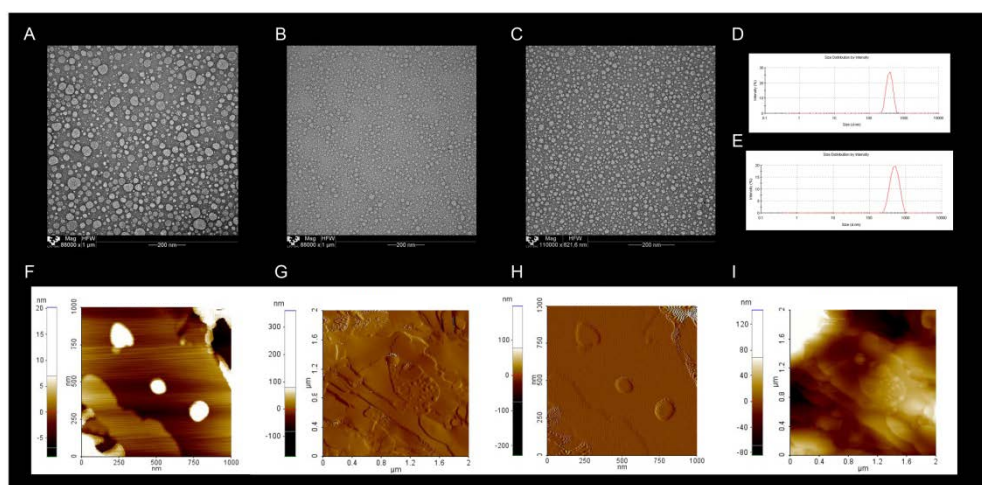
Figure 1. Transmission electron microscopy images of sodium colistimethate-loaded lipid nanoparticles, A) SLN, B) NLC after reconstitution, and C) NLC after nebulisation with vibrating mesh nebulizer. Size analysis results, D) Colist-NLC after reconstitution, and E) Colist-NLC after nebulisation with vibrating mesh nebulizer. F-I atomic force microscopy images, F and G) sodium colistimethate-loaded SLN and H and I) sodium colistimethate-loaded NLC.
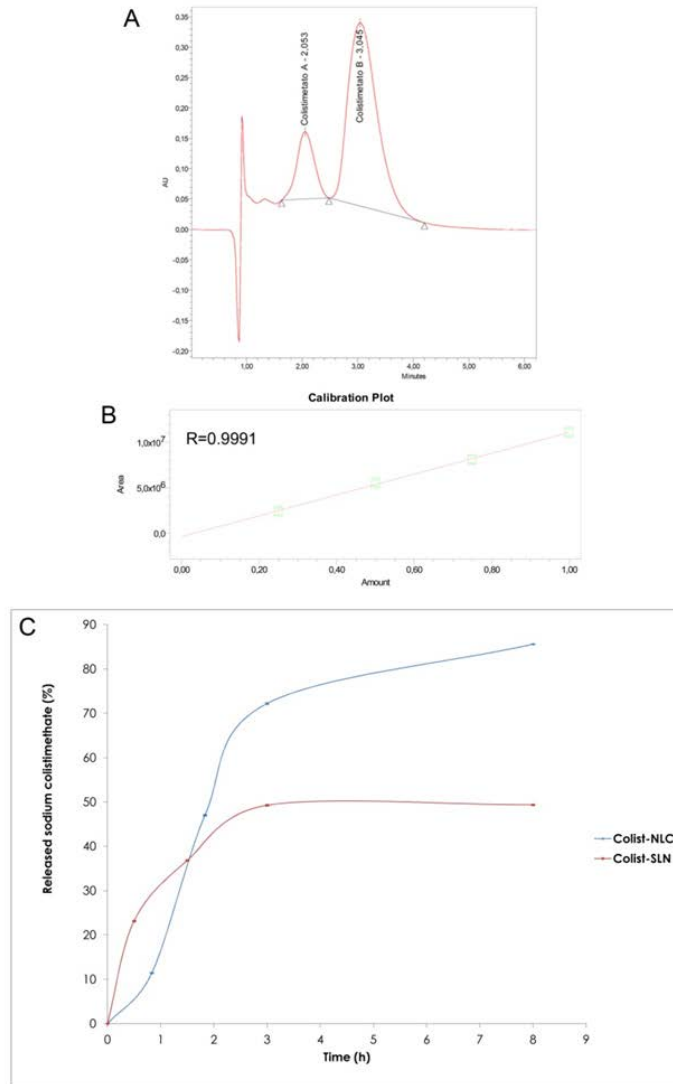
Figure 2. Sodium colistimethate determination. A) The two peak chromatogram of the API from the supernatants of the lipid nanoparticles. B) Calibration plot of the standard. C) Release profile of sodium colistimethate from the lipid nanoparticles.

Regarding the release profile, a sustained release of the antibiotic was detected for both Colist-SLNs and Colist-NLCs. As Figure 2C displays, an initial burst release was detected for all the nanoparticles. By the end of the study, a 49.3% and 85.6% of sodium colistimethate was released from Colist-SLN and Colist-NLC, respectively. With regard to the IR-labeled NLC, a slower profile was detected, releasing $18.9 \pm 1.1\%$ at the 8th hour and the $25.47 \pm 0.68\%$ of the dye content in 48h, the end of the *in vivo* sampling time points.

3.2. Microbiological experiments

P. aeruginosa is frequently isolated from sampling the respiratory tract of cystic fibrosis patients. It is also well known that both mucoid and non-mucoid types can be isolated. Figure 3A shows petri dishes containing both types of colonies. These species are characterized by its shape and size (short Gram-negative rods). Moreover, when grown on McConkey agar, lactose negative, greyish colonies were detected. In blood agar, bacterial growth was noticed, presenting beta-hemolysis in most cases. In TSA (Trypticase Soy Agar) at 42°C bacterial growth is disclosed and green coloring is detected in most of the isolates. Regarding biochemical testing, all strains presented oxidase positive results, oxidative metabolism and were strictly aerobic.

Turning to MIC determination, both Colist-NLCs and Colist-SLNs showed to be active against clinically isolated *P. aeruginosa* growth. As Figure 3B exhibits, the free antibiotic solution presented a mode of 2 µg/ml, whereas NLCs (irrespective of the cryoprotectant) displayed a 1 µg/ml MIC. The inhibitory concentration found for Colist-SLNs was 2 µg/ml. When nanoparticles were freeze dried with D-mannitol, a lower activity was determined in both cases. Although the MIC remained similar for both Colist-NLC and Colist-SLN, the final percentage of isolates susceptible to the formulation was lower when D-mannitol was incorporated, i.e., 64% vs 77% of isolates were susceptible to D-mannitol Colist-NLC and trehalose Colist-NLC, respectively at 1 µg/ml.
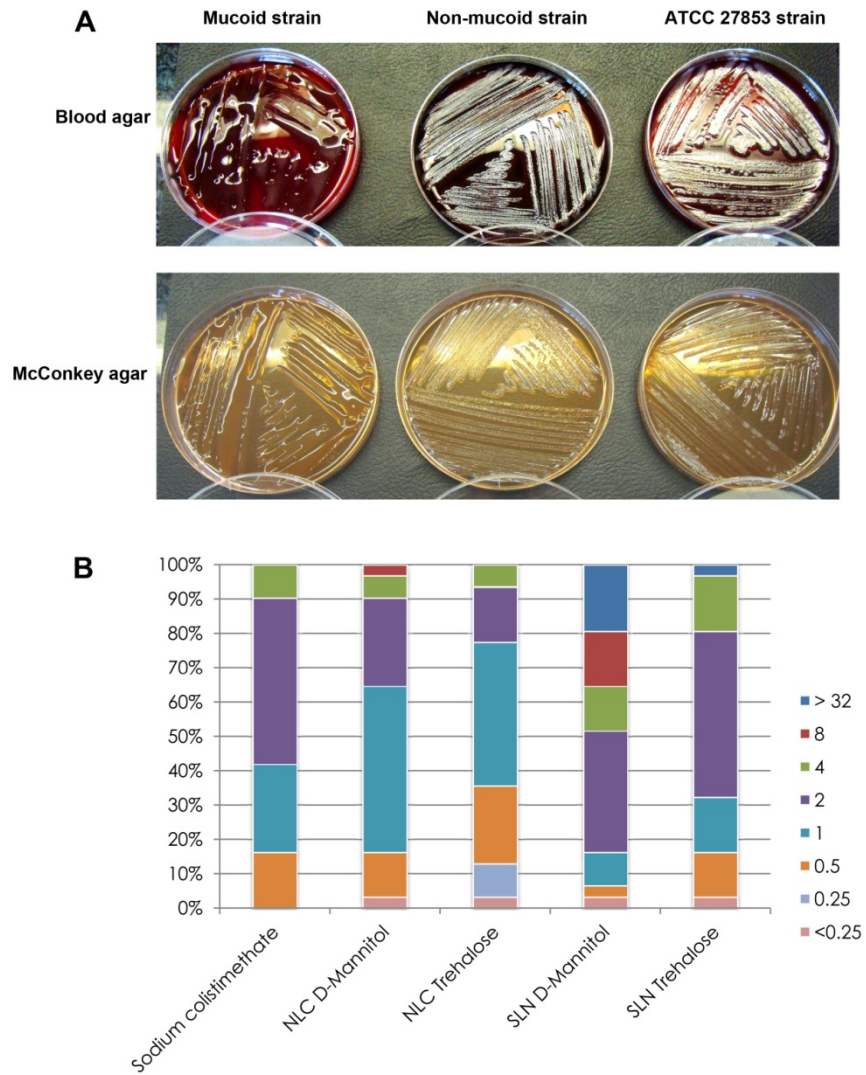
Figure 3. Microbiological experiments. A) Isolated *Pseudomonas aeruginosa* strains. Left column, mucoid strain, middle column no-mucoid strains and right column control *P. aeruginosa* from ATCC. First row represents the morphology in blood agar and second row growth in McConkey Agar. B) Bioactivity of elaborated lipid nanoparticles in terms of MIC determination in 31 strains of clinically isolated *P. aeruginosa* samples.

In the case of SLNs, 51% of isolates incubated with D-mannitol Colist-SLN and 80% of those with trehalose Colist-SLN were not able to grow at a 2 µg/ml concentration. It is noteworthy that free sodium colistimethate was unable to inhibit microorganism growth bellow 0.5 µg/ml, while lipid nanoparticles presented antimicrobial activity at 0.25 µg/ml. It should be also underlined that lipid nanoparticles were able to prevent microbial growth of the mucoid *P. aeruginosa* isolates.

As the D-mannitol containing lipid nanoparticles led to higher MIC values, trehalose was defined as the cryoprotectant to use in the following experiments. Finally, it should be underlined that NLCs presented most satisfactory results, compared to the SLNs.

3.3. Cell experiments

The IC50 of the lipid nanoparticles developed was estimated by CCK8 assay in two cell lines, H441 human lung papillary adenocarcinoma and A549 human lung carcinoma, as showed in Figure 4A. It has been previously analysed and reported in a systemic review by Doktorovova *et al.* that in terms of toxicity studies no differences in susceptibility could be achieved to the fact of employing normal or cancel cell lines. Therefore, we chose these cell lines as they came from a lung cell lineage that is the intended route of administration for the nanoparticles elaborated (Doktorovova *et al.*, 2014). The IC50 represents half of the maximum inhibitory concentration. Hence, the lower the IC50 value, the higher the toxicity. Firstly, it could be concluded that the H441 cell line presented a more sensitive behaviour displaying a lower IC50 compared to the A549 cell line. For both cell lines, sodium colistimethate showed the lowest IC50, therefore displaying the highest toxicity, 0.0065 ± 0.0007 mg/ml and 0.080 ± 0.103 mg/ml for H441 and A549, respectively. Among the lipid nanoparticles, Colist-NLC exhibited the highest IC50 ($p<0.01$) 1.08 ± 0.19 mg/ml and 2.59 ± 0.87 mg/ml for H441 and A549, respectively. Interestingly, these IC50 values are far from the 1-2 µg/ml that was
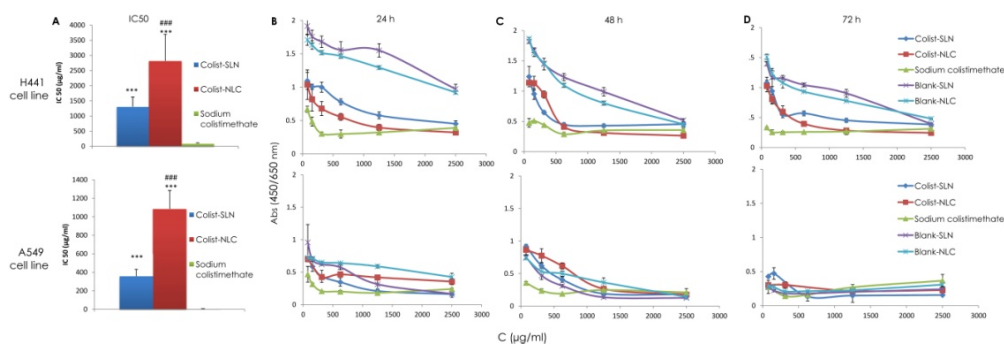
Figure 4. Cell experiments results. (A) represents the IC50 value of the formulation in both cell lines. *** describes statistically significant difference between the formulation and the free sodium colistimethate, p<0.01 and ### represents differences between Colist-NLC and Colist-SLN, p<0.01. B-D) *In vitro* cytotoxicity measured by means of CCK8 at 24h (B), 48h (C) and 72h (D). Upper row: cytotoxicity tested against H441 cell line, second row: cytotoxicity in the A549 cell line.

estimated as MIC in section 3.2., therefore, it could be inferred that lipid nanoparticles might be a safe product. These results were statistically significant compared to sodium colistimethate (p<0.01). Overall, it should be pointed out that enclosing the antibiotic in lipid nanoparticles led to a huge decrease in toxicity, as NLCs presented 160-fold less toxicity in H441 cells and 28-fold less toxicity in A549 cells than the free antibiotic. Moreover, it should be highlighted that Colist-NLC was statistically less toxic than Colist-SLN (p<0.01).

Regarding the cytotoxicity of the formulations three exposure times, 24h, 48h and 72h, and six different concentrations were assessed (78.13-2500 µg/ml). Both the H441 and A549 cell lines were used in the test. In the CCK 8 assay the number of living cells was estimated by the bio-reduction of the reagent leading to formazan. The results obtained suggest that sodium colistimethate encapsulation enhances cell viability especially at concentrations bellow 1,250 µg/ml. As described in Figures 4B-D, it could be observed that at the lowest concentration, sodium

colistimethate exhibited lower absorbance values than the nanoencapsulated formulation, thus less living cells. On the other hand, the absorbance value of sodium colistimethate became even lower as the exposure time was longer. NLCs presented higher absorbance values than SLNs when assessed in the A549 cell line. Nevertheless, the cell viability was quite similar for Colist-SLN and Colist-NLC when tested in H441 cell line. Blank lipid nanoparticles showed to be less toxic that antibiotic loaded nanoparticles when testing in H441 cells. Nevertheless, under the A549 cell line, unloaded lipid nanocarriers displayed almost the same absorbance value than loaded ones.

3.4. *In vivo* biodistribution study

Due to a more suitable release profile of NLCs along with a lower MIC and higher IC50, the IR-labeled NLCs were selected for the *in vivo* distribution experiment. Similarly, trehalose was chosen as cryopreservation agent. In this work, an inhalation tower was used to administer the nebulized lipid nanoparticles to mice. The inhalation tower enables a homogeneous dose distribution among the experimental animals. Moreover, the more aggressive intratracheal administration was avoided and the associated anaesthesia eluded. Each mouse was administered 1.66 mg of IR-labeled NLCs and IR images were recorded (Figure 5). At 0 h, immediately after the nebulization was completed, the whole body images showed abundant NLC presence in the snout and the oropharyngeal cavity, the most exposed areas to the inhalation device. Two and half hours later, swallowing and breathing have displaced most NLCs to the respiratory and digestive tracks; at this time point NLCs were homogenously distributed in both lungs and remained there until the end of the study. When comparing brightness intensities in the lungs at different time points, it could be observed that the strongest signal was displayed after 2.5 h (Figure 5A). In fact, a 1.5-fold increase in the arbitrary brightness units (ABU) value could be measured when comparing time 0 and time 2.5 h.
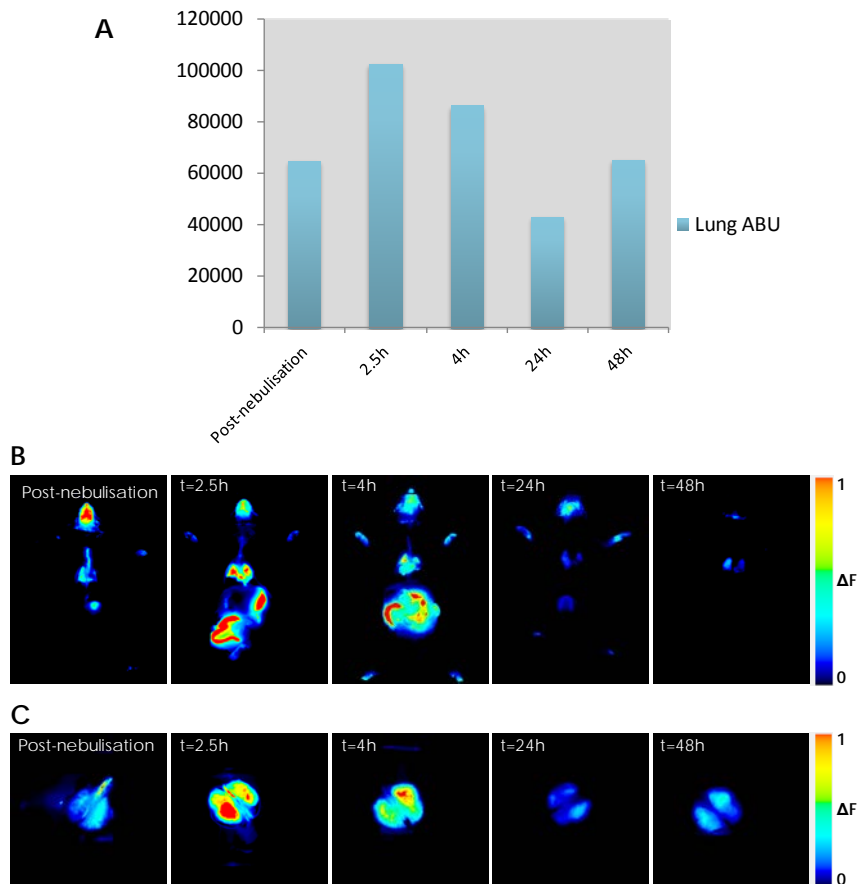
Figure 5. *In vivo* results of IR-NLC distribution after inhalation. A) Bar graph showing the mean brightness intensity in arbitrary brightness units (ABU) of the whole area of each lung pair. B and C) Pseudo-colour image representing the spatial distribution of photon counts in whole animals and lungs respectively, immediately after nebulization and at 2.5, 4, 24 and 48 h after IR-NLC inhalation. Fluorescence intensity in the 800 nm channel is related to an external reference to make images of different animals and time points comparable.

The signal at 4 h remained strong, whereas recordings at 24 h and 48 h showed a progressive decrease in intensity. No IR emission was detected in other organs, such as liver, kidney, or spleen at any time point during the experiment. It is also worth mentioning that in spite of the relatively high doses of NLCs detected in

lungs and intestine, the animals did not show any symptomatology association with the uptake. It is likely, therefore, that the nanocarriers have negligible systemic toxicity. Nevertheless, further animal experiments would be required to confirm the safety of the formulation.

The use of an inhalation tower to administer nanoparticles to mice enabled a homogeneous dose delivery throughout the lungs of the animals. Furthermore, this method led to a broad distribution of NLCs across the organ that could be detected up to 48 h after nebulization. It remains to be studied, however, whether the residual dose detected after 48 h could have an impact on the clinical outcome of the treatment of the disease.

4. Discussion

As detailed in this work, we prepared sodium colistimethate loaded lipid nanoparticles focusing on the treatment of *P. aeruginosa* in cystic fibrosis patients. The use of lipid nanoparticles gave rise to a potential enhancement of the treatment. We obtained high encapsulation efficiencies (SLN 79.7% and NLC 94.8%) that are in accordance with the results reported by Martins *et al*. who also described high EE values (>90%) for camptothecin loaded SLN. Their slightly higher results are likely to be related to the higher lipophilicity of camptothecin compared to sodium colistimethate (Martins *et al*., 2012). Likewise, Patlolla *et al*. (2010) reported similar encapsulation efficiency values when encapsulating Celecoxib in NLCs, >90%. Hence, the lipid nanoparticles described in this work presented acceptable EE values, comparable to those reported previously. Turning to the release profile of the nanoparticles, NLCs released an 86% of sodium colistimethate in 8 h and SLNs a 50%, data that were similar to those reported by Silva *et al*. (2012) for risperidone loaded SLN, i.e., 40% drug released by the 8th hour. Similarly, Zheng *et al*. also detected almost a 100% of drug release form their NLCs (Zheng *et al*., 2013). Remarkably, it could be observed that almost all the drug was released from

the Colist-NLC under the assayed conditions. This sustained release, especially the one presented by the Colist-NLC, could reduce the number of doses, improving patient adherence to the treatment and, thus, life quality. The release profile of the dye was much slower than that observed for sodium colistimethate, very likely due to its lipophilicity (Yue *et al.*, 2013). Indeed, this delayed release is very helpful for the *in vivo* imaging in order to ensure that the IR dye detected in mice is closely related to the dye incorporated into the NLCs.

Regarding the microbiological assays, other authors, such as Omri, described much higher MIC values for *P. aeruginosa* ATCC 27853, 4.0 ± 1.0 µg/ml, when incorporating Polymixin B in liposomes. Nevertheless, the MIC values were even higher when the free Polymixin B was assessed (Omri *et al.*, 2002). Wang *et al.* (2012) reported also the utility of lipid nanoparticles for tilmicosin, a macrolide, encapsulation reporting a MIC of 4.0 µg/ml. It is should be underlined that the lipid nanoparticles described in this work presented MIC values around 1-2 mg/ml and were active against the mucoid strains.

As far as cell experiments are related, it should be remarked that, in agreement with our finding, Nassimi *et al.* reported that blank SLN displayed very high IC50 values (analysed by MTT, (3-(4,5-dimethylthiazole-2-yl)- 2,5- diphenyl-tetrazolium bromide, and NRU, Neutral Red Uptake), that is 2-3 mg/ml. Although the assays were conducted under the same cell line, the results could not be directly compared as they used other techniques for determination of cell viability (Nassimi *et al.*, 2010). On an average, as reported by Doktorovova after the analysis of their published data concerning IC50, this value is usually within 0.1–1 mg/ml for lipid nanoparticles, being in our case slightly superior for Colist-NLC, 2.82 mg/ml and 1.08 mg/ml for A549 and H441, respectively (Doktorovova *et al.*, 2014). In terms of cell viability, Ribeiro de Souza described that praziquantel-loaded SLN presented a time and dose-dependent cell viability in a

hepatoma cell line, reaching up to a 70% decrease of cell viability for the free drug and 45% decrease for the loaded SLN (Souza *et al.*, 2014). Overall, it could be concluded that sodium colistimethate encapsulation led to lower toxicity values. Sodium colistimethate is transformed to colistin that is the active molecule and it is known to present an increased toxicity. Lately, due to the Gram-negative resistance, the use of colistin has re-emerged despite its side effects and toxicity (Sukhadeve *et al.*, 2012). Hence, based on these *in vitro* results, it could be postulated that enclosing sodium colistimethate into lipid nanoparticles decreases the toxicity of both the pro-drug, sodium colistimethate, and the drug, colistin, mainly because they are released in a controlled manner over time.

Finally, as the *in vivo* biodistribution has shown, NLCs displayed a suitable tissue disposition, spreading extensively throughout the lungs. Similarly, Taratula *et al.* (2013) reported that NLC presented a uniform distribution through the lungs 24 h post-nebulization, whereas i.v.

administration led to only 23% of NLCs retained in the lungs.

5. Conclusions

Taking into account the results described in this work, in terms of antimicrobial activity and toxicity, lipid nanoparticles seem to us an encouraging alternative to the currently available cystic fibrosis therapies. NLCs distributed homogenously through the respiratory tract and remained in the target tissue for at least 48 h. Furthermore, it is remarkable that both Colist-SLNs and Colist-NLCs are effective against mucoid *P. aeruginosa*. Besides, the side effects of the active drug, colistin, could be ameliorated because of the sustained drug release. Moreover, based on the release of the antibiotic and the homogeneous distribution through the lungs, the results suggest that the number of doses could be diminished. Yet other studies should be conducted in order to assess the bioavailability of sodium colistimethate and to transform the

elaborated lipid nanoparticles into an optimized inhalable CF therapy.

References

Alvarez, C.A., Wiederhold, N.P., McConville, J.T., Peters, J.I., Najvar, L.K., Graybill, J.R., Coalson, J.J., Talbert, R.L., Burgess, D.S., Bocanegra, R., Johnston, K.P., Williams III, R.O., 2007. Aerosolized nanostructured itraconazole as prophylaxis against invasive pulmonary aspergillosis. J. Infect., 55, 68-74.

Andrade, F., Rafael, D., Videira, M., Ferreira, D., Sosnik, A., Sarmento, B., 2013. Nanotechnology and pulmonary delivery to overcome resistance in infectious diseases. Adv. Drug Deliv. Rev., 65, 1816-1827.

Beloqui, A., Solinís, M.Á., Gascón, A.R., del Pozo-Rodríguez, A., des Rieux, A., Préat, V., 2013. Mechanism of transport of saquinavir-loaded nanostructured lipid carriers across the intestinal barrier. J. Control. Release, 166, 115-123.

Cancho Grande, B., García Falcón, M., Pérez-Lamela, C., Rodríguez Comesaña, M., Simal Gándara, J., 2000. Quantitative analysis of colistin and tiamulin in liguid and solid medicated premixes by HPLC with diode-array detection. Chromatographia, 53, S460-S463.

Chono, S., Tanino, T., Seki, T., Morimoto, K., 2008. Efficient drug targeting to rat alveolar macrophages by pulmonary administration of ciprofloxacin incorporated into mannosylated liposomes for treatment of respiratory intracellular parasitic infections. J. Control. Release, 127, 50-58.

Committee for Medicinal Products for Human Use, CHMP, 2011. European Medicines Agency. Guideline on Bioanalytical Method Validation. Available at: http://www.ema.europa.eu/docs/en_GB/document_library/Scientific_guideline/2011/08/WC500109686.pdf, (accessed 04.11.14.).

Doktorovova, S., Souto, E.B., Silva, A.M., 2014. Nanotoxicology applied to solid lipid nanoparticles and nanostructured lipid carriers – a systematic review of *in vitro* data. Eur. J. Pharm. Biopharm., 87, 1-18.

Fuste, E., Lopez-Jimenez, L., Segura, C., Gainza, E., Vinuesa, T., Viñas, M., 2013. Carbapenem-resistance mechanisms of multidrug-resistant *Pseudomonas aeruginosa*. J. Med. Microbiol., 62, 1317-1325.

Ghaffari, S., Varshosaz, J., Saadat, A., Atyabi, F., 2011. Stability and antimicrobial effect of amikacin loaded SLN. Int. J. Nanomed., 6, 35-43.

Gibson, R.L., Burns, J.L., Ramsey, B.W., 2003. Pathophysiology and management of pulmonary infections in cystic fibrosis. Am. J. Respir. Crit. Care Med., 168, 918-951.

Gilani, K., Moazeni, E., Ramezanli, T., Amini, M., Fazeli, M.R., Jamalifar, H., 2011. Development of respirable nanomicelle carriers for delivery of amphotericin B by jet nebulization. J. Pharm. Sci., 100, 252-259.

Gould, I., Bal, A., 2013. New antibiotic agents in the pipeline and how they can help overcome microbial resistance. Virulence, 4, 185-191.

Heijerman, H., Westerman, E., Conway, S., Touw, D., 2009. Inhaled medication and inhalation devices for lung disease in patients with cystic fibrosis: A European consensus. J. Cys.t Fibros., 8, 295-315.

Koch, C., 2002. Early infection and progression of cystic fibrosis lung disease. Pediatr. Pulmonol., 34, 232-236.

Martins, S., Tho, I., Reimold, I., Fricker, G., Souto, E., Ferreira, D., Brandl, M., 2012. Brain delivery of camptothecin by means of solid lipid nanoparticles: Formulation design, *in vitro* and *in vivo* studies. Int. J. Pharm., 439, 49-62.

Nassimi, M., Schleh, C., Lauenstein, H.D., Hussein, R., Hoymann, H.G., Koch, W., Pohlmann, G., Krug, N., Sewald, K., Rittinghausen, S., Braun, A., Müller-Goymann, C., 2010. A toxicological evaluation of inhaled solid lipid nanoparticles used as a potential drug delivery system for the lung. Eur. J. Pharm. Biopharm., 75, 107-116.

Obeidat, W.M., Schwabe, K., Müller, R.H., Keck, C.M., 2010. Preservation of nanostructured lipid carriers (NLC). Eur. J. Pharm. Biopharm., 76, 56-67.

Omri, A., Suntres, Z.E., Shek, P.N., 2002. Enhanced activity of liposomal polymyxin B against *Pseudomonas aeruginosa* in a rat model of lung infection. Biochem. Pharmacol., 64, 1407-1413.

Patlolla, R.R., Chougule, M., Patel, A.R., Jackson, T., Tata, P.N.V., Singh, M., 2010. Formulation, characterization and pulmonary deposition of nebulized celecoxib encapsulated nanostructured lipid carriers. J. Control. Release, 144, 233-241.

Proesmans, M., Vermeulen, F., Boulanger, L., Verhaegen, J., De Boeck, K., 2013. Comparison of two treatment regimens for eradication of *Pseudomonas aeruginosa* infection in children with cystic fibrosis. J. Cyst. Fibros., 12, 29-34.

Ratjen, F., Brockhaus, F., Angyalosi, G., 2009. Aminoglycoside therapy against *Pseudomonas aeruginosa* in cystic fibrosis: A review. J. Cyst. Fibros., 8, 361-369.

, M.A., Ruiz, N., Viñas, M., 2004. Relationship between clinical and environmental isolates of *Pseudomonas aeruginosa* in a hospital setting. Arch. Med. Res., 35, 251-257.

Ruiz-Martinez, L., Lopez-Jimenez, L., d'Ostun, V., Fusté, E., Vinuesa, T., Viñas, M., 2011a. A mechanism of carbapenem resistance due to a new insertion element (ISPa133) in

Pseudomonas aeruginosa. Int. Microbiol., 14, 51-58.

Ruiz-Martinez, L., Lopez-Jimenez, L., Fuste, E., Vinuesa, T., Martinez, J.P., Viñas, M., 2011b. Class 1 integrons in environmental and clinical isolates of *Pseudomonas aeruginosa*. Int. J. Antimicrob. Agents, 38, 398-402.

Silva, A.C., Kumar, A., Wild, W., Ferreira, D., Santos, D., Forbes, B., 2012. Long-term stability, biocompatibility and oral delivery potential of risperidone-loaded solid lipid nanoparticles. Int. J. Pharm., 436, 798-805.

Sims, E.J., McCormick, J., Mehta, G., Mehta, A., 2005. Neonatal screening for cystic fibrosis is beneficial even in the context of modern treatment. J. Pediatr., 147, S42-S46.

Soares, S., Fonte, P., Costa, A., Andrade, J., Seabra, V., Ferreira, D., Reis, S., Sarmento, B., 2013. Effect of freeze-drying, cryoprotectants and storage conditions on the stability of secondary structure of insulin-loaded solid lipid nanoparticles. Int. J. Pharm., 456, 370-381.

Souza, A.L.R.d., Andreani, T., de Oliveira, R.N., Kiill, C.P., Santos, F.K.d., Allegretti, S.M., Chaud, M.V., Souto, E.B., Silva, A.M., Gremião, M.P.D., 2014. *In vitro* evaluation of permeation, toxicity and effect of praziquantel-loaded solid lipid nanoparticles against *Schistosoma mansoni* as a strategy to improve efficacy of the schistosomiasis treatment. Int. J. Pharm., 463, 31-37.

Sukhadeve, K., Apte, M., Waghmare, P., 2012. Colistin for bad bugs. Pediatr. Infect. Dis., 4, 168-171.

Taratula, O., Kuzmov, A., Shah, M., Garbuzenko, O.B., Minko, T., 2013. Nanostructured lipid carriers as multifunctional nanomedicine platform for pulmonary co-delivery of anticancer drugs and siRNA. J. Control. Release, 171, 349-357.

Ungaro, F., d'Angelo, I., Coletta, C., d'Emmanuele di Villa Bianca, R., Sorrentino, R., Perfetto, B., Tufano, M.A., Miro, A., La Rotonda, M.I., Quaglia, F., 2012. Dry powders based on PLGA nanoparticles for pulmonary delivery of antibiotics: Modulation of encapsulation efficiency, release rate and lung deposition pattern by hydrophilic polymers. J. Contro. Release, 157, 149-159.

Wang, X.F., Zhang, S.L., Zhu, L.Y., Xie, S.Y., Dong, Z., Wang, Y., Zhou, W.Z., 2012. Enhancement of antibacterial activity of tilmicosin against *Staphylococcus aureus* by solid lipid nanoparticles *in vitro* and *in vivo*. Vet. J., 191, 115-120.

Weber, S., Zimmer, A., Pardeike, J., 2014. Solid Lipid Nanoparticles (SLN) and Nanostructured Lipid Carriers (NLC) for pulmonary application: A review of the state of the art. Eur. J. Pharm. Biopharm., 86, 7-22.

WHO, 2002. The Molecular Genetic Epidemiology of Cystic Fibrosis. Report of a Joint Meeting of WHO/ECFTN/ICF(M)A/ECFS, 1-26.

Wong, J.P., Yang, H., Blasetti, K.L., Schnell, G., Conley, J., Schofield, L.N., 2003. Liposome delivery of ciprofloxacin against intracellular Francisella tularensis infection. J. Control. Release, 92, 265-273.

Worlitzsch, D., Tarran, R., Ulrich, M., Schwab, U., Cekici, A., Meyer, K.C., Birrer, P., Bellon, G., Berger, J., Weiss, T., Botzenhart, K., . Yankaskas, J.R., Randell, S., Boucher, R.C., Döring, G., 2002. Effects of reduced mucus oxygen concentration in airway *Pseudomonas* infections of cystic fibrosis patients. J. Clin. Invest., 109, 317-325.

Yue, C., Liu, P., Zheng, M., Zhao, P., Wang, Y., Ma, Y., Cai, L., 2013. IR-780 dye loaded tumor targeting theranostic nanoparticles for NIR imaging and photothermal therapy. Biomaterials, 34, 6853-6861.

Zheng, M., Falkeborg, M., Zheng, Y., Yang, T., Xu, X., 2013. Formulation and characterization of nanostructured lipid carriers containing a mixed lipids core. Colloids Surf. Physicochem. Eng. Aspects, 430, 76-84.

Chapter 2

Stability study of sodium colistimethate-loaded lipid nanoparticles

Stability study of sodium colistimethate-loaded lipid nanoparticles

María Moreno-Sastre[a,b,#], Marta Pastor[a,b,#], Amaia Esquisabel[a,b], Eulàlia Sans[c], Miguel Viñas[c,d], Daniel Bachiller[e,f], José Luis Pedraz[a,b]

[a]NanoBioCel Group, Laboratory of Pharmaceutics, University of the Basque Country, School of Pharmacy, Paseo de la Universidad 7, Vitoria-Gasteiz 01006, Spain.
[b]Biomedical Research Networking Center in Bioengineering, Biomaterials and Nanomedicine (CIBER-BBN). Vitoria-Gasteiz, Spain.
[c]Department of Pathology and Experimental Therapeutics, Medical School, University of Barcelona-IDIBELL, Barcelona, Spain.
[d]IINFACTS, CESPU, Gandra, Portugal.
[e]Fundación Investigaciones Sanitarias Islas Baleares (FISIB), Development and Regeneration Program, Ctra. Sóller km 12,07110 Bunyola (Balearic Islands), Spain.
[f]Consejo Superior de Investigaciones Científicas (CSIC), Ctra. Sóller km 12, Bunyola (Balearic Islands) 07110, Spain.

[#]Both authors contributed equally.

Abstract

In the last decades, the encapsulation of antibiotics into nanoparticulate carriers has gained increasing attention as drug delivery systems for the treatment of infectious diseases. Sodium colistimethate-loaded solid lipid nanoparticles (Colist-SLNs) and nanostructured lipid carriers (Colist-NLCs) were designed in this study aiming to treat the pulmonary infection associated to cystic fibrosis patients. Nanoparticles were freeze-dried using trehalose as cryoprotectant. The stability of both nanoparticles was analyzed over one year according to the International Conference of Harmonization (ICH) guidelines by determining the minimum inhibitory concentration (MIC) against clinically isolated *Pseudomonas aeruginosa* strains and by studying their physico-chemical characteristics. The results showed that Colist-SLNs lost their antimicrobial activity at the third month; however, the antibacterial activity of Colist-NLCs was maintained throughout the study within an adequate range (MIC ≤ 16 μg/mL). In addition, Colist-NLCs exhibited suitable size (≤ 500 nm), zeta potential (≤ -20 mV), morphology and release profile at 5°C and 25°C/ 60% relative humidity over one year. Altogether, Colist-NLCs proved to have better stability than Colist-SLNs.

1. Introduction

Over the last decades, the use of lipid nanoparticles (NPs) for drug delivery in pharmaceutical technology has been extensively investigated (Das and Chaudhury 2011). Lipid nanoparticles show interesting features concerning their therapeutic application as they are able to incorporate a great variety of substances. In this regard, solid lipid nanoparticles (SLNs) have emerged as promising nanosystems to encapsulate drugs in the submicron range, from about 50 nm to 1000 nm. SLNs are composed of biocompatible and biodegradable lipids building a solid lipid matrix core but due to their low drug loading and unpredictable drug release, nanostructured lipid carriers (NLCs) have been developed as a second generation of lipid nanoparticles (Muller *et al*., 2000). The main difference between them is the structure of the lipid matrix that in the NLCs is composed of a mixture of solid and liquid lipids resulting in a less-ordered matrix with many imperfections that permit the increase of drug loading and prevent its leakage (Muller *et al*., 2007).

In principle, these NPs present some advantages over other drug delivery systems such as a controlled drug delivery, specific targeting, good tolerability, the ability to incorporate lipophilic and hydrophilic drugs and the possibility to protect the drug from degradation (Weber *et al*., 2014). Nevertheless, the major obstacle that limits the use of these nanoparticles is their physical or chemical instability in aqueous suspensions (Chacon *et al*., 1999). To overcome this drawback, the water content must be removed to convert the nanoparticle suspension into a solid phase formulation able to display suitable stability for long term storage. For this purpose of improving stability, freeze-drying, also known as lyophilization, is the technique usually applied in the pharmaceutical and technological industry (Abdelwahed *et al*., 2006). This process consists on removing the water from a frozen sample by sublimation and desorption under vacuum, hence

decreasing hydrolysis phenomena (Jennings, 1999). Before freezing the sample, the addition of cryoprotectants might be required to protect the nanoparticles against mechanical stress of ice crystals or to prevent their aggregation. The most commonly used cryoprotectants are sugars like glucose, trehalose, sucrose and mannitol. Trehalose is widely used as it possesses low hygroscopicity, very low chemical reactivity and also high glass transition temperature (Crowe *et al*., 1996; Schwarz and Mehnert 1997). It has been shown that samples lyophilized in the presence of sugars with high transition temperature (T_g) show less tendency to aggregate during storage as compared to sugars with lower Tg such as sucrose or glucose (Molina *et al*., 2004).

Sodium colistimethate, which is rapidly hydrolyzed to its active form (colistin), is a polypeptide antibiotic known to have potential bactericidal activity against a broad range of Gram-negative bacteria that is being administered in patients with pulmonary infections, particularly those suffering from with cystic fibrosis (Dijkmans *et al*., 2014). *Pseudomonas aeruginosa* is the main pathogen that affects cystic fibrosis patients showing a significant increase in its resistance to antimicrobial drugs in the last years. Sodium colistimethate has demonstrated its efficiency in combating this bacterium (minimum inhibitory concentration, MIC, susceptibility data ≤ 0.06-16 µg/mL); however, its clinical used is limited due to its toxic effects such as nephrotoxicity and neuromuscular blockade (Falagas and Kasiakou 2005). It has been reported that nano-antibiotics administered by the pulmonary route may increase local drug concentration and avoid systemic adverse effects (Moreno-Sastre *et al*., 2015). In that sense, SLNs and NLCs have emerged as alternative vehicles for antibiotic delivery to the lungs as they can protect the drug from chemical and enzymatic degradation and gradually release it from the lipid matrix in the target site, thus minimizing the toxicity and improving the antimicrobial effect (Huh and Kwon 2011).

In our previous work, the preparation and characterization of sodium colistimethate-loaded SLNs (Colist-SLNs) and NLCs (Colist-NLCs) were described (Pastor *et al.*, 2014). In the present study, the stability of Colist-SLNs and Colist-NLCs after freeze-drying was investigated by determining their antimicrobial activity against several strains of *P. aeruginosa* (ATCC 27853, 056 SJD, 086 SJD) and the maintenance of their physicochemical properties over one year. NPs were stored for 12 months under four different conditions, selected as recommended in the International Conference on Harmonization (ICH) guidelines: a) long-term refrigerator at 5 ± 3°C b) long-term room temperature at 25 ± 2°C/ 60 ± 5% relative humidity (RH), c) intermediate at 30 ± 2°C/ 65% ± 5 RH, and d) accelerate at 40 ± 2°C / 75 ± 5% RH (Grimm 1998; Guideline 2003).

2. Material and methods

2.1 Materials

Precirol® ATO 5 was kindly provided by Gattefossé (Madrid, Spain). Kolliphor® P188 (Poloxamer 188) was a kind gift from BASF (Ludwigshafen, Germany). Tween® 80 was purchased from Panreac Química (Castellar del Vallès, Barcelona, Spain). Miglyol® 812 was provided by Sasol (Johannesburg, South Africa). Sodium colistimethate was purchased from Sigma Aldrich (St. Louis, MO, USA). All the chemicals were of analytical grade.

2.2 Preparation of colistimethate-loaded SLNs and NLCs

SLNs and NLCs containing sodium colistimethate were prepared as previously reported methods (Pastor *et al.*, 2014). Colist-SLNs were elaborated by an emulsion-solvent-evaporation technique. Briefly, 10 mg of sodium colistimethate were mixed with Precirol® ATO 5 as lipid phase and dissolved in dichloromethane solution (5%, w/v). An aqueous solution containing Poloxamer 188 (1%, w/v) and Tween® 80 (1%, w/v) was also prepared. The aqueous phase was added into the lipid phase. Then, the mixture was sonicated at 20 W for 30 seconds (Branson Sonifier 250 Danbury, CT, USA). The resulting emulsion was stirred for 2 hours

allowing the evaporation of the solvent. Subsequently, SLNs were washed by centrifugation in Amicon® centrifugal filtration units (100,000 Da MWCO) at 2,500 rpm for 15 minutes three times.

On the other hand, Colist-NLCs were elaborated by the hot melt homogenization technique. In brief, solid (Precirol® ATO 5) and liquid (Miglyol® 812) lipids at 10:1 were first weighed along with the drug at 10% (w/w) and heated at 60⁰C. In a separate container, Tween® 80 (1.3%, w/v) and Poloxamer 188 (0.6%, w/v) were dissolved in Milli-Q water and heated at the same temperature as the lipid phase. The hot aqueous surfactant solution was poured into the lipid phase and emulsified by sonication for 15 seconds at 20 W. This step produced a nano-emulsion that was stored at low temperature (5 ± 3⁰C) for 12 hours. After that period, the nanoparticles were washed by centrifugation at 2,500 rpm in Amicon® centrifugal filtration units (100,000 Da MWCO) three times. Finally, all the nanoparticles prepared were freeze-dried.

2.3 Freeze-drying of the nanoparticles

Lyophilization of the nanoparticles was used to prolong the stability of Colist-SLNs and Colist-NLCs during storage. Prior to freeze-drying, trehalose (15%, w/w of the lipid solid) was added to the nanoformulations as a cryoprotectant and thereafter were freeze dried for 40 hours (Telstar Lyobeta freeze-dryer, Terrasa, Spain). Freeze-drying cycle can be divided into three steps: freezing, primary drying and secondary drying that is represented in Figure 1. The primary drying took place for 24 hours and the secondary drying step was maintained for 12 hours in order to low humidity in the sample.
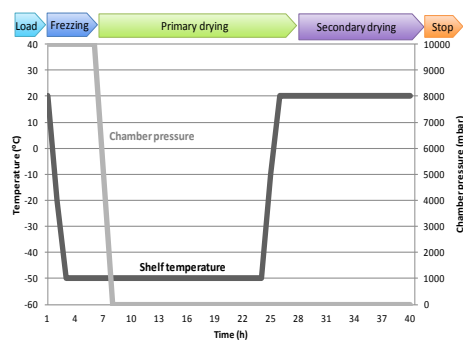
Figure 1. Schedule of the freeze-drying procedure of the SLNs and NLCs.

Table 1. Stability test store conditions of temperature and relative humidity (RH) intervals and sampling time for all the four experiments.

Samples	Groups	Storage conditions	Time points
Colist-NLC Colist-SLN	Long-term refrigerated	$5 \pm 3\,^{\circ}C$	0, 1, 3, 6, 9 and 12 months
	Long-term room temperature	$25 \pm 2\,^{\circ}C$ $60 \pm 5\%$ RH	0, 1, 3, 6, 9 and 12 months
	Intermediate	$30 \pm 2\,^{\circ}C$ $65 \pm 5\%$ RH	0, 1, 3, 6, 9 and 12 months
	Accelerated	$40 \pm 2\,^{\circ}C$ $75 \pm 5\%$ RH	0, 1, 3, 6, 9[*] and 12[*] months

[*]Additional sampling time points not established by the ICH CPMO/ICH/2736/99.

2.4 Stability study

Each different batch of Colist-SLNs and Colist-NLCs was divided into four different sample sets. All samples were stored in plain glass vials (USP type I) in environmental simulation chambers for constant climatic conditions (Binder, Tuttlingen, Germany) according to ICH Q1 A (R2) guidelines (CPMO/ICH/2736/99) that were: $5 \pm 3\,^{\circ}C$, $25 \pm 2\,^{\circ}C/60 \pm 5\%$ RH, $30 \pm 2\,^{\circ}C/65 \pm 5\%$ RH and $40 \pm 2\,^{\circ}C/75 \pm 5\%$ RH (Table 1).

Parameters such as size, zeta potential, morphological characteristics and antimicrobial activity were studied over the time until 12 months of storage and compared to the fresh formulations (after freeze-drying, time 0) so that the changes observed of these characteristics could be attributed to sample exposure to different temperatures and humidity conditions. In addition, a drug release study testing Colist-NLCs was performed at 12 months to ensure the sustained release of the drug by that time. The specifications of the freeze-dried product are described in table 2, these have been established according to the results of the fresh nanoparticles (time 0) and based on previous experience with this type of nanoformulations.

At the beginning of the stability study, an acceptance criterion was established for the microbiological assay stating the maximum MIC at 16 µg/mL. As Colist-SLNs formulations displayed a value higher than 16 µg/mL at the third month, meaning a loss of activity against bacteria, Colist-SLNs were set aside for the stability study for the following months. This is the reason why the drug release test was not carried out for this formulation at the end of the stability study.

Table 2. Specifications of the freeze-dried nanoparticles.

Parameters	Specifications
Size	≤ 500 nm
PDI	≤ 0.5
Zeta potential	≤ -20 mV
Macroscopic appearance	White powder
Microscopic morphology	Spherical shape
Antibacterial activity (MIC)	≤ 16 µg/mL
Drug release profile	≥ 80 % at 24 h

2.5 Characterization

2.5.1 Encapsulation efficiency

The encapsulation efficiency (EE) of sodium colistimethate into NPs was calculated by the following equation:

$$EE\,(\%) = \frac{Drug_{initial} - Drug_{non\text{-}encapsulated}}{Drug_{initial}} \times 100$$

In this method the non-entrapped drug was determined by a high performance liquid chromatography (HPLC) analysis from the supernatants collected after centrifugation. The HPLC technique was performed using a Waters 1525 HPLC Binary Pump (Waters Corp., Milford, USA) with a UV-detector Waters 2487 and Waters 717 plus autosampler adapted, as described in our previous work (Pastor, *et al*. 2014). The system was controlled by the Empower 3 software. A Novapak C18 x 150 mm column with a 4 µm pore size was used as the stationary phase, whereas mixture of acetonitrile and an aqueous solution 23:77 (v/v) was used as mobile phase. The aqueous phase consisted of sodium sulphate (7.1 g/L), acetic (0.6 g/L) and phosphoric acid (2.2 g/L) and adjusted with tryethylamine at pH 2.5. The column temperature, flow rate of mobile phase, injection volume for isocratic elution and detection wavelength were set as 65°C, 1.5 mL/min, 50 µL and 206 nm, respectively. This analytic technique was previously validated following EMA guidance for bioanalytical methods. The

calibration curve was linear (r^2>0.9991) within the concentration range 100-800 µg/mL. The mobile phase and surfactant presented no interference under the assessed conditions.

2.5.2 Particle size and zeta potential

The mean particle size and polydispersity index (PDI) were assessed by photon correlation spectroscopy (also known as dynamic light scattering) and Zeta potential (ZP) was determined by laser doppler velocimetry using a Zetasizer Nano ZS (Malvern Instruments, Ltd., Worcestershire, UK). Prior to the measurements all samples were diluted with purified water to reach a suitable scattering intensity. Measurements were performed at 25°C. Time 0 is considered as the time just after the lyophilization step. All the measurements of each nanoparticle formulation were performed in triplicate**.**

2.5.3 Nanoparticle morphology study

2.5.3.1 Macroscopic characteristics

The physical appearance of Colist-NPs was studied over the time by visual inspection.

2.5.3.2 Microscopic appearance

Nanoparticles morphology was examined by a transmission electron microscope (TEM, Philips CM120) at an accelerating voltage of 120 kV. Samples were prepared by drying a dispersion of the nanoparticles on a copper grid coated with an amorphous carbon film and then negative staining with 1% uranyl acetate for observation.

2.5.4 Measurement of antimicrobial activity

Pseudomonas aeruginosa strains were used to test the antimicrobial activity of the nanoparticles. Microbiological and biochemical assays were performed in order to select and identify the different bacteria, i.e. morphology and colony observation in McConkey agar, Blood agar, TSA (Triptone Soy Agar) and MHA (Mueller Hinton Agar) at 37°C for 24-48 hours, oxidase test, oxidative/fermentative test (O/F), and Kliger medium assay. Among the isolated strains, 056 SJD and 086 SJD that were recovered from the sputum of cystic fibrosis patients were selected for

the stability study, presenting non-mucoid and mucoid characteristics, respectively. Additionally, the *P. aeruginosa* ATCC 27853 strain was also assessed.

The MIC of the free drug and nanoformulations was determined by the broth microdilution method. A bacterial inoculum was prepared from an overnight culture in Mueller–Hinton II Broth Cation-Adjusted (MHBCA) and adjusted to yield 10^4 CFU/well (colony-forming units). The inoculum was then delivered onto 96-well plates containing two-fold serial dilutions of formulations starting from 128 µg/mL. Finally, the plates were incubated for 24 hours at 37℃. Free antibiotic (sodium colistimethate), Colist-SLNs and Colist-NLCs were tested simultaneously against all bacterial strains. The lowest concentration of antibiotic that prevented the appearance of a visible growth was defined as the MIC. All measurements were performed in triplicate.

2.5.5 *In vitro* release profile

A release study was carried out for Colist-NLCs at time 0 and after 12 months to test the effect of the storage at all conditions of temperature and humidity. An accurate amount of the formulation was placed in a tube and incubated at 37℃ in phosphate buffer saline (PBS) as the release medium. The tube was kept on a rotary shaker at 100 rpm. Samples were withdrawn at pre-established time intervals being subsequently centrifuged in Amicon® centrifugal filtration units (100,000 Da MWCO) for 15 minutes. The medium withdrawn was replaced with fresh PBS. The supernatants were then analyzed by HPLC for drug quantification as mentioned in section 2.5.1. Results were expressed as percentage of drug released from the NLCs at different time points. The assay was run in triplicate.

3. Result*s* and discussion

3.1. Encapsulation efficiency

The encapsulation efficiency (EE) was calculated indirectly by determining the amount of drug in the supernatants collected after the washing step. High EEs were achieved for Colist-SLNs and Colist-

NLCs, 79.70 ± 6.06% and 94.79 ± 4.20%, respectively. In agreement with this finding Gainza *et al.* (2013) found that recombinant human epidermal growth factor (rh-EGF)-loaded NLCs presented higher encapsulation efficiencies than SLN-rhEGF (around 95% versus 73%). Similarly, Pardeike *et al.* (2011) achieved a high EE up to 98% for intraconazole in NLCs. It is postulated that the high drug payload described for NLCs is related to the blending of a solid lipid with a liquid lipid leading to a less ordered solid lipid matrix providing the possibility for a high drug encapsulation (Hu *et al.*, 2006). In the case of SLNs, only a solid lipid was used giving rise to an ordered internal structure minimizing loading capacity.

3.2 Particle size and PDI

The maintenance of the nanoparticle diameter size after freeze-drying is considered as a good indication of physical stability (Uner 2006). The particle size is presented as z-average diameter in nanometric scale over the time (Figure 2). The particle size measurement after the elaboration of the nanoparticles was assigned as "time 0" being around 303 nm and 412 nm for Colist-SLNs and Colist-NLCs, respectively.

Colist-SLNs (Figure 2A) met the specifications during the first month of storage at all temperatures ranging from 245 to 336 nm. However, the size requirement (below 500 nm) was only preserved for SLNs stored at 5°C and 25°C after the 3 months. It was observed that there was a progressive increase in size for all temperatures tested, being more remarkable at 30°C and 40°C. In a similar study carried out by Venkateswarlu *et al.* (2004), clozapine-SLNs increased their size two-fold, from 40 to 78.8 nm, after 6 month-storage at 25°C. In relation with our findings, Freitas and co-workers showed a rapid particle growth within 3 days when storing SLN dispersions (consisting of 10% compritol 888 stabilized with 1.2% poloxamer 188) at 50°C. This fact was due to the high film rigidity of the emulsifier (also named microviscosity) that avoided the fusion of the film layers after particle collision. However, at room temperature (20°C) improved stability for
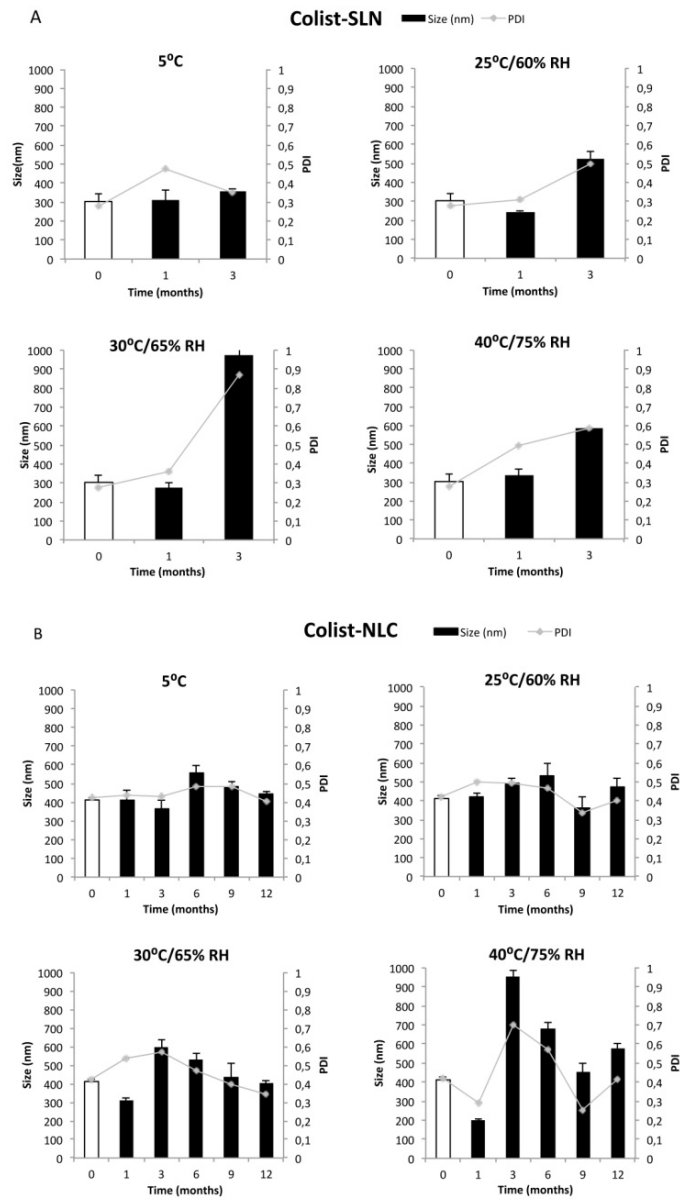
Figure 2. A) Particle size and polidispersity index (PDI) of Colist-SLNs stored at ICH recommendations of temperature and relative humidity (RH) during 3 months. B) Particle size and PDI of Colist-NLCs stored under the same conditions for 12 months (n=3).

3 months and stored the nanoparticles in darkness at 8°C prolong their stability over 3 years. By this time the mean diameter remained almost unchanged from 276 to 297 nm (Freitas and Müller 1998). Del Pozo *et al.* found that SLNs for gene therapy lyophilized with trehalose were physically stable during 9 months at 25°C/60% RH and 6 months at 30°C/65% RH. However, the stability was lost when harder conditions were employed, for example at 40°C/75% RH the size was twice higher than at time 0 resulting in unmeasured aggregates at 6 months (del Pozo-Rodriguez *et al.*, 2009).

On the other hand, Colist-NLCs (Figure 2B) met the requirements set for size at 5°C and 25°C, ranging around 400 nm overall but with a slight growth at the sixth month. However, when Colist-NLCs were stored at higher temperatures, a size enlargement was detected over the third month, exceeding 600 nm at 30°C and 40°C. The particle size fluctuations at the highest temperatures tested indicated that the size of the nanoparticles was influenced by the storage conditions.

Moreover, Das and colleages (2012) reported that clotrimazole-loaded NLCs showed better stability in terms of size than SLNs at 5°C and 25°C after 3 months of storage, especially when a high amount of drug is incorporated to the formulation (10% versus 4% drug to lipid ratio). Kim *et al.* (2010) elaborated itraconazole-loaded NLCs with the solid lipid tristearin and the liquid lipid triolein at different ratios and found sizes less than 500 nm during 90 days of storage at room temperature.

It is known that the average particle diameter of NPs can be influenced by different factors, such as the composition of the formulation, the production technique or the parameters of the process such as time, temperature, pressure, equipment type, lyophilization and storage conditions (Cavalli *et al.*, 1997; Zimmermann *et al.*, 2000). Well-formulated nanosystems should display a narrow particle size distribution in the submicron range. Particles greater than 1 μm and a particle growth over the time can be indicators of physical instability (Haskell *et al.*, 1998). Depending on the

application and route of administration, a particular attention should be paid in size control, for example, particle above 5 μm might cause embolism if they are administered by intravenous injection (Wissing *et al.*, 2004). Furthermore, particle size can modulate the capture mechanism by macrophages and influence their biological stability, as phagocytosis increases when particle size increases; hence, it could influence the biodistribution behavior of the particles. Due to the small size of the NPs developed, they have a greater chance to escape from the clearance mechanism by alveolar macrophages, compared to a microparticulate form (Chono *et al.*, 2006). Moreover, after using a nebulization system, pulmonary deposition depends on the particle size, shape and ventilation parameters; with decreasing particle diameters below 500 nm, the deposition increases in all regions of the lung due to their diffusional mobility (Yang *et al.*, 2008) and they should also be able to diffuse through the mucus pores of chronically infected lungs which typically fall in the range of around 200-500 nm (Suk *et al.*, 2009).

The measurement of the polidispersity index (PDI) indicates the wide distribution of the particle size with values ranging from 0 to 1, and it is also a parameter that is used to evaluate the preservation of nanoparticles. As expected, there were more variations in the PDI at higher temperatures for both formulations (Figure 2). In general, as the particle size increased, the PDI also augmented. The PDI of Colist-SLNs was higher when increasing time and temperature, for instance, in the third month at 30°C and 40°C, the PDI reached the highest values, 0.87 and 0.59, respectively. Only samples stored under 5°C and 25°C displayed PDI values below 0.5. This is in concordance with the PDI values (< 0.5) obtained by Ridolfi *et al* (2012) when testing chitosan-SLN-tretinoin over one year period at room temperature. The PDI of Colist-NLCs at the third month rose up to 0.57 and 0.75 at 30°C and 40°C, respectively, indicating a heterogeneous distribution of the nanoparticles that could be related to

an increase of agglomerates. However, at lower temperatures, all PDIs were less than 0.5 meeting the criteria requirement for the storage conditions, meaning that the samples were monodisperse and homogenous (Zhang *et al*., 2009). Similarly, Das *et al*. (2012) reported that the PDI of clotrimazole-NLC formulations remained practically unchanged during the 3 months of the stability study at 2-8°C and 25°C.

Altogether, the storage conditions at 5°C and 25°C met the specifications of size and PDI for Colist-SLNs and Colist-NLCs after three months and one year of storage, respectively.
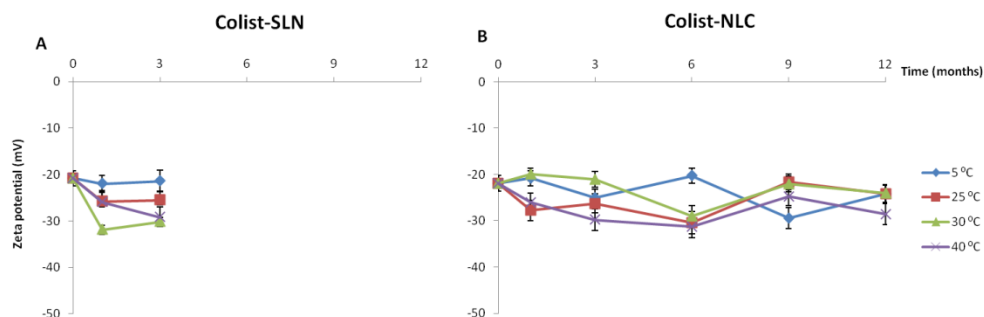
3.3 Zeta potential

The measurement of zeta potential (ZP) is a good method to evaluate the state of nanoparticle surface and to detect any eventual modification during storage. It is also a useful indicator to predict physical stability of the NPs (Freitas and Müller 1998). Positive and negative ZP indicates the degree of repulsion between close and similar particles in the dispersion; this repulsion prevents the aggregation process of particles (Heurtault *et al*., 2003).

After the lyophilization step (time 0), the charge for Colist-SLNs and Colist-NLCs was almost identical, -20.8 mV and -21.97 mV, respectively. These zeta potential values could lead to a decreased risk of particle aggregation and enlargement after re-dispersion due to electric repulsion (Heurtault *et al*., 2003).

The ZP for all Colist-SLNs formulations ranged from -20 to -30 mV during the three months of the study (Figure 3A). Similarly, Radomska-Soukhareve *et al.* (2007) reported no changes in zeta potential of their SLNs formulations (-20 to -30 mV) after two years of storage at 5°C, 25°C and 40°C, as the values at all three temperatures were identical to those of the day of preparation being the most stable ones the SLNs obtained with triglycerides compared to mono- and diglicerides. It could be noticed that when the temperature increased, the zeta potential of Colist-SLNs was more negative, reaching -30.20 mV at 30°C.

Figure 3. A) Representation of zeta potential for Colist-SLNs at 5 ± 3°C, 25 ± 2°C/ 60 ± 5% RH, 30 ± 2°C/ 65% and 40 ± 2°C / 75 ± 5% RH for 3 months. B) Representation of zeta potential for Colist-NLCs at the same conditions for 12 months.

In contrast, Freitas *et al*. stated that the ZP of their SLN formulations decreased with increasing the input of energy (light and temperature) and only the samples stored at 8°C in the dark were physically stable up to 3 years (-22 to -24 mV). They suggested that the energy input increases the kinetic energy of a system and can lead to changes in the crystalline structure of the lipid. In that study only SLN dispersions (without drug) were analyzed (Freitas and Müller, 1998).

Figure 3B shows the zeta potential values obtained for Colist-NLCs that remained below -20 mV (inside the limits of the specification values) at all conditions tested after one year indicating long term stability. Generally, zeta potential value above +20 mV or below -20 mV combined with steric stabilization predicts good stability of the nanoparticle dispersion; therefore, the NLCs prepared are expected to be stable (Das *et al*., 2012). Pardeike *et al*. (2011) found that the zeta potential of itraconazole-loaded NLCs stayed unchanged (around -31 mV) at room temperature and refrigerated conditions after 6-months of storage.

As instability such as aggregation or agglomeration of lipid nanoparticles are indicated by a decrease of the absolute zeta potential value, Colist-NLCs are expected to be stable beyond the observation period (Freitas and Müller, 1998). Moreover, surface electrostatic charge is an important factor influencing the deposition of inhaled nanoparticles. Charged NPs have higher deposition efficiencies as compared to neutrally ones (Yang *et al*., 2008). Moreover, anionic liposomes exhibited longer retention in the lung compared to the neutral liposomes that was attributed to being less prone to aggregate *in vivo* (Beaulac *et al*., 1997).

3.4 Macroscopic and microscopic observation

A critical analysis of freeze-dried products normally includes the visual observation of the final volume and appearance of the cake. An attentive examination of the macroscopic aspect of the nanoparticles was carried out to detect any degradability of the formulation. The freeze-drying process led to a fine white powder at time
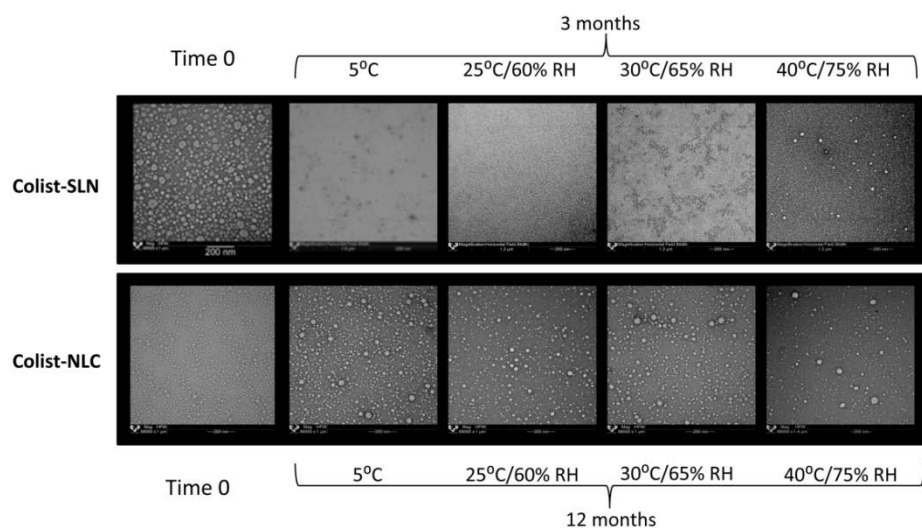
Figure 4. Upper row, transmission electron microscopy (TEM) images of Colist-SLNs at time 0 and the third month at ICH conditions. Lower row, TEM images of Colist-NLCs at time 0 and after 12 months at ICH conditions.

0 for both formulations. Colist-SLNs at the third month (when the stability study was stopped for Colist-SLNs as a result of the MIC data) showed a shrinkage appearance with a rubbery aspect and yellowish-white color especially after undergoing 40°C storage conditions. However, Colist-NLCs maintained the desired characteristics of a freeze-dried pharmaceutical formulation with a powdery aspect at each sample time and until the end of the study. Accordingly, the white color and consistency of nanoparticles remained unaltered. As a result, the effect of storing Colist-NLCs samples during 12 months at 5°C, 25°C and 60% RH, 30°C and 65% RH or as well as 40°C and 75% RH was negligible for their physical appearance. Similarly, Zhou *et al.* (2015) reported that lovastatin-loaded NLC dispersions maintained excellent stability without exhibiting any aggregation, precipitation or phase separation at 4°C for 6 months of storage and also any significant changes in appearance.

The microscopic visualization of the particles allows the observation of the structure of the matrix, the conservation of nanoparticle integrity and to check whether any modifications took place on their morphology during storage. At the beginning of the study (time 0), both NPs were spherical as other authors described. For instance, Sanjula *et al.* (2009) used TEM to study the shape of the lyophilized carvediol-loaded SLNs prepared with stearic acid (oil phase) and Poloxamer 188 (surfactant), revealing that particles were spherical, smooth and uniformly distributed. However, in that case they used mannitol (5%) as cryoprotectant. In another study, spherical and uniform particle sizes were reported for chitosan-coated NLCs (Gartziandia *et al.*, 2015).

TEM images revealed that Colist-SLNs at the third month (Figure 4, upper row) presented aggregation of particles or modifications in particle morphology in all temperatures tested. Scaning electron microscpy (SEM) pictures of amikacin-loaded SLNs dispersions developed by Ghaffari *et al* showed that the particles stored at 4°C for 60 days did not present aggregation, however, when stored at

25°C and 40°C they showed aggregation and particle size enlargement due to the melting of cholesterol used in their composition. On the other hand, SEM photos of redispersed lyophilized particles confirmed that the freeze-drying process did not have any impact on the shape and size of SLNs after 60 days stored at high temperature (40°C) (Ghaffari *et al.*, 2011).

On the contrary, Colist-NLCs (Figure 4, lower row) showed a different behavior compared to Colist-SLNs. The resulting formulation exhibited spherical particles with a homogeneous particle size distribution meaning that Colist-NLCs were well preserved without aggregation or significant changes in morphology after 12 months at different conditions of temperature and humidity. TEM observation confirmed that the size distribution was uniform, which is an important technological property for powders regarding drug release kinetics. Pastor *et al.* (2013) elaborated Eudragit L30 D-55 microparticles using a spray-drying process which did not show any shape modification, confirmed by SEM

observation, assuming ICH conditions. In addition, the physical aspect of the microparticles remained unchanged at each sample time presenting a white powder with no agglomerations and without any visually observable degradation such as erosion or swelling.

3.5 Minimum inhibitory concentration (MIC)

The antimicrobial activity of both types of nanoparticles was analyzed during the stability study for each sample time. For the data analysis, the following acceptance criterion was pre-established: as the MIC of the free antibiotic always led to 8-16 µg/mL throughout all the study; 16 µg/mL MIC was set as the critical concentration. Samples outside that value were dropped off for the stability study.

At the beginning of the study, the MIC values of Colist-SLNs and Colist-NLCs were the same as the free drug. Solleti *et al.* (2015) found that the MIC and minimum bactericidal concentration (MBC) values of liposomal azithromycin (with an average diameter around 406 nm) were

significantly lower than those of free azithromycin against *P. aeruginosa*. Furthermore, other researchers observed better antimicrobial effects testing a liposomal polymyxin B formulation in comparison with the free antibiotic against *P. aeruginosa* strains (Omri *et al.*, 2002) and clinical isolates (Alipour *et al.*, 2008). This enhanced antimicrobial activity could be attributed to the fusional interaction between the membrane phospholipids of the liposomes and the bacterial cells (Alipour *et al.*, 2008). Ghaffari *et al.* (2011) evaluated the antimicrobial activity against *P. aeruginosa* of free amikacin and amikacin-loaded SLN after freeze drying, obtaining MIC values of 8 and 16 µg/mL, respectively.

By the microbiological experiments it could be demonstrated that Colist-SLNs presented antimicrobial activity against ATCC 27853 and 056 SJD strains after one month of storage at different conditions. However, in the third month the MIC exerted was 32 or 64 µg/mL for all temperatures tested except at 5°C (MIC of 16 µg/mL) against two out of the three P.

aeruginosa strains, i.e., ATCC-27853 and 086 SJD (Figure 5A). It should be pointed out that mucoid isolate was less susceptible to Colist-SLN than non- mucoid strains. Overall, it could be inferred that Colist-SLNs were not able to keep their antimicrobial activity after three months of storage and the stability study was stopped for Colist-SLNs. In contrast, Wang *et al* prepared norfloxacin loaded-SLNs suspensions that after stored at 4°C and room temperature presented the same MIC against *Escherichia coli* as that of the native norfloxacin (0.2 µg/mL) for 9 months demonstrating drug stability (Wang *et al.*, 2012).

On the other hand, the antimicrobial efficiency of Colist-NLCs was retained during 12 months against all the strains tested as the MIC values always were ≤16 µg/mL, even during storage under harder conditions of temperature and humidity (Figure 5B). These results demonstrated that sodium colistimethate encapsulated into NLCs was capable of preserving the antimicrobial activity during the storage period at ICH conditions.
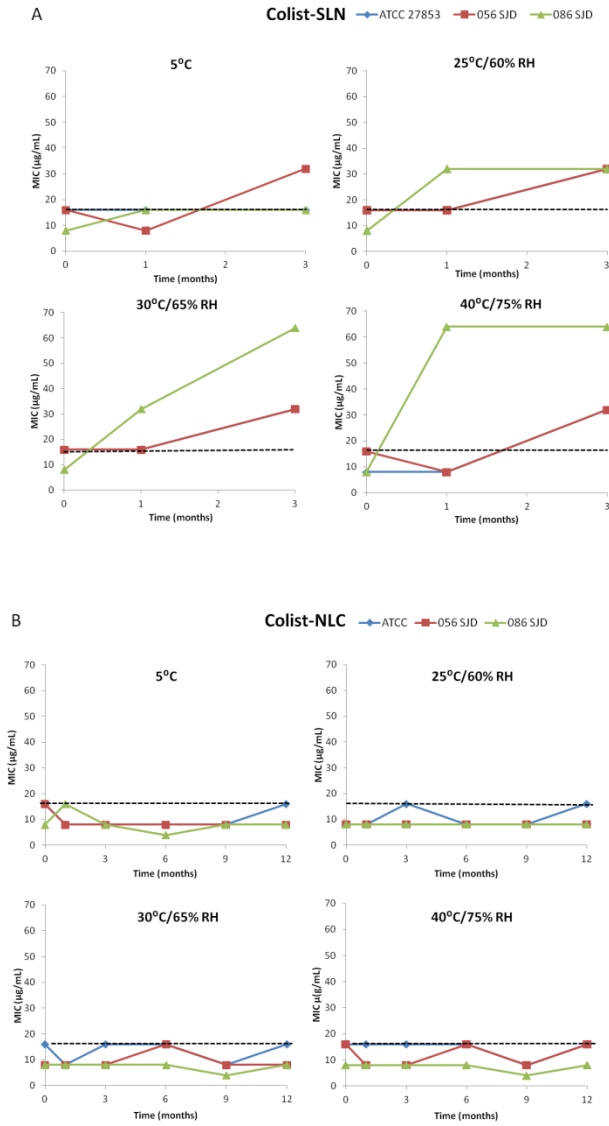
Figure 5. Minimum inhibitory concentration (MIC) of Colist-SLNs for 3 months (A) and Colist-NLCs for 12 months (B) against three strains of *Pseudomonas aeruginosa*, ATCC27853, 056SJD and 086 SJD at ICH conditions.

3.6 Drug release study

Figure 6 shows the percentage of the drug release from Colist-NLCs at the beginning of the study and after one year storage under the conditions previously described.

At time 0, the NLCs released the drug in a control manner reaching 91.53% at 24 hours and almost 100% at 48 hours. The initial fast release of the NPs may be due to the presence of the drug in the surface of the nanoparticles, while the drug incorporated into the particulate core is released in prolonged way (Misra *et al.,* 2009).

Colist-NLCs demonstrated a sustained drug release also after 12 months at 5°C and 25°C as they showed similar release profile as the fresh nanoparticles. Similar findings were reported by Das *et al.* when working with clotrimazole-loaded NLCs. The release profile of their nanoparticle was the same as fresh formulation, however, in that occasion only the refrigerated condition was tested and the storage duration was fixed in three months (Das *et al.*, 2012). A slightly slower profile was

detected at 30°C of storage, but achieving 82.87% of drug release at 24 hours and the complete released at 48 hours, meeting the specification requirements. On the contrary, Colist-NLCs at 40°C showed a significantly slower drug release rate than their counterparts reaching only 62.13% at the end of the study suggesting drug degradation.

The results obtained in our study confirmed the stability of the drug entrapped in nanoparticles as the 100% of the drug (total encapsulated drug) was able to be released from the NLCs at 5°C, 25°C/60% RH and 30°C/65% RH indicating that the antibiotic can be able to exert its antipseudomonal activity. The sustained release of a drug incorporated in a delivery system is an important characteristic quite often correlated with improved pharmacokinetics and efficacy (Chen *et al.*, 2010). According to the prolonged release profile of the NLCs, it could be suggested that sodium colistimethate delivered as lipid nanocarriers might be administered in lower doses or longer intervals, thus reducing its undesirable side effects.
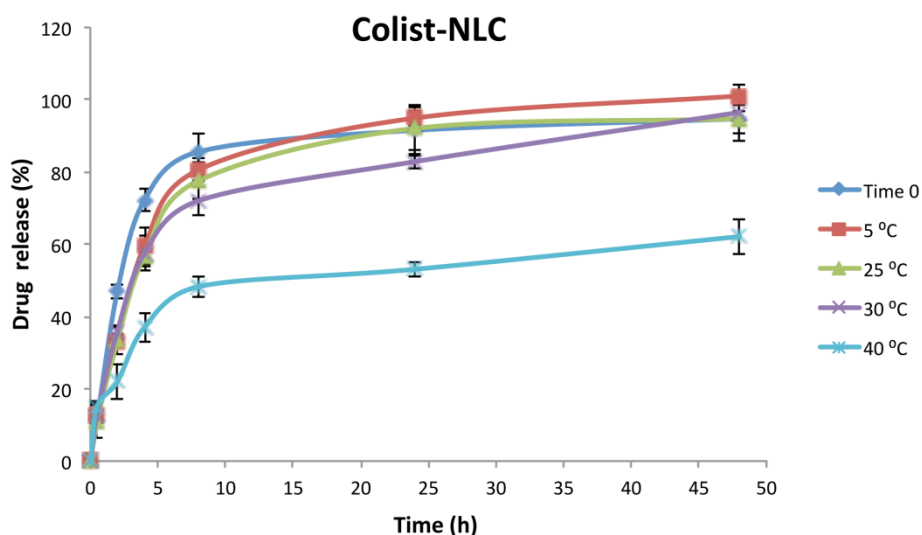
Figure 6. Sodium colistimethate release profile from NLCs after storage at 5 ± 3°C, 25 ± 2°C/ 60 ± 5% relative humidity (RH), 30 ± 2°C/ 65 ± 5% RH and 40 ± 2°C / 75 ± 5% RH after 12 months.

4. Conclusions

Stability studies are required in order to ensure that the properties of the formulation are not modified over the time. The aim of this study was to evaluate the stability of two formulations, Colist-SLNs and Colist-NLCs for a long-period by means of the analysis of their physico-chemical characteristics and antimicrobial activity. For this purpose, the NPs were freeze-dried and four stored conditions were fixed: 5°C, 25 ± 2°C/ 60 ± 5% RH, 30 ± 2°C/ 65% ± 5 RH, and 40 ± 2°C / 75 ± 5% RH.

Our results indicated that the MIC values of Colist-SLNs were up to 8 times higher than the free drug (64 µg/mL versus 8 µg/mL) exceeding the acceptance criteria at the third month; however, the storage of Colist-NLCs in all conditions of temperature and humidity did not affect its antimicrobial efficacy against

P. aeruginosa for one year, making it an attractive candidate to treat this type of infectious diseases. In that sense, sodium colistimethate-loaded NLCs exhibited improved stability and shelf-life compared to Colist-SLNs. Moreover, during the 12 months of the study, the size, PDI, zeta potential, morphology and release profile were constant for Colist-NLCs at 5°C and 25°C. Another interesting characteristic of Colist-NLCs is the fact that they are prepared with physiologically well-tolerated lipids and avoid the use of organic solvents during their preparation compared to SLNs leading to a higher environmental efficiency.

On the basis of these results, the stability of NPs depends on temperature and humidity, but long-term stability of Colist-NLCs over one year can be achieved at the optimized storage conditions (5°C and 25°C/ 60% RH). In this case, room temperature would be the most attractive one for Colist-NLCs storage as it eases supply chain management in terms of transport and storage.

To sum up, NLCs are promising carrier systems for the encapsulation of sodium colistimethate and their administration by pulmonary route could be a potential option for the treatment of respiratory infections.

Acknowledgements

References

Abdelwahed, W., Degobert, G., Stainmesse, S., Fessi, H., 2006. Freeze-drying of nanoparticles: formulation, process and storage considerations. Adv. Drug Deliv. Rev., 58, 1688-1713.

Alipour, M., Halwani, M., Omri, A., Suntres, Z.E., 2008. Antimicrobial effectiveness of liposomal polymyxin B against resistant Gram-negative bacterial strains. Int. J. Pharm., 355, 293-298.

Beaulac, C., Clement-Major, S., Hawari, J., Lagace, J., 1997. *In vitro* kinetics of drug release and pulmonary retention of microencapsulated antibiotic in liposomal formulations in relation to the lipid composition. J. Microencapsul., 14, 335-348.

Cavalli, R., Caputo, O., Carlotti, M.E., Trotta, M., Scarnecchia, C., Gasco, M.R., 1997. Sterilization and freeze-drying of drug-free and drug-loaded solid lipid nanoparticles. Int. J. Pharm., 148, 47-54.

Chacon, M., Molpeceres, J., Berges, L., Guzman, M., Aberturas, M.R., 1999. Stability and freeze-drying of cyclosporine loaded poly(D,L lactide-glycolide) carriers. Eur. J. Pharm. Sci., 8, 99-107.

Chen, C., Tsai, T., Huang, Z., Fang, J., 2010. Effects of lipophilic emulsifiers on the oral administration of lovastatin from nanostructured lipid carriers: Physicochemical characterization and pharmacokinetics. Eur. J. Pharm. Biopharm., 74, 474-482.

Chono, S., Tanino, T., Seki, T., Morimoto, K., 2006. Influence of particle size on drug delivery to rat alveolar macrophages following pulmonary administration of ciprofloxacin incorporated into liposomes. J. Drug Target., 14, 557-566.

Crowe, L.M., Reid, D.S., Crowe, J.H., 1996. Is trehalose special for preserving dry biomaterials? Biophys. J., 71, 2087-2093.

Das, S., Chaudhury, A., 2011. Recent advances in lipid nanoparticle formulations with solid matrix for oral drug delivery. AAPS PharmSciTech., 12, 62-76.

Das, S., Ng, W.K., Tan, R.B., 2012. Are nanostructured lipid carriers (NLCs) better than solid lipid nanoparticles (SLNs): development, characterizations and comparative evaluations of clotrimazole-loaded SLNs and NLCs? Eur. J. Pharm. Sci., 47, 139-151.

del Pozo-Rodriguez, A., Solinis, M.A., Gascon, A.R., Pedraz, J.L., 2009. Short- and long-term stability study of lyophilized solid lipid nanoparticles for gene therapy. Eur. J. Pharm. Biopharm., 71, 181-189.

Dijkmans, A.C., Wilms, E.B., Kamerling, I.M., Birkhoff, W., Ortiz-Zacarias, N.V., van Nieuwkoop, C., Verbrugh, H.A., Touw, D.J., 2014. Colistin: revival of an old polymyxin antibiotic. Ther. Drug Monit., 3, 419-427.

Falagas, M.E., Kasiakou, S.K., 2005. Colistin: the revival of polymyxins for the management of multidrug-resistant gram-negative bacterial infections. Clin. Infect. Dis., 40, 1333-1341.

Freitas, C., Müller, R.H., 1998. Effect of light and temperature on zeta potential and physical stability in solid lipid nanoparticle (SLN™) dispersions. Int. J. Pharm., 168, 221-229.

Gainza, G., Aguirre, J.J., Pedraz, J.L., Hernández, R.M., Igartua, M., 2013. rhEGF-loaded PLGA-Alginate microspheres enhance the healing of full-thickness excisional wounds in diabetised Wistar rats. Eur J Pharm Sci, 50, 243-252.

Gartziandia, O., Herran, E., Pedraz, J.L., Carro, E., Igartua, M., Hernandez, R.M., 2015. Chitosan coated nanostructured lipid carriers for brain delivery of proteins by intranasal administration. Colloids Surf. B Biointerfaces, 134, 304-313.

Ghaffari, S., Varshosaz, J., Saadat, A., Atyabi, F., 2011. Stability and antimicrobial effect of amikacin loaded SLN. Int J Nanomedicine, 6, 35-43.

Grimm, W., 1998. Extension of the International Conference on Harmonization Tripartite Guideline for Stability Testing of New Drug Substances and Products to countries of climatic zones III and IV. Drug Dev. Ind. Pharm., 24, 313-325.

Guideline, I.H.T., 2003. Stability testing of new drug substances and products. Q1A (R2), Current Step, 4.

Haskell, R., Shifflett, J., Elzinga, P., 1998. Particle-sizing technologies for submicron emulsions. Submicron emulsions in drug targeting and delivery. Amsterdam: Harwood Academic Publishers, 21-98.

Heurtault, B., Saulnier, P., Pech, B., Proust, J.E., Benoit, J.P., 2003. Physico-chemical stability of colloidal lipid particles. Biomaterials, 24, 4283-4300.

Hu, F., Jiang, S., Du, Y., Yuan, H., Ye, Y., Zeng, S., 2006. Preparation and characteristics of monostearin nanostructured lipid carriers. Int. J. Pharm., 314, 83-89.

Huh, A.J., Kwon, Y.J., 2011. "Nanoantibiotics": A new paradigm for treating infectious diseases using nanomaterials in the antibiotics resistant era. J. Control. Release, 156, 128-145.

Jennings, T.A., 1999. Lyophilization: Introduction and Basic Principles, CrC Press.

Kim, J., Park, J., Kim, C., 2010. Development of a binary lipid nanoparticles formulation of itraconazole for parenteral administration and controlled release. Int. J. Pharm., 383, 209-215.

Misra, R., Acharya, S., Dilnawaz, F., Sahoo, S.K., 2009. Sustained antibacterial activity of doxycycline-loaded poly (D, L-lactide-co-glycolide) and poly (ε-caprolactone) nanoparticles. Nanomedicine, 4, 519-530.

Molina, M., Armstrong, T.K., Zhang, Y., Patel, M.M., Lentz, Y.K., Anchordoquy, T.J., 2004. The stability of lyophilized lipid/DNA complexes during prolonged storage. J. Pharm. Sci., 93, 2259-2273.

Moreno-Sastre, M., Pastor, M., Salomon, C.J., Esquisabel, A., Pedraz, J.L., 2015. Pulmonary drug delivery: a review on nanocarriers for antibacterial chemotherapy. J. Antimicrob. Chemother., 70, 2945-2955.

Muller, R.H., Mader, K., Gohla, S., 2000. Solid lipid nanoparticles (SLN) for controlled drug delivery - a review of the state of the art. Eur. J. Pharm. Biopharm., 50, 161-177.

Muller, R.H., Petersen, R.D., Hommoss, A., Pardeike, J., 2007. Nanostructured lipid carriers (NLC) in cosmetic dermal products. Adv. Drug Deliv. Rev., 59, 522-530.

Omri, A., Suntres, Z.E., Shek, P.N., 2002. Enhanced activity of liposomal polymyxin B against *Pseudomonas aeruginosa* in a rat model of lung infection. Biochem. Pharmacol., 64, 1407-1413.

Pardeike, J., Weber, S., Haber, T., Wagner, J., Zarfl, H.P., Plank, H., Zimmer, A., 2011. Development of an itraconazole-loaded nanostructured lipid carrier (NLC) formulation for pulmonary application. Int. J. Pharm., 419, 329-338.

Pastor, M., Esquisabel, A., Talavera, A., Ano, G., Fernandez, S., Cedre, B., Infante, J.F., Callico, A., Pedraz, J.L., 2013. An approach to a cold chain free oral cholera vaccine: *in vitro* and *in vivo* characterization of Vibrio cholerae gastro-resistant microparticles. Int. J. Pharm., 448, 247-258.

Pastor, M., Moreno-Sastre, M., Esquisabel, A., Sans, E., Viñas, M., Bachiller, D., Asensio, V.J., Pozo, ÁD., Gainza, E., Pedraz, J.L., 2014. Sodium colistimethate loaded lipid nanocarriers for the treatment of *Pseudomonas aeruginosa* infections associated with cystic fibrosis. Int J Pharm, 477, 485-494.

Radomska-Soukharev, A., 2007. Stability of lipid excipients in solid lipid nanoparticles. Adv. Drug Deliv. Rev., 59, 411-418.

Ridolfi, D.M., Marcato, P.D., Justo, G.Z., Cordi, L., Machado, D., Durán, N., 2012. Chitosan-solid lipid nanoparticles as carriers for topical delivery of tretinoin. Colloids Surf. B Biointerfaces, 93, 36-40.

Sanjula, B., Shah, F.M., Javed, A., Alka, A., 2009. Effect of poloxamer 188 on lymphatic uptake of carvedilol-loaded solid lipid nanoparticles for bioavailability enhancement. J. Drug Target., 17, 249-256.

Schwarz, C., Mehnert, W., 1997. Freeze-drying of drug-free and drug-loaded solid lipid nanoparticles (SLN). Int. J. Pharm., 157, 171-179.

Solleti, V.S., Alhariri, M., Halwani, M., Omri, A., 2015. Antimicrobial properties of liposomal azithromycin for *Pseudomonas* infections in cystic fibrosis patients. J. Antimicrob. Chemother., 70, 784-796.

Suk, J.S., Lai, S.K., Wang, Y.Y., Ensign, L.M., Zeitlin, P.L., Boyle, M.P., Hanes, J., 2009. The penetration of fresh undiluted sputum expectorated by cystic fibrosis patients by non-adhesive polymer nanoparticles. Biomaterials, 30, 2591-2597.

Uner, M., 2006. Preparation, characterization and physico-chemical properties of solid lipid nanoparticles (SLN) and nanostructured lipid carriers (NLC): their benefits as colloidal drug carrier systems. Pharmazie, 61, 375-386.

Venkateswarlu, V., Manjunath, K., 2004. Preparation, characterization and *in vitro* release kinetics of clozapine solid lipid nanoparticles. J. Control. Release, 95, 627-638.

Wang, Y., Zhu, L., Dong, Z., Xie, S., Chen, X., Lu, M., Wang, X., Li, X., Zhou, W., 2012. Preparation and stability study of norfloxacin-loaded solid lipid nanoparticle suspensions. Colloids Surf B Biointerfaces, 98, 105-111.

Weber, S., Zimmer, A., Pardeike, J., 2014. Solid Lipid Nanoparticles (SLN) and Nanostructured Lipid Carriers (NLC) for pulmonary application: a review of the state of the art. Eur. J. Pharm. Biopharm., 86, 7-22.

Wissing, S.A., Kayser, O., Müller, R.H., 2004. Solid lipid nanoparticles for parenteral drug delivery. Adv. Drug Deliv. Rev., 56, 1257-1272.

Yang, W., Peters, J.I., Williams, R.O.,3rd, 2008. Inhaled nanoparticles a current review. Int. J. Pharm., 356, 239-247.

Zhang, J., Fan, Y., Smith, E., 2009. Experimental design for the optimization of lipid nanoparticles. J. Pharm. Sci., 98, 1813-1819.

Zhou, J., Zhou, D., 2015. Improvement of oral bioavailability of lovastatin by using nanostructured lipid carriers. Drug Des. Devel Ther., 9, 5269.

Zimmermann, E., Müller, R.H., Mäder, K., 2000. Influence of different parameters on reconstitution of lyophilized SLN. Int. J. Pharm., 196, 211-213.

Chapter 3

Pulmonary delivery of tobramycin-loaded nanostructured lipid carriers for *Pseudomonas aeruginosa* infections associated with cystic fibrosis

Pulmonary delivery of tobramycin-loaded nanostructured lipid carriers for *Pseudomonas aeruginosa* infections associated with cystic fibrosis

María Moreno-Sastre[a,b], Marta Pastor[a,b], Amaia Esquisabel[a,b], Eulàlia Sans[c], Miguel Viñas[c], Aarne Fleicher[d,e], Esther Palomino[d,e], Daniel Bachiller[d,e], José Luis Pedraz[a,b]

[a]NanoBioCel Group, Laboratory of Pharmaceutics, University of the Basque Country (UPV/EHU), School of Pharmacy, Paseo de la Universidad 7, Vitoria-Gasteiz 01006, Spain.
[b]Biomedical Research Networking Center in Bioengineering, Biomaterials and Nanomedicine (CIBER-BBN). Vitoria-Gasteiz, Spain.
[c]Department of Pathology and Experimental Therapeutics, Medical School, University of Barcelona-IDIBELL. Barcelona, Spain.
[d]Fundación Investigaciones Sanitarias Islas Baleares (FISIB), Development and Regeneration Program, Ctra. Sóller km 12, Bunyola (Balearic Islands) 7110, Spain.
[e]Consejo Superior de Investigaciones Científicas (CSIC), Ctra. Sóller km 12, Bunyola (Balearic Islands) 7110, Spain.

Abstract

Among the pathogens that affect cystic fibrosis (CF) patients, *Pseudomonas aeruginosa* is the most prevalent. As a way to fight against this infection, nanotechnology has emerged over the last decades as a promising alternative to overcome resistance to antibiotics in infectious diseases. The goal of this work was to elaborate and characterize lipid nanoparticles for pulmonary delivery of tobramycin.

Tobramycin-loaded nanostructured lipid carriers (Tb-NLCs) were prepared by hot melt homogenization technique. In addition, nanoparticles labeled with infrared dye (IR-NLCs) were used to investigate their *in vivo* performance after pulmonary administration.

Tb-NLCs displayed a mean diameter size around 250 nm, high drug encapsulation (93%) and sustained release profile. Tb-NLCs showed to be active against clinically isolated *P. aeruginosa*. Moreover, Tb-NLCs did not decrease cell viability and were able to overcome an artificial mucus barrier in the presence of mucolytics agents. During the *in vivo* assay, IR-NLCs were administered to several mice by the intratracheal route using a Penn Century® device. Next, the biodistribution of the nanoparticles was analyzed at different time points showing a wide nanosystem distribution in the lungs.

Altogether, tobramycin-loaded NLCs seem to us an encouraging alternative to the currently available CF therapies.

1. Introduction

Cystic fibrosis (CF) is a genetic disorder that affects nearly 70,000 patients worldwide. It is caused by mutations in the cystic fibrosis transmembrane conductance regulator (CFTR) gene that encodes a protein that form an ion channel in epithelial cell membranes whose dysfunction leads to the secretion and accumulation of a vicious mucus in the airways that become thick and sticky causing bronchial obstruction (Moreau-Marquis *et al.*, 2008). The tenacious mucus enables chronic bacterial infection by an opportunist Gram-negative bacterium, which is the most frequent pathogen identified in CF patients (Ratjen *et al.*, 2009). Mucoid strains of *P. aeruginosa* usually develop community of microbes in an exopolysaccharide matrix called biofilm. Although CF patients routinely take antibiotics, the mucus plugs and bacterial biofilm contribute to the poor lung penetration of antimicrobial agents, leading to clinical exacerbations (Okusanya *et al.*, 2009). Therefore the eradication of these organisms is a difficult but essential endpoint to achieve. Furthermore, over the last decades, antibiotic-resistant strains have increased due to the misuse and overuse of anti-infectious drugs (Andrade *et al.*, 2013). As a consequence, there is a high morbidity and mortality associated to the respiratory manifestations of the CF disease hampered by the lack of effective therapies (Savla and Minko, 2013).

In this regard, nanotechnology has emerged as a new alternative to drug encapsulation to overcome the limitations of conventional drugs. Nanoformulations such as nanostructured lipid carriers (NLCs) are made up of a solid lipid core stabilized by surfactants and have the possibility to incorporate both lipophilic and hydrophilic drugs. NLCs provide several advantages over other drug delivery systems (DDSs) such as good biocompatibility, biodegradable properties, higher drug loading, controlled drug release, long-term stability, as well as scaling-up feasibility (Weber *et al.*, 2014).

Nanoparticles (NPs) are currently being extensively investigated for antibiotic

inhalation therapy. Pulmonary drug delivery has gained much attention as a non-invasive route for the delivery of high amounts of therapeutic agents directly to the desired site of action minimizing systemic exposure and adverse effects (Patil and Sarasija, 2012). This route is a preferred route for agents such as aminoglycosides in CF patients. The inhalation of tobramycin is part of current CF therapies as it presents strong bactericidal activity against planktonic cells (Thellin *et al.*, 2015). For instance, TOBI® or TIS (tobramycin inhalation solution) and TIP (tobramycin inhalation powder) have recently become commercially available for the treatment of chronic lung infections caused by *P. aeruginosa* (Waters and Smyth, 2015). However, the efficacy of free drug administration in CF patients is not high enough to achieve therapeutics levels at the site of infection due to its rapid clearance and poor mucus penetration (Tseng *et al.*, 2013). These drawbacks could be overcome by nanotechnology. Encapsulation of antibiotics into nanocarriers has attracted considerable interest to improve the therapeutic index of antimicrobial drugs and for their benefits in the context of combating bacteria (Hajipour *et al.*, 2012). Moreover, many cystic fibrosis patients present an accumulation of dehydrated and thicker mucus within the airways causing respiratory problems, therefore, it is important for therapeutic agents to penetrate into this mucus in order to distribute the drug and maximize its antibacterial effect (Yang *et al.*, 2011). Nano-antibiotic represents a promising strategy to overcome the mucus barrier and to prolong the drug retention in the lung as other authors have also previously reported (Poyner *et al.*, 1995).

Taking the above into account, the goal of this work was to elaborate and characterize tobramycin-loaded lipid nanocarriers (Tb-NLCs) for pulmonary delivery for the treatment of respiratory infectious diseases; in particular CF. Two different solid lipids were selected as core agents for the NLCs (Precirol® ATO 5 and Compritol® ATO 888). The antimicrobial

activity against *P. aeruginosa* was investigated as well as the capability of the nanoparticles to cross the mucus barrier *per se* or after adding mucolytic agents. Finally, the NPs biodistribution was analyzed after intratracheal administration in mice.

2. Material and Methods

2.1 Materials

Precirol® ATO 5 (glycerol distearate, type I) and Compritol® 888 ATO (glyceryl dibehenate) were kindly provided by Gattefossé (Madrid, Spain). Kolliphor® P188 (Poloxamer 188) was a gift from BASF (Ludwigshafen, Germany). Polysorbate, Tween® 80 was purchased from Panreac Química (Castellar del Vallès, Barcelona, Spain). Miglyol® 812 was provided by Sasol (Hamburg, Germany). Tobramycin, fluorescamine, IR-783 dye, gelatine from bovin skin type B, diethylenetriaminepentaacetic acid (DPTA), type II mucine from porcin stomach, egg yolk enrichment, amino acids and were purchased from Sigma-

Aldrich Chemicals (St. Louis, MO, USA). Coomassie Brilliant Blue was provided from Bio-Rad Laboratories (Hercules, CA, USA). PBS, DPBS, DMEM, MEM-NEAA, FBS, DMSO and Trypsin-EDTA Gibco® were supplied by Life Technologies (Thermo Fisher Scientific, Waltham, MA). Blood agar was provided by Oxoid (Microbioligical Products Thermo Fisher, Hampshire, UK). Mannitol (Pearlitol® PF) and L-lysine-S-carboxymethyl-L-cysteine salt were provided from Roquette and Pharmazell (India), respectively. Hydroxyethylcellulose was purchased from Vencaser S.A (Bilbao, Spain). Other chemicals were all analytical grade.

2.2 Methods

2.2.1 Preparation of nanostructure lipid carriers (NLCs)

The nanostructured lipid carriers, NLCs, were elaborated by a hot melt homogenization technique (Pastor *et al*., 2014). In brief, Precirol® ATO 5 (NLC P) or a 50:50 Compritol® 888 ATO and Precirol® ATO 5 mixture (NLC PC) together with Miglyol® 812 were selected as lipid core. These lipids were mixed with tobramycin

(Tb) and heated above the melting temperature of the solid lipid until its fusion. As tobramycin is a hydrophilic drug, it was dispersed in the molten lipids. The aqueous phase was prepared by dispersing 1.3% (w/v) of Tween® 80 and 0.6% (w/v) of Poloxamer 188 in Milli-Q water and heating to the same temperature as the lipid phase. Straightaway, the hot aqueous phase was added to the oily phase, and then sonicated for 30 second at 20W (Branson Sonifier 250, Danbury, CT, USA). The formed emulsion was stored for 12 hours at 4⁰C to allow the re-crystallization of the lipids and the nanoparticle formation. Then, Tb-NLCs were washed by centrifugation at 2,500 rpm in Amicon® centrifugal filtration units (100.000 Da MWCO, Merck Millipore, Darmstadt, Germany) for 15 minutes three times. All the nanoparticles prepared were freeze-dried for 39 hours (Telstar Lyobeta freeze-dryer, Terrasa, Spain) using trehalose at 15% (w/w) as cryoprotectant. Different batches of blank nanoparticles without the drug (Blank-NLCs) were also prepared for comparison.

Two types of dyes were used to label NLCs. Firstly, Coomasie blue (CB) labeled NLCs (CB-NLCs) were prepared for the artificial mucus (AM) penetration assay. NLCs were prepared just as mentioned above but instead of the drug, 1.3% (w/w) of CB was added. Secondly, to prepare labeled NLCs, an infrared dye (IR-783) was embedded into the nanoparticles by adding 50 mg of IR instead of the antibiotic. This dye is an excellent stain for the observation in the near infrared region (NIR). In both cases, the nanoparticles were washed by centrifugal filtration units and trehalose 15% (w/w) was added prior to the lyophilization step.

2.2.2. Characterization of lipid nanoparticles

2.2.2.1 Size and Zeta potential

The particle size and polydispersity index (PDI) were measured in a Zetasizer Nano ZS (Malvern Instruments, Worcestershire, UK) based on dynamic light scattering. Zeta potential was also determined by Doppler velocimetry by means of the Zetasizer Nano ZS. Prior to the measurements NPs were dispersed in

Milli-Q water at optimal intensity. All the measurements of each sample were performed in triplicate**.**

2.2.2.2 Microscopy analysis

NPs morphology was examined by Transmission Electron Microscope (TEM, Philips CM120) after negative staining with 2% uranyl acetate.

2.2.2.3. Encapsulation efficiency

The encapsulation efficiency (EE) of tobramycin into NLCs was determined by indirect and direct methods. By the indirect method, the supernatants obtained during the centrifugation in Amicon® devices were analyzed for Tb content by UV-VIS spectrophotometer after derivatization with fluorescamine (Sampath and Robinson, 1990; Ungaro *et al.*, 2012). Briefly, NLCs samples were diluted 1:2 (v/v) in fluorescamine solution at 0.5% (w/v) in ethanol and incubated at room temperature protected from light for one hour before analysis. The absorbance of these samples was measured at 390 nm using a Shimadzu UV-1800 spectrophotometer (Shimadzu Co., Kyoto,

Japan) fitted out with a 0.1-cm quartz cell. The absorbance of the supernatants collected from blank particles displayed no absorption at 390 nm. The tobramycin content in the supernatants samples was calculated using a calibration curve that present linearity from 5 to 100 µg/mL ($r^2 \geq$ 0.999). Encapsulation efficiency was calculated following this equation:

EE (%) = 100 x [(initial drug or dye amount - non-encapsulated drug or dye)/ initial drug or dye amount].

In order to evaluate the total amount of tobramycin into NLCs by a direct method, a known mass of NLCs (10 mg) was dissolved in a mixture of $CHCl_3$: MeOH (1:1, v/v) and analyzed by UV-VIS spectrophotometric method after derivation with fluorescamine as mention before. NLCs particles without drug were used as background signal.

On the other hand, the encapsulation efficiency of CB-NLCs and IR-NLCs was measured by determining the absorbance of the dye from the supernatants and comparing it to a calibration curve

10-100 µg/mL using a plate reader (Infinite® 200 PRO, Tecan, Männedorf, Switzerland) at 590 and 800 nm, respectively.

2.2.2.4 *In vitro* drug release studies

In vitro drug release studies were conducted using Quix-Sep Micro Dialyzers (Membrane Filtration Products Inc, Seguin, Texas, USA) at 37°C under magnetic stirring in phosphate buffer saline (PBS). A dialysis regenerated cellulose tubular membrane having a molecular weight cut-off (MWCO) between 12,000 and 14,000 Da was used. First, cellulose membranes were soaked in the dissolution medium (PBS) for 20 minutes prior to its use to ensure thorough wetting of the membrane before placing it in a Quix-Sep cell. To carry out this study, the Tb-NLCs suspension (50 mg/mL) was placed in the cell system which was immersed in 50 mL of PBS solution at pH 7.4 as the dissolution medium. At fixed time intervals up to 96 hours, samples (500 µL) were withdrawn from the incubation and evaluated by UV-VIS spectrophotometer. The release study was carried out under sink conditions and the removed PBS was replaced with equal volumes of fresh medium. Results were expressed as percentage of tobramycin released compared to the total drug encapsulated in the sample. The experiments were run in triplicate for each point of release kinetics.

2.2.3 Determination of minimum inhibitory concentration (MIC)

Six *Pseudomonas aeruginosa* strains isolated from the sputum of adult CF patients were selected for the MIC determination of the nanoparticles among which three of them were mucoid and three non-mucoid strains. *P. aeruginosa* strains were cultivated routinely on blood agar (Sigma-Aldrich, Gillingham, UK) for 24 hours at 37°C. Furthermore, *P. aeruginosa* ATCC 27853 strain was also assessed as control.

Nanoparticles and free antibiotic were tested against *P. aeruginosa* strains by broth microdilution method in 96-well microplates. The formulations were serially diluted 2-fold in Mueller-Hinton II Broth Cation-Adjusted (MHBCA) from a

starting concentration of 128 to 0.125 µg/mL in a final volume of 100 µL. Then, 5 µL of *P. aeruginosa* inoculum were added to each well to produce a bacterial cell suspension of 10^4 cfu/mL (colony-forming units) and samples were incubated for 24 hours at 37°C. Negative and positive growth controls were included. The minimum inhibitory concentration represents the lowest antibiotic concentration that inhibits a visible planktonic bacterial growth after an overnight incubation at 37°C. The assay was run in triplicate.

2.2.4 Cell experiments

2.2.4.1 Cell culture

Human lung adenocarcinoma epithelial cell line (A549 cells) and human lung papillary adenocarcinoma epithelial cell line (H441 cells) were purchased from the American Type Culture Collection (ATCC; Manassas, USA). Cells were grown and maintained in Dulbecco´s Modified Eagle Growth Medium (DMEM) pH 7.4, supplemented with 10% (v/v) inactivated fetal bovine serum (FBS), 1% glutamine and 1% antibiotic/antimycotic and 1% Minimum Essential Medium non-essential amino acids 100x (MEM-NEAA) and incubated at 90% humidity, 5% (v/v) CO_2 atmosphere at 37°C. The cells were allowed to grow until confluence, then they were trypsinized (Trypsin-EDTA) and seeded in plates for each experiments.

2.2.4.2 *In vitro* cytotoxicity studies

The cytotoxicity of Tb-NLCs was evaluated in the A549 and H441 cell lines as reported earlier. The cells were plated in 96-well microtiter plates at a density of 10,000 cells per well in a final volume of 100 µL of DMEM medium (supplemented with 10% serum). The cells were treated with Blank-NLCs or NLCs formulations (Tb-NLC P or Tb-NLC PC) diluted in DMEM medium at concentrations of 0.25, 0.5 and 1 mg/mL for 24 h at 37 ± 2°C, 90% humidity and 5% CO_2. Controls were set with dimethyl sulfoxide (DMSO) as negative or death control, and medium without formulation as positive control. Free antibiotic was added for comparison. After overnight incubation, the determination of cell viability was carried out using the Cell

Counting Kit 8 (CCK-8, Sigma-Aldrich, St. Louis, MO; USA). Wells were washed with sterile PBS and then 10% of CCK-8 in medium was added to each well and incubated in a wet chamber for 4 hours at $37 \pm 2^{o}C$ and 5% CO_2. The resulting colored solution was quantified using a microplate reader (Infinite® 200 PRO, Tecan, Männedorf, Switzerland). The spectrophotometric absorbance was measured at 450/650 nm wavelength. Results were calculated in relation to the untreated wells (100% viability) and are expressed as percent of cell vitality ± SD of values collected from three separate experiments performed in triplicate for each sample.

2.2.4.3 Cell viability

To confirm the CCK-8 data, a second independent cell viability test was assessed using a Live/Dead® kit that consisted of two stains, calcein acetoxy-methyl and ethidium homodimer-1 (calcein AM/EthD-1) (Invitrogen, Karlsruhe, Germany). Live cells were distinguished by enzymatic conversion of calcein AM to intensely green fluorescent

and EthD-1 produced intracellular red fluorescence in nucleus of dead cells allowing to differentiate the population of live cells from the dead-cells (Nassimi *et al.*, 2010).

In brief, after 24 hours the adherent cells (A549 and H441) cultured on 96 well-plate treated with both nanoparticles and free antibiotic were washed with Dulbecco´s phosphate buffered saline (DPBS) to limit the background fluorescence and then, 100 µL of a combined reagent solution of calcein (0.5 µM) and ethidium homodimer (0.5 µM) in DPBS was added to each well. After 45 minutes of incubation at room temperature and protected from light, the fluorescence emission from both fluorophores was observed simultaneously using a conventional fluorescence microscope (Nikon Eclipse TE2000-S, TSM) equipped with an excitation filter. Both positive (living cells without formulation) and negative (dead cells treated with DMSO) controls were also assessed by dying with live/dead stained and observed.

2.2.5 Penetration of NPs through artificial mucus

The purpose of this study was to test whether mannitol or S-carboxymethylcysteine (CMC) as mucolytic agents, improved nanoparticle diffusion through artificial mucus (AM) and could enhance the antibacterial activity. The penetration of CB-NLCs (Coomassie blue-NLCs) through a mucus layer was carried out using an artificial mucus model as previously reported Yang *et al.* (2011) (Figure 1). Briefly, 50 mL of artificial mucus was elaborated by adding 500 mg of DNA in 32.5 mL DNAase-free water complemented with 250 μL of sterile egg yolk emulsion and an autoclaved solution of 250 mg of mucin, 0.295 mg diethylenetriaminepentaacetic (DTPA), 250 mg NaCl, 110 mg KCl and 12.5 mg amino acids dissolved in 17.5 mL of water. The dispersion was stirred until a homogenous mixture was obtained and the pH of the AM was adjusted to 7.0 using NaOH solution. On the other hand, a 10% (w/v) gelatin solution was prepared in hot water; one milliliter of this solution

was placed in each well of a 24-well plate, solidified at room temperature and stored at $4^{o}C$ until use (layer 2). 0.5 mL of artificial mucus was placed on the top of the hardened gelatin gel (layer 1). Then, 500 μL of an aqueous dispersion of CB-NLC (containing 75 μg of CB) at different proportions of mucolytics (75:25, 50:50 and 25:75, NLC:mucolytic, w/w) were placed on the artificial mucus layer and incubated in a closed chamber maintaining 100% relative humidity, emulating the humid environment of airways (Marini and Slutsky, 1998) until pre-determinate sampling points. The upper layer (layer 1), that is, the artificial mucus layer plus the nanoparticles that have not crossed the mucus barrier, was removed after 1 and 7 hours, and gelatin plates were washed three times with water and subsequently melted at 100°C for homogenous mixing of gelatin and CB. The amount of CB in gelatin was evaluated at 590 nm using a plate reader. The absorbance values were compared to a standard CB curve from 1 to 100 μg/mL. Results are reported as percentage of the dye penetrated through

artificial mucus [(amount of CB in gelatine plates/total amount of CB in NPs) × 100] ± SD.
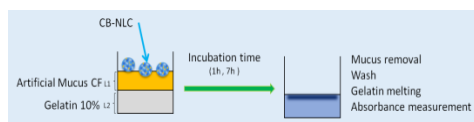
Figure 1. Scheme of the mucus penetration study. Layer 1 (L1) and 2 (L2).

2.2.6 *In vitro* **permeation study**

2.2.6.1 Rheological properties of artificial mucus

As AM was too fluid to carry on permeation studies, another mucus model named AM1 was prepared by adding 1% (w/v) of hydroxyethylcellulose (HEC) as an inert thickening agent to the preceding formula. Viscosity of AM1 was conducted using a rotational viscometer (AR1000, TA instruments, New Castle, DE, USA) based on the measurements of the torque of a rotating spindle in a sample at a specified velocity (from 1 to 1000 rpm). The probe applied was a cone plate with a 2º angle. Data were reported as Pascals per second (Pa.s) related to the rotor velocity and all the viscosity values were always between 15% and 100% of the torque range, as requested.

2.2.6.2 *In vitro* **permeation experiment**

A permeation assay was carried out to evaluate the permeation properties of Tb-NLCs formulations through AM1 by using Franz cells (Hanson Research Corporation, CA, USA), as previous reported by Donnelly *et al.* (2007). The AM1 was kept for 12 hours at room temperature before use. The receptor and donor chamber were divided by means of a cellulose membrane (pore size: 0.45 µm) that was applied between the two compartments (permeation area 0.785 cm^2). The receptor compartment was filled with 5 mL of PBS. Then, a thin layer (3 mm) of artificial mucus (AM1) was interposed between the membrane and the drug deposition area forming a film. A suspension of Tb-NLCs diluted in water and mixtures of NLC:mucolytic agents at 75:25 were uniformly added on the top. In addition, free tobramycin in presence of mucus or not was assayed as control. The cell system was stored under continuous stirring at 37°C and samples were removed (500 µL) at defined times, 1 and 7 hours, replacing the same volume with

PBS. Samples were analyzed for tobramycin content by UV-spectrophotometric method as mention in section 2.2.2.3 and results are reported by Tb permeated versus time.

On the other hand, the amount of the drug permeated per area (Q) for each time was calculated using the following equation:

$$Q\,(mg/cm^2) = \frac{V_R \times C_n + \sum_{i=0}^{n-1} V_P \times C_i}{A}$$

where, V_R is the receiver volume; C_n is the drug concentration in the receiver at the time n; V_P is the volume of the removed sample; C_i is the drug concentration in the receiver at the time n−1 and A is the permeation area (cm^2). Permeation data were reported as the quantity of drug in the receptor chamber per permeation area (mg/cm^2) related to time (Russo *et al*., 2013).

2.2.7. *In vivo* biodistribution study

Female BALB/c OlaHsd mice (12 weeks old; Harlan Laboratories, Barcelona, Spain) were used for *in vivo* pulmonary administration of IR-labeled lipid nanoparticles. The animals were maintained under controlled environmental conditions of temperature (20-24ºC) humidity (40-65%) and lighting (12-hour light-darkness cycle), with free access to standard food (A04 diet, Panlab, Barcelona, Spain) and tap water in makrolon III cages (Tecniplast, Rome, Italy). The procedures were approved by the Bioethics Committee of the Balearic Islands University and carried out in accordance with the Directive 2010/63/EU of the European Parliament and of the Council of 22 September 2010 on the protection of animals used for scientific purposes.

Once mice were anesthetized intra-peritoneally by ketamine/xylazine, 1 mg of IR-NLCs (both types, IR-NLC P and IR-NLC PC) resuspended in PBS was administered intratracheally to each mouse by a MicroSprayer™ aerosolizer (Penn Century® Liquid, Philadelphia, PA, USA). Free IR was used as a control. The mice were placed in an intubation platform for the right administration of drugs and the trachea and epiglottis of the animals were

visualized by using a small animal laryngoscope. The formulations were spray-instilled into the lungs by pushing the syringe plunger of the Penn Century® device. MicroSprayer™ aerosolizer can deliver liquid in the form of aerolized droplets (Bivas-Benita *et al.*, 2005). At given time points after intratracheal instillation (5 min, 2, 24 and 48 hours), mice were sacrificed by ketamine/xylazine anesthesia overdose and cervical dislocation. After that, respiratory tissue (trachea and lungs) and other tissues such as heart, liver, spleen and kidneys were removed and analyzed by LI-COR Pearl® impulse small animal imaging system (LI-COR Corporate, Bad Homburg, Germany) at 800 nm channel.

2.2.8. Statistical analysis

The results are expressed as the mean ± S.D. (standard deviation) for each experimental group. To evaluate the data from the different *in vitro* penetration and permeability experiments, the normal distribution of samples was assessed with the t-test and one way ANOVA, respectively. All statistical analyses were calculated using the IBM SPSS® 20.0 Statistics software (Chicago, IL, USA). *P*<0.05 was considered as significant.

3. Results

3.1. Nanoparticle characterization

The particle characterization of Blank-NLCs, Tb-NLCs, CB-NLCs and IR-NLCs is summarized in Figure 2A. All formulations displayed sizes between 250 and 300 nm after the freeze-drying step using trehalose as cryoprotectant, with polydispersity indexes below 0.4, demonstrating a narrow size distribution. In addition, all the NPs presented a negative charge of around -23 mV. Likewise, CB-labeled NLCs displayed a similar size and Zeta potential, ≈ 293 nm and -26 mV, respectively and IR-NLCs nearly 289 nm and -26 mV. The entrapment efficiency of tobramycin was around 94% for both Tb-NLCs and 99% for stained-NLCs. Moreover, all the EE values analyzed by direct method were consistent with the indirect values. The encapsulation of the drug did not affect

the size of NPs, which remained substantially unchanged compared to unloaded NP formulations. It could be observed that the Zeta potential of NLCs decreased in presence of tobramycin but without significant changes. The pH of the nanosuspension was also measured presenting an appropriate pH value, 8, within the limits that European Pharmacopeia states for liquid preparations for pulmonary administration (European Council, 2014).

TEM images (Figure 2B) revealed that nanoparticles had a regular homogeneous spherical shape without significant differences between the batches prepared.

A

Formulation	Mean size (nm)	PDI	Zeta Potential (mV)	EE (%)
Blank-NLC P	265.16 ± 19.03	0.389 ± 0.04	$- 25.22 \pm 1.23$	--------
Blank-NLC PC	291.06 ± 17.96	0.320 ± 0.02	$- 26.10 \pm 1.41$	--------
Tb-NLC P	254.05 ± 14.50	0.311 ± 0.01	$- 23.03 \pm 2.76$	93.15 ± 0.65
Tb-NLC PC	278.66 ± 20.48	0.371 ± 0.01	$- 22.25 \pm 0.49$	94.03 ± 0.22
CB-NLC P	288.46 ± 6.20	0.304 ± 0.03	-25.42 ± 1.09	99.85 ± 0.04
CB-NLC PC	298.60 ± 3.32	0.332 ± 0.02	-26.81 ± 2.15	99.83 ± 0.10
IR-NLC P	283.93 ± 5.79	0.368 ± 0.03	-25.73 ± 0.25	99.50 ± 0.02
IR-NLC PC	295.16 ± 17.35	0.304 ± 0.06	-26.30 ± 0.41	99.35 ± 0.09

B

Tb-NLC P   Tb-NLC PC

C

Figure 2. Characterization of NLCs: A) Summary table displaying the main properties of the NLCs after freeze-drying, particle size, zeta potential, polydispersity index (PDI) and encapsulation efficiency (EE). B) Transmission electron microscopy images of Tb-NLCs. C) *In vitro* release profiles of tobramycin from NLCs (Tb-NLC P and Tb-NLC PC). Data represent mean + SD values calculated on three different batches.

Table 1. Bioactivity of Tb-NLCs and free drug in terms of MIC determination in 6 strains of clinically isolated *P. aeruginosa* samples. MIC, minimum inhibitory concentration, PA, *Pseudomonas aeruginosa,* M, mucoid clinical strain and NM, non-mucoid clinical strain. P, Precirol® ATO 5 and PC, Precirol® ATO 5 plus Compritol® ATO 888.

MIC (µg/mL)	PA ATCC 27853	PA 852 (NM)	PA 056 (NM)	PA 760 (NM)	PA458 (M)	PA 428 (M)	PA 086 (M)
Free tobramycin	0.5	0.5	1	1	0.5	4	2
Tb-NLC P	0.5	0.5	0.5	0.5	0.5	2	1
Tb-NLC PC	0.5	0.5	0.5	0.5	0.5	4	1

Results from the *in vitro* release studies performed at physiological pH and temperature (pH 7.4 and 37°C, respectively) are reported in Figure 2C as percentage of tobramycin release over the time. An initial rapid release phase was observed for Tb-NLC P and Tb-NLC PC during the first 24 hours (≈80% of drug release). Following the initial burst, a sustained release of the antibiotic is detected in both cases and by the end of the study (92 hours) almost 100% of tobramycin was released from both NPs.

3.2. Microbiological experiments

To examine the antimicrobial effect of the nano-formulated tobramycin, MIC values were calculated against clinical isolated *P. aeruginosa*. Both Tb-NLCs showed to be active against bacterial growth, displaying a MIC value of 0.5 µg/mL in most of the planktonic bacteria tested. In the same experimental conditions, free tobramycin displayed the same or higher MIC value indicating that the encapsulation of the drug did not affect the antimicrobial activity (Table 1).

According to the controls, Blank-NLCs had no discernible inhibitory activity on the visible growth of bacteria.

3.3 Cell assays

The cytotoxicity of the optimized formulations was investigated on A549 and H441 as models of pulmonary epithelium cells. The exposition of NLCs at three different concentrations, 0.25, 0.5 and 1 mg/mL, for 24 hours was studied.

The results of CCK-8 are described in Figure 3 as the percentage of viability compared to control cells (100% of viability), obtained at the same time and in the same experimental conditions. It was observed that none of these formulations presented toxic effects on the cells; at least at the concentrations studied considering that the negative control (DMSO) viability was less than 8%. On the other hand, NLCs presented higher absorbance values in both cell lines when Compritol® ATO 888 was also included in the lipid core (Tb-NLC PC). Higher Tb-NLC P concentrations showed lower viability, but always above 80%, and this phenomenon was more remarkable when tested in the A549 cell line. Besides, under the H441 cell line, Tb-NLC PC, unloaded lipid nanocarriers, and free tobramycin displayed the same absorbance values over all concentrations representing a desired biocompatibility (100%). Blank-NLC formulations displayed no effect on cell viability after 24 hours of treatment, in all cases the viability value range over 80%. Hence, all nanoparticles elaborated were safe in terms of cell viability.
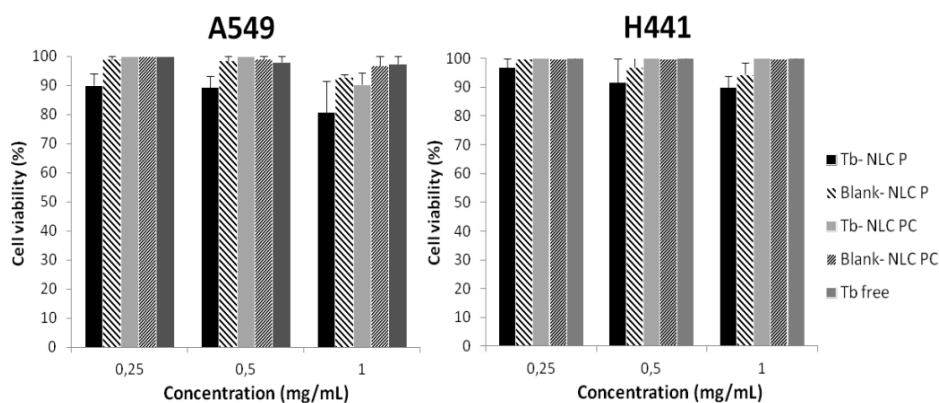
Figure 3. Effect of Tb-NLCs, Blank-NLCs and free drug at different concentrations (0.25, 0.5 and 1 mg/mL) on the viability of A549 and H441 cell lines at 24 hours.
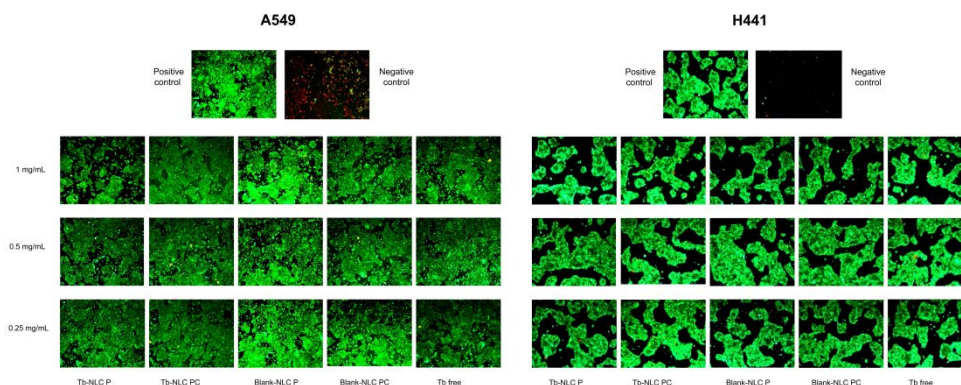
Figure 4. A549 and H441 cells (under 20x magnification) examined by fluorescent microscopy after 24 hours of incubation with Tb-NLCs, Blank-NLC and free drug at different concentrations (0.25, 0.5 and 1 mg/mL). Red color shows cell nucleus of dead cells and green color the cytoplasm of viable cells.

3.4 Artificial mucus penetration assay

Two mucolytic agents, mannitol and carboximethylcysteine (CMC), presenting the property of decreasing the mucus viscosity were used to compare the effect on drug diffusion through an artificial mucus (AM). Figure 5 shows the amount of CB (%) captured in the gelatin gel that was proportional to particle penetration. According to the results, CB-NLC P particles with CMC penetrated the AM faster at the ratio 50:50 (NLC:mucolytic agent) than nanoparticles with mannitol (60% at 7 hours versus 50% at the same time). Similarly, NLC P:CMC at 25:75, the penetration values were almost the same, around 57%. On the other hand, CB recovered from NLC PC was around 55-60% at 7 hours with both excipients independent of the proportions. In all cases, the amount of CB was higher in presence of mucolytic agents. According to these results, no significant differences were found when using various NLC: mucolytic agent ratios, therefore, for further studies, the proportion NLC: mucolytic 75:25 was selected as it contained a higher proportion of nanoparticles.
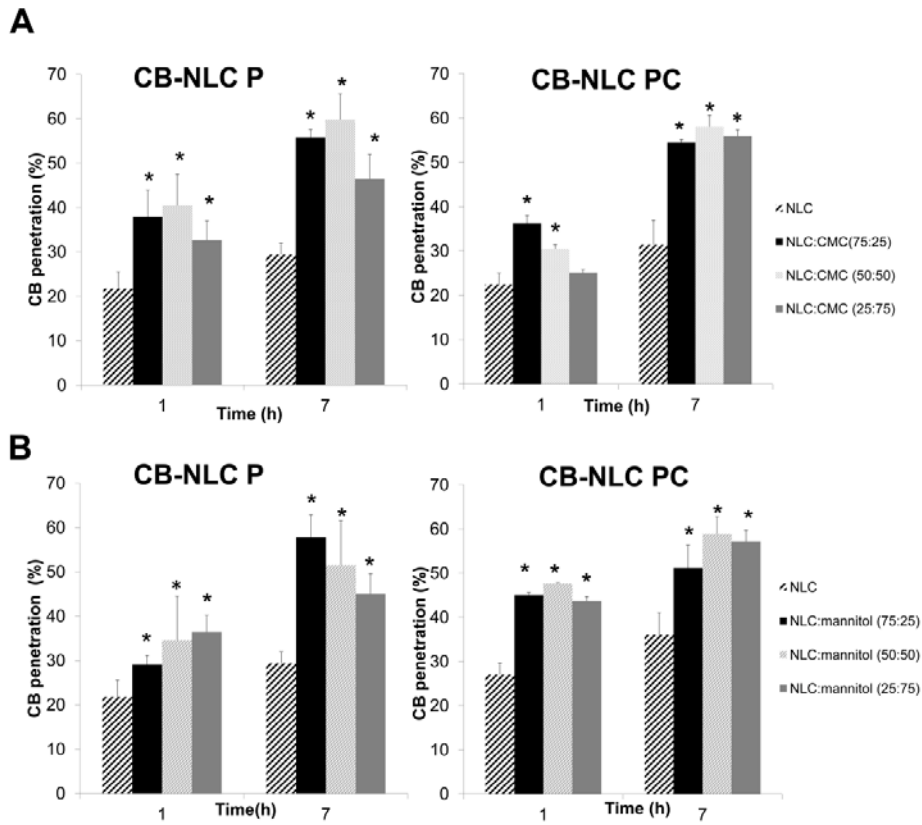
Figure 5. Ability of Coomassie Blue-loaded nanoparticles (CB-NLCs) to penetrate through artificial mucus (AM). A) CB-NLCs alone and mixture of CB-NLCs plus CMC (carboxymethylcysteine) at 75:25, 50:50 and 25:75. B) CB-NLCs alone and mixture of CB-NLCs plus mannitol at 75:25, 50:50 and 25:75. Left column, represents CB-loaded NLC Precirol® ATO 5 and right column, CB-NLC with Precirol® ATO 5 and Compritol® ATO 888.

3.5 Permeation study

In order to estimate the permeability of nanoparticles through artificial mucus, AM1 was used to better simulate the pulmonary environment in CF patients. First, its rheological behavior was analyzed and then the Tb-NLCs permeability was studied.

A

B

C
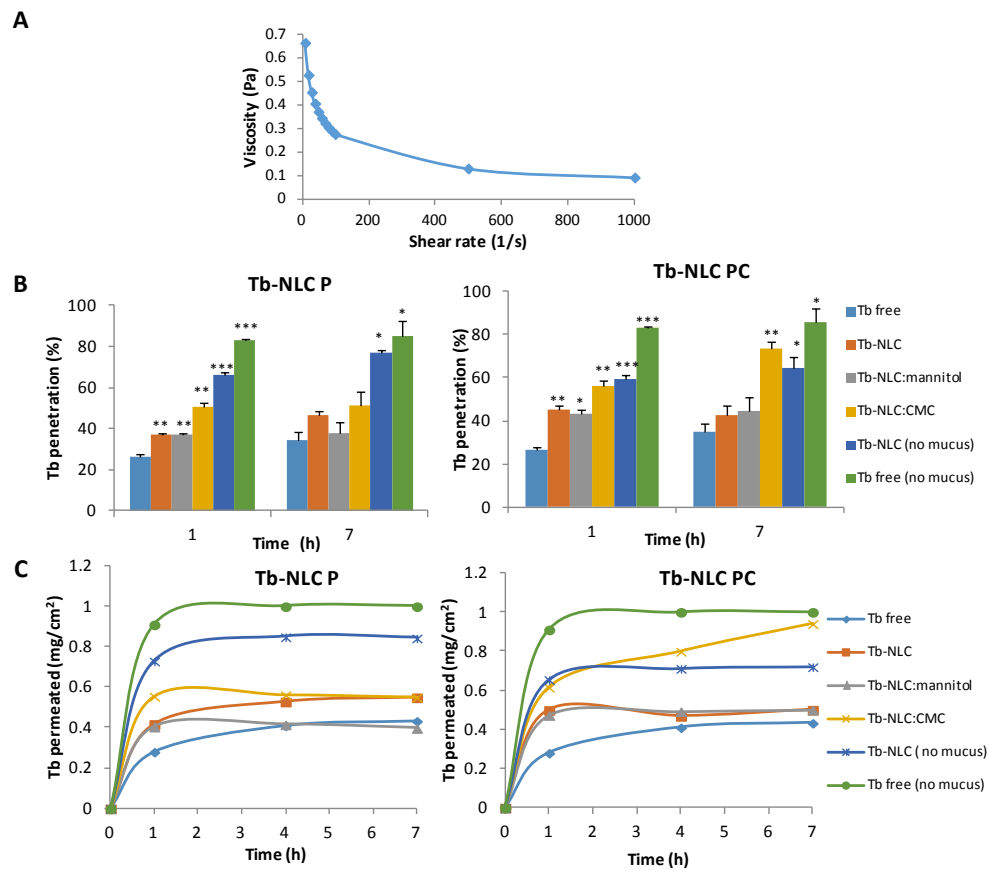
Figure 6. A) Viscosity values versus shear rate of artificial mucus (AM1). B) Percentage of tobramycin permeation from NLCs through the AM1 layer. C) Mucus permeation profile of tobramycin (mg/cm^2) from Tb-NLCs through AM1 at 1, 4 and 7 hours. Legends for B and C: Tb free, Tb-NLC, Tb-NLC: mannitol (75:25), Tb-NLC:CMC (carboxymethylcysteine) (75:25) are formulations tested in presence of a mucus layer. Tb-NLC (no mucus) and Tb free (no mucus) are used as controls without AM1.

AM1 presented a pseudo-plastic behavior (Figure 6A), the shear stress increases while viscosity decreases. Moreover, this artificial mucus was able to be retained on the membrane surface throughout the study period. In the second part of the study, Tb-NLCs with different mucolytics agents were added on the top of the mucus layer and results of the permeation through the mucus are reported in Figure 6B. It was observed that the addition of CMC enhance the permeability of the drug significantly reaching 73% (7 h) for Tb-NLC PC, whereas using mannitol only 42% crossed the AM1 at the same time. In both types of Tb-NLCs, the addition of a mucolytic agent led an increase in permeation. According to the free antibiotic, AM1 reduced significantly the permeability of tobramycin from around 85% to 30%. As Figure 6C shows, tobramycin, a very soluble and polar drug, showed a high dissolution rate from the beginning of the experiment reaching the 100% in less than 5 hours and achieving 1 mg/cm^2 permeation rate, however the presence of a mucus layer reduced it to

less than 0.4 mg/cm^2. Tb-NLCs with mannitol and CMC (75:25) demonstrated an improved permeation rate than the free drug, due to the mucolytic effect of the excipients. In this case, CMC-containing formulations showed higher permeability than mannitol-containing NPs over the time reaching 0.9 mg/cm^2 with Tb-NLCs PC. In both cases tobramycin was locally available to exert its antibiotic activity.

3.6 *In vivo* biodistribution study

IR-NLCs were used for the *in vivo* distribution study as they allow the observation of the NLCs *in vivo* avoiding the auto-fluorescence of the tissues. After intratracheal administration to mice by the Penn Century® device, each mouse was sacrificed at determinate time points and images from LI-COR Pearl® were recorded. IR emission associated with nanoparticles was detected at different levels of the pulmonary tree, suggesting a wide distribution in the lungs until 48 hours (Figure 7A). Immediately after the administration, a high concentration of IR-NLCs in the lungs was observed (Figure

7B). According to the intense red color of the images, IR signal was totally dispersed throughout the entire lung lobes including alveoli. After 2 hours of administration, a systemic absorption of NLCs could be detected in other organs such as liver and kidneys, and less intensively in spleen. At 48 hours, the nanoparticles remained in the lungs while the IR signal disappeared in all other organs suggesting that the lung functions as a NP-trapping organ. Both formulations displayed a similar behavior *in vivo*.
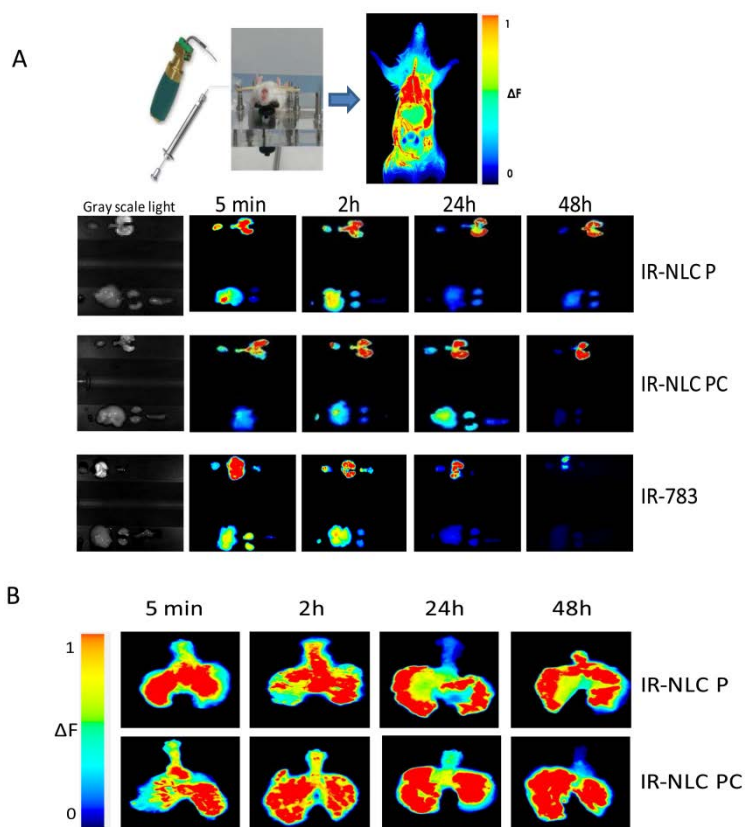
Figure 7. A) Biodistribution of IR-NLCs and free IR after intratracheal administration to mice. IR-intensity image of selected organ excised (upper row from left to right: heart, trachea and lungs, lower row from left to right: gallbladder, liver, kidneys and spleen) at different time points (5 min, 2 h, 24 h and 48 h). B) Biodistribution of IR-NLCs in the lungs.

The only difference was the lack of signal in the liver at 48 hours in the case of NLCs PC. According to the Figure 7A, free dye was faster cleared from the lung and distributed more quickly to other organs such as kidneys and liver (e.g., at 48 hours there was almost no signal in the lungs) compared to NLC formulations. No IR emission was detected in mice before the administration of the formulations.

4. Discussion

As described in this work, we developed antibiotic-loaded NLCs as pulmonary delivery system focusing on the treatment of cystic fibrosis patients. In this case, tobramycin was selected as it is an antibiotic of choice in the treatment of CF associated *P. aeruginosa* infection (Smyth *et al.*, 2014). Some clear advantages of these nanoparticles are the use of biocompatible and biodegradable lipids and the avoidance of organic solvents during their preparation leading to economic efficiency and an environmental friendly process. In addition, it has been reported that the presence of residual solvents in the final product could lead to pulmonary toxicity (Patil and Sarasija, 2012).

Nanoparticles displayed a diameter size ranging from 250 to 300 nm using trehalose as cryoprotectant. Based on our previous studies, 15% (w/w) of trehalose was chosen as cryoprotectant as it was found to be the most suitable one for the lyophilization process (Pastor *et al.*, 2014). The particle size of the nanoparticles allows them to escape from phagocytosis by macrophages, as it is generally thought that particles of 0.5-3 µm in diameter are taken by macrophages (Mansour *et al.*, 2009). The low PDI achieved meant that the particles are distributed uniformly within the formulation. The negative Zeta potential of the nanoparticles, around −24 mV, predicts good physical stability of nanoparticle dispersions (Das *et al.*, 2012). High encapsulation efficiencies (≥ 93%) were achieved for both nanoparticles. Many other studies have been reported regarding the encapsulation of tobramycin into SLN (Cavalli *et al.*, 2000, 2002),

liposomes (Messiaen *et al*., 2013), and polymeric nanoparticles (Deacon *et al*., 2015; Ungaro *et al*., 2012), and those were also able to achieve nanometric size although with less encapsulation efficiencies.

According to the release studies, results showed a biphasic profile characterized by an initial rapid release followed by a modulated and progressive release of tobramycin lasting at least for three days, in both types of formulations. The burst release could be attributed to the drug adsorbed onto or close to the surface of the nanoparticles (Nandakumar *et al*., 2013). This profile release is very similar to the one reported by Patlolla *et al.* (2010) where Colecoxib-NLCs formulation incorporating Compritol® were able to release the drug in a controlled manner and almost completely (over 80% of the drug) during 72 hours. The sustained release of tobramycin via a nanocarrier delivery system may provide the opportunity to maintain prolonged targeted lung exposures and enhance the uptake of drug to the site of infection.

Moreover, in case of a biofilm development, the biphasic release profile might be beneficial, where the fast antibiotic release in the beginning ensures a high initial antibiotic concentration enough to inhibit the biofilm growth, followed by a sustained antibiotic concentration above the MIC value that permits the eradication of the surviving cells minimizing the exacerbation (Cheow *et al*., 2010). It is remarkable that the number of doses could be reduced or longer the dosing interval and therefore enhance patient compliance.

CF patients usually suffer for chronic infections caused by *P. aeruginosa,* which frequently become resistant to antibiotics. For that reason, the efficacy of Tb-NLCs was evaluated using a *P. aeruginosa* strain from CF patients finding the same or higher antipseudomonal activity than free tobramycin. Similar results were reported by Deacon *et al.*, who found that tobramycin NPs and free tobramycin reflected the same MIC values against *P. aeruginosa* PA01 (0.625 µg/mL) (Deacon *et al*., 2015). According to Mugabe *et al.*

(2005), the MIC of liposomal gentamicin formulations were significantly lower than the MICs of free gentamicin against resistant mucoid and non-mucoid clinical strains of *P. aeruginosa* (≤8 µg/mL versus ≥32 µg/mL). This phenomenon was explained by the liposome-bacterial membrane fusion mechanism that led to the deformation of bacterial membrane (Mugabe *et al.*, 2005).

To determine whether Tb-NLCs exerted cell toxicity, *in vitro* cytotoxicity and viability assays using human epithelial cell (A549 and H441) lines was performed after 24h of exposition. None of the formulations tested presented toxicity, at least at the concentrations studied. This finding is in accordance with other reports that demonstrated the good tolerability of lipid nanoparticles *in vitro* using A549 cell lines (Hu and Jia, 2010; Liu *et al.*, 2008; Patlolla *et al.*, 2010). Furthermore, the concentration of 1 mg/mL is 2,000 times higher than the MIC of Tb-NLCs against *P. aeruginosa* (MIC 0.5 µg/mL). In the next step, cell viability was analyzed under fluorescent microscopy where the

predominance of green color in all the samples confirmed the safety of the lipid nanoparticles.

Mucus covers many body surfaces forming a gel-like barrier to protect the body from pathogens and other kind of environmental ultrafine particles (Cone, 2009). However, in CF patients this natural mucus becomes tenacious housing many bacterial pathogens that hinder the penetration of antibiotics and the efficiency of therapies. In order to overcome this abnormal mucus barrier and to prolong the NLCs retention in the lung two mucolytic agents, i.e mannitol and carboxymethylcisteine were selected. We tested whether our particles could cross the mucus and facilitate the drug transport through it using the AM model, reported before by Yang *et al.* (2011) CB dye was chosen as the active ingredient because the gelatin interfered with the amino groups of the tobramycin and it was impossible to quantify. As the nanoparticle diffusion across the mucus is dictated by the size of the mucus pores, Tb-NLCs particles with an approximate diameter of

250 nm, theoretically, should be able to overcome the mucus barrier as they are small enough to diffuse through the mucus pores which typically fall in the range of 200-500 nm in chronically infected lungs (Suk *et al.*, 2009). Forier *et al.* (2013) also reported that negatively charged nanoparticles exhibited superior mucus penetration. As expected, the penetration of the particles across the mucus layer was improved by the addition of mucolytic agents that facilitated the drug transport through it. Suk *et al* also demonstrated an increased in particle penetration through CF sputum when using another mucolytic, N- acetylcysteine (Suk *et al.*, 2011).

To carry out permeation studies for tobramycin quantification, another artificial mucus (AM1) was elaborated with similar physico-chemical properties to the mucus that have CF patients as described by Shur *et al.* (2008). This model reproduces pulmonary environment and allows *in vitro* experiments performing because AM passed through membranes pores. According to our previous penetration study, the highest proportion of NLC: mucolytic agent was selected (75:25). The permeability assay revealed that the maximum drug permeation across the mucus layer was observed for the Tb-NLC PC incorporating carboxymethyl-cysteine (CMC), whereas the addition of mannitol did not improve significantly the drug permeability at 7 hours. Similarly, Suk *et al.* also reported a close to 13-fold improvement in the diffusion velocity of NPs through a sputum layer upon the addition of acetylcysteine (Suk *et al.*, 2011). The presence of tobramycin in the receptor compartment suggests that the drug from NLCs may slowly release, permeate and distribute into the abnormal mucus layer being locally available for its antimicrobial activity. According to these results, we developed a mucus penetrating drug carrier that after formulate with appropriate mucolytic agents, could offer sustained levels of antibiotic at the mucus barrier. However, a complementary studies incubating *P. aeruginosa* with AM should be performance in order to find out what

could happen in an infection scenario such as in CF patient sputum.

Finally, the administration of IR-NLCs exerted a strong IR signal in the lungs of the mice lasting until 48 hours allowing the drug release from the lipid matrix. The intratracheal instillation by Penn Century® device provides a fast and quantifiable technique for drug delivery directly to the lungs (Patil and Sarasija, 2012) presenting large distribution and minimal drug loss during application compared to nebulization processes (Bivas-Benita *et al.*, 2005). Nevertheless, intratracheal instillation does not reflect the natural inhalation mechanism because the formulation is required to be administered to anesthetized animals (Nahar *et al.*, 2013). Regarding to the free drug, Poyner *et al.* (1995) reported that the endotracheal administration of radiolabeled tobramycin led to a higher dissemination to the kidney and in a lower extent at the lung tissue compared to liposomal and microcapsular tobramycin which were primarily retained in the lungs, thus decreasing nephrotoxicity. Similar results were reported by Varshosaz *et al.* (2013) who confirmed that amikacin-loaded SLNs remained 6 hours longer in lungs after pulmonary administration by microsprayer compared to i.v. route. Moreover, in another study by Patlolla *et al.* (2010), authors also showed that celecoxib-loaded NLCs deposited in the alveolar region with prolonged residence time, up to 24 hours, after inhalational administration in mice. Therefore, it might be concluded that tobramycin encapsulation within DDS such as liposomes or nanoparticles may represent an advantage for prolonging lung residence time of the encapsulated drug that would be slowly released to the media allowing continuous bacterial killing.

5. Conclusions

In this work, we report the development and the characteristics of a new tobramycin nanocarrier formulation. Tb-NLCs (both Tb-NLC P and Tb-NLC PC) demonstrated efficacy against

P. aeruginosa in vitro, mucus penetration ability and large pulmonary distribution and retention in the *in vivo* studies. Tb-NLCs can provide the advantage of a sustained drug release in the target site, resulting in reduced-dose schedule and improved patient compliance. Therefore, Tb-NLCs could represent an alternative drug delivery system for pulmonary infection treatment. As yet, the results presented in this study are not sufficient to predict the effectiveness of the lipid-based nanosystem in CF patients although the features of the developed formulation so far examined could be considered promising in a perspective of an efficacious CF inhalable therapy.

Acknowledgments

References

Andrade, F., Rafael, D., Videira, M., Ferreira, D., Sosnik, A., Sarmento, B., 2013. Nanotechnology and pulmonary delivery to overcome resistance in infectious diseases. Adv. Drug. Deliv. Rev., 65, 1816-1827.

Bivas-Benita, M., Zwier, R., Junginger, H.E., Borchard, G., 2005. Non-invasive pulmonary aerosol delivery in mice by the endotracheal route. Eur. J. Pharm. Biopharm., 61, 214-218.

Cavalli, R., Gasco, M.R., Chetoni, P., Burgalassi, S., Saettone, M.F., 2002. Solid lipid nanoparticles (SLN) as ocular delivery

system for tobramycin. Int. J. Pharm., 238, 241-245.

Cavalli, R., Zara, G.P., Caputo, O., Bargoni, A., Fundarò, A., Gasco, M.R., 2000. Transmucosal transport of tobramycin incorporated in SLN after duodenal administration to rats. Part I-A pharmacokinetic study. Pharmacol. Res., 42, 541-545.

Cheow, W.S., Chang, M.W., Hadinoto, K., 2010. Antibacterial efficacy of inhalable antibiotic-encapsulated biodegradable polymeric nanoparticles against *E. coli* biofilm cells. J Biomed. Nanotechnol., 6, 391-403.

Cone, R.A., 2009. Barrier properties of mucus. Adv. Drug Deliv. Rev., 61, 75-85.

Das, S., Ng, W.K., Tan, R.B.H., 2012. Are nanostructured lipid carriers (NLCs) better than solid lipid nanoparticles (SLNs): Development, characterizations and comparative evaluations of clotrimazole-loaded SLNs and NLCs? Eur. J. Pharm. Sci., 47, 139-151.

Deacon, J., Abdelghany, S.M., Quinn, D.J., Schmid, D., Megaw, J., Donnelly, R.F., Jones, D.S., Kissenpfennig, A., Elborn, J.S., Gilmore, B.F., Taggart, C.C., Scott, C.J., 2015. Antimicrobial efficacy of tobramycin polymeric nanoparticles for *Pseudomonas aeruginosa* infections in cystic fibrosis: Formulation, characterisation and functionalisation with dornase alfa (DNase). J. Control. Release, 198, 55-61.

Donnelly, R.F., McCarron, P.A., Cassidy, C.M., Elborn, J.S., Tunney, M.M., 2007. Delivery of photosensitisers and light through mucus: Investigations into the potential use of photodynamic therapy for treatment of *Pseudomonas aeruginosa* cystic fibrosis pulmonary infection. J. Control. Release, 117, 217-226.

European Council, 2014. European Pharmacopeia 8.0. Council of Europe: European Directorate for the Quality of Medicines and Healthcare, Strabourg; 363-365.

Forier, K., Messiaen, A.S., Raemdonck, K., Deschout, H., Rejman, J., De Baets, F., Nelis, H., De Smedt, S.C., Demeester, J., Coenye, T., Braeckmans, K., 2013. Transport of nanoparticles in cystic fibrosis sputum and bacterial biofilms by single-particle tracking microscopy. Nanomedicine (Lond), 8, 935-949.

Hajipour, M.J., Fromm, K.M., Ashkarran, A.A., Jimenez de Aberasturi, D., de Larramendi, I.R., Rojo, T., Serpooshan, V., Parak, W.J., Mahmoudi, M., 2012. Antibacterial properties of nanoparticles. Trends Biotechnol., 30, 499-511.

Hu, L., Jia, Y., 2010. Preparation and characterization of solid lipid nanoparticles loaded with epirubicin for pulmonary delivery. Die Pharmazie-An Int. J. Pharm. Sci., 65, 585-587.

Liu, J., Gong, T., Fu, H., Wang, C., Wang, X., Chen, Q., Zhang, Q., He, Q., Zhang, Z., 2008. Solid lipid nanoparticles for pulmonary delivery of insulin. Int. J. Pharm., 356, 333-344.

Mansour, H.M., Rhee, Y.S., Wu, X., 2009. Nanomedicine in pulmonary delivery. Int. J. Nanomed., 4, 299-319.

Marini, J.J., Slutsky, A.S., 1998. Physiological Basis of Ventilatory Support, Marcel Dekker New York.

Messiaen, A., Forier, K., Nelis, H., Braeckmans, K., Coenye, T., 2013. Transport of nanoparticles and tobramycin-loaded liposomes in Burkholderia cepacia complex biofilms. Nanomedicine, 8, 895-949.

Moreau-Marquis, S., Stanton, B.A., O'Toole, G.A., 2008. *Pseudomonas aeruginosa* biofilm formation in the cystic fibrosis airway. Pulm. Pharmacol. Ther., 21, 595-599.

Mugabe, C., Azghani, A.O., Omri, A., 2005. Liposome-mediated gentamicin delivery: development and activity against resistant strains of *Pseudomonas aeruginosa i*solated from cystic fibrosis patients. J. Antimicrob. Chemother., 55, 269-271.

Nahar, K., Gupta, N., Gauvin, R., Absar, S., Patel, B., Gupta, V., Khademhosseini, A., Ahsan, F., 2013. *In vitro*, *in vivo* and ex vivo models for studying particle deposition and drug absorption of inhaled pharmaceuticals. Eur. J. Pharm. Sci., 49, 805-818.

Nandakumar, V., Geetha, V., Chittaranjan, S., Doble, M., 2013. High glycolic poly (DL lactic co glycolic acid) nanoparticles for controlled release of meropenem. Biomed. Pharmacother., 67, 431-436.

Nassimi, M., Schleh, C., Lauenstein, H.D., Hussein, R., Hoymann, H.G., Koch, W., Pohlmann, G., Krug, N., Sewald, K., Rittinghausen, S., Braun, A., Muller-Goymann, C., 2010. A toxicological evaluation of inhaled solid lipid nanoparticles used as a potential drug delivery system for the lung. Eur. J. Pharm. Biopharm., 75, 107-116.

Okusanya, O.O., Bhavnani, S.M., Hammel, J., Minic, P., Dupont, L.J., Forrest, A., Mulder, G.J., Mackinson, C., Ambrose, P.G., Gupta, R., 2009. Pharmacokinetic and pharmacodynamic evaluation of liposomal amikacin for inhalation in cystic fibrosis patients with chronic pseudomonal infection. Antimicrob. Agents Chemother., 53, 3847-3854.

Pastor, M., Moreno-Sastre, M., Esquisabel, A., Sans, E., Viñas, M., Bachiller, D., Asensio, V.J., Pozo, ÁD., Gainza, E., Pedraz, J.L., 2014. Sodium colistimethate loaded lipid nanocarriers for the treatment of *Pseudomonas aeruginosa* infections associated with cystic fibrosis. Int. J. Pharm., 477, 485-494.

Patil, J.S., Sarasija, S., 2012. Pulmonary drug delivery strategies: A concise, systematic review. Lung India., 29, 44-49.

Patlolla, R.R., Chougule, M., Patel, A.R., Jackson, T., Tata, P.N., Singh, M., 2010. Formulation, characterization and pulmonary deposition of nebulized celecoxib encapsulated nanostructured lipid carriers. J. Control. Release, 144, 233-241.

Poyner, E.A., Alpar, H.O., Almeida, A.J., Gamble, M.D., Brown, M.R.W., 1995. A comparative study on the pulmonary delivery of tobramycin encapsulated into liposomes and PLA microspheres following intravenous and endotracheal delivery. J. Control. Release, 35, 41-48.

Ratjen, F., Brockhaus, F., Angyalosi, G., 2009. Aminoglycoside therapy against *Pseudomonas aeruginosa* in cystic fibrosis: A review. J. Cyst. Fibros., 8, 361-369.

Russo, P., Stigliani, M., Prota, L., Auriemma, G., Crescenzi, C., Porta, A., Aquino, R.P., 2013. Gentamicin and leucine inhalable powder: what about antipseudomonal activity and permeation through cystic fibrosis mucus? Int. J. Pharm., 440, 250-255.

Sampath, S.S., Robinson, D.H., 1990. Comparison of new and existing spectrophotometric methods for the analysis of tobramycin and other aminoglycosides. J. Pharm. Sci., 79, 428-431.

Savla, R., Minko, T., 2013. Nanotechnology approaches for inhalation treatment of fibrosis. J. Drug Target., 21, 914-925.

Shur, J., Nevell, T.G., Ewen, R.J., Price, R., Smith, A., Barbu, E., Conway, J.H., Carroll, M.P., Shute, J.K., Smith, J.R., 2008. Cospray-dried unfractionated heparin with L-leucine as a dry powder inhaler mucolytic for cystic fibrosis therapy. J. Pharm. Sci., 97, 4857-4868.

Smyth, A.R., Bell, S.C., Bojcin, S., Bryon, M., Duff, A., Flume, P., Kashirskaya, N., Munck, A., Ratjen, F., Schwarzenberg, S.J., Sermet-Gaudelus, I., Southern, K.W., Taccetti, G., Ullrich, G., Wolfe, S., European Cystic Fibrosis Society, 2014. European Cystic Fibrosis Society Standards of Care: Best Practice guidelines. J. Cyst. Fibros., 13 (Suppl 1), S23-S42.

Suk, J.S., Lai, S.K., Boylan, N.J., Dawson, M.R., Boyle, M.P., Hanes, J., 2011. Rapid transport of muco-inert nanoparticles in cystic fibrosis sputum treated with N-acetyl cysteine. Nanomedicine (Lond), 6, 365-375.

Suk, J.S., Lai, S.K., Wang, Y.Y., Ensign, L.M., Zeitlin, P.L., Boyle, M.P., Hanes, J., 2009. The penetration of fresh undiluted sputum expectorated by cystic fibrosis patients by non-adhesive polymer nanoparticles. Biomaterials, 30, 2591-2597.

Thellin, O., Zorzi, W., Jolois, O., Elmoualij, B., Duysens, G., Cahay, B., Streel, B., Charif, M., Bastin, R., Heinen, E., Quatresooz, P., 2015. *In vitro* approach to study the synergistic effects of tobramycin and clarithromycin against *Pseudomonas aeruginosa* biofilms using prokaryotic or eukaryotic culture media. Int. J. Antimicrob. Agents, 46, 33-38.

Tseng, B.S., Zhang, W., Harrison, J.J., Quach, T.P., Song, J.L., Penterman, J., Singh, P.K., Chopp, D.L., Packman, A.I., Parsek, M.R., 2013. The extracellular matrix protects *Pseudomonas aeruginosa* biofilms by limiting the penetration of tobramycin. Environ. Microbiol., 15, 2865-2878.

Ungaro, F., d'Angelo, I., Coletta, C., d'Emmanuele di Villa Bianca, R., Sorrentino, R., Perfetto, B., Tufano, M.A., Miro, A., La Rotonda, M.I., Quaglia, F., 2012. Dry powders based on PLGA nanoparticles for pulmonary delivery of antibiotics: modulation of encapsulation efficiency, release rate and lung deposition pattern by hydrophilic polymers. J. Control. Release, 157, 149-159.

Varshosaz, J., Ghaffari, S., Mirshojaei, S.F., Jafarian, A., Atyabi, F., Kobarfard, F., Azarmi, S., 2013. Biodistribution of amikacin solid lipid nanoparticles after pulmonary delivery. Biomed. Res. Int., 13685, 9.

Waters, V., Smyth, A., 2015. Cystic fibrosis microbiology: Advances in antimicrobial therapy. J. Cyst Fibros., 14 (5) 551-560

Weber, S., Zimmer, A., Pardeike, J., 2014. Solid Lipid Nanoparticles (SLN) and Nanostructured Lipid Carriers (NLC) for pulmonary application: A review of the state of the art. Eur. J. Pharm. Biopharm., 86, 7-22.

Yang, Y., Tsifansky, M.D., Shin, S., Lin, Q., Yeo, Y., 2011. Mannitol-guided delivery of Ciprofloxacin in artificial cystic fibrosis mucus model. Biotechnol. Bioeng., 108, 1441-1449.

DISCUSSION

Cystic fibrosis (CF) is a genetic disorder that affects nearly 80,000 patients worldwide. It is caused by mutations in the cystic fibrosis transmembrane conductance regulator (CFTR) gene that encodes a protein that forms an ion channel in epithelial cell membranes [1]. CFTR mutations cause malfunctioning of the membrane-bound cAMP regulated chloride channel, which in turns, produces plugs of mucus and obstruction that lead with bronchial infections in the lung being *Pseudomonas aeruginosa* the most prevalent pathogen that affects CF patients [2]. *P. aeruginosa* is known to be one of most drug-resistant bacteria. The resistance mechanism is largely based on the very low, non-specific permeability of its outer membrane or the presence of an efflux pump system removing drugs from the cell [3]. For this reason, the treatment of this infection is often difficult and, as a consequence, there is a high morbidity and mortality associated to the respiratory manifestations of the CF disease hampered by the lack of effective therapies [4]. Nowadays, sodium colistimethate, which is rapidly hydrolyzed to its active form (colistin), is one of the first-choice options for inhaled therapy to treat respiratory infections in CF patients [5]. Colistin is a polycationic peptide antibiotic that disrupts the integrity of the outer membrane of the cell wall of gram-negative bacteria by binding to the lipopolysaccharides leading to cell death [6]. It has proved to be effective against *P. aeruginosa*, however, its clinical used is limited due to its toxic effects such as nephrotoxicity and neuromuscular blockade [7].

As it is becoming increasingly difficult to fight against antibiotic resistances, new approaches have been carried out, putting efforts in the discovery of new antibiotics or in the chemical modification of existing antimicrobial drugs. Since only a few new antimicrobial entities have been discovered recently [8], nanoencapsulation of antibiotics into drug delivery systems (DDS) seems to be an interesting alternative for improving current treatments. Over the last decades, the use of lipid nanoparticles (NPs) for drug delivery has been extensively investigated in order to overcome some limitations of the already current drug formulations [9]. In this regard, solid lipid nanoparticles (SLNs) have emerged as promising nanosystems to encapsulate drugs in the submicron range from about 50 nm to 1000 nm (Figure 1). SLNs are composed of biocompatible and biodegradable lipids building a solid lipid matrix core but due to their low drug loading and unpredictable drug release, nanostructured lipid carriers (NLCs) have been developed as a second generation of lipid nanoparticles (Figure 1) [10]. The main difference between them is the structure of the lipid matrix that in the NLCs is composed of a mixture of solid and liquid lipids resulting in a less-ordered matrix with many imperfections that permit the increase of the drug loading and prevent its leakage [11]. In principle, these NPs present some advantages over other DDS such as a controlled drug delivery, specific targeting, good tolerability, the ability to protect the drug from degradation and the possibility to incorporate lipophilic and hydrophilic drugs [12].

SLN   NLC
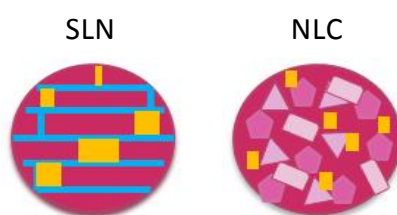
Figure 1. Schematic representation of solid lipid nanoparticles (SLN) and nanostructured lipid carriers (NLC).

Considering that pulmonary infection with *P. aeruginosa* is located in the lower conducting airways, the treatment is usually accessible with the use of inhaled aerosolized antibiotics [13]. In this sense, pulmonary drug delivery has gained much attention as a non-invasive route for the delivery of high amounts of therapeutic agents directly to the desired site of action minimizing systemic exposure and adverse effects [14]. Many research groups have focused their efforts in developing inhalable nanoparticles to fight against bacterial resistances by encapsulating different drugs such as amikacin [15], tobramycin [16], ciprofloxacin [17,18], itraconazole [19] or amphotericin B [20]. However, new alternatives must be considered due to the rapid emergence of bacterial resistances, being lipid nanoparticles such as SLNs and NLCs encouraging candidates for drug delivery to the lungs.

Bearing in mind these considerations, this doctoral thesis experimental work focuses on the use of lipid nanoparticles for antibiotic delivery to the lungs with the aim to treat *Pseudomonas aeruginosa* infections associated with cystic fibrosis. One of the main goals of CF treatment is to prevent, limit and eradicate *P. aeruginosa* from the respiratory tract of patients. This could enlarged survival and improved their quality of life [21].

For this purpose, in the first part of this doctoral thesis, we wanted to answer the following questions:

1. **Are SLNs and NLCs suitable for the encapsulation of sodium colistimethate? Have sodium colistimethate-loaded NPs antimicrobial activity against *Pseudomonas aeruginosa* infections? How is their biodistribution after their pulmonary delivery?**

The first step of this work was the design and optimization of two nanoformulations containing sodium colistimethate with desired physico-chemical and biopharmaceutical characteristics for the delivery of the encapsulated drug after pulmonary administration. With this purpose, Colist-SLNs and Colist-NLCs were elaborated by the emulsion solvent

evaporation technique [22] and by the hot melt homogenization method [23,24], respectively. SLNs were made of Precirol® ATO 5 (1%, w/v) stabilized with Tween® 80 and Poloxamer 188 at 1% (w/v) while NLCs are prepared with Precirol® ATO 5 (6.6% w/v) and Mygliol® 812 (0.6%, w/v) using Poloxamer 188 (0.6% ,w/v) and Tween® 80 (1.3%, w/v) as surfactants. Both types of NPs were elaborated at 10% of drug concentration (w/w, lipid content). All the nanoparticles prepared were freeze-dried with two different cryoprotectacts, either D-mannitol or trehalose at 15% (w/w, lipid content) in order to select the most suitable one.

Once prepared, the *in vitro* characterization of the nanoparticles was undergone allowing to study the nanoparticles obtained into a greater detail. The *in vitro* characterization included size measurement, zeta potential, drug content, morphology and drug release.

Table 1. Characteristics of sodium colistimethate-loaded lipid nanoparticles.

Formulation	Cryoprotectant	Size (nm)[a]	Polydispersity index (PDI)[a]	Zeta potential (mV)[a]
Colist-NLC	Trehalose	412.5 ± 13.9	0.442	-21.97 ± 1.72
	D-Mannitol	254.5 ± 20.3	0.339	-26.1 ± 7.05
Colist-SLN	Trehalose	303.4 ± 39.5	0.276	-20.80 ± 1.63
	D-Mannitol	302.6 ± 20.5	0.361	-20.5 ± 6.09
IR-NLC	Trehalose	439.3 ± 20.1	0.439	-23.03 ± 1.8

[a] The results are expressed as the mean ± S.D. (n=3).

Nanoparticles displayed a mean diameter size of 412.5 ± 13.9 nm and 303.4 ± 39.5 nm, for Colist-NLCs and Colist-SLNs, respectively, when trehalose was used as cryoprotectant. The addition of D-mannitol led to particle sizes of 254.5 ± 20.3 nm for Colist-NLCs and 302.6 ± 20.5 nm for Colist-SLNs. The polydispersity index was below 0.5 for both NPs demonstrating that were monodisperse [25]. All the nanoformulations

elaborated presented a negative zeta potential, from -20 to -26 mV (Table 1). Transmission electron microscopy (TEM) and atomic force microscope (AFM) images revealed that the nanoparticles (lyophilized with trehalose) presented a spherical shape and a smooth surface (Figure 2).
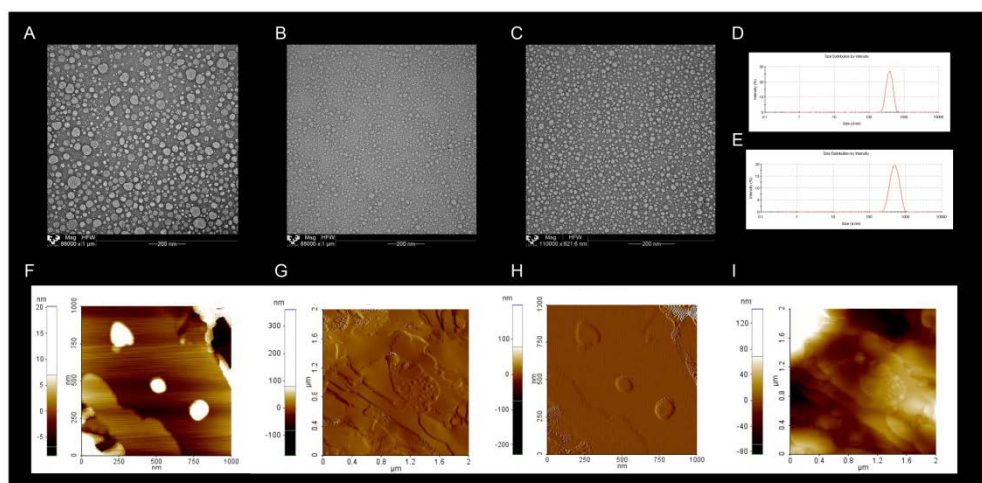

Figure 2. Transmission electron microscopy images of sodium colistimethate loaded lipid nanoparticles, A) SLN, B) NLC after reconstitution, and C) NLC after nebulization with a vibrating mesh nebulizer. Size analysis results, D) Colist-NLC after reconstitution, and E) Colist-NLC after nebulization with vibrating mesh nebulizer. F-I atomic force microscopy images, F and G) Sodium colistimethate loaded SLN and H and I) Sodium colistimethate-loaded NLC.

Moreover, high encapsulation efficiencies were achieved for Colist-SLNs and Colist-NLCs, i.e., 79.70% and 94.79%, respectively, that are in accordance with the results reported by Martins *et al.* who also described high EE values (>90%) for camptothecin-loaded SLN. Their slightly higher results are likely to be related to the higher lipophilicity of camptothecin compared to sodium colistimethate [26]. Likewise, Patlolla *et al*. reported similar encapsulation efficiency values when encapsulating celecoxib in NLCs (>90%) [27].

The next step was to determine the ability of these NPs to provide a sustained release of the drug. The determination of the *in vitro* release profile of a formulation gives

us guidance on how the particles would behave when administered in an *in vivo* model. As it is represented in Figure 3, SLNs released a 50% of sodium colistimethate in 8 hours, data that were similar to those reported by Silva *et al.* for risperidone-loaded SLN, i.e., 40% drug released by the 8th hour [28]. On the other hand, NLCs released an 86% of the drug by that time (end of study) which is in accordance with Zheng *et al*. who also detected almost a 100% of drug release from their NLCs [29]. Remarkably, it could be observed that almost all the drug was released from the Colist-NLCs under the assayed conditions. This sustained release, especially the one presented by the Colist-NLCs, could reduce the number of doses, improving patient adherence to the treatment and, thus, life quality.
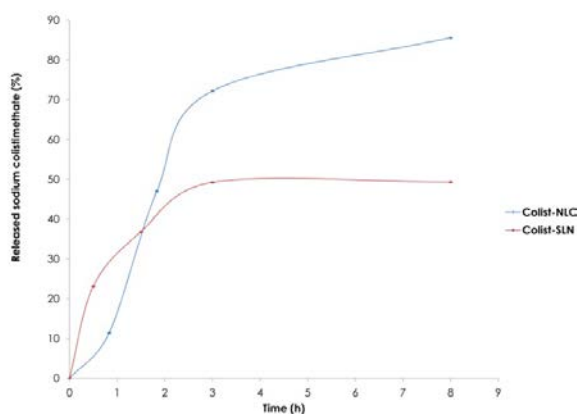
Figure 3. Release profile of sodium colistimethate from the lipid nanoparticles elaborated.

Following the characterization of the NPs, we wanted to check their antimicrobial efficacy against *Pseudomonas aeruginosa* strains. For this purpose, *P. aeruginosa* was isolated from the sputum of cystic fibrosis patients obtaining two types: mucoid and non-mucoid. Both Colist-NLCs and Colist-SLNs inhibit the growth of clinically isolated *P. aeruginosa*. As Figure 4 displays, the free antibiotic solution presented a mode of 2 µg/mL, whereas Colist-NLCs and Colist- SLNs displayed a 1 µg/mL and 2 µg/mL MIC, respectively. When nanoparticles were freeze-dried with D-mannitol, a lower activity was determined in both cases and for that reason, trehalose was defined as the cryoprotectant to be used

in the subsequent experiments. Other authors reported much higher MIC values for *P. aeruginosa* ATCC 27853, 4.0 ± 1.0 µg/mL, when incorporating Polymixin B in liposomes. Nevertheless, the MICs were even higher when the free Polymixin B was assessed [30]. Wang *et al*. reported also the utility of lipid nanoparticles for tilmicosin encapsulation describing a MIC of 4.0 µg/mL [31].
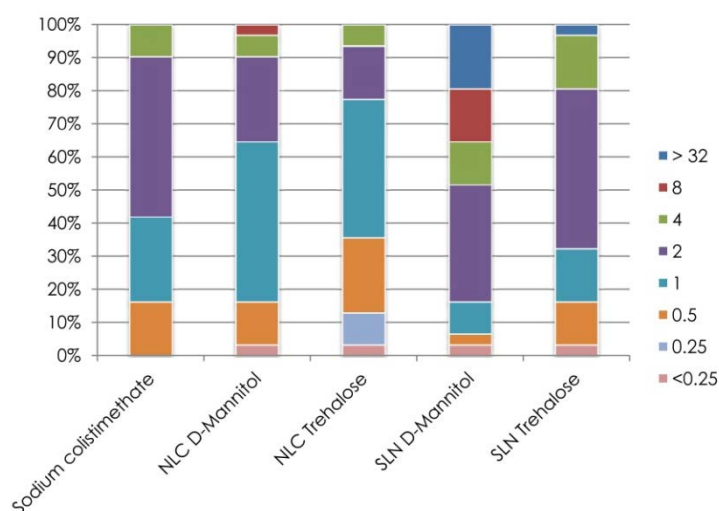
Figure 4. Bioactivity of the lipid nanoparticles elaborated in terms of MIC determination in 31 strains of clinically isolated *P. aeruginosa* samples.

Apart from being efficient against bacteria pathogens, another requirement for lipid nanoparticles is the lack of toxicity. Therefore, the IC50 of the lipid nanoparticles developed was estimated by the CCK-8 assay in two cell lines: human lung papillary adenocarcinoma (H441) and human lung carcinoma (A549), as shown in Figure 5A. According to the FDA, IC50 represents the concentration of a drug that is required for the 50% inhibition *in vitro*. For both cell lines, sodium colistimethate showed the lowest IC50, therefore displaying the highest toxicity whereas Colist-NLCs exhibited the highest IC50, 1.08 ± 0.19 mg/mL and 2.59 ± 0.87 mg/mL for H441 and A549 cells, respectively.

Interestingly, these IC50 values are far from the 1-2 μg/mL that was estimated as MIC, consequently, it could be inferred that the lipid nanoparticles might be a safe product. Doktorovova and colleagues reported that IC50 values for lipid nanoparticles are usually within 0.1-1 mg/mL, being in our case slightly higher [32]. Overall, it should be pointed out that entrapping the antibiotic in lipid nanoparticles led to a huge decrease in toxicity, as NLCs presented 160-fold less toxicity in H441 cells and 28-fold less toxicity in A549 cells than the free antibiotic. Moreover, Colist-NLCs was statistically less toxic than Colist-SLNs (p<0.01).
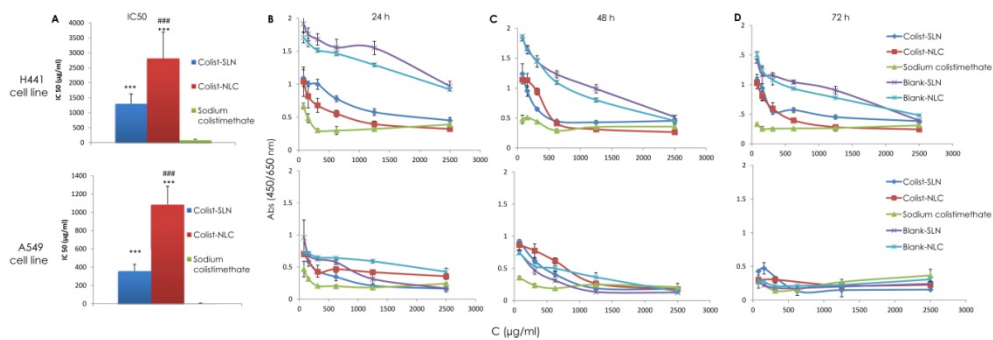
Figure 5. Cell experiments results. A) Represents the IC50 value of the formulation in both cell lines. *** Describes statistically significant difference between the formulation and the free sodium colistimethate, p<0.01 and ### represents differences between Colist-NLC and Colist-SLN, p<0.01. B-D) *In vitro* cytotoxicity measured by means of CCK8 at 24 h (B), 48 h (C) and 72 h (D). Upper row: cytotoxicity tested against H441 cell line, second row: cytotoxicity in the A549 cell line.

In order to complete this study, the citotoxicity of the formulations at three exposures times was assayed. The results obtained suggest that sodium colistimethate encapsulation enhances cell viability especially at concentrations bellow 1250 μg/mL (Figure 5B-D). In terms of cell viability, Ribeiro de Souza *et al.* reported that praziquantel-loaded SLNs presented a time and dose-dependent cell viability in a hepatoma cell line, reaching up to a 70% decrease of cell viability for the free drug and a 45% decrease for the loaded SLN [33]. Hence, based in these *in vitro* results, it could be postulated that

enclosing sodium colistimethate into lipid nanoparticles decreases the toxicity of both the pro-drug, sodium colistimethate, and the drug, colistin, mainly because they are released in a controlled manner over time.

Taking the aforementioned findings together, the NLCs presented most satisfactory results (more suitable release profile along with a lower MIC and toxicity) compared to the SLNs, thus, Colist-NLCs (freeze-dried with trehalose) were selected for the *in vivo* experiments. Before we started them, some previous *in vitro* studies needed to be carried out. As the final formulation may need to be administered by the pulmonary route, we selected a mesh vibrating nebulizer (eFlow® rapid, Figure 6A) to analyze the impact of the nebulization on the NLCs. The size distribution and zeta potential slightly varied from the pre-nebulization to the post-nebulization stage (Figure 2E) but were not significant changes. Besides, the TEM images showed that the nebulization process did not affect nanoparticle morphology (Figure 2C).
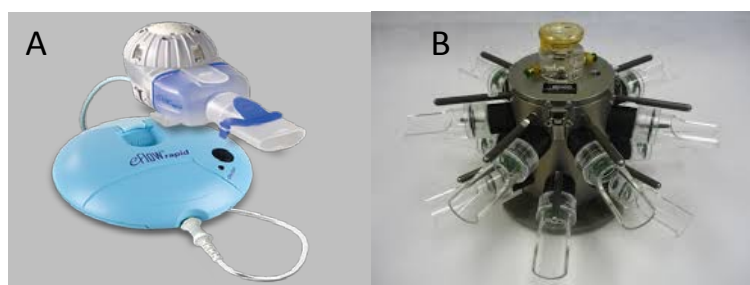
Figure 6. Images of eFlow® rapid nebulizer system (A) and inhalation tower for mice (B).

In the last stage of this first chapter, *in vivo* experiments were conducted to further analyze the biodistribution of NLCs after pulmonary administration to mice. For these *in vivo* studies, infrared (IR-783) labeled NLCs were prepared just as mentioned previously, but by adding 50 mg of IR-783 instead of the antibiotic. Likewise, IR-NLCs displayed a size and charge very similar to the antibiotic-loaded NLCs (Table 1). An inhalation tower (Figure

6B) was used to administer the nebulized lipid nanoparticles to mice and IR images were recorded at predetermined time points (post-nebulization, 2.5, 4, 24 and 48 hours) as Figure 7A shows.
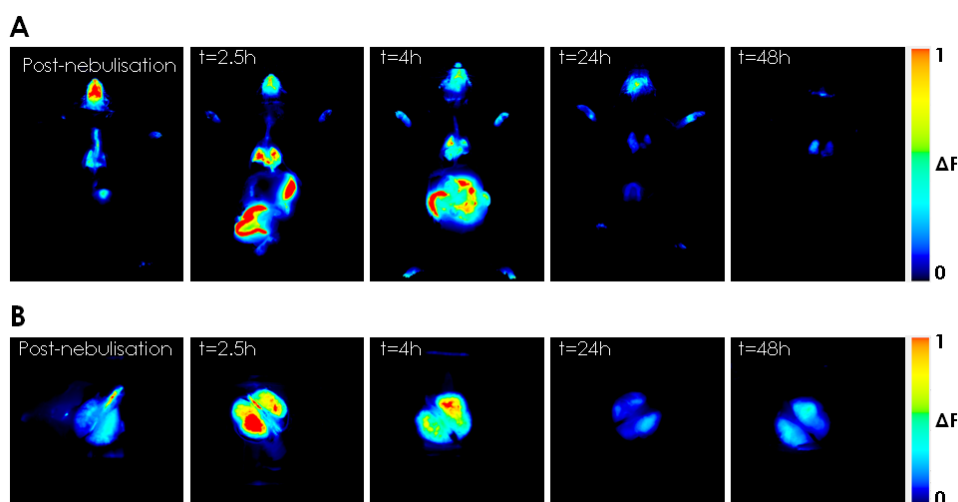
Figure 7. *In vivo* results of IR-NLC distribution after inhalation. A and B) Pseudo-color image representing the spatial distribution of photon counts in whole animals and lungs respectively, immediately after nebulization and at 2.5, 4, 24 and 48 hours after IR-NLC inhalation.

At 0 hours, immediately after the nebulization was completed, the whole body images showed abundant NLCs presence in the snout and the oropharyngeal cavity, the most exposed areas to the inhalation device. Two and half hours later, swallowing and breathing have displaced most NLCs to the respiratory and digestive tracts; at this time point NLCs were homogenously distributed in both lungs and remained there until the end of the study. Thus, NLCs displayed a suitable tissue disposition, spreading extensively throughout the lungs that could be detected up to 48 hours after nebulization (Figure 7B). Similarly, Taratula *et al.* reported that NLCs presented a uniform distribution through the lungs 24 h post-nebulization, whereas i.v. administration led to only 23% of NLCs retained in the lungs [34].

In this part of this doctoral thesis, we verified that Colist-SLNs and Colist-NLCs were physico-chemically suitable for the delivery of sodium colistimethate. In terms of tolerability and antimicrobial activity, Colist-NLCs freeze-dried with trehalose seem to us an encouraging alternative to the currently available cystic fibrosis therapies as they are effective against mucoid *Pseudomonas aeruginosa*. Besides, the side effects of the active drug, colistin, could be improved because of the sustained drug release and also the number of dose could be decreased. The NLCs were homogenously distributed throughout the respiratory tract and remained in the target tissue for at least 48 hours. In summary, these preliminary results suggest that NLCs could be a better option for sodium colistimethate delivery than SLNs; however, the stability of both NPs should be assessed in order to find the adequate condition for their storage and finally achieve a suitable formulation that can be used clinically.

2. Are these nanoparticles stable in terms of their physico-chemical characteristics, biopharmaceutical properties and antimicrobial activity? Which is the optimal storage condition for our NPs?

We wondered if the prolonged storage at different conditions of temperature and humidity could alter, somehow, the properties of the NPs. In order shed light on this question, the stability of Colist-SLNs and Colist-NLCs was analyzed over one year according to the International Conference on Harmonization (ICH) guidelines in terms of their antimicrobial activity and physico-chemical and biopharmaceutical properties.

An important limitation of aqueous suspensions is their poor stability that could be overcome by transforming them in a powder. Freeze-drying is one of the most extensively employed methods in the pharmaceutical field to get dehydrated formulations which can be stored for longer periods [35]. For that purpose, a good stabilizer or cryoprotectant is

needed, in this case trehalose was chosen for our NPs as it showed an improvement on antimicrobial activity and tolerability in our previous work compared to mannitol.

In this second part, Colist-SLNs and Colist-NLCs were stored in plain glass vials (USP type I) in environmental simulation chambers for constant climatic conditions as recommended ICH Q1 A (R2) guidelines (CPMO/ICH/2736/99): i) long-term refrigerator at 5 ± 3°C, ii) long-term room temperature at 25 ± 2°C/ 60 ± 5% relative humidity (RH), iii) intermediate at 30 ± 2°C/ 65% ± 5 RH, and iv) accelerate at 40 ± 2°C / 75 ± 5% RH [36,37].

The parameters to be studied and the specifications of the freeze-dried product are described in Table 2. These acceptance criteria was established according to the results of the fresh nanoparticles (time 0) and based on previous experience with this type of nanoformulations.

Table 2. Specifications of the freeze-dried nanoparticles.

Parameters	Specifications
Size	≤ 500 nm
PDI	≤ 0.5
Zeta potential	≤ -20 mV
Macroscopic appearance	White powder
Microscopic morphology (TEM)	Spherical shape
Antibacterial activity (MIC)	≤ 16 µg/mL
Drug release profile	≥ 80 % at 24 h

As Colist-SLNs formulations displayed a higher value than 16 µg/mL at the third month failing to meet the acceptance criteria, this formulation was set aside for the following testing periods.

The maintenance of the nanoparticle diameter size after freeze-drying is considered as a good indication of physical stability [38]. Colist-SLNs met the specifications during the first month of storage at all temperatures, ranging from 245 to 336 nm. However, the size

requirement (below 500 nm) was only preserved for SLNs stored at 5°C and 25°C after the first 3 months. On the other hand, Colist-NLCs met the requirements set for size at 5°C and 25°C for one year (Figure 8A), ranging around 400 nm overall but with a slight growth at the sixth month. Similarly, Das and colleagues reported that clotrimazole-loaded NLCs showed better stability in terms of size than SLNs at 5°C and 25°C after 3 months of storage, especially when a high amount of drug was incorporated to the formulation (10% versus 4% drug to lipid ratio) [39]. In addition, Kim *et al.* elaborated itraconazole-loaded NLCs using the solid lipid tristearin and the liquid lipid triolein at different ratios and found sizes less than 500 nm during 90 days of storage at room temperature [40]. However, when Colist-NLCs were stored at higher temperatures, a size enlargement was detected over the third month, exceeding 600 nm at 30°C and 40°C.

Well-formulated nanosystems should display a narrow particle size distribution in the submicron range. Particles greater than 1 µm and a particle growth over the time can indicate physical instability [41]. Furthermore, the particle size can modulate the capture mechanism by macrophages and influence nanoparticle biological stability, as phagocytosis increases when the particle size increases; hence, due to the small size of the NPs developed, they have a greater chance to escape from the clearance mechanism by alveolar macrophages, compared to a microparticulate form [42]. Moreover, after using a nebulization system, pulmonary deposition depends on the particle size, shape and ventilation parameters; with decreasing particle diameters below 500 nm, the deposition increases in all regions of the lung due to their diffusional mobility [43] and they should also be able to diffuse through the mucus pores of chronically infected lungs which typically fall in the range of around 200-500 nm [44].

According to PDI values, as expected, there were more variations in the PDI at higher temperatures for both formulations. In general, as the particle size increased, the PDI also augmented. Only Colist-SLNs samples stored under 5°C and 25°C displayed PDI values below 0.5. This is in concordance with the PDI values (< 0.5) obtained by Ridolfi *et al.*

when testing chitosan-SLN-tretinoin over one year at room temperature [45]. On the other hand, the PDI of Colist-NLCs at the third month rose up to 0.57 and 0.75 at 30°C and 40°C, respectively, indicating a heterogeneous distribution of the nanoparticles that could be related to an increase of agglomerates. However, at lower temperatures, all PDIs kept below 0.5 (Figure 8A) meeting the criteria requirement for the storage conditions, meaning that the samples were monodisperse and homogenous [25]. In addition, Das *et al* reported that the PDI of clotrimazole-NLC formulations remained practically unchanged during the 3 months of the stability study at 2-8°C and 25°C [39].

Altogether, the storage conditions at 5°C and 25°C met the specifications of size and PDI for Colist-SLNs and Colist-NLCs after three months and one year of storage, respectively.

Turning to the zeta potential, all Colist-SLNs formulations ranged from -20 to -30 mV during the three months of the study. Figure 8B shows the zeta potential values obtained for Colist-NLCs that remained below -20 mV (inside the limits of the specification values) at all conditions tested after one year indicating long term stability. Generally, zeta potential values above +20 mV or below -20 mV combined with sterically stabilization predicts good stability of the nanoparticle dispersion; therefore, the NLCs prepared are expected to be stable [39]. Pardeike and co-workers found that the zeta potential of itraconazole-loaded NLCs stayed unchanged (around -31 mV) at room temperature and refrigerated conditions after 6-month of storage [46]. As instability such as aggregation or agglomeration of lipid nanoparticles is indicated by a decrease in the absolute zeta potential value, Colist-NLCs are expected to be stable beyond the observation period [47]. Moreover, surface electrostatic charge is an important factor influencing the deposition of inhaled nanoparticles. For example, charged NPs have higher deposition efficiencies as compared to neutrally ones [43]. In addition, anionic liposomes exhibited longer retention in the lung compared to the neutral liposomes that was attributed to being less prone to aggregate *in vivo* [48].

With regards to drug release, Colist-NLCs showed a similar release profile as the fresh formulation after one-year storage at 5$^\mathrm{o}$C and 25$^\mathrm{o}$C (Figure 8C). Similar findings were reported by Das *et al* when working with clotrimazole-loaded NLCs although in that occasion only the refrigerated condition was tested and the storage duration was fixed in three months [39]. A slightly slower profile was detected at 30$^\mathrm{o}$C of storage, but meeting the specification requirements. On the contrary, Colist-NLCs at 40$^\mathrm{o}$C showed a significantly slower drug release rate than their counterparts reaching only 62.13% of drug release at the end of the study suggesting drug degradation. The results obtained in our study confirmed the stability of the drug entrapped in nanoparticles as the 100% of the drug (total encapsulated drug) was able to be released from the NLCs at 5$^\mathrm{o}$C and 25$^\mathrm{o}$C/60% RH indicating that the antibiotic could be able to exert its antipseudomonal activity after one-year storage under these conditions. According to the prolonged release profile of the NLCs, it could be suggested that sodium colistimethate delivered as lipid nanocarriers might be administered in lower doses or longer intervals, thus reducing its undesirable side effects.

Regarding morphology characteristics, the freeze-drying process led to a fine white powder at time 0 for both formulations. Colist-SLNs at the third month showed a shrinkage appearance with a rubbery aspect and yellowish-white color especially after undergoing 40$^\mathrm{o}$C storage conditions. In accordance with these results, TEM images revealed that Colist-SLNs at the third month presented aggregation of particles or modifications in particle morphology in all temperatures tested. On the other hand, Colist-NLCs maintained the desired characteristics of a freeze-dried pharmaceutical formulation with a powdery aspect at each sample time and until the end of the study. Furthermore, Colist-NLCs exhibited spherical particles without aggregation or significant changes in morphology after 12 months at different conditions of temperature and humidity (Figure 8D).
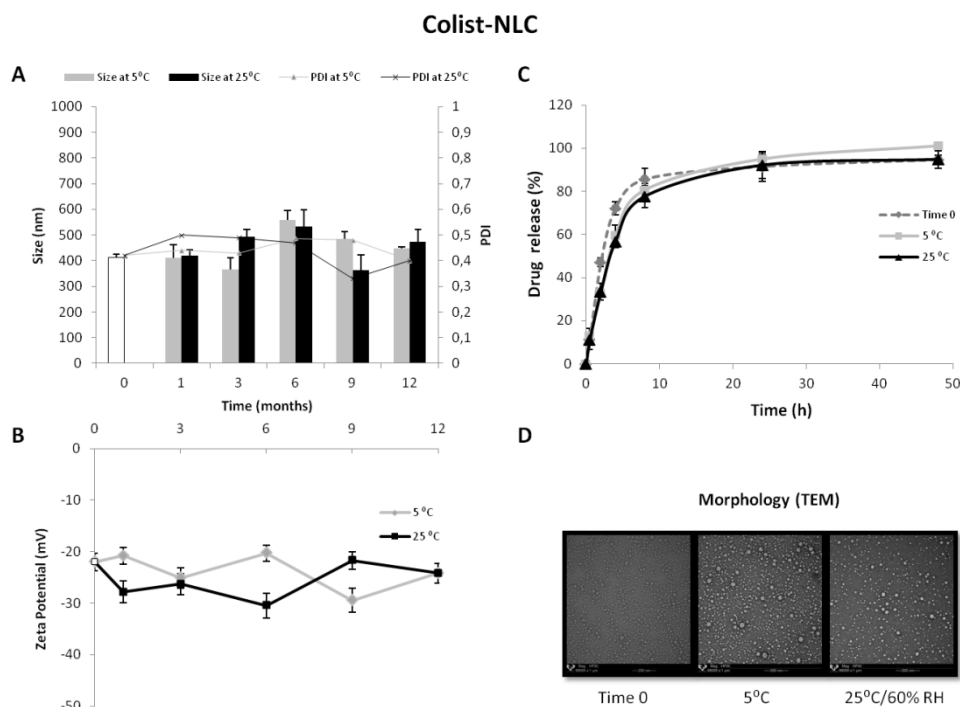
Colist-NLC

Figure 8. Characterization of Colist-NLCs: Representation of particle size and PDI (A) and zeta potential (B) of Colist-NLCs stored under 5 ± 3°C, 25 ± 2°C/ 60 ± 5% RH conditions for 12 months (n=3). Sodium colistimethate release profile from NLCs (C) and TEM images of Colist-NLCs (D) at time 0 and after 12-month storage at 5 ± 3°C, 25 ± 2°C/ 60 ± 5% RH.

Following the characterization of the NPs, the antimicrobial activity of both types of nanoparticles was analyzed against two clinically isolated of *P. aeruginosa* (the non-mucoid 056 SJD and the mucoid 086 SJD) recovered from the sputum of CF patients. Additionally, ATCC 27853 was used as a control strain. For the data analysis, the following acceptance criterion was pre-established: as the MIC of the free antibiotic always led to 8-16 μg/mL throughout all the study; 16 μg/mL MIC was set as the critical concentration (Table 3). Samples outside that value were dropped off for the stability study. At the

beginning of the study, the MIC values of Colist-SLNs and Colist-NLCs were the same as the free drug. Similarly, Ghaffari *et at.* evaluated the antimicrobial activity against *P. aeruginosa* of free amikacin and amikacin-loaded SLNs after freeze drying, obtaining MIC values of 8 and 16 μg/mL, respectively [15].
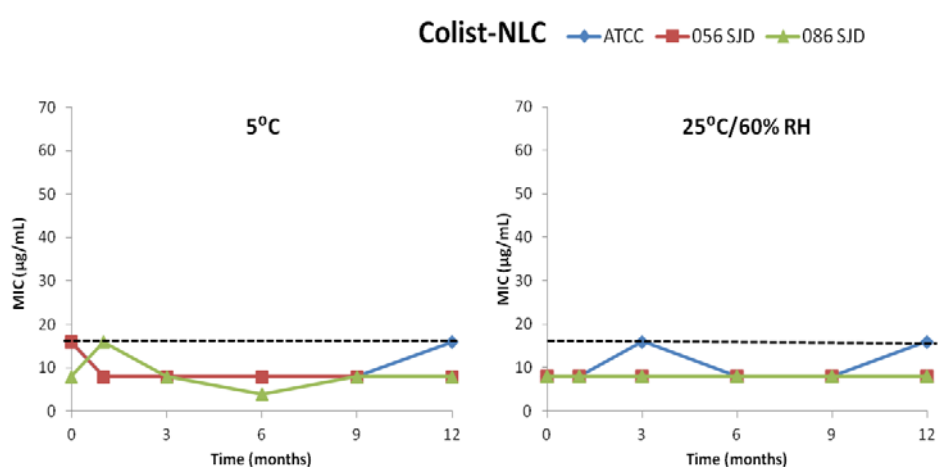
Figure 9. Minimum inhibitory concentration (MIC) of Colist-NLCs against three strains of *Pseudomonas aeruginosa*, ATCC27853, 056SJD and 086 SJD at 5°C and 25°C/60% relative humidity (RH) during 12 months.

By the microbiological experiments it could be demonstrated that Colist-SLNs were not able to maintain their antimicrobial activity after three months of storage because MIC values were 8 times higher than the free drug, exceeding the acceptance criteria and, as consequence, the stability study was stopped for sodium colistimethate-loaded SLNs. On the other hand, the antimicrobial efficiency of Colist-NLCs was retained during 12 months against all the strains tested as the MIC values always were ≤16 μg/mL at 5°C and 25°C (Figure 9) and also even during storage under harder conditions of temperature and humidity. These results demonstrated that sodium colistimethate encapsulated into NLCs

was capable of preserving the antimicrobial activity during the storage period at different ICH conditions.

Finally, this work revealed important differences between both types of nanoparticles which it is summarized in table 3. It is noteworthy that the storage of Colist-NLCs in all conditions of temperature and humidity did not affect its antimicrobial efficacy against *P. aeruginosa* for one year. Moreover, during the 12 months of the study, the size, PDI, zeta potential, morphology and release profile remained constant for Colist-NLCs at 5°C and 25°C/60% RH. Another interesting characteristic of Colist-NLCs is the fact that they are prepared with physiologically well-tolerated lipids and avoid the use of organic solvents during their preparation compared to SLNs leading to a higher environmental efficiency. The results collected in the present study indicate that long-term stability of Colist-NLCs over one year can be achieved at the optimized storage conditions (5°C and 25°C/ 60% RH), but it should be highlighted that room temperature would be the most attractive one for Colist-NLCs storage as it eases supply chain management not only in terms of storage but also of transport.

In view of these findings and once confirmed that sodium colistimethate-loaded NLCs exhibited improved stability and shelf-life than Colist-SLNs, the type of lipid nanoparticle considered to be used in further studies was NLCs.

Table 3. Stability of Colist-SLN and Colist-NLC. √: meets the requirements, X: do not meet the requirements.

	SLN				NLC			
	5°C	25°C	30°C	40°C	5°C	25°C	30°C	40°C
Size								
1 month	√	√	√	√	√	√	√	√
3 months	√	√	X	X	√	√	X	X
6 months	---	---	---	---	X	X	X	X
9 months	---	---	---	---	√	√	√	√
12 months	---	---	---	---	√	√	√	X
PDI								
1 month	√	√	√	√	√	√	X	√
3 months	√	√	X	X	√	√	X	X
6 months	---	---	---	---	√	√	√	X
9 months	---	---	---	---	√	√	√	√
12 months	---	---	---	---	√	√	√	√
ZP								
1 month	√	√	√	√	√	√	√	√
3 months	√	√	√	√	√	√	√	√
6 months	---	---	---	---	√	√	√	√
9 months	---	---	---	---	√	√	√	√
12 months	---	---	---	---	√	√	√	√
TEM								
1 month	√	√	√	X	√	√	√	√
3 months	√	X	X	X	√	√	√	√
6 months	---	---	---	---	√	√	√	√
9 months	---	---	---	---	√	√	√	√
12 months	---	---	---	---	√	√	√	√
MIC								
1 month	√	X	X	X	√	√	√	√
3 months	X	X	X	X	√	√	√	√
6 months	---	---	---	---	√	√	√	√
9 months	---	---	---	---	√	√	√	√
12 months	---	---	---	---	√	√	√	√

In the next step, we decided to focus our research on the encapsulation of another type of antibiotic into NLCs with the ultimate purpose of a combination therapy for the treatment of CF. In this approach, we chose an aminoglycoside, more precisely tobramycin, as it is an antibiotic of choice in the treatment of CF associated *P. aeruginosa* infection [49]. Furthermore, a significant reduction of *P. aeruginosa* cell counts in a rat lung infection model and in patients with cystic fibrosis when combined both antibiotics has been reported [50]. Tobramycin is a bactericidal antibiotic that works by binding to a specific receptor protein on the 30S subunit of bacterial ribosomes and 50S ribosome preventing the formation of the 70S complex. As a result, the mRNA base sequence

cannot be into proteins, and cell death ensues [51]. The inhalation of tobramycin is part of current CF therapies as it presents strong bactericidal activity against planktonic cells [52]. For instance, TOBI® or TIS (tobramycin inhalation solution) and TIP (tobramycin inhalation powder) have recently become commercially available for the treatment of chronic lung infections caused by *P. aeruginosa* [53]. However, the efficacy of free drug administration in CF patients is not high enough to achieve therapeutics levels at the site of infection due to its rapid clearance and poor mucus penetration [54]. These drawbacks could be overcome by the use of nanotechnology, fact that has been considered with the use of a formulation based on an inhaled liposomal tobramycin which is currently in phase II (Axentis Pharma, Fluidosome™-Tobramycin ARB-CF0223) [55].

Taking the above into consideration, NLCs appear to be a promising option for tobramycin delivery as they have previously demonstrated good stability for sodium colistimethate and several advantages over liposomes such as, high stability during storage, high encapsulation efficiency or the avoidance of the use of organic solvents during the preparation process [56].

3. **Tobramycin-loaded NLCs: are they active against *P. aeruginosa* and are they capable of penetrating the typical CF mucus layer? Are they suitable for pulmonary delivery?**

The goal of the third work was to prepare and characterize tobramycin-loaded lipid nanocarriers (Tb-NLCs) for targeting the antibiotic to the bacterial infested lungs of patients suffering from chronic lung infections, in particular CF.

In this case, Precirol® ATO 5 (NLC P) and a mixture of Compritol® ATO 888 and Precirol ATO® 5 (1:1) (NLC PC) together with Mygliol® 812 were selected as lipid core for the preparation of these new NPs. Based on our previous work, Precirol® ATO 5 was again selected and we moved onto the evaluation of another lipid, Compritol® ATO 888, which

was chosen taking into consideration that it has been broadly used for the production of nanoparticles [27,57] and presents a similar chemical structure to Precirol® ATO 888 (both are C22 fatty acids). Both NLCs were elaborated by a hot melt emulsification technique as mentioned before, at a 10% of tobramycin load (w/w) and using trehalose (15%, w/w) as cryoprotectant for the freeze-drying process. Thereafter, the formulations were characterized in terms of size, PDI, zeta potential, TEM and release profile, as summarized in Figure 10.
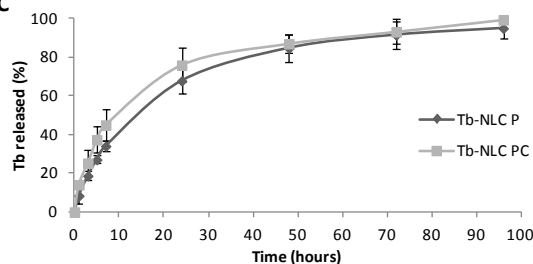
A

Formulation	Mean size (nm)	PDI	Zeta Potential (mV)	EE (%)
Tb-NLC P	254.05 ± 14.50	0.311 ± 0.01	- 23.03 ± 2.76	93.15 ± 0.65
Tb-NLC PC	278.66 ± 20.48	0.371 ± 0.01	- 22.25 ± 0.49	94.03 ± 0.22
IR-NLC P	283.93 ± 5.79	0.368 ± 0.03	-25.73 ± 0.25	99.50 ± 0.02
IR-NLC PC	295.16 ± 17.35	0.304 ± 0.06	-26.30 ± 0.41	99.35 ± 0.09

B
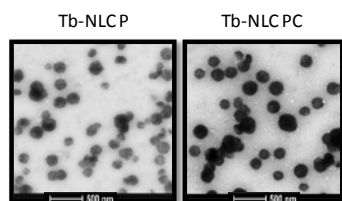
C

Figure 10. Characterization of NLCs: A) Summary table displaying the main properties of the NLCs after freeze-drying, particle size, zeta potential, polydispersity index (PDI) and encapsulation efficiency (EE). B) Transmission electron microscopy images of Tb-NLCs. C) *In vitro* release profiles of tobramycin from NLCs (Tb-NLC P and Tb-NLC PC). Data represent mean + SD values calculated on three different batches.

All the formulations prepared displayed average particle sizes between 250-300 nm after the freeze-drying step with polydispersity indexes below 0.4, demonstrating a narrow size distribution. In addition, all the NPs presented a negative charge of around − 23 mV. The entrapment efficiency of tobramycin was around 94% for both types of Tb-NLCs (Figure 10A). Many other studies have been reported regarding the encapsulation of

tobramycin into SLN [58,59], liposomes [60], and polymeric nanoparticles [61,62], and those were also able to achieve nanometric size although presenting lower encapsulation efficiencies. TEM images revealed that nanoparticles had a regular homogeneous spherical shape (Figure 10B).

According to Figure 10C, an initial rapid release phase was observed for Tb-NLC P (prepared with Precirol® ATO 5) and Tb-NLC PC (prepared with Precirol® ATO 5 plus Compritol® ATO 888) during the first 24 hours (≈80% of drug release). Following the initial burst, a sustained release of the antibiotic is detected in both cases and by the end of the study (92 hours) almost 100% of tobramycin was released from both NPs. The burst release could be attributed to the drug adsorbed onto or close to the surface of the nanoparticles [63]. This profile release is very similar to the one reported by Patlolla *et al.* where a Colecoxib-NLCs formulation incorporating Compritol® was able to release the drug in a controlled manner and almost completely (over 80% of the drug) during 72 hours [27]. The sustained release of tobramycin via a nanocarrier delivery system may provide the opportunity to maintain prolonged lung exposures and enhance the uptake of the drug in the site of infection.

Once we confirmed that the NLCs presented suitable physico-chemical properties, their antimicrobial activity was analyzed. With this purpose, MIC values were calculated against clinical isolated *P. aeruginosa*. Both Tb-NLCs showed to be active against bacterial growth, displaying MIC values of 0.5 µg/mL in most of the planktonic bacteria tested. In the same experimental conditions, free tobramycin displayed the same or higher MIC value indicating that the encapsulation of the drug did not affect the antimicrobial activity. According to the controls, Blank-NLCs had no discernible inhibitory activity on the visible growth of bacteria. Similar results were reported by Deacon *et al.*, who found that tobramycin NPs and free tobramycin reflected the same MIC values against *P. aeruginosa* PA01 (0.625 g/mL) [61].

In a further study, *in vitro* cytotoxicity and viability assays using human epithelial cell (A549 and H441) lines were carried out in order to determine whether Tb-NLCs exerted cell toxicity. None of the formulations tested presented toxicity, at least at the concentrations studied (0.25, 0.5 and 1 mg/mL) after 24 hours of exposition (Figure 11). This finding is in accordance with other reports that demonstrated the good tolerability of lipid nanoparticles *in vitro* using A549 cell lines [64,65]. Furthermore, the concentration of 1 mg/mL is 2,000 times higher than the MIC of Tb-NLCs against *P. aeruginosa* (MIC 0.5 µg/mL). In the next step, cell viability was analyzed under fluorescent microscopy where the predominance of green color in all the samples confirmed the safety of the lipid nanoparticles.
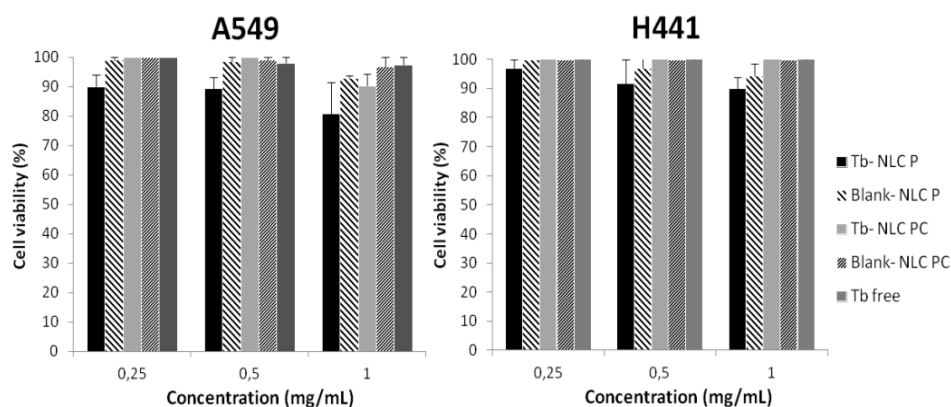
Figure 11. Effect of Tb-NLCs, Blank-NLCs and free drug at different concentrations (0.25, 0.5 and 1 mg/mL) on the viability of A549 and H441 cell lines at 24 hours.

Taking into account that many cystic fibrosis patients present an accumulation of dehydrated and thicker mucus within the airways which leads to respiratory problems, it is important for the therapeutic agents to penetrate into this mucus in order to distribute the drug and maximize its antibacterial effect [66]. In order to overcome this abnormal mucus barrier and to prolong the NLCs retention in the lung, two mucolytic agents, i.e., mannitol and carboxymethylcisteine, (CMC) were selected and used at the proportion

NLC: mucolytic agent 75:25 (based on a previous study using CB-NLCs). We tested whether our particles could cross the mucus and facilitate the drug transport through it by using an artificial mucus model with similar composition and rheological properties to the mucus that CF patients present, as described by Shur *et al.* [67].
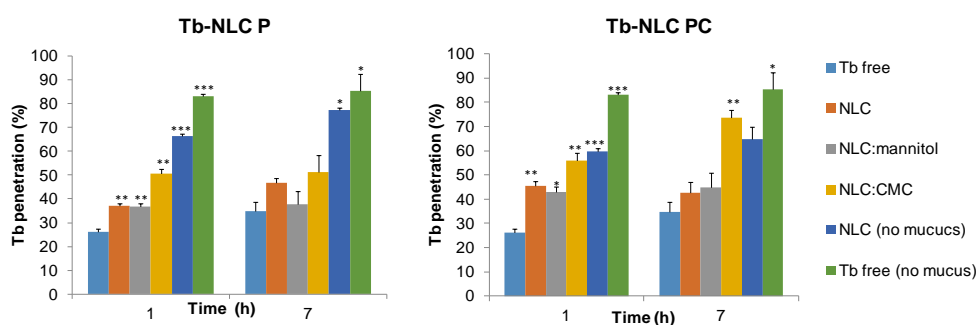

Figure 12. Percentage of tobramycin permeation from NLCs through the AM1 layer. Tb free, Tb-NLC, Tb-NLC: mannitol (75:25), Tb-NLC:CMC (carboxymethylcysteine) (75:25) are formulations tested in presence of a mucus layer. P, Precirol and PC, Precirol plus Compritol. Tb-NLC (no mucus) and Tb free (no mucus) are used as controls without AM1.

The permeability assay was carried out by using Franz cells, observing that the maximum drug permeation across the mucus layer was detected for the Tb-NLC-PC incorporating CMC, whereas the addition of mannitol did not improve significantly the drug permeability at 7 hours (Figure 12). As expected, the penetration and permeation of the particles across the mucus layer was improved by the addition of mucolytic agents that facilitated the transport through it. Similarly, Suk *et al.* also reported a close to 13-fold improvement in the diffusion velocity of NPs through a sputum layer upon the addition of acetylcysteine [68]. The presence of tobramycin in the receptor compartment suggests that the drug may be slowly released from the NLCs, permeate and distribute into the abnormal mucus layer being locally available for its antimicrobial activity. Moreover, as the nanoparticle diffusion across the mucus is dictated by the size of the mucus pores, Tb-NLCs particles, with an approximate diameter of 250 nm, should be theoretically able to overcome the mucus barrier as they are small enough to diffuse

through the mucus pores in chronically infected lungs [44]. Similarly, Forier *et al.* also reported that negatively charged nanoparticles exhibited superior mucus penetration, which is also the case of the NLCs prepared in this study [69].

The final step of the present work was to analyze the biodistribution of the NPs after their intratracheal administration to mice using a MicroSprayer™ aerosolizer (Penn Century® Liquid) in order to test another alternative device for inhalation therapy. As in our first work, IR dye was used again to prepare IR-NLC P and IR-NLC PC that presented similar physic-chemical properties as Tb-NLCs (Figure 10). The fluorescent images of the extracted organs revealed NPs at different levels of the pulmonary tree with a wide distribution in the lungs until 48 hours (Figure 13).
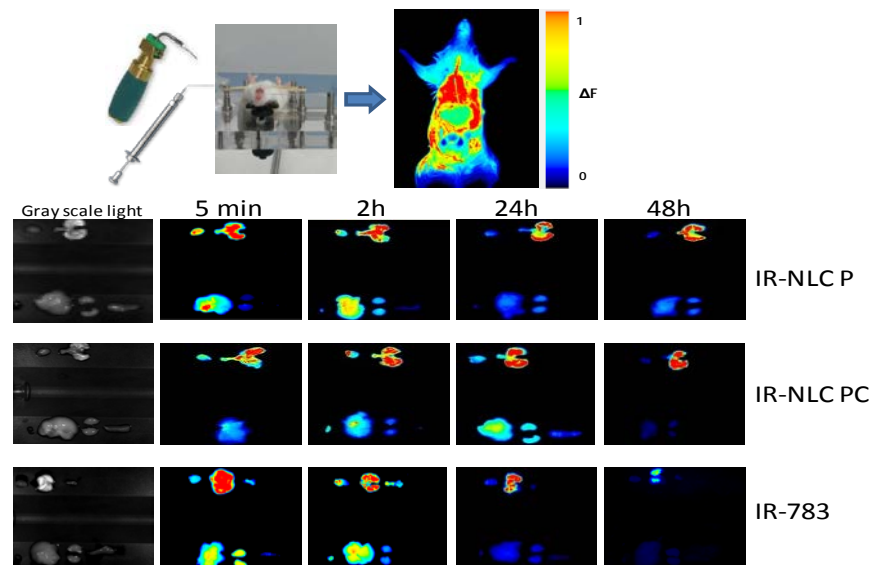
Figure 13. Biodistribution of IR-NLCs and free IR after intratracheal administration to mice. IR-intensity image of selected organ excised (upper row from left to right: heart, trachea and lungs, lower row from left to right: gallbladder, liver, kidneys and spleen) at different time points (5 min, 2 h, 24 h and 48 h).

On the other hand, free dye was faster cleared from the lung and distributed more quickly to other organs such as kidneys and liver compared to NLC formulations (e.g., at 48 hours there was almost no signal in the lungs). In summary, nanoparticles can deposit in the respiratory tract with higher efficiency and for a longer period allowing the drug to be released from the lipid matrix. Similar results were reported by Varshosaz *et al.* who confirmed that SLNs of amikacin remained 6 hours longer in the lungs after the pulmonary administration by microsprayer compared to the i.v. route [70]. Moreover, in another study by Patolla *et al.* celecoxib-loaded NLCs were able to be deposited in the alveolar region with a prolonged residence time, up to 24 hours, after their inhalational administration in mice [27].

In this research work, we have reported an *in vitro* and *in vivo* study of a new tobramycin nanocarrier formulation. Tb-NLCs (both Tb-NLC P and Tb-NLC PC) demonstrated efficacy against *P. aeruginosa in vitro*, mucus penetration ability and large pulmonary distribution and retention in the *in vivo* studies. Tb-NLCs can provide the advantage of a sustained drug release in the target site, resulting in a reduced-dose schedule and improving patient compliance. Therefore, Tb-NLCs could represent an alternative drug delivery system for the treatment of pulmonary infections.

As a whole, in this doctoral thesis we have developed two different lipid nanoparticles (Colist-NLC and Tb-NLC) as a promising strategy to deal with the difficulties of infectious diseases. NLCs are systems with good perspectives to be successfully marketed as they were developed considering industrials needs, e.g.; scale up, qualification and validation, simple technology, low cost, regulatory excipients status (GRAS), tolerability, etc. We believe that these nanocarriers offer a good alternative for antibiotic delivery; however, we are aware that there is much work to be done and limitations that must be overcome.

The continued development and optimal usage of new antimicrobial compounds, including antibiotic combinations, are essential to improve the quality and survival of people with CF; thus, for future studies a combination therapy of tobramycin and sodium colistimethate-loaded NLCs should be considered with the aim to improve the anti-pseudomonal efficacy and reduce the antibiotic resistance. In addition, we have demonstrated that these NPs presented high antimicrobial efficacy against *P. aeruginosa* mucoid strains; hence, a synergistic effect of both formulations could be expected. It would also be interesting to test both nanoformulations in an animal infection model in order to ensure their effectiveness and, finally, further investigation would be needed to develop a dry powder formulation to make possible a clinical application of this combined therapy by using a dry powder inhaler that is a simple device that reduces administration time and improves patient adherence.

In conclusion, sodium colistimethate and tobramycin-loaded NLCs appear to be promising systems for the future therapy of cystic fibrosis.

References

[1] S. Moreau-Marquis, B.A. Stanton, G.A. O'Toole, *Pseudomonas aeruginosa* biofilm formation in the cystic fibrosis airway, Pulm. Pharmacol. Ther. 21 (2008) 595-599.

[2] F. Ratjen, F. Brockhaus, G. Angyalosi, Aminoglycoside therapy against *Pseudomonas aeruginosa* in cystic fibrosis: A review, J. Cyst. Fibros. 8 (2009) 361-369.

[3] E. Drenkard, F.M. Ausubel, *Pseudomonas* biofilm formation and antibiotic resistance are linked to phenotypic variation, Nature. 416 (2002) 740-743.

[4] R. Savla, T. Minko, Nanotechnology approaches for inhalation treatment of fibrosis, J. Drug Target. 21 (2013) 914-925.

[5] H. Heijerman, E. Westerman, S. Conway, D. Touw, Inhaled medication and inhalation devices for lung disease in patients with cystic fibrosis: A European consensus, J Cyst Fibros. 8 (2009) 295-315.

[6] A.C. Dijkmans, E.B. Wilms, I.M. Kamerling, W. Birkhoff, N.V. Ortiz, C.V.N. Zacarías, H.A. Verbrugh, D.J. Touw, Colistin: revival of an old polymyxin, Ther. Drug Moni. 37 (2015) 419-427.

[7] M.E. Falagas, S.K. Kasiakou, Colistin: the revival of polymyxins for the management of multidrug-resistant gram-negative bacterial infections, Clin. Infect. Dis. 40 (2005) 1333-1341.

[8] I. Gould, A. Bal, New antibiotic agents in the pipeline and how they can help overcome microbial resistance, Virulence. 4 (2013) 185-191.

[9] S. Das, A. Chaudhury, Recent advances in lipid nanoparticle formulations with solid matrix for oral drug delivery, AAPS Pharm. Sci. Tech. 12 (2011) 62-76.

[10] R.H. Muller, K. Mader, S. Gohla, Solid lipid nanoparticles (SLN) for controlled drug delivery - a review of the state of the art, Eur. J. Pharm. Biopharm. 50 (2000) 161-177.

[11] R.H. Muller, R.D. Petersen, A. Hommoss, J. Pardeike, Nanostructured lipid carriers (NLC) in cosmetic dermal products, Adv. Drug Deliv. Rev. 59 (2007) 522-530.

[12] S. Weber, A. Zimmer, J. Pardeike, Solid Lipid Nanoparticles (SLN) and Nanostructured Lipid Carriers (NLC) for pulmonary application: a review of the state of the art, Eur. J. Pharm. Biopharm. 86 (2014) 7-22.

[13] M. Ballmann, A. Smyth, D.E. Geller, Therapeutic approaches to chronic cystic fibrosis respiratory infections with available, emerging aerosolized antibiotics, Respir. Med. 105 (2011) S2-S8.

[14] J.S. Patil, S. Sarasija, Pulmonary drug delivery strategies: A concise, systematic review, Lung India. 29 (2012) 44-49.

[15] S. Ghaffari, J. Varshosaz, A. Saadat, F. Atyabi, Stability and antimicrobial effect of amikacin loaded SLN, Int. J. Nanomedicine. 6 (2011) 35-43.

[16] F. Ungaro, I. d'Angelo, C. Coletta, R. d'Emmanuele di Villa Bianca, R. Sorrentino, B. Perfetto, M.A. Tufano, A. Miro, M.I. La Rotonda, F. Quaglia, Dry powders based on PLGA nanoparticles for pulmonary delivery of antibiotics: Modulation of encapsulation efficiency, release rate and lung deposition pattern by hydrophilic polymers, J Control. Release. 157 (2012) 149-159.

[17] S. Chono, T. Tanino, T. Seki, K. Morimoto, Efficient drug targeting to rat alveolar macrophages by pulmonary administration of ciprofloxacin incorporated into mannosylated liposomes for treatment of respiratory intracellular parasitic infections, J Control. Release. 127 (2008) 50-58.

[18] J.P. Wong, H. Yang, K.L. Blasetti, G. Schnell, J. Conley, L.N. Schofield, Liposome delivery of ciprofloxacin against intracellular Francisella tularensis infection, J Control. Release. 92 (2003) 265-273.

[19] C.A. Alvarez, N.P. Wiederhold, J.T. McConville, J.I. Peters, L.K. Najvar, J.R. Graybill, J.J. Coalson, R.L. Talbert, D.S. Burgess, R. Bocanegra, K.P. Johnston, R.O. Williams III, Aerosolized nanostructured itraconazole as prophylaxis against invasive pulmonary aspergillosis, J. Infect. 55 (2007) 68-74.

[20] K. Gilani, E. Moazeni, T. Ramezanli, M. Amini, M.R. Fazeli, H. Jamalifar, Development of respirable nanomicelle carriers for delivery of amphotericin B by jet nebulization, J. Pharm. Sci. 100 (2011) 252-259.

[21] E. Westerman, H. Heijerman, H. Frijlink, Dry powder inhalation versus wet nebulisation delivery of antibiotics in cystic fibrosis patients, Expert Opin Drug Deliv. 4(2007) 91-94.

[22] S. Soares, P. Fonte, A. Costa, J. Andrade, V. Seabra, D. Ferreira, S. Reis, B. Sarmento, Effect of freeze-drying, cryoprotectants and storage conditions on the stability of secondary structure of insulin-loaded solid lipid nanoparticles, Int. J. Pharm. 456 (2013) 370-381.

[23] A. Beloqui, M.Á Solinís, A.R. Gascón, A. del Pozo-Rodríguez, A. des Rieux, V. Préat, Mechanism of transport of saquinavir-loaded nanostructured lipid carriers across the intestinal barrier, J. Control. Release. 166 (2013) 115-123.

[24] W.M. Obeidat, K. Schwabe, R.H. Müller, C.M. Keck, Preservation of nanostructured lipid carriers (NLC), European Journal of Pharmaceutics and Biopharmaceutics. 76 (2010) 56-67.

[25] J. Zhang, Y. Fan, E. Smith, Experimental design for the optimization of lipid nanoparticles, J. Pharm. Sci. 98 (2009) 1813-1819.

[26] J. Jain, S. Arora, J.M. Rajwade, P. Omray, S. Khandelwal, K.M. Paknikar, Silver nanoparticles in therapeutics: development of an antimicrobial gel formulation for topical use, Mol. Pharm. 6 (2009) 1388-1401.

[27] R.R. Patlolla, M. Chougule, A.R. Patel, T. Jackson, P.N. Tata, M. Singh, Formulation, characterization and pulmonary deposition of nebulized celecoxib encapsulated nanostructured lipid carriers, J. Control. Release. 144 (2010) 233-241.

[28] A.C. Silva, A. Kumar, W. Wild, D. Ferreira, D. Santos, B. Forbes, Long-term stability, biocompatibility and oral delivery potential of risperidone-loaded solid lipid nanoparticles, Int. J. Pharm. 436 (2012) 798-805.

[29] M. Zheng, M. Falkeborg, Y. Zheng, T. Yang, X. Xu, Formulation and characterization of nanostructured lipid carriers containing a mixed lipids core, Colloids Surf. Physicochem. Eng. Aspects. 430 (2013) 76-84.

[30] A. Omri, Z.E. Suntres, P.N. Shek, Enhanced activity of liposomal polymyxin B against *Pseudomonas aeruginosa* in a rat model of lung infection, Biochem. Pharmacol. 64 (2002) 1407-1413.

[31] X. Wang, S. Zhang, L. Zhu, S. Xie, Z. Dong, Y. Wang, W. Zhou, Enhancement of antibacterial activity of tilmicosin against Staphylococcus aureus by solid lipid nanoparticles *in vitro* and *in vivo*, The Veterinary Journal. 191 (2012) 115-120.

[32] S. Doktorovova, E.B. Souto, A.M. Silva, Nanotoxicology applied to solid lipid nanoparticles and nanostructured lipid carriers – A systematic review of *in vitro* data, Eur. J. Pharm. Biopharm. 87 (2014) 1-18.

[33] A.L.R.d. Souza, T. Andreani, R.N. de Oliveira, C.P. Kiill, F.K.d. Santos, S.M. Allegretti, M.V. Chaud, E.B. Souto, A.M. Silva, M.P.D. Gremião, *In vitro* evaluation of permeation, toxicity and effect of praziquantel-loaded solid lipid nanoparticles against *Schistosoma mansoni* as a strategy to improve efficacy of the schistosomiasis treatment, Int. J. Pharm. 463 (2014) 31-37.

[34] O. Taratula, A. Kuzmov, M. Shah, O.B. Garbuzenko, T. Minko, Nanostructured lipid carriers as multifunctional nanomedicine platform for pulmonary co-delivery of anticancer drugs and siRNA, J. Control. Release. 171 (2013) 349-357.

[35] W. Abdelwahed, G. Degobert, S. Stainmesse, H. Fessi, Freeze-drying of nanoparticles: formulation, process and storage considerations, Adv. Drug Deliv. Rev. 58 (2006) 1688-1713.

[36] W. Grimm, Extension of the International Conference on Harmonization Tripartite Guideline for Stability Testing of New Drug Substances and Products to countries of climatic zones III and IV, Drug Dev. Ind. Pharm. 24 (1998) 313-325.

[37] I.H.T. Guideline, Stability testing of new drug substances and products, Q1A (R2), Current Step. 4 (2003).

[38] M. Uner, Preparation, characterization and physico-chemical properties of solid lipid nanoparticles (SLN) and nanostructured lipid carriers (NLC): their benefits as colloidal drug carrier systems, Pharmazie. 61 (2006) 375-386.

[39] S. Das, W.K. Ng, R.B. Tan, Are nanostructured lipid carriers (NLCs) better than solid lipid nanoparticles (SLNs): development, characterizations and comparative evaluations of clotrimazole-loaded SLNs and NLCs? Eur. J. Pharm. Sci. 47 (2012) 139-151.

[40] J. Kim, J. Park, C. Kim, Development of a binary lipid nanoparticles formulation of itraconazole for parenteral administration and controlled release, Int. J. Pharm. 383 (2010) 209-215.

[41] R. Haskell, J. Shifflett, P. Elzinga, Particle-sizing technologies for submicron emulsions, Submicron emulsions in drug targeting and delivery. 9 (1998) 21-98.

[42] S. Chono, T. Tanino, T. Seki, K. Morimoto, Influence of particle size on drug delivery to rat alveolar macrophages following pulmonary administration of ciprofloxacin incorporated into liposomes, J. Drug Target. 14 (2006) 557-566.

[43] W. Yang, J.I. Peters, R.O. Williams 3rd, Inhaled nanoparticles--a current review, Int. J. Pharm. 356 (2008) 239-247.

[44] J.S. Suk, S.K. Lai, Y.Y. Wang, L.M. Ensign, P.L. Zeitlin, M.P. Boyle, J. Hanes, The penetration of fresh undiluted sputum expectorated by cystic fibrosis patients by non-adhesive polymer nanoparticles, Biomaterials. 30 (2009) 2591-2597.

[45] D.M. Ridolfi, P.D. Marcato, G.Z. Justo, L. Cordi, D. Machado, N. Durán, Chitosan-solid lipid nanoparticles as carriers for topical delivery of tretinoin, Colloids Surf. B Biointerfaces. 93 (2012) 36-40.

[46] J. Pardeike, S. Weber, T. Haber, J. Wagner, H.P. Zarfl, H. Plank, A. Zimmer, Development of an itraconazole-loaded nanostructured lipid carrier (NLC) formulation for pulmonary application, Int. J. Pharm. 419 (2011) 329-338.

[47] C. Freitas, R.H. Müller, Effect of light and temperature on zeta potential and physical stability in solid lipid nanoparticle (SLN™) dispersions, Int. J. Pharm. 168 (1998) 221-229.

[48] C. Beaulac, S. Clement-Major, J. Hawari, J. Lagace, *In vitro* kinetics of drug release and pulmonary retention of microencapsulated antibiotic in liposomal formulations in relation to the lipid composition, J. Microencapsul. 14 (1997) 335-348.

[49] A.R. Smyth, S.C. Bell, S. Bojcin, M. Bryon, A. Duff, P. Flume, N. Kashirskaya, A. Munck, F. Ratjen, S.J. Schwarzenberg, I. Sermet-Gaudelus, K.W. Southern, G. Taccetti, G. Ullrich, S. Wolfe, European Cystic Fibrosis Society, European Cystic Fibrosis Society Standards of Care: Best Practice guidelines, J. Cyst. Fibros. 13 Suppl 1 (2014) S23-42.

[50] G. Herrmann, L. Yang, H. Wu, Z. Song, H. Wang, N. Hoiby, M. Ulrich, S. Molin, J. Riethmuller, G. Doring, Colistin-tobramycin combinations are superior to monotherapy concerning the killing of biofilm *Pseudomonas aeruginosa*, J. Infect. Dis. 202 (2010) 1585-1592.

[51] B.D. Davis, Mechanism of bactericidal action of aminoglycosides, Microbiol. Rev. 51 (1987) 341-350.

[52] O. Thellin, W. Zorzi, O. Jolois, B. Elmoualij, G. Duysens, B. Cahay, B. Streel, M. Charif, R. Bastin, E. Heinen, P. Quatresooz, *In vitro* approach to study the synergistic effects of tobramycin and clarithromycin against *Pseudomonas aeruginosa* biofilms using prokaryotic or eukaryotic culture media, Int. J. Antimicrob. Agents. 46 (2015) 33-38.

[53] V. Waters, A. Smyth, Cystic fibrosis microbiology: Advances in antimicrobial therapy, J. Cyst. Fibros. 14 (2015) 551-560.

[54] B.S. Tseng, W. Zhang, J.J. Harrison, T.P. Quach, J.L. Song, J. Penterman, P.K. Singh, D.L. Chopp, A.I. Packman, M.R. Parsek, The extracellular matrix protects *Pseudomonas aeruginosa b*iofilms by limiting the penetration of tobramycin, Environ. Microbiol. 15 (2013) 2865-2878.

[55] R. Diab, B. Khameneh, O. Joubert, R. Duval, Insights in Nanoparticle-Bacterium Interactions: New Frontiers to Bypass Bacterial Resistance to Antibiotics, Curr. Pharm. Des. 21 (2015) 4095-4105.

[56] G. Barratt, Colloidal drug carriers: achievements and perspectives, Cell. Mol. Life Sci. 60 (2003) 21-37.

[57] V. Jenning, A.F. Thünemann, S.H. Gohla, Characterisation of a novel solid lipid nanoparticle carrier system based on binary mixtures of liquid and solid lipids, Int. J. Pharm. 199 (2000) 167-177.

[58] R. Cavalli, M.R. Gasco, P. Chetoni, S. Burgalassi, M.F. Saettone, Solid lipid nanoparticles (SLN) as ocular delivery system for tobramycin, Int. J. Pharm. 238 (2002) 241-245.

[59] R. Cavalli, G.P. Zara, O. Caputo, A. Bargoni, A. Fundarò, M.R. Gasco, Transmucosal transport of tobramycin incorporated in SLN after duodenal administration to rats. Part I- A pharmacokinetic study, Pharmacological Research. 42 (2000) 541-545.

[60] A. Messiaen, K. Forier, H. Nelis, K. Braeckmans, T. Coenye, Transport of nanoparticles and tobramycin-loaded liposomes in Burkholderia cepacia complex biofilms, Nanomedicine. 8 (2013) 935-945.

[61] J. Deacon, S.M. Abdelghany, D.J. Quinn, D. Schmid, J. Megaw, R.F. Donnelly, D.S. Jones, A. Kissenpfennig, J.S. Elborn, B.F. Gilmore, C.C. Taggart, C.J. Scott, Antimicrobial efficacy of tobramycin polymeric nanoparticles for *Pseudomonas aeruginosa* infections in cystic fibrosis: Formulation, characterisation and functionalisation with dornase alfa (DNase), J. Control. Release. 198 (2015) 55-61.

[62] F. Ungaro, I. d'Angelo, C. Coletta, R. d'Emmanuele di Villa Bianca, R. Sorrentino, B. Perfetto, M.A. Tufano, A. Miro, M.I. La Rotonda, F. Quaglia, Dry powders based on PLGA nanoparticles for pulmonary delivery of antibiotics: modulation of encapsulation efficiency, release rate and lung deposition pattern by hydrophilic polymers, J. Control. Release. 157 (2012) 149-159.

[63] V. Nandakumar, V. Geetha, S. Chittaranjan, M. Doble, High glycolic poly (DL lactic co glycolic acid) nanoparticles for controlled release of meropenem, Biomed. Pharmacother. 67 (2013) 431-436.

[64] J. Liu, T. Gong, H. Fu, C. Wang, X. Wang, Q. Chen, Q. Zhang, Q. He, Z. Zhang, Solid lipid nanoparticles for pulmonary delivery of insulin, Int. J. Pharm. 356 (2008) 333-344.

[65] L. Hu, Y. Jia, Preparation and characterization of solid lipid nanoparticles loaded with epirubicin for pulmonary delivery, Die Pharmazie. Int. J. Pharm. Sci. 65 (2010) 585-587.

[66] Y. Yang, M.D. Tsifansky, S. Shin, Q. Lin, Y. Yeo, Mannitol-guided delivery of ciprofloxacin in artificial cystic fibrosis mucus model, Biotechnol. Bioeng. 108 (2011) 1441-1449.

[67] J. Shur, T.G. Nevell, R.J. Ewen, R. Price, A. Smith, E. Barbu, J.H. Conway, M.P. Carroll, J.K. Shute, J.R. Smith, Cospray-dried unfractionated heparin with L-leucine as a dry powder inhaler mucolytic for cystic fibrosis therapy, J. Pharm. Sci. 97 (2008) 4857-4868.

[68] J.S. Suk, S.K. Lai, N.J. Boylan, M.R. Dawson, M.P. Boyle, J. Hanes, Rapid transport of muco-inert nanoparticles in cystic fibrosis sputum treated with N-acetyl cysteine, Nanomedicine (Lond). 6 (2011) 365-375.

[69] K. Forier, A.S. Messiaen, K. Raemdonck, H. Deschout, J. Rejman, F. De Baets, H. Nelis, S.C. De Smedt, J. Demeester, T. Coenye, K. Braeckmans, Transport of nanoparticles in cystic fibrosis sputum and bacterial biofilms by single-particle tracking microscopy, Nanomedicine (Lond). 8 (2013) 935-949.

[70] J. Varshosaz, S. Ghaffari, S.F. Mirshojaei, A. Jafarian, F. Atyabi, F. Kobarfard, S. Azarmi, Biodistribution of amikacin solid lipid nanoparticles after pulmonary delivery, Biomed. Res. Int. 2013 (2013) 1-8.

CONCLUSIONS

Based on the results obtained from the experimental studies of this dissertation, the following conclusions were derived:

1. Emulsion-solvent evaporation and hot melt homogenization resulted in appropriated techniques to prepare SLNs and NLCs, respectively, enabling the encapsulation of sodium colistimethate with adequate physico-chemical and biopharmaceutical properties against clinically isolated *Pseudomonas aeruginosa* strains. Among the formulations developed Colist-NLCs freeze-dried using trehalose as cryoprotectant showed the optimal features for pulmonary administration.

2. Colist-SLNs were not stable after three months of storage according to ICH Q1 A (R2) conditions in terms of physico-chemical characteristics, biopharmaceutical properties and antimicrobial activity.

3. Colist-NLCs maintained their physico-chemical, biopharmaceutical and antibacterial properties against *P. aeruginosa* (inside the fixed limits of acceptability) after 12-month storage at 5°C and 25°C/60% relative humidity, demonstrating optimal stability. Therefore, NLCs were considered better candidates for further studies.

4. Two formulations based on NLCs were developed for tobramycin encapsulation (Tb-NLC P and Tb-NLC PC). Both Tb-NLCs showed satisfactory physico-chemical characteristics and biopharmaceutical properties for pulmonary delivery. Mucoid and non-mucoid *P. aeruginosa* clinically isolates were susceptible to Tb-NLCs. Tb-NLCs co-formulated with carboxymethylcysteine demonstrated mucus penetration and permeation ability through an artificial mucus model that simulates the one that cystic fibrosis patients present.

5. After the pulmonary administration of NLCs to mice using a nebulizer system or a microsprayer aerolizer, NLCs demonstrated a large distribution and retention in the lungs for at least 48 hours.

APPENDIX I

This dissertation is part of the ZabaldUz program whose main objective is to strengthen the relationship between universities and companies by addressing research programs that may be of interest to companies and that advance on the transfer of knowledge to the industrial environment. An important part of this process is the protection of intellectual property for the results, which allows them to be exploited by businesses. In this context, this dissertation has resulted in a joint patent whose reference is included in this annex.

The present invention relates to a lipid nanoparticle comprising at least one antibiotic, tobramycin, a pharmaceutical composition comprising this nanoparticle and the use of this nanoparticle in the prevention and/or treatment of infections by bacteria sensitive to tobramycin, preferably in the respiratory tree.

Justificante de presentación electrónica de solicitud de patente

Este documento es un justificante de que se ha recibido una solicitud española de patente por vía electrónica, utilizando la conexión segura de la O.E.P.M. Asimismo, se le ha asignado de forma automática un número de solicitud y una fecha de recepción, conforme al artículo 14.3 del Reglamento para la ejecución de la Ley 11/1986, de 20 de marzo, de Patentes. La fecha de presentación de la solicitud de acuerdo con el art. 22 de la Ley de Patentes, le será comunicada posteriormente.

Número de solicitud:	P201431894
Fecha de recepción:	19 diciembre 2014, 16:33 (CET)
Oficina receptora:	OEPM Madrid
Su referencia:	BIO002
Solicitante:	BIOPRAXIS RESEARCH AIE
Número de solicitantes:	5
País:	ES
Título:	Nanopartícula lipídica de tobramicina
Documentos enviados:	Descripcion.pdf (21 p.) package-data.xml Reivindicaciones.pdf (3 p.) es-request.xml Dibujos.pdf (1 p.) application-body.xml Resumen.pdf (1 p.) es-fee-sheet.xml OLF-ARCHIVE.zip feesheet.pdf request.pdf
Enviados por:	CN=Ismael Igartua Irizar 28226
Fecha y hora de recepción:	19 diciembre 2014, 16:33 (CET)
Codificación del envío:	4E:73:E8:97:CA:39:DC:FF:4B:33:56:BE:CD:CC:E6:03:CC:A0:BF:A7

ADVERTENCIA: POR DISPOSICIÓN LEGAL LOS DATOS CONTENIDOS EN ESTA SOLICITUD PODRÁN SER PUBLICADOS EN EL BOLETÍN OFICIAL DE LA PROPIEDAD INDUSTRIAL E INSCRITOS EN EL REGISTRO DE PATENTES DE LA OEPM, SIENDO AMBAS BASES DE DATOS DE CARÁCTER PÚBLICO Y ACCESIBLES VÍA REDES MUNDIALES DE INFORMÁTICA.
Para cualquier aclaración puede contactar con la O.E.P.M.